

**SENSORIMOTOR INTEGRATION IN
DYSTONIA: PATHOPHYSIOLOGY AND
POSSIBLE NON-INVASIVE APPROACHES
TO THERAPY**



Lorenzo Rocchi

University College London

UCL Queen Square Institute of Neurology

Department of Clinical and Movement Neurosciences

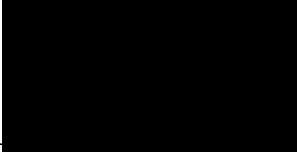
University College London

This dissertation is submitted for the degree of Doctor of Philosophy

September 2020

DECLARATION

I, Lorenzo Rocchi, confirm that the work presented in this thesis is my own. Where information has been derived from other sources, I confirm that this has been indicated in the thesis.

Signed: _____


Date: _____01/SEP/2020_____

Lorenzo Rocchi

University College London

ABSTRACT

Dystonia is a condition characterized by excessive and sustained muscle contractions causing abnormal postures and involuntary movements. The pathophysiology of dystonia includes loss of inhibition and abnormal plasticity in the somatosensory and motor systems; however, their contribution to the phenomenology of dystonia is still uncertain, and the possibility to target these abnormalities in an attempt to devise new treatments has not been thoroughly explored. This thesis describes how abnormal inhibition and plasticity in the somatosensory system of dystonic patients can be manipulated to ameliorate motor symptoms by means of peripheral stimulation.

First, we characterized electrophysiological and behavioural markers of inhibition in the primary somatosensory cortex in a group of patients with idiopathic cervical dystonia (CD). Outcome measures included a) somatosensory temporal discrimination threshold (STDT); b) paired-pulse somatosensory evoked potentials (PP-SEP) tested with interstimulus intervals (ISIs) of 5, 20 and 40 ms; c) spatial somatosensory inhibition ratio (SIR) by measuring SEP interaction between simultaneous stimulation of the digital nerves in thumb and index finger; d) high-frequency oscillations (HFO) extracted from SEP obtained with stimulation of digital nerves of the index finger. This first investigation demonstrated that increased STDT in dystonia is related to reduced activity of inhibitory circuits within the primary somatosensory cortex, as reflected by reduced PP-SEP inhibition at ISI of 5 ms and reduced area of the late part of the HFO (l-HFO).

In a second set of experiments, we applied high frequency repetitive somatosensory stimulation (HF-RSS), a patterned electric stimulation applied to the skin through surface electrodes, to the index finger in a sample of healthy subjects, with the aim to manipulate excitability and inhibition of the primary somatosensory (S1) and motor (M1) cortices. The former was assessed by the same methods used before (STDT, PP-SEP, HFO), with the addition of two psychophysical tasks designed to assess tactile spatial discrimination (grating orientation and bumps tests). Assessment of physiology of M1 was performed by means of short intracortical inhibition (SICI) assessed with TMS; this was performed with multiple conditioning stimulus (CS) intensities (70%, 80%, 90% of the active motor threshold) and with an interstimulus interval (ISI) between conditioning and test stimulus of 3 ms.

It was found that HF-RSS increased inhibition in S1 tested by PP-SEP and HFO; these changes were correlated with improvement in STDT. HF-RSS also enhanced bumps detection, while there was no change in grating orientation test. Finally, there was an increase in SICI, suggesting widespread changes in cortical sensorimotor interactions. Overall, these findings demonstrated that HF-RSS is able to modify the effectiveness of inhibitory circuitry in S1 and M1.

The results obtained so far led us to hypothesize that HF-RSS could restore inhibition in dystonic patients, similar to what observed in healthy subjects. To test this, we applied HF-RSS on the index finger in a sample of patients with CD, and tested its effects with some of the outcome measures used before (STDT, PP-SEP, HFO, SIR, SICI). Unexpectedly, the results were opposite to what was predicted. Patients with CD showed a consistent, paradoxical response: after HF-RSS, they had reduced suppression of PP-SEP, as well as decreased HFO area and SICI, and increased SIR. STDT deteriorated after the stimulation protocol, and correlated with reduced measures of inhibition within S1 (PP-SEP at 5 ms ISI, 1-HFO area). It was hypothesized that patients with CD have abnormal homeostatic inhibitory plasticity within the sensorimotor cortex and that this is responsible for their abnormal response to HF-RSS. Interestingly, this alteration in plasticity seems to be specific to idiopathic dystonia: when the same protocol was applied to patients with dystonia caused by lesions in the basal ganglia, the response was similar to healthy controls. This result suggests that reduced somatosensory inhibition and abnormal cortical plasticity are not strictly required for the clinical expression of dystonia, and that the abnormalities reported in idiopathic dystonia are not necessarily linked to basal ganglia damage.

We then directed our attention to another form of peripheral electrical stimulation, delivered at low frequency (LF-RSS). Previous literature demonstrated that this pattern of stimulation had effects opposite to HF-RSS on tactile performance in healthy subjects; therefore, given the previous findings of abnormal response to HF-RSS in CD, we hypothesized that an inverse response might occur in these patients following LF-RSS as well. Our hypothesis was confirmed by the observation that LF-RSS, applied to the fingers in patients with CD, induced an increase in inhibition in the primary somatosensory and motor cortices. This was reflected by an improvement of STDT and an increase in PP-SEP suppression, HFO area and SICI.

With this in mind, in the final project of the thesis, we tested the effects of HF-RSS and LF-RSS applied directly over two affected muscles in different groups of patients with

focal hand dystonia (FHD), in an attempt to modulate involuntary muscle activity and, consequently, to ameliorate motor symptoms. Whereas HF-RSS was delivered synchronously over the two muscles, LF-RSS was given either synchronously or asynchronously. Outcome measures included a) PP-SEP obtained by direct stimulation of affected muscles, with ISIs of 5 and 30 ms; b) quantification of electromyographic (EMG) activity from tested muscles; c) SICI recorded from the affected muscles, with CS intensities ranging from 50% to 100% RMT and with an ISI of 3 ms; d) evaluation of hand function, assessed by the box and blocks test (BBT) and the nine-hole peg test (NHPT); e) SIR by measuring SEP interaction between simultaneous stimulation of the two muscles receiving repetitive stimulation. We confirmed the paradoxical response of dystonic patients to HF-RSS, which was reflected in decreased PP-SEP suppression and SICI and increased SIR. Importantly, this was paralleled by an increase in involuntary EMG activity and worse scores at the BBT and NHPT. This results were opposite when LF-RSS was delivered, either in its synchronous or asynchronous version, the latter being slightly more effective. Thus, LF-RSS was able to increase PP-SEP suppression and SICI, decrease SIR and reduce involuntary EMG activity, with consequent improvement in performance in the BBT and NHPT.

Overall, our data provide novel insight into the neural mechanisms underlying loss of inhibition and deranged somatosensory plasticity in idiopathic dystonia and bring preliminary evidence that peripheral electrical stimulation can be used as a treatment in idiopathic focal hand dystonia.

IMPACT STATEMENT

We anticipate that the findings in this thesis will be relevant to a range of clinical and non-clinical neuroscientists interested in dystonia. Some pathophysiological features of dystonia, such as decreased inhibition and deranged plasticity, have been known for some time, but they have not so far clearly framed into the clinical context, nor have they been successfully addressed as potential therapeutical targets. In this work we have first thoroughly characterized alterations in somatosensory inhibition in dystonia. Then, we have demonstrated that deranged homeostatic plasticity at inhibitory synapses, both in the primary somatosensory cortex and subcortical somatosensory relay structures, represents a pathophysiological hallmark of idiopathic dystonia. Finally, we have provided preliminary results that this deranged plasticity can be partly restored with peripheral repetitive electrical stimulation, with resulting amelioration of dystonia. Overall, we have characterized a novel mechanism which might contribute to dystonia and have shown that it can be used as a target for non-invasive forms of therapy. We hope that this will prompt future research in the field, allowing for further characterization of inhibition in dystonia, as well as refinement of non-invasive therapeutical approaches.

ACKNOWLEDGEMENTS

The results described in this thesis would not have been obtained without the assistance of many colleagues, whose contributions in the following aspects of the work have been invaluable:

Neurophysiological testing: Dr Elena Antelmi, Dr Roberto Erro, Dr Anna Latorre.

Patient recruitment: Dr Anna latorre, Dr Elena Antelmi, Dr Roberto Erro, Dr Carla Cordivari,

Clinical assessment: Dr Anna latorre, Dr Elena Antelmi, Dr Roberto Erro.

Significant intellectual contribution: Dr Roberto Erro, Dr Anna Latorre, Prof Kailash Bhatia, Prof John Rothwell.

I am particularly grateful to Prof John Rothwell for his advice, guidance and continuous support during the years spent at UCL. Special thanks also go to Mr Paul Hammond, for his precious technical assistance and impeccable management of the lab environment.

CONTENTS

1	Introduction.....	19
1.1	Overview of the subtypes of dystonic disorders and the known underlying pathophysiological mechanisms.....	19
1.2	Treatment options for dystonia.....	22
1.3	Somatosensory temporal discrimination abnormalities in dystonia.....	24
1.4	An introduction to inhibition in the nervous system.....	25
1.5	Inhibition in the primary somatosensory cortex.....	29
1.6	Assessing inhibition in the human somatosensory cortex.....	33
1.6.1	<i>Introduction to the somatosensory evoked potential.....</i>	<i>33</i>
1.6.1.1	<i>Somatosensory pathways involved in the generation of the somatosensory evoked potential.....</i>	<i>34</i>
1.6.1.2	<i>Electrophysiological properties of somatosensory evoked potentials.....</i>	<i>35</i>
1.6.2	<i>The somatosensory evoked potential as a measure of somatosensory inhibition.....</i>	<i>41</i>
1.6.2.1	<i>Paired-pulse somatosensory evoked potential.....</i>	<i>41</i>
1.6.2.2	<i>High-frequency oscillations.....</i>	<i>46</i>
1.6.3	<i>Behavioural measures of somatosensory discrimination.....</i>	<i>49</i>
1.6.3.1	<i>Somatosensory temporal discrimination threshold.....</i>	<i>49</i>
1.6.3.2	<i>Tactile spatial discrimination and tactile threshold.....</i>	<i>51</i>
1.7	Inhibition in the motor system.....	54
1.8	Introduction to transcranial magnetic stimulation.....	56
1.8.1	<i>Paired-pulse transcranial magnetic stimulation.....</i>	<i>58</i>
1.9	Plasticity induced in the nervous system by repetitive peripheral stimulation.....	62
1.10	Aims of the current thesis.....	66
2	General methods.....	59
2.1	Participants, institutional and ethical approval.....	68
2.2	Transcranial magnetic stimulation.....	68
2.2.1	<i>TMS coils and magnetic stimulators.....</i>	<i>68</i>

2.2.2	<i>Hotspot location and test stimulus threshold measurement</i>	68
2.3	Electrical stimulation.....	69
2.4	Recording of evoked responses.....	69
2.4.1	<i>Evoked responses from muscles</i>	69
2.4.2	<i>Evoked responses from the scalp</i>	69
2.5	Somatosensory behavioural tasks.....	69
2.6	Hand motor function tests.....	70
2.7	Clinical assessment.....	71
3	Neurophysiological correlates of abnormal somatosensory temporal discrimination in Dystonia	73
3.1	Introduction.....	73
3.2	Materials and methods.....	74
3.2.1	<i>Subjects</i>	74
3.2.2	<i>Somatosensory temporal discrimination threshold</i>	74
3.2.3	<i>Somatosensory evoked potentials recording and analysis</i>	75
3.2.4	<i>Analysis of HFO</i>	77
3.2.5	<i>Statistical analysis</i>	77
3.3	Results.....	77
3.4	Discussion.....	82
4	High frequency somatosensory stimulation increases sensorimotor inhibition and leads to perceptual improvement in healthy subjects	86
4.1	Introduction.....	86
4.2	Materials and methods.....	87
4.2.1	<i>Subjects</i>	87
4.2.2	<i>Somatosensory temporal discrimination threshold</i>	87
4.2.3	<i>Tactile tasks</i>	88
4.2.4	<i>Somatosensory evoked potentials recording and analysis</i>	89

4.2.5	<i>High frequency oscillations analysis</i>	89
4.2.6	<i>Transcranial magnetic stimulation and electromyographic recording</i>	90
4.2.7	<i>Experimental Procedure</i>	91
4.2.8	<i>Statistical analysis</i>	91
4.3	Results	92
4.3.1	<i>Somatosensory temporal discrimination threshold</i>	92
4.3.2	<i>N20/P25 and P14 latency and amplitude</i>	93
4.3.3	<i>N20 and P14 recovery cycle</i>	94
4.3.4	<i>Early and late high-frequency oscillations</i>	95
4.3.5	<i>Tactile tasks</i>	95
4.3.6	<i>Correlation between the effect of HF-RSS on STDT and neurophysiological - behavioural measures</i>	96
4.3.7	<i>Effect of HF-RSS on inhibitory circuitry of the primary motor area</i>	98
4.4	Discussion	100
4.4.1	<i>Electrophysiological results</i>	101
4.4.2	<i>Relation between temporal and spatial perception and electrophysiological inhibition</i>	102
4.4.3	<i>HF-RSS effects on motor cortex inhibition</i>	104
4.4.4	<i>Conclusion</i>	104
5	High Frequency Somatosensory Stimulation in Dystonia: Evidence for Defective Inhibitory Plasticity	106
5.1	Introduction	106
5.2	Materials and methods	107
5.2.1	<i>Subjects and experimental protocol</i>	107
5.2.2	<i>Somatosensory temporal discrimination threshold</i>	108
5.2.3	<i>Somatosensory evoked potentials recording and analysis</i>	108
5.2.4	<i>Transcranial magnetic stimulation and electromyographic recording</i>	109
5.2.5	<i>High frequency repetitive somatosensory stimulation</i>	110
5.2.6	<i>Statistical analysis</i>	111

5.3	Results.....	111
5.3.1	<i>Somatosensory temporal discrimination threshold.....</i>	<i>111</i>
5.3.2	<i>Somatosensory evoked potentials.....</i>	<i>112</i>
5.3.3	<i>Somatosensory evoked potentials recovery cycle.....</i>	<i>114</i>
5.3.4	<i>Somatosensory lateral inhibition.....</i>	<i>115</i>
5.3.5	<i>High frequency oscillations.....</i>	<i>116</i>
5.3.6	<i>Corticospinal excitability.....</i>	<i>116</i>
5.3.7	<i>Cortical inhibition in the motor system.....</i>	<i>117</i>
5.3.8	<i>Correlations.....</i>	<i>118</i>
5.4	Discussion.....	120
5.4.1	<i>Paradoxical effect of HF-RSS in patients with idiopathic cervical dystonia.....</i>	<i>120</i>
5.4.2	<i>Defective homeostatic plasticity in patients with idiopathic cervical dystonia.....</i>	<i>121</i>
5.4.3	<i>Limitations.....</i>	<i>123</i>
6	Defective inhibition and plasticity in the somatosensory System are not required to developed dystonia.....	124
6.1	Introduction.....	124
6.2	Materials and methods.....	125
6.2.1	<i>Statistical analysis.....</i>	<i>125</i>
6.3	Results.....	126
6.4	Discussion.....	133
7	Reversal of abnormal somatosensory temporal discrimination in cervical dystonia following low-frequency repetitive sensory stimulation.....	136
7.1	Introduction.....	136
7.2	Materials and methods.....	137
7.2.1	<i>Statistical analysis.....</i>	<i>137</i>

7.3	Results.....	138
7.4	Discussion.....	147
8	Amelioration of focal hand dystonia via low-frequency Repetitive somatosensory stimulation.....	149
8.1	Introduction.....	149
8.2	Materials and methods.....	150
8.2.1	<i>Patients and clinical evaluation.....</i>	<i>150</i>
8.2.2	<i>Hand motor function tasks.....</i>	<i>151</i>
8.2.3	<i>Electromyographic recording and transcranial magnetic stimulation.....</i>	<i>151</i>
8.2.4	<i>Somatosensory evoked potentials recording and analysis.....</i>	<i>154</i>
8.2.5	<i>Repetitive somatosensory stimulation.....</i>	<i>155</i>
8.2.6	<i>Experimental procedure.....</i>	<i>156</i>
8.2.7	<i>Statistical analysis.....</i>	<i>156</i>
8.3	Results.....	157
8.3.1	<i>Hand motor function tests and EMG activity during posture.....</i>	<i>163</i>
8.3.2	<i>Motor evoked potentials and short intracortical inhibition.....</i>	<i>164</i>
8.3.3	<i>Somatosensory evoked potentials.....</i>	<i>165</i>
8.3.4	<i>Correlations.....</i>	<i>170</i>
8.4	Discussion.....	172
8.4.1	<i>Effects of RSS on somatosensory function.....</i>	<i>172</i>
8.4.2	<i>Effects of RSS on motor function.....</i>	<i>173</i>
8.4.3	<i>Correlations and putative mechanisms underlying the effect of RSS.....</i>	<i>174</i>
8.5	Conclusions and limitations.....	166
9	General discussion.....	178
9.1	Evidence for defective inhibition in the somatosensory system in dystonia.....	179
9.2	Evidence for defective inhibitory plasticity in idiopathic dystonia.....	180
9.3	Low-frequency repetitive somatosensory stimulation as a means to ameliorate dystonia.....	181

9.4	Contribution of the present findings to the understanding of the pathophysiology of dystonia	182
9.5	Limitations and future perspectives.....	185
9.6	Conclusion.....	185
10	References.....	186

LIST OF FIGURES

FIGURE 1.1: synaptic interaction between neocortical neurons and pyramidal cells.....	26
FIGURE 1.2: main circuits involving cortical inhibitory interneurons.....	30
FIGURE 1.3: feedback inhibition motif.....	32
FIGURE 1.4: main upper limb SEP waveform and generators.....	40
FIGURE 1.5: paired pulse suppression of SEP at different interstimulus intervals.....	42
FIGURE 1.6: subtraction of single pulse SEP from paired-pulse SEP.....	43
FIGURE 1.7: SEP suppression by simultaneous stimulation of median and ulnar nerves.....	45
FIGURE 1.8: N20/P25 components of SEP and superimposed HFO.....	48
FIGURE 1.9: mechanics of STDT testing.....	49
FIGURE 1.10: correlation between STDT, PP-SEP and HFO.....	50
FIGURE 1.11: JVP domes.....	52
FIGURE 1.12: the bumps device.....	54
FIGURE 1.13: mechanisms underlying D and I waves generation.....	58
FIGURE 1.14: short intracortical inhibition.....	59
FIGURE 1.15: effects of SICI and Lorazepam on I waves.....	60
FIGURE 1.16: principles of plasticity induction.....	63
FIGURE 1.17: training-independent somatosensory learning.....	65
FIGURE 3.1: experimental protocol.....	81
FIGURE 3.2: example of PP-SEP and SIR.....	72
FIGURE 3.3: correlations between STDT, PP-SEP and I-HFO.....	82
FIGURE 4.1: STDT values obtained before and after HF-RSS.....	93
FIGURE 4.2: effects of HF-RSS on the latency and amplitude of SEP.....	94
FIGURE 4.3: effects of HF-RSS on PP-SEP.....	96
FIGURE 4.4: effects of HF-RSS on HFO area.....	97
FIGURE 4.5: effects of HF-RSS on TSD and TT.....	98
FIGURE 4.6: correlations between RSS-induced changes on STDT, R5 and I-HFO.....	99
FIGURE 4.7: effects of HF-RSS on SICI recorded from the APB.....	100

FIGURE 5.1: STDT values obtained from HC and CD patients before and after HF-RSS.....	112
FIGURE 5.2: effects of HF-RSS on PP-SEP in HC and CD patients.....	115
FIGURE 5.3: effects of HF-RSS on SICI recorded in HC and CD patients from APB, FDI and ADM.....	118
FIGURE 5.4: effects of HF-RSS on LICI recorded in HC and CD patients in the APB.....	119
FIGURE 5.5: correlations between HF-RSS-induced changes on STDT, R5 and IHFO.....	119
FIGURE 6.1: effects of HF-RSS in HC and SD patients on STDT, SEP amplitude and SICI.....	132
FIGURE 6.2: effects of HF-RSS in HC and SD patients on PP-SEP and SIR.....	133
FIGURE 7.1: effects of LF-RSS on STDT.....	144
FIGURE 7.2: effects of LF-RSS on PP-SEP, SIR and HFO.....	145
FIGURE 7.3: effects of LF-RSS on SICI recorded from the APB and ADM.....	146
FIGURE 7.4: correlations between LF-RSS-induced changes on STDT, R5 and l-HFO.....	147
FIGURE 8.1: effects of RSS on BBT, NHPT and RMS of EMG signal in FHD patients.....	164
FIGURE 8.2: effects of RSS on test MEP and SICI in FHD patients.....	165
FIGURE 8.3: examples of SEP obtained my muscle stimulation.....	166
FIGURE 8.4: effects of RSS on SEP latencies in FHD patients.....	167
FIGURE 8.5: effects of RSS on SEP amplitudes in FHD patients.....	168
FIGURE 8.6: effects of RSS on PP-SEP in FHD patients.....	169
FIGURE 8.7: effects of RSS on SIR in FHD patients.....	170
FIGURE 8.8: correlations between LF-RSS-induced changes in variables.....	171
FIGURE 9.1: graphical summary of the key findings of the PhD.....	183

LIST OF TABLES

TABLE 1.1: features of main components of the somatosensory evoked potential.....	36
TABLE 3.1: summary of clinical and electrophysiologic features in patients and healthy controls.....	78
TABLE 5.1: clinical details of CD patients.....	113
TABLE 5.2: values of variables related to the SEP.....	113
TABLE 5.3: data related to corticospinal excitability.....	117
TABLE 6.1: values related to demographic and clinical variables, thresholds and stimulation intensities in HC and SD patients.....	126
TABLE 6.2: raw values of variables unchanged by HF-RSS in HC and CD patients.....	127
TABLE 6.3: statistics relative to main effects and interactions of the ANOVAs.....	128
TABLE 7.1: values related to demographic and clinical variables, thresholds and stimulation intensities in HC and CD patients.....	138
TABLE 7.2: raw values of variables unchanged by LF-RSS in HC and CD patients.....	139
TABLE 7.3: statistics relative to main effects and interactions of the ANOVAs.....	140
TABLE 8.1: clinical and demographic variables of FHD patients.....	152
TABLE 8.2: effects of RSS on thresholds and stimulation intensities of FHD patients.....	157
TABLE 8.3: statistics relative to main effects and interactions of the ANOVAs.....	159
TABLE 9.1: overlap between healthy controls tested across different projects.....	178
TABLE 9.2: overlap between patients tested across different projects.....	179

LIST OF ABBREVIATIONS AND ACRONYMS

Abbreviation	Meaning
ADDS	Arm dystonia disability scale
ADM	Abductor digiti minimi
AMT	Active motor threshold
AMPA	α -amino-3-hydroxy-5-methyl-4-isoxazolepropionic acid
APB	Abductor pollicis brevis
BBT	Box and block test
BoNT	Botulinum toxin
CD	Cervical dystonia
CNS	Central nervous system
CS	Conditioning stimulus
cTBS	Continuous theta burst stimulation
DLPFC	Dorsolateral prefrontal cortex
DBS	Deep brain stimulation
EBCC	Eyeblink classical conditioning
EEG	Electroencephalography
EMG	Electromyography
e-HFO	Early high-frequency oscillations
FS	Fast-spiking
FDI	First dorsal interosseous
fMRI	Functional magnetic resonance imaging
FHD	Focal hand dystonia
GABA	γ -aminobutyric acid
GPe	External globus pallidus
GPi	Internal globus pallidus
ICF	Intracortical facilitation
HFO	High-frequency oscillations
HF-RSS	High-frequency repetitive somatosensory stimulation
HC	Healthy controls
IPSP	Inhibitory post-synaptic potential
ISI	Inter-stimulus interval
l-HFO	Late high-frequency oscillations

LF-RSS	Low-frequency repetitive somatosensory stimulation
LFas-RSS	Low-frequency asynchronous somatosensory stimulation
LICI	Long intracortical inhibition
LTD	Long-term depression
LTP	Long-term potentiation
MEG	Magnetoencephalography
M1	Primary motor area
MEP	Motor evoked potential
NHPT	Nine-hole peg test
NMDA	N-methyl-D-aspartate
PA	Posterior to anterior
PAS	Paired associative stimulation
PP-SEP	Paired-pulse somatosensory evoked potential
Pre-SMA	Pre-supplementary motor area
RA	Rapidly adapting
RMT	Resting motor threshold
RS	Regular spiking
RSS	Repetitive somatosensory stimulation
S1	Primary somatosensory area
S2	Secondary somatosensory area
SA	Slowly adapting
SD	Secondary dystonia
SEP	Somatosensory evoked potentials
SICI	Short intracortical inhibition
SIR	Spatial inhibition ratio
SMA	Supplementary motor area
STDP	Spike timing dependent plasticity
STDT	Somatosensory temporal discrimination threshold
STN	Subthalamic nucleus
TMS	Transcranial magnetic stimulation
TSD	Tactile spatial discrimination
TT	Tactile threshold
TWSTRS	Toronto western spasmodic torticollis rating scale
UDRS	Unified dystonia rating scale

1 Introduction

1.1 Overview of the subtypes of dystonic disorders and the known underlying pathophysiological mechanisms

Dystonia is a heterogeneous disorder with variable distribution, phenomenology and aetiology. According to the last criteria ¹, dystonia is classified along two axes: clinical characteristics and aetiology. The clinical characteristics fall into several specific dystonia syndromes that help to guide diagnosis and treatment, and include age at onset, body distribution, temporal pattern and associated features. According to the latter, dystonia is divided in “isolated” (where dystonia is the only motor feature, with the exception of tremor) and “combined” (where dystonia is associated with other movement disorders, such as myoclonus and parkinsonism). With regards to the aetiology, dystonia can be inherited (autosomal dominant and recessive, X-linked recessive, mitochondrial), acquired (due to a known, specific cause) or idiopathic (familial or sporadic).

To investigate the pathophysiology of dystonia, studies have mainly focused on isolated forms and their subtypes. Isolated dystonia is typically genetic or idiopathic and follows a characteristic pattern with regards to age at onset, sex and anatomical distribution. Isolated generalized dystonia manifests in childhood or adolescence and, generally, has no sex predilection. Conversely, focal dystonia normally start in the fourth-sixth decade of life, with a male predominance in task-specific upper limb dystonia (i.e. writer’s cramp, musician dystonia), and female predominance in cervical dystonia, spasmodic dysphonia, blepharospasm and oromandibular dystonia (or a combination of the last two, called Meige syndrome) ². Generalized dystonia is often genetic, and most commonly due to *TOR1A* and *THAP1* gene mutations, respectively causing DYT1 and DYT6. Cervical dystonia is the most common adult-onset dystonia, followed by task-specific upper limb dystonia. Most of the studies aiming to elucidate the pathophysiology of dystonia are based on data collected in cervical dystonia, task-specific upper limb dystonia, DYT1 and DYT6.

The anatomical basis for dystonia has been debated for years, and is still not completely understood. Almost 30 years ago, David Marsden recognized dystonia as a basal ganglia disorder, based on the observation of dystonic patterns in the context of damage to the basal ganglia. According to the first model proposed to explain the involvement of basal ganglia in dystonia, the direct pathway is hyperfunctional, while the indirect one is hypofunctional, as a

consequence of reduced activity along the putamen-external globus pallidus (GPe) connections and increased inhibition of the subthalamic nucleus (STN) and internal globus pallidus (GPi) by the GPe; these abnormalities would result in reduced inhibition of the thalamus and increased excitation of the cortex^{3,4}. Single-cell recording in dystonic patients undergoing functional neurosurgery demonstrated several abnormalities in the activity of GPe and GPi neurons, consisting in decreased discharge rate⁵ and overall irregular firing^{6,7}. These changes contribute to dystonia, as confirmed by the fact that deep brain stimulation (DBS) improves it by restoring more physiological firing patterns in the GPi⁸. Another electrophysiological abnormality in the basal ganglia of dystonic patients is represented by an excess of synchronized low-frequency (4-10 Hz) activity⁹. It is to note that a decrease in basal ganglia output in dystonia has not always been confirmed¹⁰, likely due to the different dystonia phenotypes studied; it has been proposed that the final common pathway linking the different forms of dystonia needs to be found in cortical processing¹¹. The basal ganglia are, indeed, part of a group of parallel closed circuits that originate in the cerebral cortex, traverse the thalamus, and then project back to the cortical areas of origin³. Cortical motor areas are one of the primary projection target of the basal ganglia (i.e. the motor loop) and their involvement in dystonia have been largely investigated.

Three are the main abnormalities that have been associated with the pathophysiology of dystonia at the cortical level: loss of inhibition, alterations of synaptic plasticity and sensory dysfunction (the latter reviewed in the following paragraph)¹². Reduced inhibition in the motor cortex, spinal cord¹³ and brainstem¹⁴, has been demonstrated in dystonia¹⁵⁻¹⁷. Regarding the motor cortex, in the pioneering study of Ridding et al. (1995)¹⁵, dystonic patients showed significant less inhibition compared to healthy controls when tested by means of short-interval intracortical inhibition (SICI), a transcranial magnetic stimulation (TMS) paradigm which investigates γ -aminobutyric acid-a (GABA_A) receptors function¹⁸. Later studies strengthened this result and showed that reduced intracortical inhibition not only contributes to dystonia, but also predispose to its development¹⁶. Reduced SICI is a common finding in most forms of idiopathic dystonia¹⁹⁻²¹, but also in dopa-responsive-dystonia²², asymptomatic carriers of the DYT1 gene mutation¹⁶, in the affected side of patients with secondary dystonia²³ and also in functional dystonia^{24,25}. Despite the impressive number of papers that report reduced SICI in dystonia, several others have found it to be within the normal range^{23,26-29}. Some discrepancies between studies could be due to the large inter-individual variability of SICI^{30,31} as well as subtle methodological differences. Nevertheless, despite its reduction, the role played by SICI

in dystonia is still not completely clear, but it is possible that it predisposes to the development of a dystonic phenotype and that additional factors (for instance genetic or psychological) are needed to develop the symptoms^{12, 16}. Some authors claim that another possible factor determining the development of dystonia in people with reduced SICI is the susceptibility to plastic change³².

Abnormal synaptic plasticity in the motor cortex seems to be the key mechanism that underlies the development of dystonia. As a matter of fact, while other electrophysiological measures (like intracortical inhibition and sensory abnormalities) are similarly abnormal in manifesting and non-manifesting individuals with inherited primary dystonia (DYT1), susceptibility to plastic change in response to TMS appears to differentiate such individuals³². Spike-timing dependent plasticity has often been reported to be enhanced in dystonia, compared to healthy subjects^{23, 33-35}. However, this result has not been confirmed in all studies³⁶⁻³⁸. This variable response to plasticity protocols is also seen in healthy subjects, but it might be possible that the different forms of dystonia (focal and generalized) involve diverse pathophysiological mechanisms, with plasticity having a variable contribution to each¹².

Reports of cerebellar lesions causing dystonia have raised the question of a cerebellar involvement in its pathophysiology and encouraged researcher to investigate it further. Associative motor learning, investigated through the eyeblink classic conditioning (EBCC), related to the integrity of the olivo-cerebellar circuit, is impaired in patients with primary focal dystonia^{23, 39}, but it is normal in patients with generalised and segmental inherited dystonia caused respectively by DYT1 and DYT6 gene mutation⁴⁰. This discrepancy might suggest that the cerebellar contribution differs according to the form of dystonia, or that EBCC abnormalities segregate with the presence of dystonic tremor⁴¹. However, this form of learning represents only part of the computation usually performed by the cerebellum, and a normal EBCC might not necessarily reflect a normal cerebellar physiology from a more general perspective⁴⁰.

Taken together, this body of evidence suggests that dystonia does not result from dysfunction of a single brain region, but most likely from the dysfunction of a network⁴². This explains why it is so difficult to identify a single pathological locus in dystonia and is in line with evidence that secondary dystonia can be caused by lesions in basal ganglia, as well as other structures, in particular the thalamus, brainstem and cerebellum. The network model posits that all subtypes of dystonia result from a network disorder that includes the basal

ganglia, cerebellum, thalamus, and sensorimotor cortex; however, the precise role and the relevance of each component have not yet been elucidated. According to the model, dystonia can be produced by a single or multiple nodes dysfunction, in addition to an abnormal interplay among the nodes ⁴². It is therefore plausible that the various forms of dystonia (e.g. focal, generalised, and task-specific) reflect derangement at different levels of the network. This might explain the incongruent results among studies investigating patients with different clinical manifestations.

1.2 Treatment options for dystonia

The concept that different dystonias may have different neuroanatomical substrates ⁴³ and pathophysiology ⁴⁴ has also an impact on the treatment strategies and their outcomes ⁴⁵⁻⁴⁷. The treatment of dystonia is only symptomatic, and it is based on three main approaches: pharmacological treatment (drugs), local treatment (Botulinum toxin injections) and surgery. The appropriate therapy is selected on the basis of distribution, severity of the dystonia and other factors (such as side effects, age, etc.). In general, botulinum toxin is the initial treatment of choice for patients with focal or segmental dystonia, whereas generalized dystonia is typically treated pharmacologically or surgically.

Botulinum toxins used for dystonia treatment (BoNT) are synthetic derivatives of naturally occurring toxins made by the bacterium *Clostridium botulinum*. Seven serotypes are known, and two have been developed as therapeutics, serotypes A and B. The most commonly available formulations of serotype A include abobotulinumtoxinA (Dysport), incobotulinumtoxinA (Xeomin), and onabotulinumtoxinA (Botox). Serotype B is available as rimabotulinumtoxinB (Myobloc). Each serotype is made of a heavy and light chain; the heavy chain binds to peripheral cholinergic nerve terminals and facilitates endocytosis of BoNT, following which the light chain is released into the cytoplasm and cleaves the soluble N-ethylmaleimide-sensitive factor attachment protein that is required for synaptic transmission (specifically, for the fusion of the acetylcholine-containing synaptic vesicle with the presynaptic membrane) ⁴⁸. BoNT therefore works reducing the release of acetylcholine at the neuromuscular junction level and, consequently, muscle activity related to abnormal movements. BoNT, administered directly into dystonic muscles, has been used for the treatment of nearly all forms of focal and segmental dystonia. The clinical benefit can be observed within a few days and usually persists for 3–4 months, after which the injection is

repeated. The most common adverse effects of BoNT is transient, focal focal muscle weakness at the injection site or surrounding muscles.

Although evidence-based reviews have been published ^{49, 50}, none of the available agents for dystonia has been tested in rigorously controlled clinical trials. The most commonly symptomatic drugs useful for many types of dystonia are anticholinergics and antispastic drugs. Anticholinergics are most effective for the treatment of generalized and segmental dystonia, rather than focal dystonia. Among oral anticholinergics, trihexyphenidyl is the most commonly used, especially in children. Its side effects include blurry vision, dry mouth, urinary retention, constipation and cognitive impairment. Antispastic agents include baclofen, tizanidine and benzodiazepines. They are used by 5% to 10% of adults and 40% to 50% of children with dystonia ⁵¹. Baclofen, a GABAB agonist, is popular in childhood, when there is coexisting spasticity, such as in cerebral palsy, but also for the treatment of oromandibular dystonia. According to in an international cross-sectional study, benzodiazepines are the most commonly used oral treatment of all types of isolated dystonia ⁵². These drugs act as muscles relaxants and have an important role in the off-label treatment of dystonia, although their usefulness is limited by potential adverse effects such as drowsiness and addiction. Levodopa is the treatment of choice for dopa-responsive dystonias, a group of dystonias caused by dopamine biosynthesis pathways deficit.

Surgical options are grouped here into two main categories, namely DBS and ablative procedures. DBS has emerged as the most effective therapy for patients with medically refractory and disabling dystonia, both generalized or focal and segmental. The two main target of stimulation are the GPi and the STN. Aetiology plays an important role in predicting outcomes, which are reliably good for some causes and consistently poor for others. For instance, DYT1 has a very good response to DBS, while in DYT6 the response is less predictable ⁵³. Good outcomes can also be expected for some combined dystonia syndromes such as myoclonus-dystonia or dystonia secondary to tardive syndromes. Dysarthria is the most frequent complication associated with GPi DBS, but parkinsonism has been observed in some patients ⁵⁴. The most common adverse effect with STN DBS is chorea ⁵⁵. Other stimulation-related adverse events related to GPi or STN DBS include incoordination, paresthesias and perioral tingling, whereas the most frequently reported hardware-related complications are infection, haematomas and wire displacement ⁵⁶. Before DBS, pallidotomy and thalamotomy were commonly used for the treatment of dystonia. These procedures, albeit less commonly

used, may be preferable to DBS in some circumstances, such as task-specific dystonias of the upper limb, since they can give permanent result with few apparent side effects ⁵⁷.

1.3 Somatosensory temporal discrimination abnormalities in dystonia

Epidemiological and clinical studies have reported that patients with focal dystonias occasionally complain of sensory symptoms. These usually include ill-defined pain, discomfort, distortion of sensory modalities and ‘phantom’ kinetic or postural sensations in the affected region ⁵⁸. One of the most robust alteration in the somatosensory domain found in dystonic patients is abnormally high STDT. The STDT is altered in patients with blepharospasm ⁵⁹⁻⁶¹, with increased values being observed in the affected body part (face) and unaffected body parts (neck and hand) ^{60, 61}. STDT values have also been reported to be abnormal in patients with increased blinking ⁶², a prodromal form of blepharospasm. One study showed that patients with increased blinking who had altered STDT values at baseline developed orbicularis oculi muscle spasms during a 5-year follow-up period ⁶³. Several research groups have investigated the STDT in patients with cervical dystonia (CD) ^{59, 61, 64-69}. Although most studies reported altered STDT in this patient population, two reported normal values ^{65, 66}. A convincing body of evidence also indicates that the STDT is abnormal in unaffected first-degree relatives of patients with sporadic or familial CD ⁷⁰⁻⁷². When compared with relatives with a normal STDT, unaffected relatives with an abnormal STDT had larger putaminal volumes, as demonstrated by voxel-based morphometry ⁷¹, and displayed reduced putaminal activity when performing a temporal discrimination task during functional magnetic resonance imaging (fMRI) ⁷². STDT values seem to be unaffected by therapeutic strategies for CD (BoNT and DBS) ^{68, 73}. Patients with focal hand dystonia (FHD) also display higher STDT values than healthy individuals ^{61, 74}. Only two studies have compared the extent of STDT abnormalities among the various types of focal dystonia ^{59, 61}, and they found no significant differences. Repetitive transcranial magnetic stimulation (TMS) to modulate the activity in the primary somatosensory area (S1) failed to normalize STDT values in patients with FHD ⁷⁴.

A number of conclusions can be drawn by these data. The observation that the degree of STDT increase does not differ between patients with blepharospasm and with CD, which have different ages at onset ^{59, 61}, suggests that age-related effects become negligible when a dystonic trait is present. Several lines of evidence indicate that increased STDT represents a

mediational endophenotype that makes individuals susceptible to the development of dystonia⁷⁵. First, increased STDT values are present before dystonic symptoms become manifest^{62, 63} and are also observed in unaffected relatives of patients with dystonia⁷⁵. Second, the values do not correlate with disease severity^{61, 71} and remain unchanged over time⁷⁶. Last, STDT values are similarly altered in patients with generalized dystonia⁷⁷ and patients with focal dystonias^{61, 73, 78}. Therefore, mechanisms underlying abnormal temporal processing of tactile input might predispose individuals to motor symptoms. Overall, a link between dystonia and derangement of inhibitory mechanisms within S1 has been established in the literature; however, it has not been investigated whether interventional protocols aimed at restoring these mechanisms can be useful to treat dystonia as well. Dystonia has recently been construed as a network disorders, the somatosensory system being one of the dysfunctional nodes⁷⁹. Even if not directly linked to motor symptoms, it might be possible that an improvement in the balance between excitation and inhibition in one of the nodes (i.e. the somatosensory system) would result in a more physiological activity in the whole brain network involved in dystonia. The next section introduces the basic inhibitory mechanisms in the nervous system, since most of this work is based on the application of translational electrophysiological methods to study inhibition in the intact human.

1.4 An introduction to inhibition in the nervous system

Inhibition was established as an active process in neural computation in the early 20th century by Sherrington. In the brain, inhibition is mostly mediated by a neurotransmitter called GABA. Since the early days of study, it was clear that only some neurons (about 20% of all cortical neurons) contained this neurotransmitter at their synaptic terminals; hence, these were called inhibitory interneurons. In time, many morphologically distinct types of interneurons have been described; despite some differences, they all share some similarities, i.e. a distinctive short axon and local connections with the pyramidal neurons which, in turn, send projections to other cortical and subcortical structures. Despite a large number of morphological and electrophysiological studies, the role of cortical inhibition in the representation of behavioural information and in the shaping of action is still largely unknown. This lack of integration between the information generated from microcircuits analysis and system neurophysiology is mostly due to methodological problems, such as the lack of definite, global signatures of inhibitory interneuronal activity in behaving, complex organisms⁸⁰. However, some general

information about the organization of inhibitory interneurons in the cortex, as well as examples about how their activity can influence behaviour, can be given here.

It is useful to introduce the concept of neural microcircuit, defined as the minimal number of interacting neurons that can collectively produce a functional output ⁸¹ (figure 1.1). These microcircuits are usually referred to as cortical columns, i.e. vertical assemblies of highly interconnected neurons spanning cortical layers II – VI, and they are especially well characterized in primary sensory cortices ^{82, 83}. Despite the fact that the concept of a cortex consisting of repetitions of the same fundamental microcircuit has been questioned due to the variable size and cell composition of the columns ^{84, 85}, it is well known that neurons in the same columns share similar functional properties ^{86, 87}.

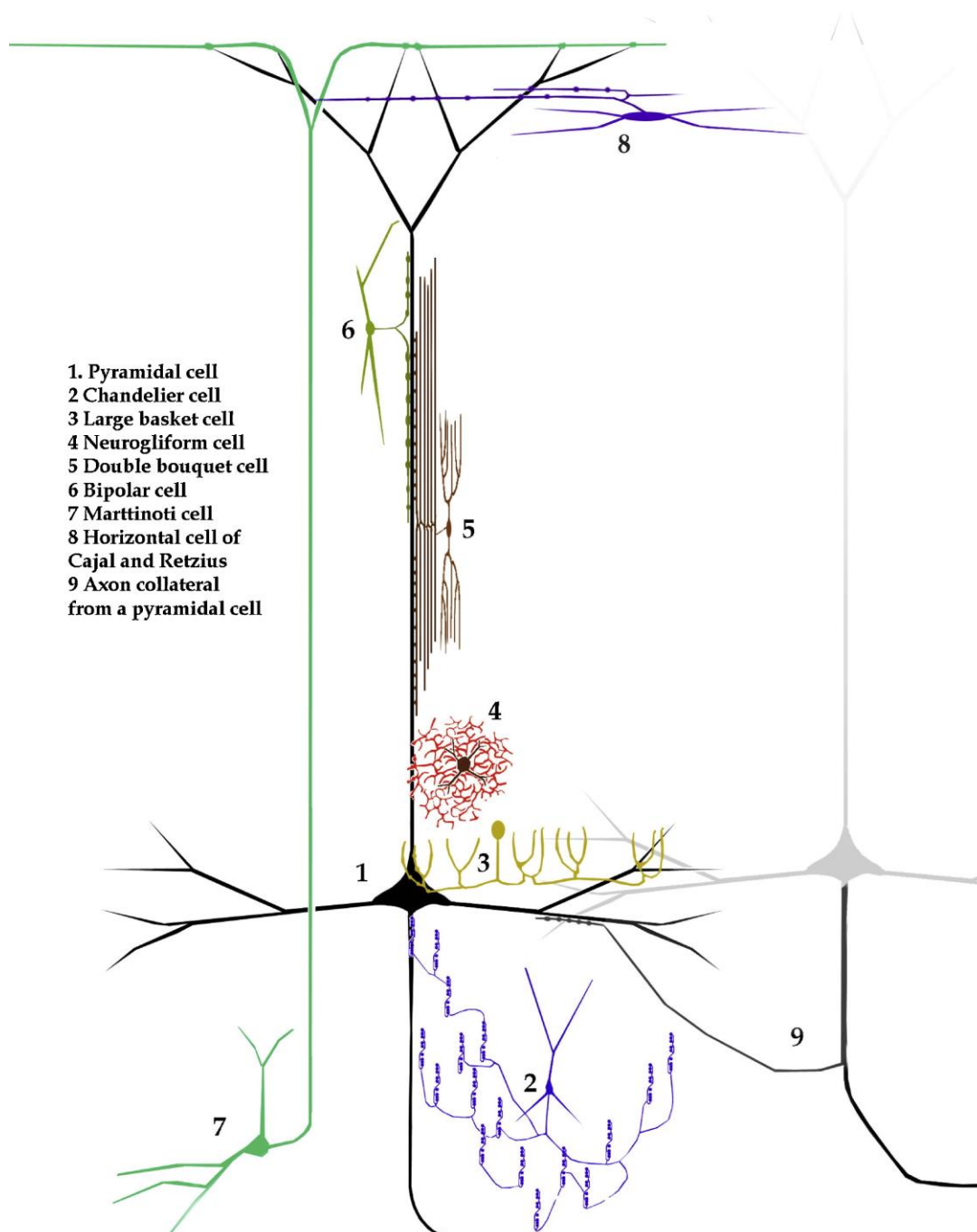


Figure 1.1: synaptic interactions between neocortical interneurons and pyramidal cells (black and grey). Inhibitory neurons are depicted according to the region of the pyramidal cell where their axon establishes the main contact (adapted from Merchant et al., 2012).

Whereas columnar organization represents the anatomical substrate for cortical computation, tuning of cellular activity to motor, sensory and cognitive information is considered the building block of cortical physiology. Cell tuning depends on anatomically precise convergence of inputs and microcircuit dynamics; these two factors not only vary between

cortical areas, but even between layers inside a column. Thus, cell tuning can show a columnar organization accompanied by a tangential mapping of the behavioural variable. These three features (tuning, columns, and maps) are closely interrelated and largely depend on inhibitory mechanisms.

It is intuitive that sculpting cortical activity needs to rely on very precise timing. Mountcastle was the first ⁸⁸ to suggest that cortical neurons could be segregated into regular-spiking (RS) and fast-spiking (FS) cells in the awake monkey. FS cells were subsequently shown to correspond mainly to multipolar parvalbumin-positive basket and chandelier cells, whereas RS correspond to pyramidal neurons ^{89, 90}. FS interneurons generate short-duration action potentials and are capable of discharging at high frequencies with little spike frequency adaptation; their role in sculpting excitatory cortical activity has been reported in several cortical areas, such as the primary auditory cortex ⁹¹, the inferior temporal cortex ⁹², the frontal eye field ⁹³, the primary motor area (M1) ⁹⁴⁻⁹⁶, the dorsal premotor cortex ⁹⁷ and the posterior parietal cortex ⁹⁸. The relationship between activity of FS interneurons and some behavioural variables has been characterized in the visual system in an interesting series of experiments. It has been observed that the firing rate of FS interneurons in area V4 increases in parallel with allocation of attentional resources during a visual task, together with a reduction in response variability ⁹⁹. It is possible that, in this context, the increase in inhibitory activity is able to suppress neural responses evoked by distracter stimuli and to initiate the characteristic high-frequency synchronization during attentive periods. The same modulation of discharge pattern from FS interneurons has been demonstrated also in the primary visual area; interestingly, pyramidal neurons showed an opposite behaviour, i.e. their responses were suppressed during periods of increased attention ¹⁰⁰. These data are important to underline that activity from FS interneurons and RS pyramidal cells can be dissociated. Further proving this point, recent studies using optogenetics have shown that activation of FS interneurons, but not RS pyramidal cells, induces gamma band oscillation and enhances signal transmission in the cortical microcircuitry ^{101, 102}. A further interesting point concerns the promotion of information transmission by activation of interneurons. Experiments involving multiple-site recording have shown an increase in synchrony between pairs of inhibitory, but not pyramidal, cells in M1 after tactile stimulation ⁹⁶ and in the prefrontal motor cortex of the monkey during a memory-guided saccade task ¹⁰³.

Overall, these studies highlight the importance of studying inhibitory interneurons to investigate cortical activity during presentation of various stimuli, information processing and complex behaviour. A more thorough description of the role of inhibitory interneurons in the motor and

somatosensory systems, which are the focus of the present investigation, follows, together with details on some neurophysiological techniques which can be used to study somatosensory and motor inhibition in the intact human.

1.5 Inhibition in the primary somatosensory cortex

It is important, in the present context, to give some background about basic physiology of thalamic input to S1, and in particular to inhibitory interneurons. Most studies so far focused on thalamocortical projections from primary sensory thalamic nuclei that carry information from the sensory organs to the cortex. Thalamocortical afferents directly target both pyramidal cells and FS inhibitory interneurons, the latter located in the in the principal input layers of S1 and often expressing the calcium binding protein parvalbumin^{104, 105}. Depending on the target region, inputs onto FS neurons activate both α -amino-3-hydroxy-5-methyl-4-isoxazolepropionic acid (AMPA) and N-methyl-D-aspartate (NMDA) receptors¹⁰⁶, or drive primarily AMPA receptors¹⁰⁴. The composition of postsynaptic receptors directly affects kinetics and short-term dynamics of synaptic responses¹⁰⁴. Thalamocortical inputs onto inhibitory neurons are plastic, and inputs to distinct groups of inhibitory neurons can be differentially affected by changes in sensory experience¹⁰⁷. All these factors influence how inhibitory circuits are engaged by incoming activity and may provide specificity on how distinct groups of neurons exert their function.

Afferent inputs can activate inhibitory neurons above threshold for action potentials leading to the release of GABA, the primary inhibitory neurotransmitter in the central nervous system. Many factors can determine how activation of GABAergic inhibition will affect local cortical circuits. Type, laminar location and pattern of connectivity of specific populations of inhibitory interneurons determine the subcellular location targeted by the GABAergic axon¹⁰⁸. Firing patterns of inhibitory interneurons in response to incoming stimuli and the organization of presynaptic release sites of inhibitory synapses determine how much GABA will be released. Many other factors, including uptake and degradation mechanisms, and expression of membrane transporters will control the duration of the signal. Once released, the effect of GABA on postsynaptic neurons depends on the properties of the receptor that binds it. GABA can modulate neuronal excitability through a variety of mechanisms depending on whether receptors are ionotropic (GABA-A), mediating the opening of an anion channel, or metabotropic (GABA-B), activating a G-protein-dependent signalling cascade¹⁰⁹. This distinction determines timing and duration of GABA signalling. Lastly, the location of GABA

receptors - presynaptic, postsynaptic or extrasynaptic ¹¹⁰ - will influence the role of inhibition. The effect of inhibition on cortical circuits is often viewed as a shift in circuit excitability, by modulation of action potentials generation. Indeed, GABAergic inhibition affects the capacity of a postsynaptic neuron to fire by hyperpolarizing the membrane potential ¹¹¹, or by shunting its depolarization ¹¹². These factors likely contribute to shaping the tuning of neuronal response curves and to modulating input/output functions and can limit the propagation of signals in the circuit ¹¹³.

Activation of FS inhibitory interneurons may influence the activity of cortical excitatory neurons through a number of different pathways. As FS interneurons contact the perisomatic region of pyramidal neurons ¹¹⁴, they can impair the ability of the postsynaptic neurons to fire action potentials. Based on circuits characteristics, two main types of inhibition are recognized in S1: feedforward inhibition and feedback inhibition (figure 1.2). Feedforward inhibition is the process by which an afferent excitatory input source, in addition to contacting principal neurons, also synapses onto local inhibitory neurons, which in turn provide inhibition to the principal cells receiving the excitatory input. In most cases, feedforward inhibition is mediated by FS basket cells. The involvement of perisomatic targeting neurons, in combination with their intrinsic properties enabling high speed and temporal fidelity, provides unique high pass filtering properties to these feedforward inhibitory circuits, imposing coincidence detection onto postsynaptic neurons. Crucial for thalamocortical transformation and by extension sensory processing in neocortex, this microcircuit involves layer 4 primary sensory thalamic afferents, layer 4 pyramidal cells projecting locally and to other layers, and local FS basket interneurons.

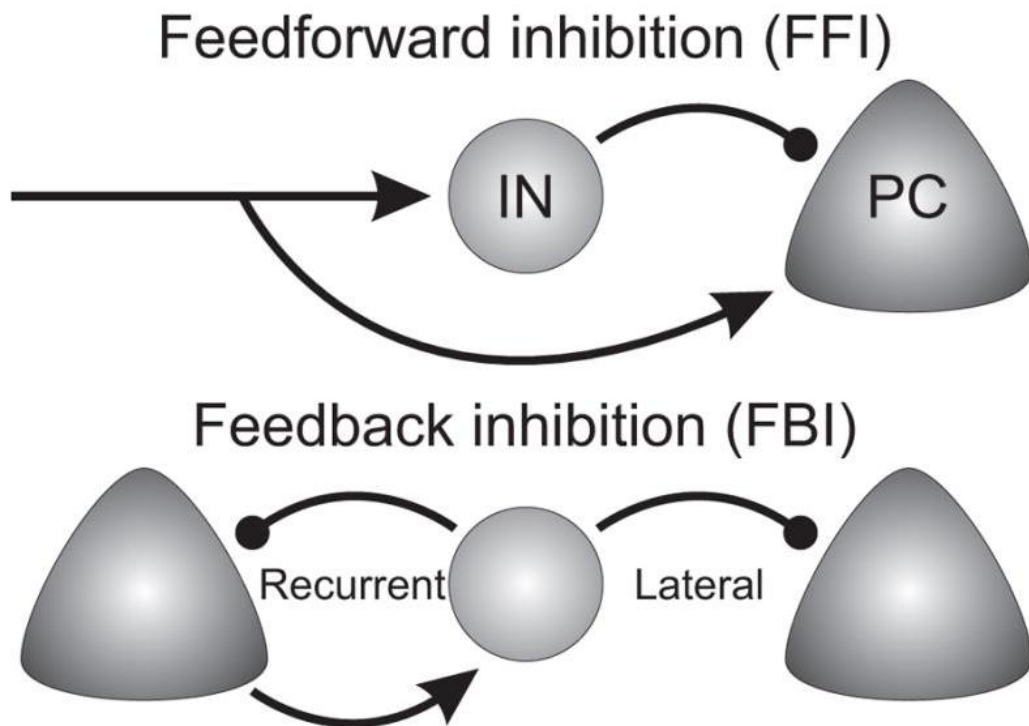


Figure 1.2: main circuits involving cortical inhibitory interneurons. In feedforward inhibition (top), an external source makes excitatory synapses (arrows) onto both local principal cells and interneurons. Interneurons in turn provide inhibitory inputs (black dot) to principal cells. Feedback inhibition (bottom) occurs when the source of excitation is local. Interneurons can in turn make inhibitory synapses on the local principal cells that provided the excitation (recurrent) or other neighbouring principal cells that did not participate in the recruitment of the interneurons (lateral) (adapted from Tremblay et al., 2016).

Unitary thalamocortical connections onto FS inhibitory interneurons are faster and fourfold stronger than those onto the pyramidal cells¹¹⁵⁻¹¹⁷, due to high quantal amplitude with calcium permeable AMPA receptors¹¹⁸ and multiple synaptic contacts forming clusters of neurotransmitter release sites¹¹⁹. As a result of these synaptic specialization, very few inputs are required to drive FS interneurons, which in turn form strong, perisomatic GABAergic synapses onto pyramidal cells, resulting in a powerful disynaptic feedforward inhibition of these neurons. Because inhibition of pyramidal cells by FS inhibitory interneurons is delayed by one synapse, disynaptic feedforward inhibition of pyramidal cells lags behind their monosynaptic thalamocortical excitation by few ms, creating a limited temporal “window of opportunity” for pyramidal cells to summate afferent inputs that will bring them to fire and transduce somatosensory signals^{116, 120-123}. As a result of this circuit, cortical pyramidal cells in S1 act as coincidence detectors of thalamic input and improve the sensitivity of cortical

neurons to the temporal distribution of thalamic spiking activity^{121, 124-127}. Therefore, this mechanism allows cortical neurons in layer IV to encode the temporal features of somatosensory inputs and produce cortical responses that more precisely represent the timing of sensory input^{116, 128}. Modulation of the feedforward inhibitory circuit and the window of opportunity has been shown to be of functional relevance. Upon repetitive thalamic firing, stimulus adaptation occurs, as input from thalamic relay neurons to FS inhibitory interneurons decreases. Inputs to FS inhibitory interneurons changes more than those to pyramidal cells; this results in a decreased fidelity in the recruitment of inhibitory interneurons and a widening of the temporal window of opportunity of pyramidal cells following repetitive stimulation¹¹⁶.

In contrast to the feedforward inhibition circuit motif, where the source of excitation of inhibitory interneurons originates from incoming external excitatory afferent axons, in feedback inhibition the source of excitation is locally generated and interneurons synapse back to the local pyramidal cells population (figure 1.2). The feedback action from interneurons then reduces or prevents further discharges of the excitatory cells. While feedforward inhibition is an incoming input tracking circuit mechanism and does not depend on local activity level, feedback inhibition is the opposite, i.e. a circuit mechanism tracking the local outputs that are being generated. Given the divergence of interneuron connectivity, any given interneuron will inhibit not only pyramidal cells from which it received excitation but also others that are part of the local population. This is due to the fact that interneurons generally show dense local connectivity^{129, 130}. In addition, some cortical interneurons have axons that extend beyond the local area where their soma is located, which can be in a transcolumar and/or translaminar fashion^{131, 132}. Thus, interneurons can provide inhibition to neighbouring populations of principal cells located at a certain distance that may not have provided excitation to that particular interneuron population, a phenomenon more generally referred to as lateral inhibition (figure 1.3). In lateral inhibition, a population of pyramidal cells receives feedback inhibition from interneurons that did not received excitation from this population, regardless if the pyramidal cells are within or flanking the cells driving the interneurons which provide feedback.

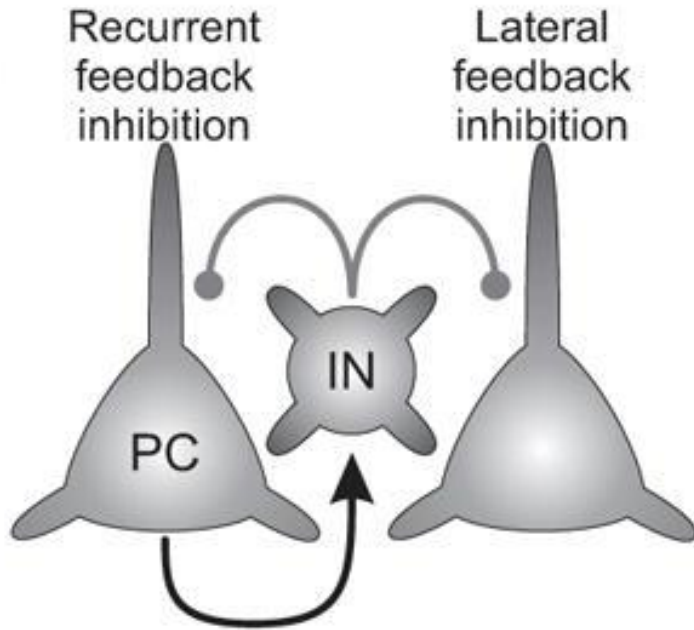


Figure 1.3: *feedback inhibition motif, encompassing both recurrent and lateral feedback inhibition (adapted from Tremblay et al., 2016).*

These different forms that feedback inhibition encompasses have been proposed to participate in important phenomena such as surround suppression ¹³³.

1.6 Assessing inhibition in the human somatosensory system

1.6.1 Introduction to the somatosensory evoked potential

Somatosensory evoked potentials (SEP) are time-locked potentials evoked by electrical stimulation of the sensory or mixed peripheral nerves and recorded along the large fibre somatosensory (dorsal column–medial lemniscus) pathway. Usually, the recorded potentials are of small amplitude and thus require averaging and amplification during the recording. The electrical stimulation applied over peripheral nerves elicits predictable SEP of certain values (amplitude and latency) based on the recording montages used. In the upper extremities median and ulnar SEP are frequently recorded, while in the lower extremities posterior tibial and peroneal SEP are commonly used. Contributions from muscle afferents produce recordings of higher amplitude and shorter latency while generating action potentials that are propagated along the somatosensory pathway and lead to sequential activation of the sensory relay stations.

1.6.1.1 Somatosensory pathways involved in the generation of the somatosensory evoked potential

The somatosensory system consists of two major parts: the dorsal column–lemniscal system and the spinothalamic system. The dorsal column–lemniscal system subserves mechanoreception (tactile object recognition, localization of skin contact, detection of vibration and texture) and proprioception (joint position, movement and force). The spinothalamic tract system subserves thermoreception, nociception and visceroreception. Each of the two systems can be divided into four neuronal populations. The somata of the first-order neuron are situated in the dorsal root ganglia, the trigeminal ganglion, the midbrain trigeminal nucleus and the vagal ganglion nodosum. The second-order neuron lies in the dorsal column nuclei (lemniscal system) or the dorsal horn of the spinal cord (spinothalamic tract system); axons of the second neuron cross the midline. Both systems project to the ventroposterior nuclei of the thalamus (third-order neuron) and from there into the network of somatosensory cortex areas, which include S1 and the secondary somatosensory cortex (S2), posterior parietal cortex, posterior and mid-insula and mid-cingulate cortex. Besides these two main systems, other pathways have been suggested to be involved in mediating somatosensory functions, such as the dorsal spinocerebellar tract (lower limb proprioception), postsynaptic dorsal column pathway (pelvic organ pain), and vagus nerve (non-painful visceral percepts). It should be kept in mind that the standard SEP techniques only assess function of the dorsal column–lemniscal system.

Primary afferent nerve fibres that project into the lemniscal system are of large diameter and myelinated (groups I and II, or Aa and Ab) with conduction velocities of 30–80 m/s. Their peripheral terminals are corpuscular nerve endings in the skin, joint capsule and muscle. These afferents have the lowest threshold for electrical stimulation and hence are preferentially activated. Since electrical stimulation directly excites the axons, deficits of the transduction process in the nerve terminals are not assessed by SEPs. The large afferent fibres are the first to be blocked or damaged by nerve compression. The central axon branches of the first neuron travel a long distance in the ipsilateral dorsal column pathways until they reach the second neuron in the dorsal column nuclei of the lower brainstem. Axons of the second neuron cross the midline and project as medial lemniscus to the ventroposterior thalamus. Fibres in the medial lemniscus reach the ventroposterior thalamus, which in turn projects to S1. Within S1, Brodmann areas 3b and 1 mainly receive mechanoreceptive inputs from the skin, whereas areas 3a and 2 mainly receive proprioceptive inputs. Tactile object recognition starts with simple

feature extraction in S1 (detection of edges, line orientation and movement direction). Object recognition continues in a ventral stream directed towards the S32 in the parietal operculum and further into the insula; these regions receive bilateral input. Stimulus location is further processed in a dorsal stream comprising Brodmann areas 5 and 7 in the posterior parietal cortex. The distinction of dorsal and ventral streams in the somatosensory system is comparable to that in the visual system, the ventral stream being mostly involved in tactile object recognition and the dorsal one in somatosensory–visual integration.

1.6.1.2 Electrophysiological properties of somatosensory evoked potentials

A traveling potential created by electrical stimulation passes along the pathway and SEP responses are recorded from locations where the signal changes direction or reaches a subsequent generator. All changes in direction of the traveling signal are reflected by peaks that are predictable, relatively steady, and reproducible. These individual peaks are named based on their latency after the stimulus and by their polarity. By convention, the recording arrangements are such that upward deflections reflect negativity (labeled N) of the potential at the active electrode and downward deflections reflect positivity (P). Polarity is determined by the recording montage used: a cephalic bipolar montage in which both electrodes are active and placed on the head, or a referential montage in which an inactive reference electrode is placed at a non-cephalic site. The number following N or P refers to the average latency at which this particular potential is recorded in normal subjects. For example, N9 potential of the median nerve SEP is a negative peak that typically occurs at 9 ms latency. However, peak nomenclature has not been standardized and numbers used to identify the same evoked potentials may differ slightly from laboratory to laboratory. SEP are considered short-latency potentials, occurring in the first 30 ms after stimulation of upper-limb mixed nerves and within 50 ms after stimulation of lower-limb mixed nerves. By comparison, long-latency SEP waveforms occur after 100 ms following stimulation, and mid-latency SEP potentials occur between short- and long-latency values ¹³⁴.

A combination of bipolar and referential recording montages is used for SEP recordings. In a bipolar montage, both recording electrodes are electrically active. The waveforms that are common to both closely spaced electrodes are cancelled by the differential amplifier (common-mode rejection) and only the remaining waveforms are displayed. In a referential montage, the inactive electrode should be placed far enough from the generator to be electrically silent and is usually noncephalic (e.g., on the opposite mastoid, shoulder, arm, hand, or knee; linked mastoids or ear lobes also may be used). The larger the distance between

the electrodes, the higher the likelihood of introducing unwanted noise to the recording, especially muscle artefact that may obscure smaller potentials. Both bipolar and referential montages are usually required for recording SEP in order to obtain the most accurate and comprehensive recordings. The obtained signal is composed of so called near-field and far-field potentials, based on the montage used. It is important to highlight the difference between these two types of potentials, as they will both be used in the present work. Near-field potentials are recorded from electrodes close to the generator site, such as the peripheral nerve, spinal cord, or cerebral cortex, and have a narrow recording distribution. These potentials are characteristically of negative polarity (e.g. the cortical N20), of relatively large amplitude, and sensitive to electrode placement. Cortical near-field potentials are best recorded with a bipolar cephalic derivation. Their amplitude decreases as the recording electrode is moved away from the generator source. These potentials, sometimes described as traveling waves, are usually triphasic with a large negativity preceded and followed by a smaller positivity. The initial positivity occurs as the propagated potential approaches the recording electrode. The large negativity occurs as the potential passes beneath the recording electrode, and the final small positivity occurs due to repolarization as the potential moves on from the electrode. Far-field potential waveforms are generated distant from the recording electrodes and have a broad distribution. The amplitude of the recorded potential is less sensitive to the recording site relative to the generator source. These potentials are usually of small amplitude, are best seen in referential montages, and are related to a change in shape or size of the volume conductor through which the impulses travel to reach the recording electrode. Specific volume conductors include the extremity tested, the spine/brain tissue, or the cerebrospinal fluid ¹³⁵. These potentials are usually positive and monophasic ¹³⁶, with the active electrode picking up only a moving phase of depolarization at the junction between volume conductors. Under some circumstances they may be biphasic and of either polarity. They can be recorded over a wide area of scalp with equal ease and amplitude. Evoked potentials recorded from brainstem structures (e.g. the P14) are examples of far-field potentials. The advantage of far-field recording is the ability to obtain information along the whole sensory pathway from a single recording montage encompassing multiple generators and recording sites. The disadvantages include the small amplitude of the responses and electrical noise introduced from muscle artefact due to long interelectrode distances. Table 1.1 summarizes the main SEP waves and their characteristics.

Upper extremity generators	Estimated peaks	Pathway	Estimated peaks	Lower extremity generators
<p>Primary somatosensory cortex:</p> <p>N20: area 3b in the posterior bank of the rolandic fissure</p> <p>P22: motor area 4</p> <p>P27: parietal cortex</p> <p>N30: supplementary motor area</p>	N20/P22 (near field)	Cortex	P37/38 (near field)	Primary somatosensory cortex (analogous to median N20, multiple cortical generators are involved)
VPL nucleus of the thalamus	N18 (far field)	Thalamocortical pathway/VPL nucleus of the thalamus between upper pons and midbrain	N34 (far field)	VPL nucleus of the thalamus (analogous to median N18)
Dorsal column fasciculus cuneatus synapses at nucleus cuneatus in lower medulla (postsynaptic)	P13/14 (far field)	Medial lemniscus decussation (cervico-medullary junction)	N30/P31 (far field)	Dorsal column tract synapses at nucleus gracilis (cervical fasciculus gracilis and possibly gracile nucleus in caudal medulla, analogous to median P14)

<p>Cervical cord:</p> <p>P/N11: cervical dorsal roots into dorsal horns entry zone</p> <p>N12/P12: dorsal column level</p> <p>N13/P13: dorsal column fasciculus cuneatus</p>	N13 (near field)	Dorsal column of the spinal cord	N22 (LP) (near field)	Lumbar cord: lumbosacral dorsal roots into dorsal horns of lumbar cord into dorsal column fasciculus gracilis
Erb point (brachial plexus afferent volley)	N9 (EP) (near field)	Peripheral potential	P18 (near field)	Sacral plexus, analogous to median P9
Median/ulnar nerve	N5	Peripheral mixed nerve	N8(PF)	Popliteal fossa (tibial peripheral nerve) Posterior tibial/peroneal nerve

Table 1.1: features of the main components of the SEP (adapted from Muzyka and Estephan, 2019).

Because needles are more invasive than surface electrodes, needle electrodes are not typically used for SEP recording. Electrode impedance should be below 5 KOhms. Higher impedances degrade the ability of the amplifier to average low-amplitude signals and cause discomfort to the patient. Most laboratories utilize a system passband of approximately 30 - 3000 Hz with some minor variations. Use of a wider passband, extending down to 1 Hz, for example, may have certain advantages for recording long duration signals, but it also introduces additional low-frequency noise that requires averaging a greater number of responses and may substantially prolong recording time.

While various stimulation techniques have been investigated, electrical stimulation of peripheral mixed nerves provides the best control over the stimulus onset, discontinuation, and intensity in the clinical setting. Unilateral stimulation of upper and lower-limb peripheral

nerves is used most often for lateralization of abnormalities, as each dorsal column pathway can be assessed independently. Bilateral stimulation of the lower extremities can be performed if obligate peaks cannot be reliably identified with unilateral stimulation. Cerebral evoked potentials increase in amplitude and are easier to identify with bilateral stimulation, due to a potentiated effect from the opposite side, as long as there is no significant asymmetry in the peripheral or central conduction velocities. However, unilateral lesions may be missed during bilateral stimulation, as the response from the intact side may dominate and mask the abnormality. The stimulus applied should be of sufficient intensity to produce a small visible twitch of the muscle. Higher stimulation intensity does not increase SEP amplitudes considerably and can be uncomfortable. SEP are usually evoked by bipolar transcutaneous electrical stimulation applied over the skin of the selected nerve. Monophasic square-wave constant current or constant voltage electrical pulses of 0.2 ms (0.1 - 0.3 ms) should be delivered. Stimulation rates are 2 - 5 Hz for upper limb and 1 - 2 Hz for lower limb. A lower frequency of leg stimulation is used since the recording time to activate the entire pathway is longer compared with the arm. A rate as low as 0.5 Hz may be required to avoid a flexor withdrawal reflex in a spastic limb. The notch filter should be turned off if possible. The stimulating cathode should be proximal to reduce the likelihood of anodal block. Averaging of 1000 - 2000 trials is often required for each repetition of the testing, although sometimes as few as 500 trials suffice.

The correlation of SEP peaks with specific generators has been based on associated structural and autopsy findings. There is a lack of agreement regarding the underlying generators for a number of SEP peaks, due to multiple impulse pathways, connections, and overlapping sources¹³⁷. The most commonly used peaks in clinical practice for localization purposes are displayed in table 1.1. When a particular mandatory waveform is absent or prolonged, the site of pathology is considered to be at or distal to its generator.

Since upper limb SEP are one of the outcome measures of the present set of investigations, their main technical aspects will be outlined here. For median nerve stimulation at the wrist, the cathode is placed between the tendons of the palmaris longus and flexor carpi radialis muscles 2 cm (cm) proximal to the wrist crease. The anode is placed 2 - 3 cm distal to the cathode. The ground electrode is placed between stimulation and recording sites. Slight abduction of the thumb is observed with adequate stimulation. The following components are identified with multichannel recordings (figure 1.4). N9 is the afferent volley recorded over the brachial plexus. It represents orthodromic activity involving a wide range of somatosensory fibres (C6 - C7 cutaneous, C8-T1 muscle afferents)¹³⁸, as well as antidromic motor fibre

impulses via C8 - T1 cervical roots. It is predominantly generated by sensory fibres as it remains prominent in patients with avulsion of the brachial plexus roots. N13 is derived from cervical dorsal roots entering the dorsal horn entry zone and the cuneate fasciculus of the dorsal column of the spinal cord. This is a cervical potential recorded referentially from the dorsal neck, mainly reflecting postsynaptic activity in the cervical cord ¹³⁹⁻¹⁴¹. It is usually referenced to Fz or to a non-cephalic reference. The C5/8–Fz channel records N13, earlier potentials such as N11, and later potentials such as N14. The N11 potential is likely due to presynaptic activity from near the dorsal root entry zones of C5 to C7 roots and ascending signal in the dorsal columns. N11 is also referred to as the dorsal column volley. The P/N13 response is a near-field potential with a horizontal dipole: negative posteriorly (C5) and positive anteriorly. P14 is generated from cuneate dorsal column fibres synapsing at the nucleus cuneatus in the lower medulla and continuing as the medial lemniscus after the cervico-medullary junction decussation. This is a subcortical far-field potential recorded referentially from scalp electrodes. It has a widespread scalp distribution and probably reflects activity in the caudal medial lemniscus ¹⁴²⁻¹⁴⁴. N18 is a subcortically generated far-field potential, best recorded referentially from scalp electrodes ipsilateral to the stimulated nerve. It most likely reflects postsynaptic activity from multiple brainstem generator sources between the upper pons and the midbrain and the ventral posterolateral nucleus of thalamus ^{142, 145, 146}. Studies of patients with brainstem lesions suggest that N18 reflects excitatory postsynaptic potentials evoked by dorsal column axons in the cuneate nucleus of the accessory inferior olive but may reflect presynaptic depolarization in the cuneate nucleus ^{147, 148}. N20 reflects activation of the hand area of the primary cortical somatosensory receiving area from the thalamocortical volley ^{139, 149}. N20 is recorded using a bipolar derivation to subtract the widespread far-field signals (e.g., P14 and N18) from the superimposed primary cortical activity recorded locally over the centroparietal region contralateral to the stimulated median nerve ¹³⁹.

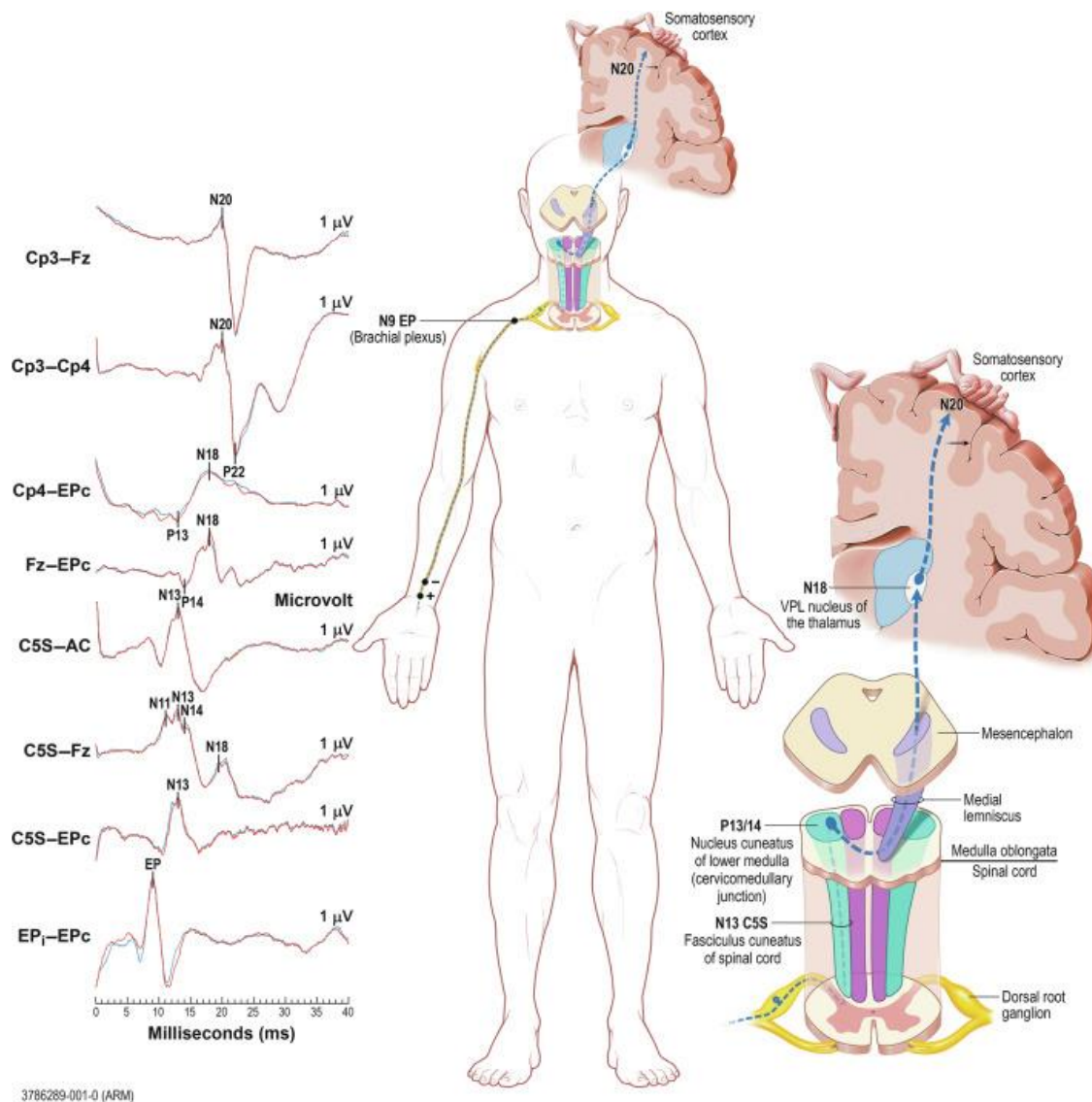


Figure 1.4: main upper limb SEP waveform and generators. Right median SEP with annotated SEP peak waveforms and their corresponding recording channels (left). Right median SEP/somatosensory pathway: pathway neuroanatomy and corresponding SEP peak generators (middle and right). Black arrow (on postcentral gyrus) shows N20 horizontal dipole orientation SEP (adapted from Muzyka and Estephan, 2019).

1.6.2 The somatosensory evoked potential as a measure of somatosensory inhibition

1.6.2.1 Paired-pulse somatosensory evoked potential

Paired-pulse techniques are commonly used tools to investigate excitability changes in somatosensory, visual and motor cortical areas¹⁵⁰⁻¹⁵². Paired-pulse somatosensory evoked

potentials (PP-SEP) is a useful technique to investigate the changes in, and the balance between, cortical excitation and intracortical inhibition in the somatosensory system. When two stimuli are applied in close temporal succession, the response to the second stimulus is significantly suppressed at short interstimulus intervals (ISI), but approaches the magnitude of the response to a single stimulus with increasing ISIs (figure 1.5) ¹⁵³. To assess paired-pulse interaction, linear superposition effects need to be accounted for by subtracting the response to a single pulse stimulation from the paired-pulse stimulation trace (figure 1.6) A recovery curve clearly shows this dependence of paired-pulse suppression on the length of the ISI. Despite being investigated in several animal studies, the cellular mechanism underlying paired-pulse suppression in the somatosensory system is not fully understood. Animal studies have described synaptic depression of thalamocortical ¹⁵⁴ and intracortical ¹⁵⁵ synapses, as well as feed-forward inhibition elicited by the activation of GABAergic interneurons by thalamic afferents ¹⁵⁶. In humans, the origin of paired-pulse suppression of SEP has been the object of a limited number of investigations, and results are partly conflicting. Hoffken and colleagues ¹⁵⁷ applied single and paired electrical stimulation to the median nerve, bilaterally, with an interstimulus interval (ISI) of 30 ms. Recording sites included the left and right brachial plexus, the second cervical vertebrae (fasciculus cuneatus/nucleus cuneatus), CP3 and CP4 electrodes (bilateral S1). To assess paired-pulse interaction, linear superposition effects were factored out by subtracting the response to a single pulse stimulation from the paired-pulse stimulation trace. The authors did not find evidence of inhibition of the N9 and N13 components, but suppression occurred in cortical SEP components (N20/P25). These results suggest that inhibition does not occur at the level of the brachial plexus or the medulla, but it is rather a phenomenon occurring rostrally to the brainstem, possibly due to an enhancement of intracortical GABAergic inhibition ^{158, 159}, a reduction of intracortical glutamatergic excitation ¹⁶⁰, or a mixture of both.

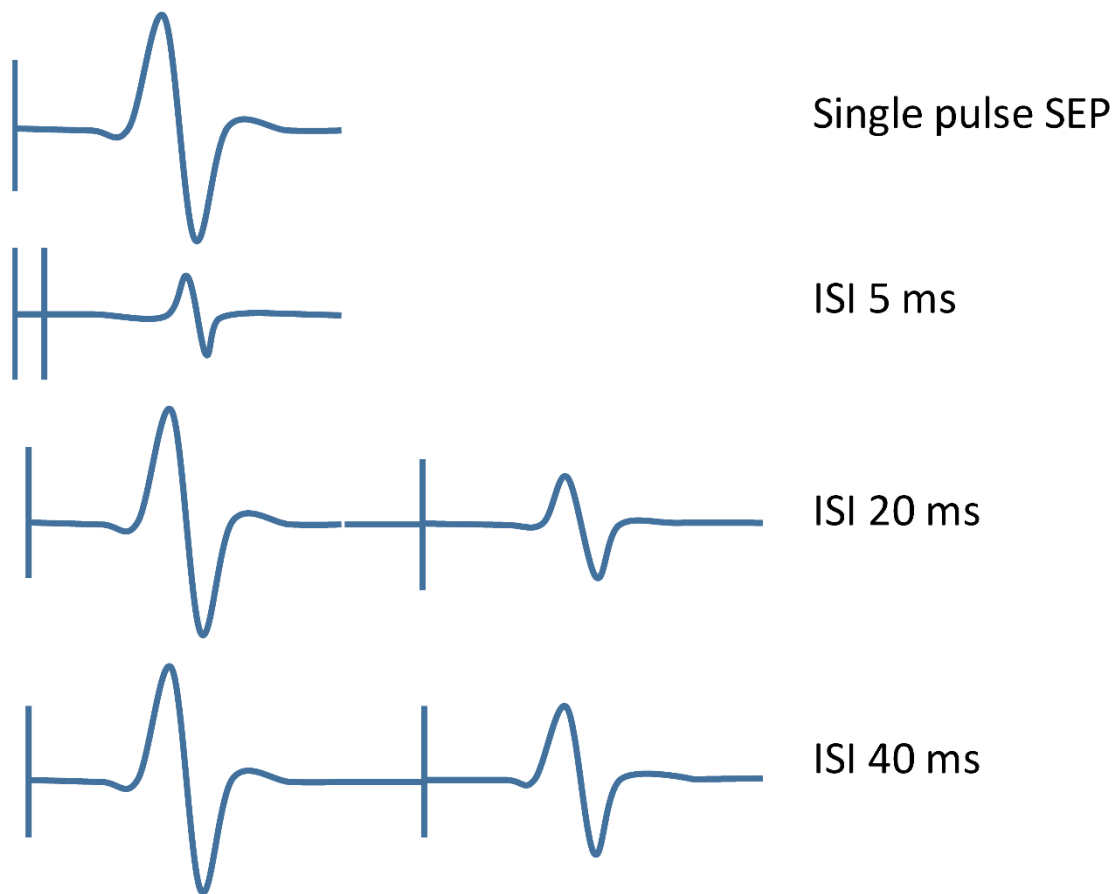


Figure 1.5: *example of paired-pulse suppression of SEP at different ISI.*

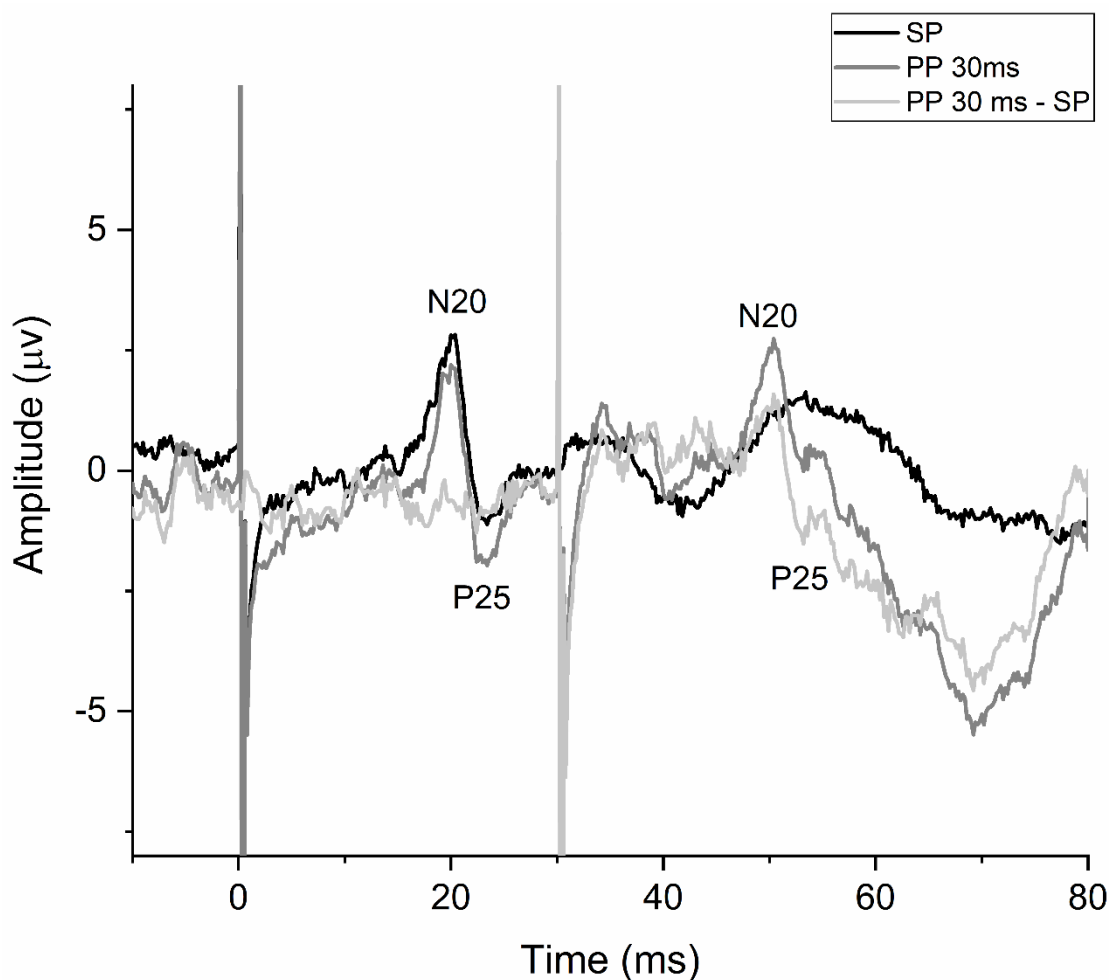


Figure 1.6: paired-pulse unfiltered SEP recorded over CP3 while stimulating the right median nerve. The black trace represent single-pulse SEP, the dark gray trace represents paired-pulse stimulation at 30 ms ISI, the light grey line results from subtracting the single-pulse trace from the paired-pulse trace. In this example, the N20/P25 amplitude of the single-pulse SP is 3.93 μV , while the amplitude of the N20/P25 complex after subtraction is 3.10 μV .

Enhancement of GABAergic inhibition would be more in agreement with evidence in animal models^{161,162}. Suppression is also probably not peripheral in origin, since for peripheral nerves in humans, an absolute refractory period of 0.75 ms with a complete recovery within 2 ms is reported¹⁶³. The mentioned data obtained in humans, however, do not provide robust physiological evidence about the origin of PP-SEP suppression, and are limited by the fact that only one ISI was explored. The work by Rocchi and coworkers¹⁶⁴ expanded on these results by taking into account multiple ISIs (5, 20 and 40 ms) and investigating another electrophysiological signature of inhibitory activity within S1, i.e. SEP high-frequency

oscillations (HFO) (see below for a more thorough explanation). In this study, the authors measured PP-SEP and HFO before and after the application of continuous theta burst stimulation (cTBS), a repetitive TMS protocol known to induce cortical inhibition, on S1. cTBS induced a decrease in PP-SEP inhibition and late-HFO area, probably due to a decreased effectiveness of inhibitory neurotransmission in S1. Two additional findings are worth mentioning here. The first is that the decrease in PP-SEP suppression only occurred at 5 ms ISI, and not at ISIs of 20 and 40 ms. This is important since it suggests that only PP-SEP at short ISIs actually takes place in S1. In contrast, inhibition at longer ISI may involve distant structures, such as the dorsal column nuclei¹⁶³ or thalamus¹⁵⁷. Secondly, cTBS induced a correlated decrease in late HFO (l-HFO) area and PP-SEP inhibition at 5 ms. The conclusion was that both l-HFO and PP-SEP at short ISI are expression of inhibitory activity in S1 and, therefore, can be used as useful in-vivo readouts of inhibitory interactions occurring in S1.

PP-SEP can also be used to probe lateral inhibition in S1, by giving simultaneous electrical pulses on two different locations. The interaction of afferent stimuli coming from spatially distinct receptive fields in the same sensory channel is a known phenomenon, as explained in previous paragraphs, and it has been investigated with different stimulation characteristics. Tinazzi and colleagues described suppression of SEP to dual input to median and ulnar nerves of the same limb, which contain mixed afferents from muscles, skin and joints¹⁶⁵. The same phenomenon has been observed with electrical stimulation of the skin of different fingers of the same hand, suggesting that surround inhibition in the somatosensory domain occurs also with selective stimulation of skin afferents¹⁶⁶. A similar suppression also occurs with stimulation of heterogeneous fibres, i.e. cutaneous and muscle afferents, from the tibial nerve¹⁶⁷. Importantly, this form of SEP inhibition occurs at multiple levels of the nervous system, including the spinal cord, cuneate nucleus, sensory thalamic nuclei, as well as somatosensory and motor cortices; this has been confirmed with recording from the surface¹⁶⁵ and from deep structures, during surgery¹⁶⁶. It is to note that an opposite effect has been described as well. Gandevia and colleagues¹⁶⁸ suggested that, by using very low intensity electrical stimulation of digital nerves, an increase of SEP to dual input can occur. However, this is not the object of the present investigation and, therefore, it will not be further described. Suppression of SEP by simultaneous input to different nerves or skin areas can be evaluated in humans by comparing SEP amplitudes obtained after dual stimulation with the arithmetic sum of SEP amplitudes obtained after stimulating each site individually¹⁶⁵⁻¹⁷⁰. In normal subjects, spinal, brainstem, and cortical SEP to dual input are smaller than the expected size calculated from the arithmetic sum of the two single inputs (figure 1.7). This suppression originates from

the phenomenon of surround inhibition that is present at multiple levels of the somatosensory system.

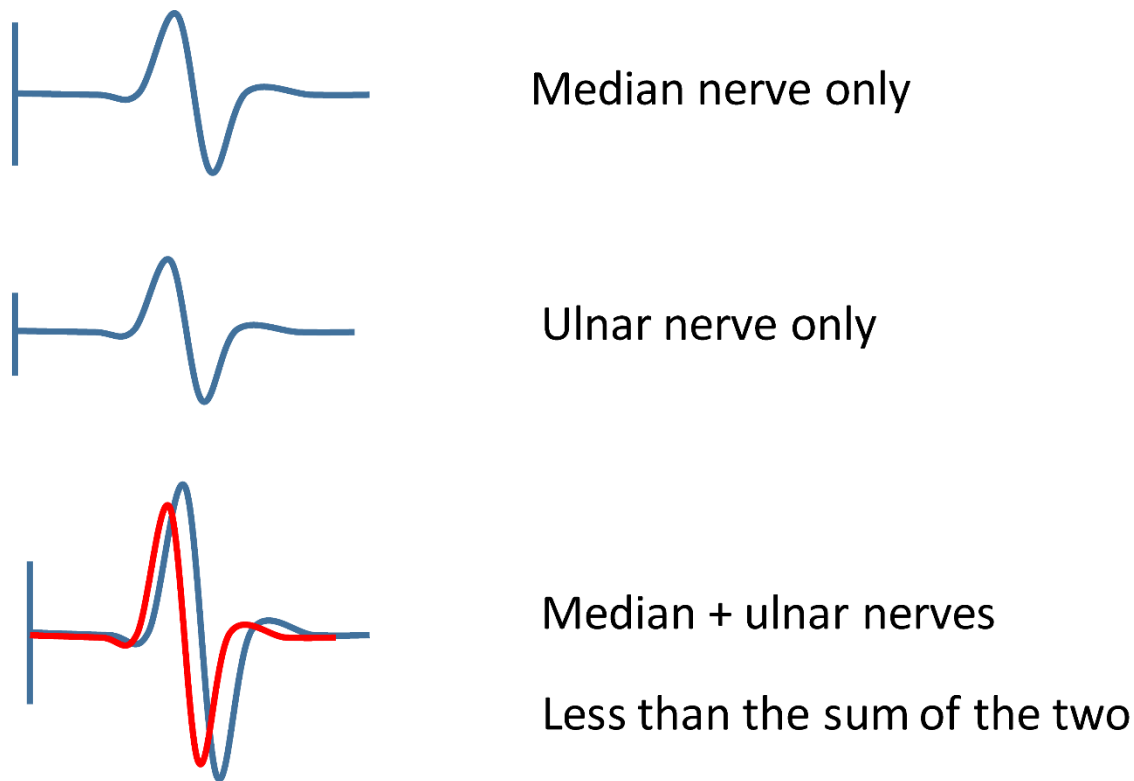


Figure 1.7: *example of SEP suppression caused by simultaneous stimulation of median and ulnar nerves. The red line represent SEP obtained by simultaneous stimulation of the two nerves and is smaller than the arithmetic sum of SEP amplitudes obtained after stimulating each site individually.*

1.6.2.2 High-frequency oscillations

Neuronal networks in the mammalian forebrain manifest several oscillatory bands covering frequencies from 0.05 to 600 Hz ¹⁰⁸. Fast oscillations at around 600 Hz (HFO) have been discovered in normal subjects to overlie the initial cortical response (N20/ P25) in SEP or somatosensory evoked magnetic field following median nerve stimulation ¹⁷¹⁻¹⁷⁸. These were first seen as notches on the N20 - P25 parietal SEP response; later, digital band-pass filtering allowed the separation between HFO and wide-band SEP. Since human somatosensory HFO share the common features of the HFO recorded from S1 of other mammals such as rats, rabbits, piglets, and monkeys, it is plausible that common physiological mechanisms underlie the genesis of the somatosensory HFO.

The early part of the HFO (e-HFO), i.e., the wavelets before the peak latency of initial cortical response such as N20 or N20m (the latter being the N20 counterpart recorded through magnetoencephalography), is presumably generated from action potentials of thalamocortical fibres at the time when they arrive to the area 3b and 1¹⁷⁹⁻¹⁸¹. This is supported by several lines of evidence: (1) the early HFO in humans are resistant to high stimulus rate (>10 Hz)^{179, 182, 183} or hypocapnia¹⁸⁴; (2) the early HFO in piglet are localized in cortical layer IV and insensitive to cortically injected kynurenic acid, a nonspecific antagonist of glutamatergic receptors¹⁸⁵. Furthermore, Kimura and colleagues¹⁸⁶ succeeded in visualizing impulse propagation along the thalamocortical fibres to S1 by recording somatosensory evoked fields with magnetoencephalography (MEG) following median nerve stimulation.

The l-HFO are the wavelets that start at around the peak latency of initial cortical N20 response^{187, 188} and usually last halfway up to the second cortical response (P25), or sometimes until its end. They are thought to originate from cortical post-synaptic activity, since they are abolished after cortical injection of glutamatergic receptors antagonists¹⁸⁵. However, there remains a controversy about the generation of l-HFO, i.e. whether they reflect excitatory activities such as pyramidal cells¹⁸⁹ or they are produced directly or indirectly by activities of inhibitory interneurons^{177, 190-192}. Furthermore, an inhibitory hypothesis for late HFO genesis comprises two possible circuits: a feedforward inhibitory circuit and a feedback inhibitory circuit. The most likely hypothesis is that l-HFO represent activity of FS interneurons in S1, as suggested by several lines of evidence, both in animals and humans. In animal experiments, FS interneurons in S1 produce bursts of action potentials that are closely correlated in frequency, phase and latency to the late HFO¹⁹². Jones and coworkers¹⁹² suggested that HFO recorded from cortical surface reflect fast inhibitory post-synaptic potentials (IPSP) of the apical dendrites of the pyramidal cells that receive the axons from the FS cells at the base of the apical dendrites. It has been generally assumed that action potentials of FS cells cannot produce a dipolar electric field that is recordable from cortical surface, due to a diversity of axonal orientation of FS cells. However, FS cells are mutually interconnected with gap junctions¹⁹³⁻¹⁹⁵ and, due to electrical synapses, respond early and synchronously to thalamic input with high-frequency burst (> 500 Hz)^{196, 197}. Considering these findings, it was proposed that l-HFO represent the activity of combined vertically and horizontally oriented GABAergic FS interneurons in S1^{177, 190, 191}. Even accepting the interneuronal hypothesis for the l-HFO, the idea that HFO recorded by MEG or electroencephalography (EEG) reflect action potentials of FS neurons might appear questionable. Instead, it might be supposed that fast IPSP of the pyramidal neurons as a result of a feedforward inhibition produces a dipolar field that is

recordable by MEG and EEG, since the apical dendrites of pyramidal neurons have a parallel orientation. If that is the case, the orientation of HFO and that of underlying N20m should be identical. In a study using MEG, Ozaki et al.¹⁹⁰ compared the orientation of HFO current sources and of the underlying N20m source, and found a wide distribution in the angle formed by pairs of concurrent HFO and N20m sources; the mean difference in the angle between the two was about 20 degrees. This divergence in the orientation of the dipoles probably results from a variety of dendrite arborization of FS interneurons that are activated. As compared to a pronounced diversity of axonal branches of FS interneurons, their dendrites are less arborized and oriented mainly in a vertical direction. More recent electron-microscopic work examining gap junctions in the neocortex has shown dendro-dendritic and dendro-somatic gap junctions between GABAergic interneurons including FS cells^{195, 198}. Accordingly, ensemble activity of mainly vertically oriented dendrites of FS interneurons that are synchronously made active can produce a dipolar field within the neocortical column that is recordable with EEG and MEG. Presumably, the difference in orientation between the apical dendrites of pyramidal neurons and the dendrites of FS interneurons results in divergence in the orientation of the dipoles between HFO current sources and N20m source. To recap, averaging somatosensory evoked response following median nerve stimulation in EEG and MEG can non-invasively record 600 Hz HFO that overlies initial N20 and P25 responses. The early part of these high-frequency components reflects action potentials of the thalamocortical axon terminals and the late part presumably results from burst of FS interneurons that monosynaptically receive thalamocortical projections and induce inhibition of pyramidal neurons in a feedforward manner (figure 1.8).

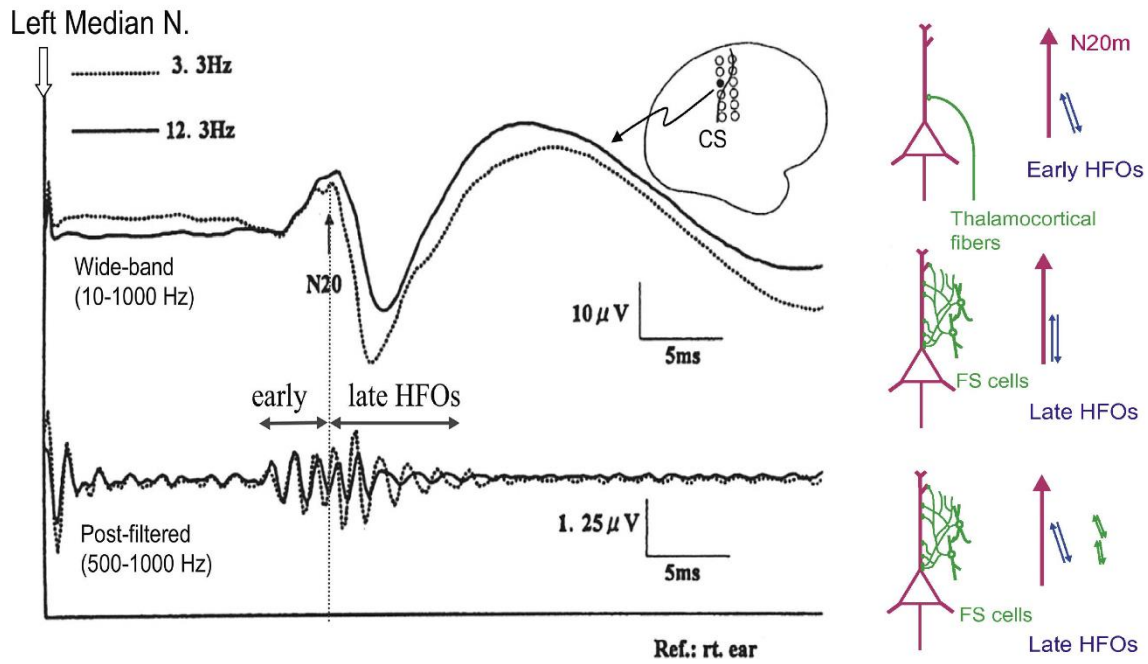


Figure 1.8: example of N20/P25 components of SEP and HFO (left side); possible neural mechanisms of HFO (right side) (adapted from Ozaki et al., 2011). See text for details.

1.6.3 Behavioural measures of somatosensory discrimination

1.6.3.1 Somatosensory temporal discrimination threshold

An experimental approach for investigating how cerebral structures contribute to timing for sensory information entails studying the temporal threshold for perceiving two tactile stimuli applied to the skin as clearly distinct, namely the somatosensory temporal discrimination threshold (STDT) (figure 1.9). Despite inter-subject variability, most healthy individuals perceive two tactile stimuli as sequential when the ISI exceeds 30–50 ms¹⁹⁹. Interest for this variable mostly comes from the finding that it is increased in several disorders of the central nervous system, including dystonia⁷⁹ and Parkinson’s Disease²⁰⁰. STDT testing activates neural processes involved in sensory discrimination uninfluenced by memory formation^{199, 201, 202}, and probably involves the activation of multiple neural structures, but the underlying mechanisms are only partially known. For instance, a fMRI study showed that STDT selectively activates the pre-supplementary motor area (pre-SMA)²⁰³, supporting previous observations of altered STDT in patients with focal lesion of this area after neurosurgery¹⁹⁹.

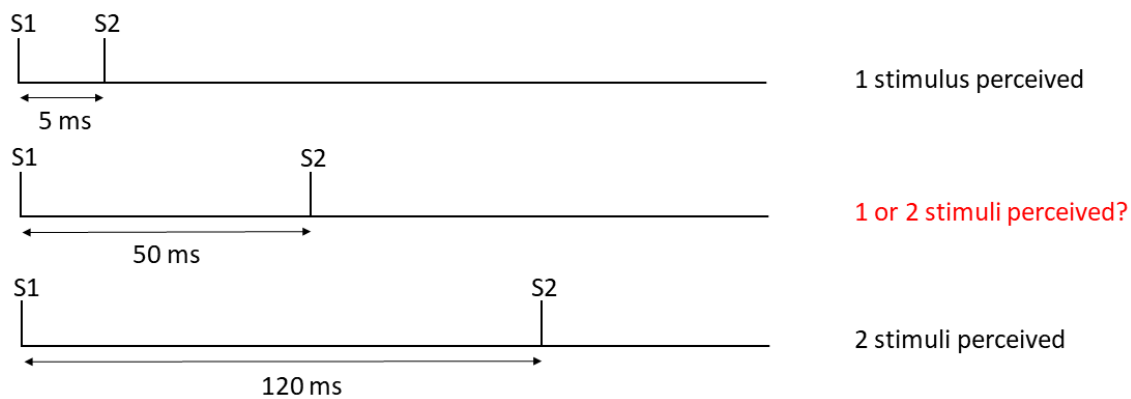


Figure 1.9: *mechanics of STDT testing.*

Another candidate relevant area for STDT is the dorsolateral prefrontal cortex (DLPFC), due to its involvement in time estimation ^{204, 205}, although its role in STDT has been little investigated. The same holds true for the cerebellum, which intervenes in temporal processing at long ISI (hundreds of milliseconds) ²⁰⁶ or during acquisition and coding of learned timing ²⁰⁷. A work from Conte and colleagues ²⁰⁸ shed some light on brain areas causally involved in STDT. In this study, the authors applied cTBS on the mentioned structures. No changes in STDT were found after cTBS on the cerebellum or the DLPFC. Conditioning of the pre-SMA led to an increase in errors that subjects made in distinguishing trials testing a single stimulus and those testing paired stimuli, but average STDT values were not modified.

Another area whose role in STDT was investigated is S1. Single-pulse TMS delivered to S1 about 50 ms before the presentation of tactile stimuli has been shown to impair discrimination of two temporally separated stimuli ^{209, 210}. In one study, cTBS applied on S1 increased STDT values, whereas intermittent theta-burst stimulation, a repetitive TMS protocol known to increase cortical excitability, decreased STDT. Additionally, the decrease in STDT after cTBS was paralleled by a decreased amplitude of the N20/P25 SEP components ²⁰⁸. Overall, these data pointed towards a causal role of S1 in STDT, although the intrinsic S1 circuits involved were not clarified. These were the object of a following investigation. Rocchi and colleagues ²¹¹ performed a more in-depth analysis of the contribution of somatosensory areas to STDT. A possible role of the S2 was hypothesized, based on previous findings of spiking rate modulation of its neurons according to the frequency of tactile stimuli ²¹², and on its involvement in a vibrotactile sequential discrimination task ^{213, 214}. In this work, a substantial role of S2 was excluded by showing that cTBS applied locally did not have any effects on STDT and on the N120 component of SEP; the latter is an evoked response, recorded over the temporal area contralateral to stimulation, that have been suggested to reflect activity in S2 ²¹⁵.

²¹⁶. Importantly, in the same study, STDT was linked to activity of inhibitory interneurons in S1. This was suggested by the finding of a baseline correlation between STDT and both l-HFO area and PP-SEP suppression and an ISI of 5 ms. Also, cTBS applied on S1 induced correlated changes in the three variables (figure 1.10). These findings allow to hypothesize that STDT relies on feedforward inhibitory circuits within S1. It is conceivable that feedforward inhibition interacts with both the initial input and subsequent ones. Feedforward inhibition might rapidly terminate initial excitatory action in pyramidal cells, sharpening up its temporal profile; in addition, it could reduce the amplitude of other inputs that arrive a short time later. The first effect is important for STDT because it will prevent prolonged discharge from the first stimulus from interfering with perception of the second.

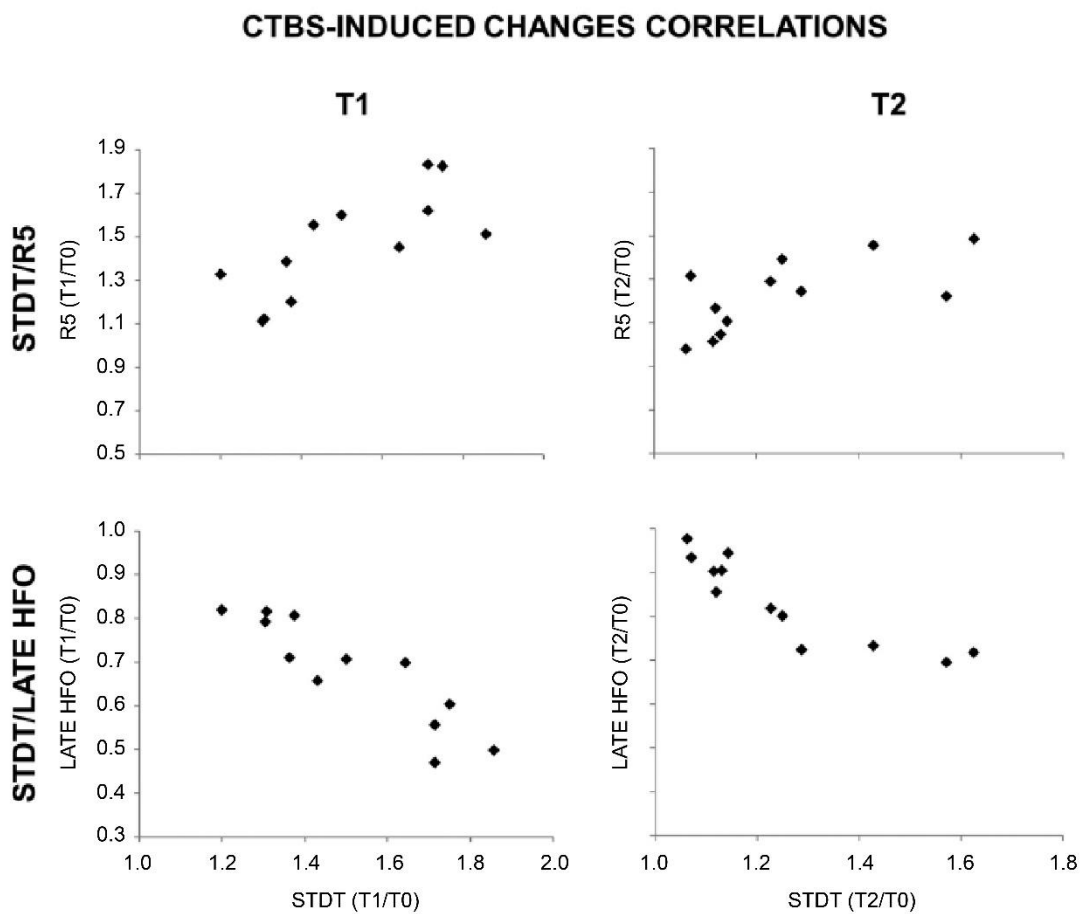


Figure 1.10: correlations between STDT, PP-SEP suppression at 5 ms ISI and l-HFO area. T0 refers to baseline, while T1 and T2 refer to time points tested after baseline (adapted from Rocchi et al., 2016).

Overall, it is likely that the ability to temporally discriminate two distinct afferent stimuli relies on inhibitory mechanisms in S1; therefore, STDT may represent a direct behavioural correlate of feedforward inhibition in S1.

1.6.3.2 Tactile spatial discrimination and tactile threshold

The tasks described in this section have been used to measure tactile spatial abilities, with the assumption, supported by animal and human studies, that that they reflect, to some extent, neural computation occurring in S1. The first is a grating orientation discrimination task, referred to as tactile spatial discrimination (TSD) task in the present work. In this task, a set of JVP domes is used. Each dome is a circular, convex grating surface of 20 mm diameter, on top of a cylindrical handle 30 mm long. The set is made of eight domes with equidistant groove and bar widths ranging from 3.0 to 0.35 mm (figure 1.11).



Figure 1.11: *a set of JVP domes (see text for details).*

The aim of the task is to judge the orientation of the grating. The thinnest grating which is reliably detected 75% of the times provides an estimate of the spatial resolution. Part of the performance in this task is dependent on peripheral innervation. This has been especially demonstrated in the fingertips, which present dense mechanoreceptive innervation²¹⁷⁻²¹⁹. The available evidence from studies at the fingertip suggests that the human capacity to resolve spatial detail at these regions operates at the limits determined by the peripheral innervation density of a fibre population that is specialized for spatial information processing^{220, 221}. This task has a number of advantages, compared to others, in the study of spatial resolution. First, the skin surface area engaged by the grating is unaffected by the grating orientation, thus eliminating non-spatial cues²²². Second, the grating orientation task yields a measure of spatial resolution that is consistent with measures obtained with more complex stimuli such as embossed letters or Braille characters, which can only be resolved by spatial cues²²². Third, among all tests of spatial discrimination²²³, its underlying neural mechanisms are best understood^{224, 225}. Combined psychophysical and neurophysiological data from the human and the monkey fingertip have shown that tactile spatial resolution is based on information conveyed by the spatial modulation of neural activity in the slowly adapting (SA) afferent population^{222, 224}. Among the four afferent fibre classes innervating the fingertip, only the SA population response transmits the spatial details of gratings to the limit of human performance: their individual spatial response profiles are modulated by gratings with grooves and bars as fine as 0.5 mm. Also, subjects' mean thresholds for spatial resolution at the fingertip correspond closely with the mean centre to centre spacing between afferent fibres at the skin^{218, 219} and with the theoretical, behavioural limit imposed by this spacing according to the Shannon sampling theorem in two dimensions²²⁶.

The second tactile discrimination task will be referred here as tactile threshold (TT) measurement, using the Bumps device²²⁷. It is a smooth surface divided into 12 squares, each containing 5 coloured circles, only one of which one has a circular bump in the middle. Bumps are 550 μm in diameter but have different height. The device consists of two such plates (plates A and B), which are identical but for bumps heights: the latter are 2.5 - 8 μm and 8.5 - 14 μm , on plate A and B, respectively (e.g., bump heights on each plate increases in 0.5 μm increments) (figure 1.12).

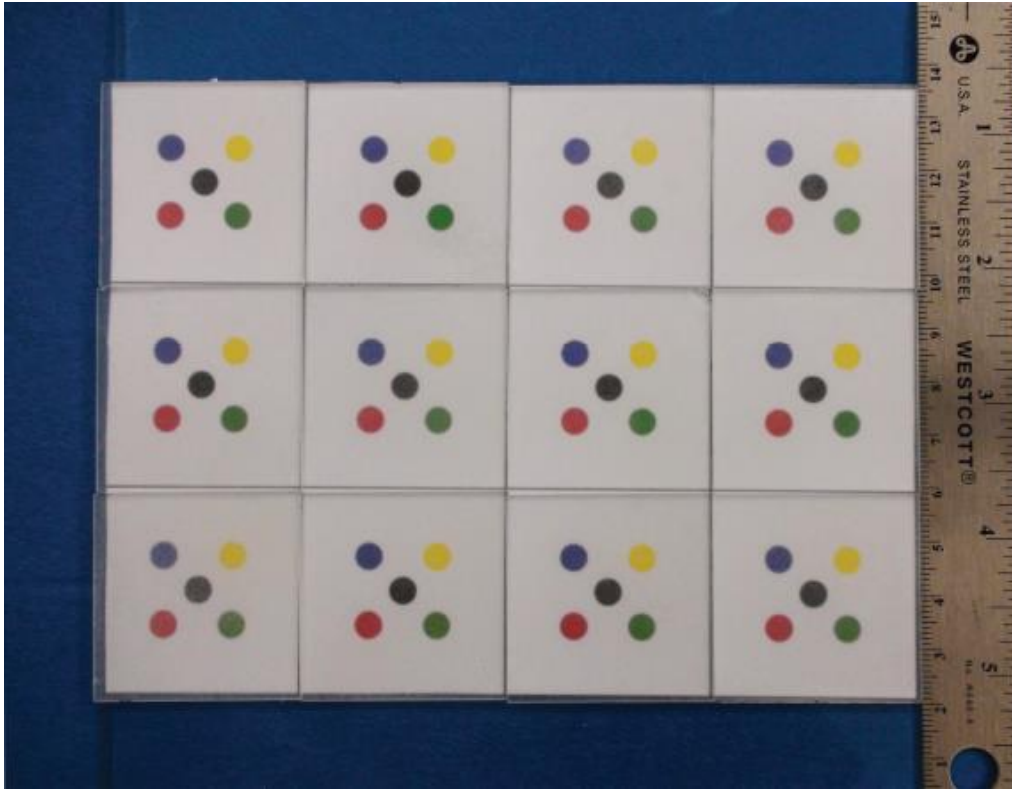


Figure 1.12: *The Bumps device (see text for details).*

Participants are asked to locate the bump in each square (testing order: plate B always first). Two trials are usually performed for each plate and TT is defined as the lowest bump such that it and the following two higher bumps are successfully detected in either trial ²²⁷. Functional studies of touch conveyed by cutaneous mechanoreceptors in glabrous skin found that detection of small raised dots (bumps) on a smooth surface using the finger pad is signalled by Meissner corpuscles ^{228, 229}. In contrast to receptors tested by the JVP domes, Meissner corpuscles are rapidly adapting (RA) and, therefore, they are more suited to detect transient cutaneous stimuli. It is to note that segregation between SA and RA receptors is maintained centrally: within S1, all neurons within each column respond to the same class of receptors, i.e. columns that receive afferents from cutaneous SA and RA receptors are distinct ^{230, 231}. Accordingly, they are called, respectively, SA and RA cortical neurons ²³⁰. It is conceivable, then, that a behavioural task which rely on activation of a different pattern of skin receptors can also give specific information on S1 patterns of activation.

1.7 Inhibition in the motor system

Despite the columnar organization in M1 is, to some extent, similar to the one present in S1, computation occurring in the motor cortex, reflective of movement generation, is less characterized than activity in S1 underlying basic somatosensory perception. In particular, the role of interneurons in M1 in shaping voluntary movement is far from been clarified. For instance, a traditional view suggests that inhibitory interneurons inhibit excitatory neurons encoding antagonistic movements (e.g. through lateral inhibition). However, FS inhibitory interneurons present in M1, unlike pyramidal cells, generally exhibit phasic movement-related activity in relation to voluntary movement ⁹⁵. It is therefore unlikely that FS inhibitory interneurons simply suppress actual muscle movements through inhibitory synaptic transmission. Several possibilities could be considered to account for this phasic activation during voluntary movement. One is feedforward inhibition, in which FS inhibitory interneurons shape a motor command together with excitatory pyramidal cells. This hypothetical function is similar to balanced inhibition observed in the auditory cortex ¹²² and S1 ²³². The other is recurrent inhibition, in which pyramidal cells for a specific movement selectively inactivate nearby neurons coding unnecessary movements via collateral activation of inhibitory interneurons ²³³. The relationship between firing of pyramidal neurons and inhibitory interneurons in M1, however, as well as the functional relevance of inhibition, are still incompletely understood. It is known that in M1, as in all cortical areas, information can be represented by neurons that are tuned to distinct behavioural parameters. This is the case for the coding of movement direction in M1, where cells show an orderly variation in activity as a function of movement direction, with a peak of activity in their preferred direction ²³⁴. Directional tuning in M1 has a columnar and short-scale organization ^{235, 236}, as well as a large-scale organization where the complete distribution of preferred directions is represented multiple times ²³⁷. Merchant and coworkers ⁹⁴ identified two groups of pyramidal cells in M1, one with a broad directional tuning, and another showing a gradation of directional tuning curves. An increase in directional specificity in this second group of cells could be accomplished by inhibition provided by local interneurons; consequently, the selectivity in directional response increased as a function of the suppression strength. Importantly, the dynamic coupling between inhibition and tuning specificity was observed on a cell-by-cell basis. The magnitude and time span of the effect was between 160 ms before to 120 ms after movement onset and was accompanied by an increase in discharge rate of interneurons. These results suggest that tuning by inhibitory mechanisms may play an important role on directional information processing during the preparation and execution of movement ⁹⁴. These findings were expanded by Isomura and colleagues ⁹⁵. The authors confirmed that activity of FS

interneurons in M1 mostly occur during movement expression and probably participate in an ongoing modulation of activity of pyramidal cells during the execution of a single voluntary movement. Notably, in this study, no FS interneurons with movement-off activity were found, excluding the possibility of intracortical gating of motor commands. FS interneurons were also activated slightly after command-like activation of pyramidal neurons, suggesting that balanced and delayed inhibition may achieve temporal sharpening of motor command. Moreover, FS interneurons might suppress other functions such as hold-related activity during motor execution. It has been hypothesized that this balanced inhibition might work effectively at the surround as well as the centre of intended movement, presumably to sharpen the direction specificity of pyramidal cells through the so-called iceberg effect¹²². In fact, a pharmacological blockade of GABAergic inhibition in the primate motor cortex increases the phasic discharge activity in a preferred direction and decreases its directionality²³⁸.

Another line of evidence in support of the local shaping of preferred directions in M1, but with a different mechanism, comes from electrophysiological studies that described the impact of recurrent collaterals of pyramidal axons and the associated interneurons on the inhibition of motor cortical pyramidal cells. Specifically, Stefanis and Jasper^{239, 240} recorded motor cortical post-synaptic potentials elicited by electrical stimulation of the pyramidal tract and described the existence of strong recurrent inhibition, probably mediated by local interneurons that were driven by pyramidal collaterals. These findings strengthened the idea that the recurrent collateral inhibition plays a fundamental role in the spatial sharpening of the focus of excitation in M1²³³. FS interneurons activated by movement pyramidal cells might accomplish recurrent inhibition of other pyramidal cells activity to suppress competing (unnecessary) movements. In the primate motor cortex, where putative FS interneurons show directional tuning properties⁹⁴, the corticospinal tract cells elicit disynaptic inhibitory responses in neighbouring neurons^{233, 239}. However, further data are needed to conclude whether the FS inhibitory interneurons are engaged in balanced inhibition, recurrent inhibition, or both.

1.8 Introduction to transcranial magnetic stimulation

Transcranial Magnetic Stimulation (TMS) is a non-invasive brain stimulation tool, which can specifically activate targeted brain regions. TMS employs an external coil of wire; a high-voltage capacitor is discharged through the wire, creating a transient peak current of several thousand amperes. This creates a magnetic field perpendicular to the coil that penetrates the

brain with little impedance. The magnetic field reaches a peak of several tesla within 100 μ s, and then declines back to zero over the following millisecond. This changing magnetic field induces a pulse of electrical current in the brain which, depending on its intensity, is able to cause a degree of activation of cortical neurons. Effectively, the magnetic field carries an electrical current pulse across the barrier of the scalp to stimulate the brain ²⁴¹. The advantage of TMS is that the current induced on the scalp is little different from that in the brain, so that sensory and muscle activation is minimal, making this type of stimulation much more tolerable for the human subjects than other forms of brain stimulation, such as transcranial electrical stimulation. TMS can be used to stimulate any cortical areas located on the cerebral convexity; for historical reasons, and because it provides a convenient readout, M1 has received considerable attention in the TMS literature. Stimulation of the motor cortex is also the object of the present investigation; therefore, basic concepts about responses of M1 following electrical stimulation will be given here.

Magnetic stimulation of M1 readily evokes responses in contralateral, particularly distal, muscles; this compound responses, recordable with EMG, are called motor evoked potentials (MEP). The MEP is a complex and indirect measure of the motor cortex output, since descending activity is been filtered by activity in synaptic connections in the spinal cord. This descending activity is composed of different wavelets, visible with epidural recordings, named according to their origin. The earliest wave which appears is the D wave, where “D” stands for “direct”. It is not modified in amplitude or latency by changes in motor cortical excitability (such as voluntary contraction) and is therefore believed to originate from direct excitation of corticospinal axons in the subcortical white matter at some distance from the cell body ^{242, 243}. D waves are preferentially obtained with a latero-medial current direction, whereas eliciting them with different current directions requires higher stimulation intensities. The I1 wave, where “I” stands for “indirect”, follows the D wave, with a latency about 1 ms longer than the D wave ^{242, 244, 245}. It is possible to elicit I1 waves with a low intensity by stimulating the motor cortex with a posterior to anterior (PA) induced current. It has been suggested that this wave is the result of monosynaptic activation of pyramidal tract neurons originating from presynaptic axons. The sensitivity of this wave to the level of cortical excitability ²⁴⁵ supports its presynaptic origin. At higher stimulus intensities, later volleys appear: these are termed late I waves, and they are preferentially obtained by using anterior-posterior current direction. The interpeak interval between I waves is about 1.5 ms, which indicates a discharge frequency of about 600 Hz. Similar bursts in the monkey have been shown to result from bursts of activity at the same frequency in neocortical neurons of S1 ²⁴⁶. Neocortical neurons fire once or multiple

times at an interval of around 1.5 ms, with spikes tightly locked to the stimulus ²⁴⁶. If similar neurons are present in M1 and have synaptic connections with pyramidal tract neurons, their activation by magnetic stimuli could in turn evoke bursts of activity that produce the I waves. Figure 1.13 summarizes current concepts of descending activity, along the corticospinal tract, evoked by TMS of M1.

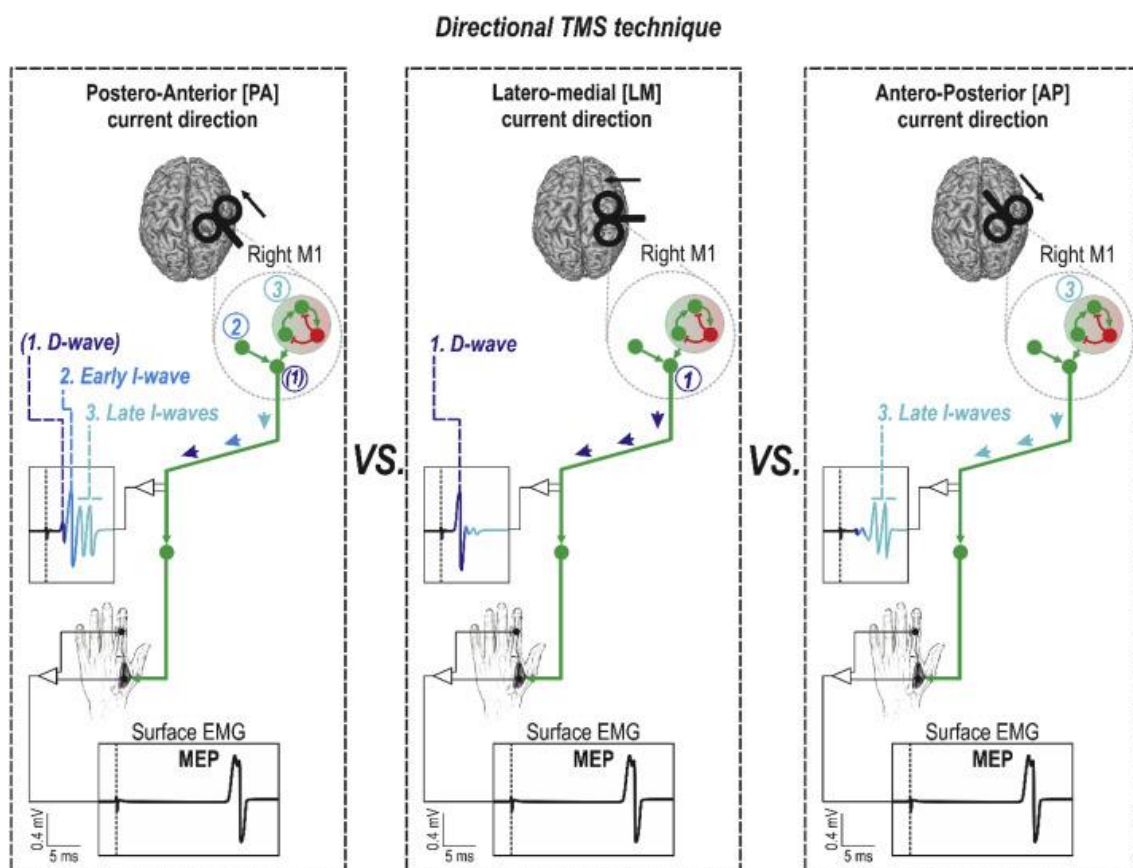


Figure 1.13: mechanisms underlying the generation of D and I waves following TMS of M1 (adapted from Derosiere et al., 2020).

1.8.1 Paired-pulse transcranial magnetic stimulation protocols

Paired-pulse TMS paradigms are used to probe M1 intracortical circuitry. Two magnetic pulses are delivered through the same coil, the first usually referred to as “conditioning” and the second as “test” pulse. In the context of assessment of corticospinal function, only one MEP is evoked (by the test stimulus), but its characteristics change based on the properties of the conditioning pulse. The intensity of both the conditioning and the test pulse is variable, and can be at subthreshold, threshold or suprathreshold intensity (referring to resting or active motor threshold). The ISI between conditioning and test pulses is highly variable, depending

on the protocol, ranging from 1 to 200 or more ms. Usually, the effect of the conditioning pulse is quantified by the amplitude ratio between MEP obtained with conditioned and unconditioned pulses. A brief explanation of the paired-pulse TMS protocols used in this work follows.

SICI is probably the most commonly used paired-pulse TMS paradigm. SICI refers to a suppression of MEP, elicited by a suprathreshold stimulus, by a preceding subthreshold stimulus, with an ISI between 1 and 6 ms. This phenomenon was first demonstrated by Kujirai and coworkers²⁴⁷ (figure 1.14).

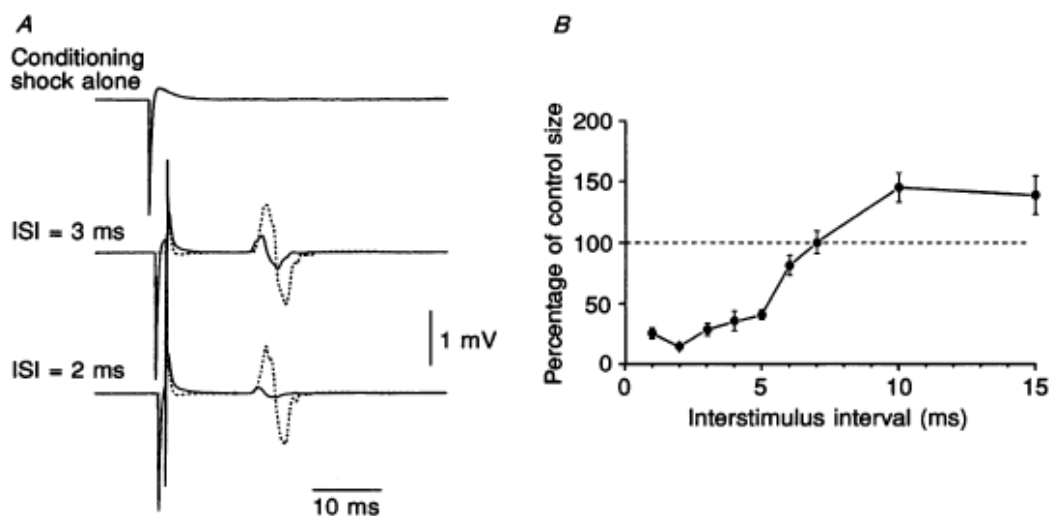


Figure 1.14: *short intracortical inhibition (adapted from Kujirai et al., 1993).*

SICI is influenced by the intensity of both the conditioning and test stimuli. It has been demonstrated that the relationship between SICI and the strength of the conditioning pulse is roughly “U” shaped; this means that SICI has a threshold around 50% of resting motor threshold, reaches a peak around 80%, and disappears for an intensity of the conditioning stimulus of 100% motor threshold or higher, although this is subject to interindividual variability. It is also known that the amount of SICI increases with larger test MEP²⁴⁸. Although originally investigated with peripheral responses, such as MEP, several lines of evidence suggest that SICI is an intracortical phenomenon, such as the fact that a) the H reflex of the flexor carpi radialis muscle is not modulated by TMS applied on M1 with an ISI and intensity similar to those used for SICI, and b) magnetic conditioning stimuli fail to suppress test MEP evoked by a low-intensity test stimulus to M1, which is known to activate corticospinal neurons directly at the axonal level. The neural mechanisms underlying SICI are not completely clarified, but several arguments suggest that it is mediated by GABAergic

neurotransmission within M1. Direct epidural recordings of the descending corticospinal volleys demonstrated the cortical origin of SICI²⁴⁹. A subthreshold conditioning stimulus, that does not evoke descending corticospinal activity alone, produced significant suppression of late I wave if the ISI to the subsequent suprathreshold test stimulus was between 1 and 5 ms. In contrast, the I1 wave was virtually unaffected in the SICI protocol. Kujirai and colleagues²⁴⁷ originally suggested that SICI represents GABAergic inhibition, and supportive evidence was provided for this by pharmacological experiments that showed an increase in SICI after oral intake of Lorazepam, a positive allosteric modulator of the GABA-A receptors²⁵⁰. This hypothesis was further supported by the observation that administration of Lorazepam increases the inhibition of the late I waves but not the I1 wave in the SICI protocol²⁵¹. Because conditioning stimulation that is subthreshold for the activation of pyramidal tract neurons produces SICI, this form of inhibition probably originates presynaptically to these cells. Since the I1 wave remains unaffected, it is unlikely that the subthreshold conditioning stimulus modifies the response of the pyramidal tract neurons to the excitatory inputs but enhances selectively GABAergic neurotransmission leading to suppression of the late I waves according to the canonical microcircuit model (figure 1.15).

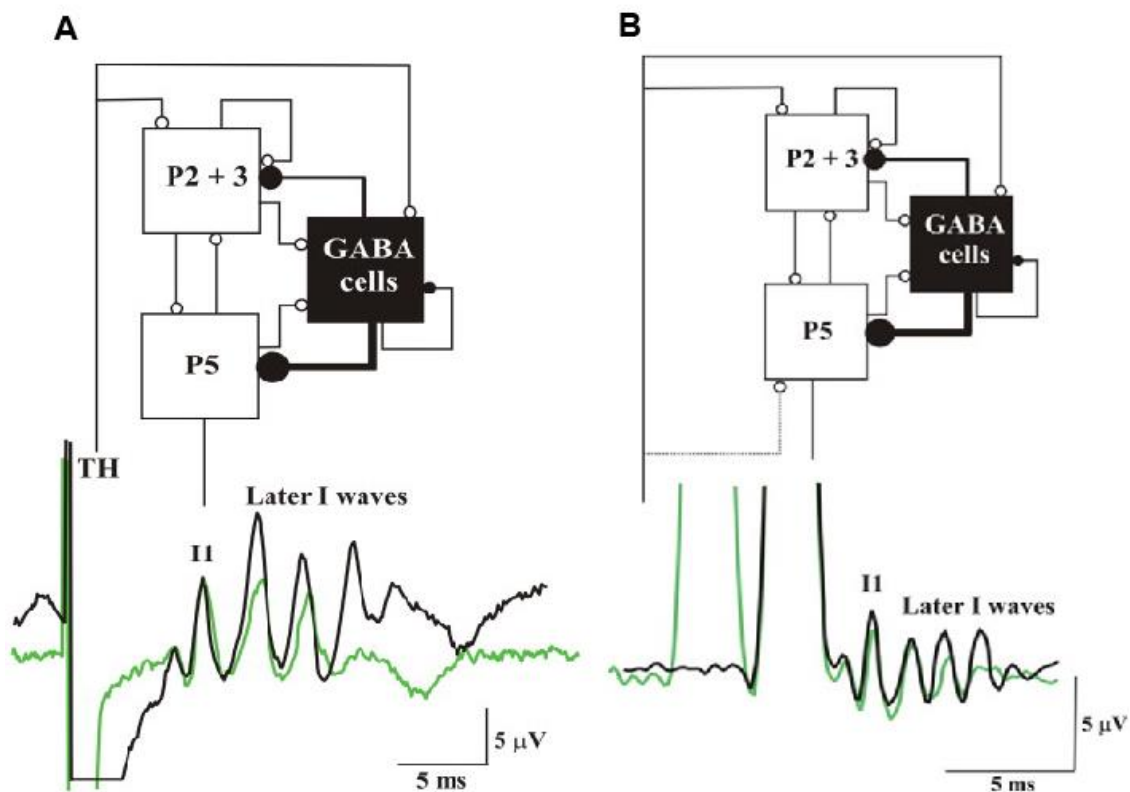


Figure 1.15: decrease in amplitude of late I waves induced by oral intake of Lorazepam (panel A) and SICI (panel B) (adapted from Di Lazzaro et al., 2012).

This is consistent with TMS experiments which indicated that the SICI circuitry has a lower excitation threshold than the excitatory circuits in M1 ^{247, 252, 253}. It should be considered that the functional characteristics of the inhibitory networks have a pronounced tendency to synchronize through axonal interconnections between GABAergic cells, a property that increases their efficiency over excitatory networks ²⁵⁴. Thus, it can be speculated that subthreshold depolarization of the superficial pyramidal cell axons produces a short-term facilitation of GABAergic neurotransmission that is expressed as significant late I-wave suppression in response to the test stimulus.

By contrast to SICI, in the long intracortical inhibition (LICI) protocol, conditioning and test pulses are separated by a longer ISI, usually 100 ms or more. Other differences are that both stimuli are above motor threshold, and that the amount of LICI increases with smaller test MEP ^{255, 256}. The length of the ISI in LICI is similar to the length of the cortical silent period, which represents a pause in EMG activity occurring when a suprathreshold TMS pulse is delivered during voluntary muscle contraction ²⁵⁷; therefore, it has been speculated that LICI and the cortical silent period rely on similar mechanisms. The recording of corticospinal volleys in this paired-pulse paradigm showed that later I waves are reduced at an ISI of 100 ms, but the I1 wave remains unaffected ²⁵⁸⁻²⁶⁰. Because of its duration, it is believed that LICI is mediated by slow inhibitory post-synaptic potentials mediated by the GABA-B receptors ²⁶¹. This received direct support by the finding that Baclofen, a specific GABA-B receptor agonist, increases the magnitude of LICI ²⁶². In analogy with SICI, the inhibition observed at 100 ms ISI originates from a selective suppression of the recurrent activity producing late I waves with no effect on the I1 wave that, accordingly to the canonical circuit model, originates from monosynaptic excitatory connections not modulated by GABAergic connections.

In the same work where SICI was originally investigated, the authors also reported that a test MEP could be facilitated by a subthreshold conditioning stimulus, at ISIs of 10-15 ms, using the same intensity used for SICI; this phenomenon was called intracortical facilitation (ICF) ²⁴⁷. The mechanisms of ICF elicited by paired-pulse stimulation are more complex and less well understood, compared to SICI and LICI. Epidural recordings showed that there is no significant change in the amplitude or number of descending corticospinal waves in the ICF protocol in the presence of a significant MEP facilitation ^{263, 264}. One possible explanation for this dissociation is that ICF results from the recruitment of circuits separate from those involved in I waves generation ²⁶³: according to the canonical microcircuit model these could be the same circuits that are being activated by anterior-posterior magnetic stimulation. These circuits

might be long-range connections (e.g. from the ventral premotor cortex) that might not be activated by single pulse PA stimulation, but might be recruited by paired pulse stimulation. However, since the additionally evoked activity is more dispersed, it may not be evident in the epidural records in the presence of clear I waves. The activation of long-range connections originating from remote areas is also suggested by the strong dependence of ICF upon the direction of the conditioning current in the brain, a phenomenon not observed for SICI²⁵². Another possibility for the lack of correlation between descending I waves and ICF is that the latter is at least partly mediated by circuits in the spinal cord, as suggested by recent evidence²⁶⁵.

1.9 Plasticity induced in the nervous system by repetitive peripheral stimulation

Activity-dependent plasticity of neurotransmission is central to memory encoding and also plays a key role in the development of the nervous system. Persistent changes in communication among neurons also probably represent both adaptive and maladaptive responses to many forms of injury to the central nervous system (CNS). Plasticity in all its forms is thus inextricably intertwined with almost all aspects of brain function. Persistent changes in synaptic transmission underlie plasticity and learning. From cellular studies, long-term potentiation (LTP) and long-term depression (LTD) of synaptic transmission are the leading candidates for being the relevant activity-dependent changes in synaptic connection strength²⁶⁶⁻²⁷⁰. Typically, high-frequency stimulation (10 Hz or higher) is used to induce LTP in brain slices, whereas LTD can be reliably evoked by low-frequency stimulation of around 1 Hz²⁶⁹ (figure 1.16, panel A). In addition to LTP/LTD mechanisms, spike-timing-dependent plasticity (STDP) mechanisms have attracted much interest over the last few years. STDP assumes that there are narrow and cell-type-specific temporal windows for synaptic modification induced by the correlated spiking of presynaptic and postsynaptic neurons, depending on the temporal order of spiking²⁷¹⁻²⁷⁴. LTP effects are induced when presynaptic spikes are emitted before the postsynaptic neuron starts to spike, and LTD effects are induced when presynaptic spikes are emitted after the postsynaptic neuron starts to spike. The strength of the LTP and LTD effects depends on the proximity in time of presynaptic neuron activity to that of the postsynaptic neuron (figure 1.16, panel B).

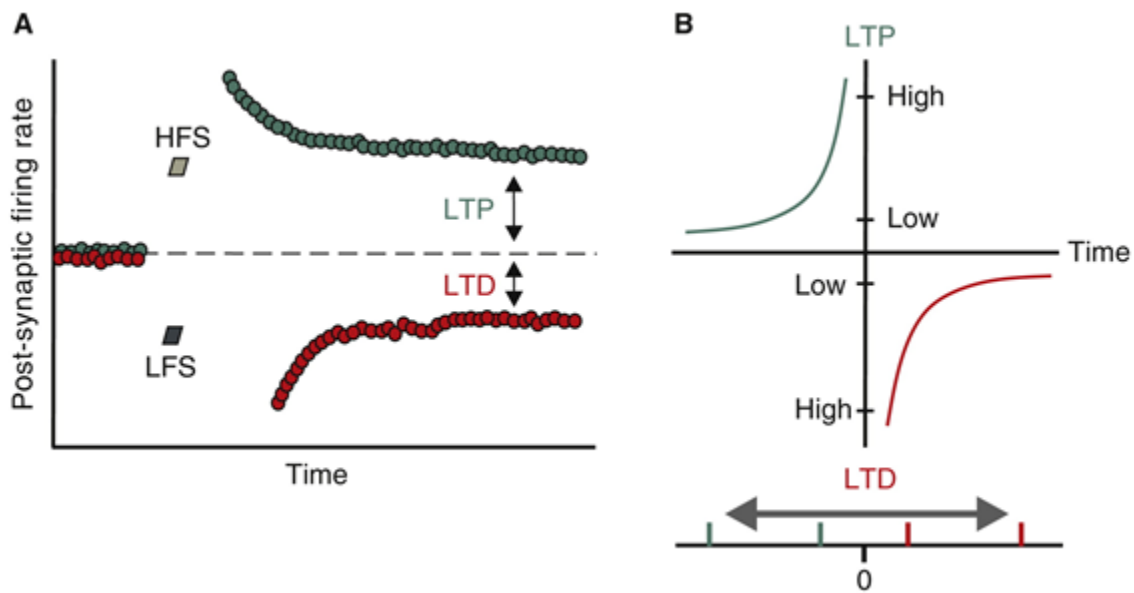


Figure 1.16: principles for inducing plasticity. *Panel A:* Long-term potentiation (LTP) is induced using high-frequency stimulation (HFS) and leads to increases in post-synaptic firing rate. Opposed to this, long-term depression (LTD) is induced using low-frequency stimulation (LFS) and leads to decreases in post-synaptic firing rate. *Panel B:* principles underlying spike-time-dependent plasticity (STDP). If spiking in the pre-synaptic neuron occurs closely to activity of the post-synaptic neuron, LTP and LTD effects are strong. When the time difference in presynaptic neuron spikes and activity of the postsynaptic neuron is longer, the LTP or LTD effect is weaker. LTP and LTD effects depend on whether the presynaptic neuron fires before or after the postsynaptic neuron (adapted from Beste and Dinse, 2013).

The concept of sensory stimulation protocols to induce learning has attracted substantial interest as a means to drive learning and plasticity. In particular, recent findings demonstrate the feasibility and effectiveness of training-independent sensory learning approaches in the somatosensory domain. In several tactile repetitive stimulation protocols, the fingertips or other skin areas are repeatedly stimulated, either mechanically or electrically, for many minutes to hours in order to induce plasticity in the somatosensory cortices²⁷⁵⁻²⁷⁷. Because of the induced plasticity, tactile perception at the stimulated skin sites is altered. Spatial tactile discrimination, or ‘tactile acuity’, is often assessed as a simple measure of change in tactile perception abilities. In a typical repetitive somatosensory (RSS) experiment, two-point discrimination thresholds are lowered, indicating improved tactile acuity, which reaches baseline levels after 24 hours²⁷⁵. This improvement does not transfer to fingers of the unstimulated hand, and there is no transfer to the neighbouring fingers of the stimulated hand.

The relation between learning-induced changes in behaviour and individual changes in brain organization has been studied using a combination of psychophysical tests and non-invasive imaging. Neuroimaging and electric source localization by multi-channel EEG showed that RSS led to an increase in the size of the cortical representation specific to the stimulated finger^{276,277}, which can be regarded as a recruitment of processing resources. The changes observed in cortical map representation were found to be linearly related to the degree of improvement in two-point discrimination thresholds. Accordingly, a large gain in spatial discrimination abilities was associated with large changes in cortical maps^{276,277}. A similar result was obtained for changes in cortical excitability. Cellular studies have shown that increased excitability is a typical signature of effective LTP induction. In humans, paired-pulse stimulation protocols provide a reliable marker of excitability: the paired-pulse behaviour is characterized by a significant suppression of the second response at short ISI. Paired-pulse suppression of SEP was reduced after RSS, and the amount of suppression was positively correlated with the individual gain in performance²⁷⁸. Taken together, these data show that training-independent sensory learning results in selective reorganization in the primary somatosensory cortical areas. As outlined above, LTP and LTD are activity-dependent changes in the strength of synaptic connections which are leading candidate mechanisms of neuronal plasticity²⁶⁸⁻²⁷⁰. Several studies specifically investigated the efficacy of in vitro stimulation protocols in driving perceptual changes by applying high-frequency and low-frequency stimulation. High-frequency stimulation consisted of cutaneous pulse trains applied to the tip of the right index finger with a stimulation frequency of 20 Hz. Each train consisted of 20 single pulses of 20 Hz lasting one second with an inter-train interval of five seconds. Low-frequency stimulation was applied at 1 Hz with stimulus trains consisting of 1200 pulses. It was found that 20 minutes of high-frequency stimulation induced a lowering of tactile discrimination thresholds, whereas low-frequency stimulation resulted in an impaired discrimination performance. Most interestingly, 24 hours after high-frequency stimulation, it was found that spatial two-point discrimination thresholds were still lower than the baseline values. In contrast, 24 hours after low frequency stimulation, the discrimination thresholds had recovered to the baseline values²⁷⁹ (figure 1.17).

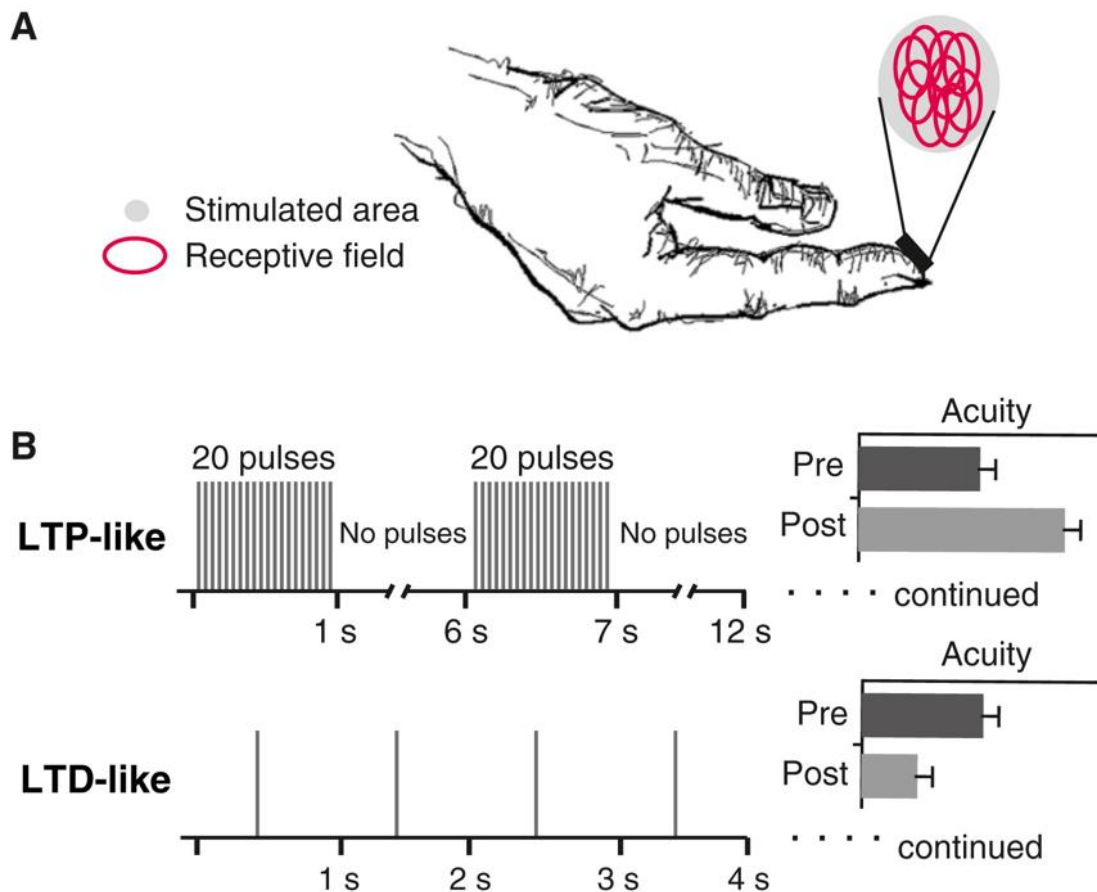


Figure 1.17: Training-independent sensory learning in the tactile modality. *Panel A:* schematic representation of a stimulation device placed on the top of an index finger. The red circles denote the different receptive fields that were stimulated in the area underneath the stimulation patch. *Panel B:* depiction of LTP- and LTD-like stimulation protocols, together with their effects on tactile two-point discrimination threshold. Acuity thresholds are lowered after LTP-like stimulation but increased after LTD-like stimulation (adapted from Beste and Dinse, 2013).

These results indicate that brief stimulation protocols resembling those used in cellular LTP and LTD studies can induce meaningful and persistent alterations in tactile discrimination behaviour of humans.

In summary, the data from tactile training-independent sensory learning experiments have demonstrated the following. First, tactile perception can be bi-directionally altered by protocols that present stimuli at a pace resembling that of protocols used to induce LTP and LTD at a cellular level. Second, changes in tactile perception are paralleled by alterations in cortical maps, cortical activation and cortical excitability in S1.

1.10 Aims of the current thesis

The main aim of this PhD project is to investigate the physiological abnormalities in central processing of somatosensory input in patients with dystonia, and then to test possible interventions that might improve sensory discrimination first in healthy individuals and then in patients. This dissertation describes initial experiments in patients that provided some clues as to potential central somatosensory deficits in patients. We then tested whether an intervention known to improve sensory discrimination in healthy participants would affect the circuits involved in patient deficits.

In a first investigation, we tested if electrophysiological markers of reduced inhibition in the somatosensory system correlate with abnormal somatosensory temporal discrimination in dystonia. STDT was measured in patients with idiopathic CD and age-matched healthy controls (HC). We evaluated temporal somatosensory inhibition using PP-SEP, spatial somatosensory inhibition by measuring the SEP interaction between simultaneous stimulation of the digital nerves in thumb and index finger, and GABAergic sensory inhibition using the early and late components of HFO in digital nerves SEP. Then we investigated the mechanisms through which RSS acts on S1 circuitry, by testing its effects on the same measures of inhibition used in the first experiment. In particular, we hypothesized that refinement of inhibition induced by high-frequency RSS might be responsible for an improvement in spatial and temporal perception. As an additional item, we also tested inhibition in M1 by means of TMS, under the hypothesis that changes in S1 inhibition could be transmitted to M1, as observed in previous work on RSS. Following this, the effect of high-frequency RSS was tested in a group of patients with idiopathic CD, with the expectation that a refinement in S1 inhibition would occur, as hypothesized for HC. Unexpectedly, we found that patients with idiopathic CD showed a paradoxical reduction in S1 intracortical inhibition after high-frequency RSS, resulting in an increase in STDT, a reduced suppression of PP-SEP, as well as reduced HFO and lateral inhibition. This led to the speculation that patients with idiopathic dystonia might have abnormal homeostatic plasticity in the inhibitory circuitry within the S1. It is known that dystonia can develop after lesions in the basal ganglia, but it is still unknown whether lesions in these deep nuclei result in altered S1 inhibition, which might then lead to the development of dystonia, or whether the dystonic phenomenon is independent from altered S1 plasticity. To address this question, the same experimental protocol was used in patients with dystonia secondary to lesions in the basal ganglia.

The paradoxical response of dystonic patients to high-frequency RSS led us to speculate that a reverted response would also occur to other plasticity-inducing protocols. In previous work, as will be explained in the relevant section, it was shown that low-frequency RSS had effects opposite to high-frequency RSS in HC, i.e. a decline in tactile spatial discrimination. We hypothesized that, as for high frequency RSS, patients might have a reversal of plastic effects induced by low-frequency RSS, so that the response consisted in a decrease in STDT and a global improvement in S1 inhibition. Since this was the case, we devised a final experiment to test the effects of RSS applied directly on a body part affected by dystonia and not just to probe S1 inhibition. We tested patients affected by FHD, dividing them in three groups, according to the different type of stimulation received. The first group received high-frequency RSS on the two forearm muscles mostly affected by dystonia; the second received synchronous low-frequency RSS over the same muscles at 1 Hz frequency; in the third group, low-frequency RSS was delivered asynchronously over the two muscles. In the latter case, we assumed that the asynchronicity would act at the cortical level by LTD-like mechanisms following the principle of STDP, thus possibly inducing an inhibition of the abnormal muscle synergies characterizing dystonia. The effects of RSS were assessed similarly to experiment 3, but this time SEP were obtained by motor-point stimulation of the muscles where RSS was applied.

2 General methods

2.1 Participants, institutional and ethical approval

HC were recruited from a database of healthy volunteers at the Institute of Neurology, University College London, or were relatives/spouses to patients. Patients with a diagnosis of CD or FHD were recruited from Professor Kailash Bathia's or Dr Carla Cordivari's outpatient clinics at The National Hospital of Neurology and Neurosurgery. All experiments were performed at the Institute of Neurology (London) and were approved by the University College London Research Ethics Committee. All studies were performed in accordance with the Declaration of Helsinki.

2.2 Transcranial magnetic stimulation

2.2.1 TMS coils and magnetic stimulators

All experiments used monophasic, single pulse TMS delivered via a figure-of-eight coil with 70 mm internal wing diameter (D70 Alpha Flat Coil, The Magstim Company, Dyfed, UK). Figure of eight-shaped coils are more focal than other models (e.g. round coils); with their configuration, the induced current under the point where the coil windings overlap is approximately twice that of the coil edges, and thus stimulation can be considered to occur within that smaller area. We used one or two magnetic stimulators to deliver stimuli (Magstim 200, The Magstim Company, Dyfed, UK); when testing SICI, ICF and LICI, pulses from two stimulators were delivered through the same coil, by means of a connecting module (Magstim BiStim²), linking the two stimulators.

2.2.2 Hotspot location and test stimulus threshold measurement

The primary motor cortex corresponding to the muscle of interest was targeted in all experiments. The hotspot was identified as the area on the scalp where the largest and most stable MEP could be obtained, using a given suprathreshold intensity. The coil was always held approximately perpendicular to the presumed central sulcus and tangentially to the skull, with the coil handle pointing backwards, to induce a posterior to anterior directed current in the brain.

2.3 Electrical stimulation

Electrical stimulation was delivered with a DS7A Current Stimulator (Digitimer, Welwyn Garden City, United Kingdom). It provides up to 100 mA constant current high voltage pulses of brief duration (from 50 μ s to 2 ms) and a maximum compliance voltage of 400 V. Square wave pulses were used in all experiments, with intensity varying according to the output required in each experiment. Depending on the experiment, current was delivered through ring electrodes (in case digital fingers were stimulated) or through 9 mm Ag–AgCl surface electrodes (when stimulation was applied on mixed nerves or directly over muscles). When nerve trunks were stimulated, the stimulating cathode was always placed proximally, to avoid the risk of anodal block.

2.4 Recording of evoked responses

2.4.1 Evoked responses from muscles

Surface EMG was obtained using a belly-tendon montage for hand muscles or bipolar montage for forearm muscles; 9 mm Ag-AgCl surface electrodes were used in both cases. The raw signals were amplified (1000x), and a bandpass filter was applied (5 Hz to 2 kHz (Digitimer, Welwyn Garden City, United Kingdom). Signals were digitised at 5 kHz (CED Power 1401; Cambridge Electronic Design, Cambridge, United Kingdom) and data were stored on a computer for offline analysis (Signal or Spike2 softwares, Cambridge Electronic Design, United Kingdom).

2.4.2 Evoked responses from the scalp

Scalp evoked responses were recorded via 9 mm Ag-AgCl surface electrodes. Electrodes positioning varied depending on the signals of interests, but was always based on the international 10-20 system of EEG electrode placement²⁸⁰. The raw signals were amplified (100000x), and a bandpass filter was applied (2 Hz to 3 kHz (Digitimer, Welwyn Garden City, United Kingdom). Signals were digitised at 5 kHz (CED Power 1401; Cambridge Electronic Design, Cambridge, United Kingdom) and data were stored on a computer for offline analysis (Signal software, Cambridge Electronic Design, United Kingdom).

2.5 Somatosensory behavioural tasks

STDT was measured with an ascending method²¹¹ in all experiments. It was investigated by delivering paired stimuli on the distal phalanx of different fingers, starting with an ISI of 0 ms

(simultaneous pair) and progressively increasing the ISI steps by 10 ms. The stimulation intensity was defined for each subject by delivering series of stimuli, manually increasing the intensity from 2 mA in steps of 0.5 mA; the intensity used for the STDT was the minimal intensity perceived by the subject in 10 of 10 consecutive stimuli. Before STDT testing started, subjects familiarized themselves with the task and achieved a stable performance. Subjects were asked to report verbally whether they perceived a single stimulus or two temporally separate stimuli. The first of three consecutive ISI at which participants recognized the stimuli as temporally separated was considered the STDT. To keep the subject's attention level constant during the test and to minimize the risk of perseverative responses, the STDT testing procedure included "catch" trials consisting of a single stimulus delivered randomly. Each session comprised four separate blocks. The STDT was defined as the average of four STDT values.

TSD was measured using a set of JVP domes²⁸¹. Each dome is a circular, convex grating surface of 20 mm diameter, on top of a cylindrical handle 30 mm long. The set is made of eight domes with equidistant groove and bar widths ranging from 3.0 to 0.35 mm. Subjects were required to judge the orientation of the grating (i.e., horizontal, or vertical to the fingertip). The thinnest grating which was reliably detected 75% of the times provided an estimate of the spatial resolution.

TT was tested using the Bumps device²²⁷. It is a smooth surface divided into 12 squares, each containing 5 coloured circles, only one of which one has a circular bump in the middle. Bumps are 550 μm in diameter but have different height. The device consists of two such plates (plates A and B), which are identical but for bumps heights: the latter are 2.5 - 8 μm and 8.5 - 14 μm , on plate A and B, respectively (e.g., bump heights on each plate increases in 0.5 μm increments). Participants were asked to locate the bump in each square (testing order: plate B always first). Two trials were performed for each plate and TT was defined as the lowest bump such that it and the following two higher bumps were successfully detected in either trial, as previously described.

2.6 Hand motor function tests

In one of the projects, two tests were used to assess hand motor function, in particular manual dexterity, i.e. the box and block test and the nine-hole peg test.

The box and block test (BBT) measures unilateral gross manual dexterity²⁸². It is a quick, simple and inexpensive test, and has been validated in a range of neurological disorders

affecting manual dexterity, including stroke ^{283, 284}. The BBT is composed of a wooden box divided in two compartments by a partition and 150 blocks. Administration of the BBT consists of asking the participant to move, one by one, the maximum number of blocks from one compartment of a box to another of equal size, within sixty seconds. The box is oriented lengthwise and placed at the participant's midline, with the compartment holding the blocks oriented towards the hand being tested. Participants are scored based on the number of blocks transferred from one compartment to the other compartment in 60 seconds.

The nine-hole peg test (NHPT) is used to measure finger dexterity in patients with various neurological diagnoses, including stroke and Parkinson's disease ^{283, 285}. It is composed of a plastic board with 9 holes (10 mm diameter, 15 mm depth), placed apart by 32 mm, and a container for the pegs (a round dish at the end of the board) ²⁸⁶⁻²⁸⁹. It is administered by asking the subject to take the pegs from a container, one by one, and place them into the holes on the board, as quickly as possible; participants must then remove the pegs from the holes, one by one, and replace them back into the container. The board is placed at the participant's midline, with the container holding the pegs oriented towards the hand being tested, and only the hand being evaluated should perform the test. Scores are based on the time taken to complete the test activity, recorded in seconds.

2.7 Clinical assessment

Several clinical rating scales were used to assess dystonia in patients. Patients with CD were assessed by means of the Toronto Western Spasmodic Torticollis Rating Scale (TWSTRS). The TWSTRS is a comprehensive scale designed to assess objective physical (severity subscale) and subjective findings (disability and pain subscales) ²⁹⁰. The reliability and validity of the TWSTRS have been well established, and the severity scores rated by physicians positively correlate with patient's self-reported improvement in disability and pain after treatment with BoNT injections ²⁹¹. Two different assessment scales were administered to patients with FHD. The first is the Unified dystonia rating scale (UDRS), designed to include a detailed assessment of the severity of dystonia in individual body areas. Each of 14 body regions are rated for dystonia severity and duration. The proximal and distal limbs are given separate ratings. Ratings for each body region are totaled for an overall rating of dystonia severity. The UDRS was tested in a large sample of dystonia patients at multiple sites exhibiting the full spectrum of dystonia severity ²⁹². The second is the Arm dystonia disability scale (ADDS). It contains seven items that score the impairment of manual motor control, and

is used to evaluate functional impairment of the dystonic hand in everyday life. The lower the ADDS score, the more severe is the functional impairment caused by hand dystonia. Patients who are unaware of any motor dysfunction have an ADDS score of 100%. The ADDS score is 90% if there are no limitations of activities, but patients are socially affected by the dystonia. Patients who are limited in their functional activities have to answer seven questions. The scale uses a range of points from 0 to 3 for each of the seven questions. The total number of points scored by each patient is divided by the maximum possible points, the quotient is multiplied by 90, and the result subtracted from 90% ²⁹³.

3 Neurophysiological correlates of abnormal somatosensory temporal discrimination in dystonia

3.1 Introduction

The aim of the first project was to establish whether neurophysiological markers of reduced inhibition in S1 contribute to abnormal STDT in dystonia. STDT is possibly one of the most consistent somatosensory abnormalities found in dystonia^{61, 74, 200}. It is defined as the shortest time interval necessary for a pair of tactile stimuli to be perceived as separate¹⁹⁹. In young healthy subjects, it is in the order of 30 to 50 milliseconds, although this interval tends to increase with age^{72, 294}. Work on healthy individuals^{74, 203} and on patients with focal cerebral lesions¹⁹⁹ has shown that several brain regions are involved in STDT, including S1, the pre-SMA, and the basal ganglia. STDT is increased in patients with different types of dystonia where it is thought to indicate a deficit of temporal sensory processing^{60, 61, 202, 295}. STDT has been considered an endophenotype of dystonia because it does not correlate with disease severity^{296, 297}, is abnormal in non-dystonic body regions⁷³ and is altered in about half of the unaffected first-degree relatives of patients^{70, 72}. Besides abnormalities in the temporal somatosensory domain, other behavioural or electrophysiological studies showed that patients with dystonia have deficits in the spatial domain, such as impaired orientation sensitivity at the fingertips²⁹⁸ and abnormal processing of simultaneous stimulation of median and ulnar nerves as a putative marker of impaired lateral somatosensory inhibition¹⁶⁵. Furthermore, patients with focal cervical dystonia have a reduced area of HFO²⁹⁹, measuring the activity of the GABAergic inhibitory mechanism within the somatosensory system³⁰⁰. It is, however, unknown whether the aforementioned abnormalities relate to each other and are somewhat linked to increased STDT in dystonia.

As already suggested in patients with focal hand dystonia by Tamura and colleagues²⁰², increased STDT in dystonia may be related to reduced PP-SEP suppression at short ISI, which is indicative of a deficit in somatosensory temporal processing within S1. Indeed, STDT can be increased in both healthy individuals and patients with FHD if PP-SEP suppression is reduced by preconditioning the excitability of S1 with cTBS^{74, 164}, a protocol able to induce LTD-like changes in the cortex. Rocchi and colleagues¹⁶⁴ also found in HC that cTBS reduced

the amplitude of the late component of the HFO, linking this marker of cortical inhibition to STDT.

The aim of this first set of experiments was to provide further information on the relationship between physiological measures of somatosensory processing in S1 and measures of STDT in HC and in patients with dystonia. We also included measures of subcortical somatosensory processing since imaging studies have highlighted that abnormal STDT in dystonia correlates with changes in the cerebellum and the basal ganglia^{71, 301}, suggesting widespread involvement of a subcortical striatal re-entrant looped pathway. Therefore, we used an extensive neurophysiological battery involving paired-pulse median nerve SEP, somatosensory lateral inhibition during simultaneous stimulation of the digital nerves of the thumb and index finger, and measures of early and late HFO during the N20/P25 components of the SEP. Logistic regression analysis was then used to test which of these measures contributed to the variance of STDT.

3.2 Materials and methods

3.2.1 Subjects

A total of 19 consecutive patients with a diagnosis of idiopathic isolated CD according to current criteria (Albanese et al 2013) were prospectively recruited from those attending the outpatient clinics at the Sobell Department of Motor Neuroscience and Movement Disorder, Institute of Neurology, University College London, London, UK. Patients were assessed at least 3 months after their last BoNT injection, and their disease severity was assessed with the TWSTRS. A total of 19 HC with similar age and gender distribution and no reported family history for any neurological disorders, including dystonia, were recruited. Additional exclusion criteria for both patients and HC were (1) no history of other neurological or psychiatric diseases, (2) no history of medications acting on the central nervous system, and (3) no symptoms or signs suggestive of peripheral neuropathy. All subjects were all right-handed³⁰² and they signed a written informed consent before the experimental session. All experimental procedures were approved by the local ethical committee and conducted in accordance with the Declaration of Helsinki and according to international safety guidelines.

3.2.2 Somatosensory temporal discrimination threshold

STDT was investigated with an ascending method³⁰³. Paired stimuli starting with an ISI of 0 milliseconds (simultaneous stimuli) and progressively increasing the ISI (in 10 milliseconds steps) were consecutively delivered over the right index finger according to the experimental procedures used in previous studies^{70, 164}. To maintain participants' attention and to minimize the risk of perseverative responses, random catch trials (single stimulus) occurred at least once in each of the ascending series¹⁶⁴. Each stimulus consisted of a square-wave electrical pulse with a width of 0.2 milliseconds delivered with a constant current stimulator (Digitimer DS7A, Digitimer Ltd, Welwyn Garden City, UK) through surface skin electrodes (5 mm in diameter; Neurospec GA, Stans, Switzerland); both were placed on the terminal phalanx of the tested finger, with the anode located distal to the cathode and the distance of the edges of the two electrodes being 5 mm. The stimulation intensity was defined for each participant by delivering a series of stimuli at increasing intensity from 2 mA in steps of 0.5 mA; the intensity used for STDT was the minimal intensity perceived by the participant in 10 of 10 consecutive stimuli. Participants were asked to report verbally whether they perceived a single stimulus or two temporally separated stimuli. The first (i.e. lowest) of three consecutive ISI at which participants recognized the stimuli as temporally separated was considered the STDT. The intertrial interval was dependent on the subjects' response time (around 3 s). Each session comprised three separate blocks. The STDT was defined as the average of the three STDT values (i.e. 1 for each block) and entered in the analysis.

3.2.3 Somatosensory evoked potentials recording and analysis

We evaluated the P14 and N20 SEP amplitude and latency, the SEP recovery cycle, and the spatial inhibition ratio (SIR). The experimental protocol is described in figure 3.1.

SEP were recorded from scalp silver/silver-chloride (Ag/AgCl) surface electrodes arranged according to the international 10 to 20 system of EEG electrode placement²⁸⁰. To record the N20/P25 component, the active electrode was placed at Cp3 and the reference electrode at Fz, while the P14 component was recorded with the active electrode at Fz and the reference on the contralateral mastoid³⁰⁴. Digital nerves of right thumb (T) and index (I) fingers were stimulated with a constant current stimulator (Digitimer DS7A) through ring electrodes (Technomed Europe, The Netherlands); these were adjustable, metal noose electrodes with separate leadwires. The cathode was placed at the base of the first phalanx and the anode was placed 2 cm distal to the cathode¹⁶⁵. Monophasic square wave pulses of 200 microseconds duration were delivered at 250% of the sensory threshold (defined as the lowest current intensity at

which the subject could perceive the stimulus in five out of five trials) and at a frequency of 5 Hz. Recordings were collected at a sampling rate of 5 KHz, beginning 20 milliseconds before each stimulus and lasting for 100 milliseconds.

<u>Block/stimuli</u>	<u>Stimulation target</u>	<u>Analyses</u>
1000 square wave pulses (200 μ sec each) at 5 Hz	Index finger	SSEPs/HFOs
750 paired square wave pulses (200 μ sec each) given randomly at 5, 20 or 40 ms interstimulus intervals	Index finger	SSEPs recovery cycle
750 square wave pulses (200 μ sec each) at 5 Hz	Thumb finger	SSEPs from thumb (used to calculate SIR)
750 square wave pulses (200 μ sec each) at 5 Hz	Index/thumb fingers (simultaneous stimulation)	SSEPs SIR

Figure 3.1: *experimental protocol.*

Data were band-passed filtered from 3 Hz to 2 kHz³⁰⁴. Trials containing high-amplitude artefacts ($> 200 \mu\text{V}$) were automatically rejected. In the first block, 1000 sweeps were averaged; N20 peak latency and N20/P25 peak-to peak amplitude were measured. The recording from this block was also used to extract and measure HFO, as explained in the next paragraph. Three more recording blocks of 750 frames each were performed to measure the N20/P25 recovery cycle. In each, 750 trials were averaged and paired pulses at ISI of 5, 20, and 40 milliseconds were delivered. In the frames obtained using paired stimuli, the responses following the second stimulus were obtained by subtracting the SEP waveform obtained by the first stimulus from the waveform following each double stimulus. R5, R20, and R40 were defined as the ratio between the second and the first responses^{305, 306}. Finally, two more blocks of 750 trials each were recorded, the first stimulating the right thumb only and the second stimulating both the thumb and index finger concomitantly by giving two simultaneous stimuli delivered through two constant current stimulators. The SIR of N20/P25 (Q20) and P14 (Q14) was calculated as the ratio $\text{TI}/(\text{T} + \text{I}) \times 100$, where TI is the SEP amplitude obtained by simultaneous stimulation of the thumb and index finger and T+I is the arithmetic sum of the

SEP obtained by the individual stimulation of the two fingers ¹⁶⁵. In healthy volunteers, spinal, brainstem and cortical SEP to simultaneous dual inputs are expected to be smaller than the sum of each alone because of the lateral inhibition between the two inputs ¹⁶⁵.

3.2.4 Analysis of HFO

To extract HFO from the underlying wideband N20, the stimulus artifact was removed manually from -10 to 15 milliseconds to avoid ringing induced by filtering ³⁰⁷. The SEP wideband signal was bandpass, digitally filtered (400-800 Hz) and averaged. HFO waveform was divided in two components, namely e-HFO and l-HFO, separated by the latency of the N20 peak. Onset of e-HFO and offset of l-HFO were defined as the time point at which their amplitudes exceeded the averaged background noise level by three standard deviations ³⁰⁸; the signal was then corrected for direct current (DC) shift and rectified. e-HFO and l-HFO area under the curve were measured and analysed.

3.2.5 Statistical analysis

Given that some of the gathered variables did not distribute normally, non-parametric analyses, including the Mann–Whitney U-test and the Kruskal–Wallis test, along with the χ^2 test, were used, as appropriate to check differences between patients and HC. Correlations between variables were evaluated with the Spearman’s rank correlation coefficient. Finally, a logistic regression analysis with forward stepping (likelihood ratio method) was used to evaluate the major contributors to the variation in STDT. Thus, STDT (dependent variable) was dichotomized to the median value in HC. All significant variables in the bivariate analysis as well as those that have been demonstrated to influence the outcome (e.g age, dystonia) were included in the model with forward stepping until adding any further single variable did not improve the model.

3.3 Results

No side effects were recorded during the experimental sessions. Table 3.1 summarizes the demographic, clinical, behavioural and electrophysiological findings in patients and HC. There were no significant differences between rejected SEP trials in the two groups ($p > 0.05$).

	Healthy controls	Patients	<i>p value</i>
Age (years)	57.6 ± 14.5	62.6 ± 9.2	.21
Gender, F/M	7/12	10/9	.32
Handeness, R/L	19/0	19/0	-
Disease duration (years)	-	9.4 ± 4.7	-
Disease severity (TWSTRS score)	-	26.5 ± 3.7	-
STDT (ms)			
Mean values	80.1 ± 29.9	100.1 ± 25.3	0.03
Range	23.3-116.7	53.3-146.7	
SEP latency, ms			
N20 thumb	22.35 ± 0.9	22.71 ± 1.1	0.16
N20 index	22.96 ± 0.9	22.49 ± 1.1	0.12
P14 thumb	16.33 ± 0.6	16.41 ± 0.6	0.54
P14 index	16.48 ± 0.6	16.53 ± 0.6	0.44
SEP amplitude, μV			
P14 thumb	0.43 ± 0.1	0.41 ± 0.1	0.27
P14 index	0.55 ± 0.1	0.49 ± 0.1	0.26

	Healthy controls	Patients	<i>p</i> value
N20 thumb	0.71 ± 0.1	0.69 ± 0.1	0.31
N20 index	0.68 ± 0.1	0.65 ± 0.1	0.54
SEP P14 recovery cycle amplitude ratio, μV			
R5	0.54 ± 0.1	0.63 ± 0.1	0.02
R20	0.75 ± 0.1	0.79 ± 0.1	0.17
R40	0.91 ± 0.1	0.95 ± 0.1	0.02
SEP N20 recovery cycle amplitude ratio, μV			
R5	0.53 ± 0.16	0.68 ± 0.27	<0.01
R20	0.71 ± 0.13	0.82 ± 0.89	<0.01
R40	0.91 ± 0.05	0.91 ± 0.05	<0.01
Sensory lateral inhibition amplitude ratio, μV			
P14 sum	0.91 ± 0.2	0.89 ± 0.2	0.45
P14 pair	0.69 ± 0.1	0.84 ± 0.2	<0.01
Q14	0.72 ± 0.1	1.03 ± 0.1	<0.01
N20 sum	1.31 ± 0.2	1.29 ± 0.3	0.18

	Healthy controls	Patients	<i>p</i> value
N20 pair	0.89 ± 0.2	1.27 ± 0.2	<0.01
Q20	0.73 ± 0.1	1.09 ± 0.1	<0.01
HFOs area amplitude, μV			
Early	3.9 ± 1.1	3.2 ± 0.9	0.02
Late	3.9 ± 1.5	3.2 ± 0.9	0.09

Table 3.1: summary of clinical and electrophysiologic features in patients and healthy controls. Significant differences are expressed in bold. *F*, female; *M*, male; *R*, right; *L*, left; *HFO*, high-frequency oscillations; *ms*, milliseconds; *mV*, microvolts; *R*, recovery cycle; *SSEP*, somatosensory evoked potential; *SIR*, spatial inhibition ratio; *STDT*, somatosensory temporal discrimination threshold; *TWSTRS*, Toronto Western Spasmodic Torticollis Rating Scale.

In summary, *STDT* was significantly higher in patients than HC (100.1 ± 25.3 vs 80.1 ± 29.9 , respectively, $p = 0.03$). Many of the sensory electrophysiological measures of temporal inhibition were also abnormal in patients. When compared with HC, paired-pulse SEP data showed reduced P14 suppression at ISIs of 5 and 40 milliseconds, whereas N20 suppression was reduced at all ISI (i.e. 5, 20, and 40 milliseconds). Electrophysiological measures of spatial inhibition following simultaneous stimulation from the thumb and index finger were also reduced. In patients, the P14 and N20 SEP responses elicited by dual stimulation were larger than the expected sum of each alone, whereas this was not the case in HC (figure 3.2).

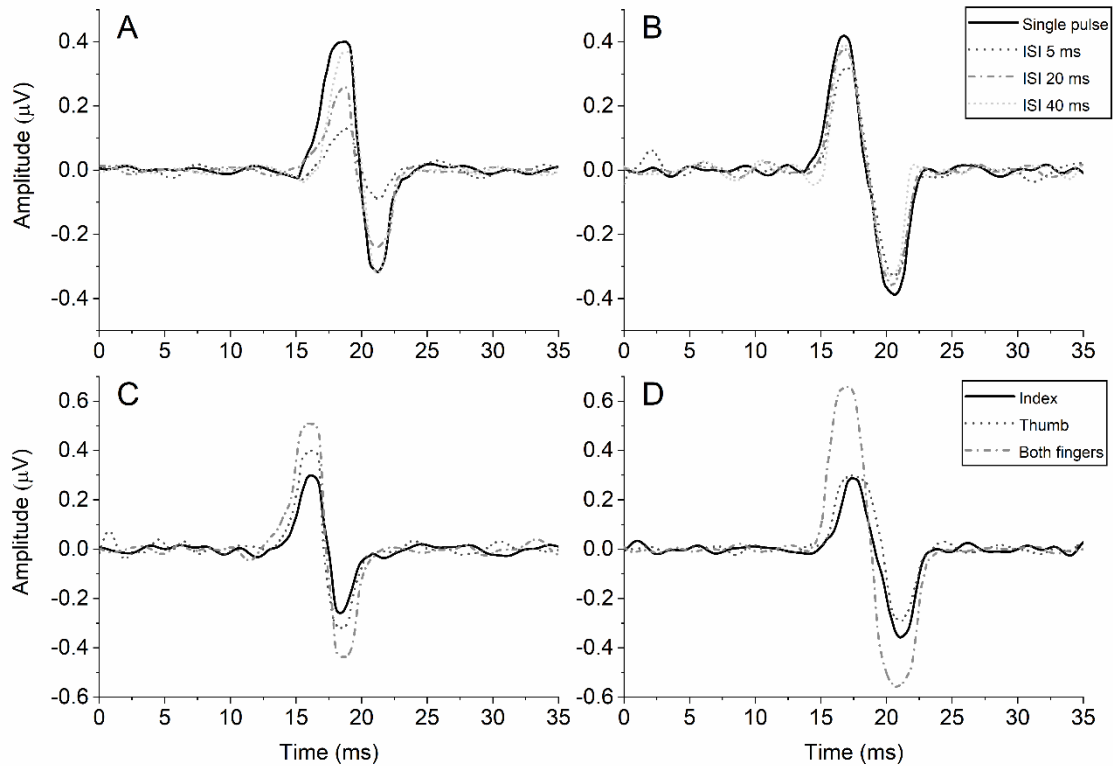


Figure 3.2: example of paired-pulse somatosensory evoked potentials (SEP; upper row) and surround inhibition ratio (lower row) measured on the N20 wave in one healthy participant (panels A and C) and in a patient with dystonia (panels B and D). SEP recorded from dystonic patient show less paired-pulse inhibition at all ISI and less suppression when the thumb and index finger were stimulated at the same time when compared with the healthy participant. The signals were band-passed between 20 and 500 Hz for visualization purposes. ISI, interstimulus interval; μV , microvolts; ms, milliseconds.

The e-HFO area was smaller in patients than HC, whereas there was a nonsignificant tendency for l-HFO to be smaller in patients. In both the HC and patients, there was a strong correlation between STDT and N20/P25 suppression at an ISI of 5 milliseconds (Spearman's rho 0.73, $p = 0.001$ and 0.80, $p < 0.001$, HC and patients respectively) and between STDT and l-HFO area (Spearman's rho -0.73, $p = 0.001$ and -0.78, $p < 0.001$, HC and patients respectively). In addition, N20/P25 suppression at an ISI of 5 milliseconds was correlated with l-HFO area (Spearman's rho 20.84 and 20.81, HC and patients, respectively, both $p < 0.001$; figure 3.3). There were no significant correlations with any of the other physiological measures. There were also no correlations between STDT and disease duration ($r = -0.230$, $p = 0.344$) or severity in the patient group as assessed by the TWSTRS ($r = 0.289$, $p = 0.229$). Finally, the logistic regression model showed that reduced N20 suppression at an ISI of 5 milliseconds

(coefficient 67.33; $p < 0.01$), smaller l-HFO area (coefficient -11.05; $p < 0.01$), and (dystonia) group (coefficient 9.62; $p < 0.05$), were independently associated with higher STDT, explaining a variance of 64% ($R^2 = 0.64$). The Hosmer–Lemeshow goodness-of-fit test supported our regression model as being valid.

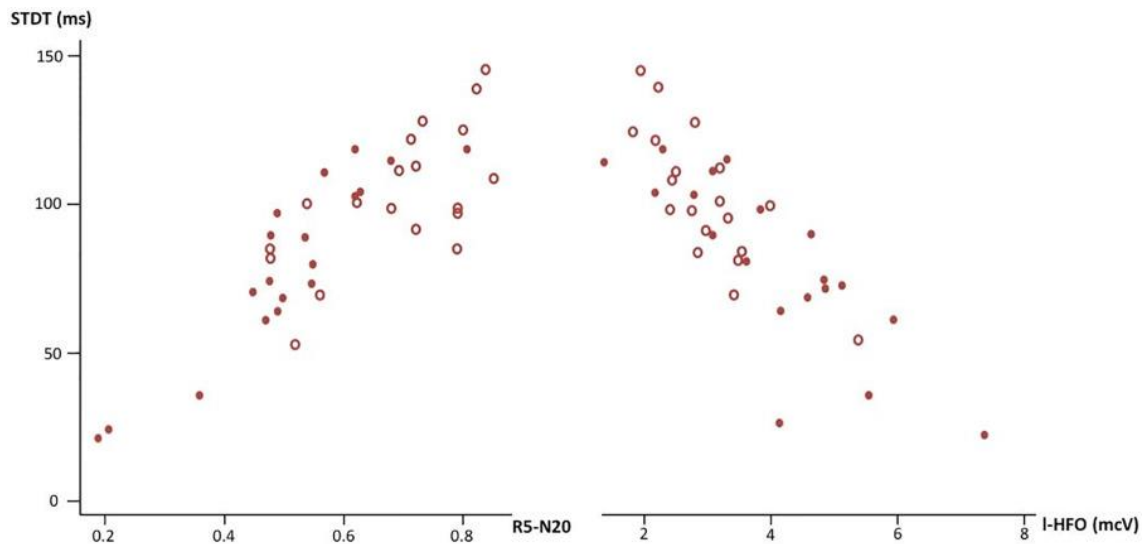


Figure 3.3: correlations between somatosensory temporal discrimination threshold (STDT) and somatosensory evoked potentials suppression at an interstimulus interval of 5 milliseconds (left panel) and l-HFO (right panel) in healthy participants (red dots) plain circles and patients (blue dots) empty circles. l-HFO, late high-frequency oscillations; R5-N20, recovery cycle at 5 milliseconds interstimulus interval for the N20/P25 component. CD: patients with cervical dystonia; HC: healthy controls.

3.4 Discussion

In line with previous studies, we found higher STDT in patients than in HC^{60, 61, 70, 72, 73, 202, 295-297}. The fact that we observed abnormal STDT in non-dystonic body regions, together with the lack of correlation between STDT and dystonia severity further confirms the notion that higher STDT in patients is not merely a consequence of overt manifestations of dystonia^{61, 296}.

Our mean STDT values in both HC and patients were slightly higher than reported in some previous studies^{60, 70, 78, 296, 309}. Several factors could contribute to this, including the older age of our cohorts as well as the different procedures that have been used in different studies (i.e. ascending or descending method, use of different intensity for the stimuli,

assessment of uni- vs multimodal temporal discrimination threshold, etc.). In line with this, Giersch and colleagues³¹⁰ demonstrated that temporal discrimination threshold obtained using different protocols/equipment are only comparable within each individual experimental paradigm.

In a previous study, Tamura and colleagues²⁰² found that patients with FHD had reduced suppression of the P27 component of the SEP following pairs of stimuli at 5 milliseconds, but not at other ISI. The aim of the present study was to extend those findings to another focal dystonia group, further probing other electrophysiological measures of somatosensory inhibition at cortical and subcortical levels. The present results confirm that paired-pulse suppression of the N20/P25 at ISI of 5 milliseconds (that is equivalent to the P27 of Tamura and colleagues because we measured the same peak-to-peak N20/P27 SEP component) was reduced in patients when compared with the control group. We also observed a reduced suppression at ISI of 20 and 40 milliseconds, which were not evident in the previous study²⁰². This may be a result of the fact that our SEP were elicited by stimulation of the digital nerves of the index finger rather than the median nerve at the wrist. The smaller SEP from digital stimulation may be in fact more sensitive to changes in cortical inhibition. Moreover, reduced suppression at ISI of 20 and 40 milliseconds, but not at shorter ISIs, has already been reported in patients with segmental and generalized dystonia³¹¹. SEP suppression of the N20/P25 at short intervals (ISI of 5 milliseconds) is thought to be primarily of cortical origin^{182, 305, 312, 313}, whereas suppression at longer ISIs (ie, ISI of 20 and 40 milliseconds) is reported to be mediated by inhibitory postsynaptic interneurons within the dorsal column nuclei and the thalamus (ventral posterolateral nucleus)³¹⁴. The evidence that abnormal processing of paired-pulse SEP occurs in dystonia also at the subcortical levels is supported by the fact that we found reduced suppression of the SEP P14 component. In fact, suppression of the P14 component of the SEP is also of subcortical origin, reflecting inhibitory activity within the dorsal columns - lemniscus medialis³¹⁴.

As to lateral inhibition, we found a significant difference between dystonic patients and HC, which was not obvious in the study by Tinazzi and colleagues¹⁶⁵. Given that lateral inhibition is mediated by intracortical connections within a limited range³¹⁵ and that contiguous fingers are represented adjacently in S1³¹⁶, it is likely that inhibition is stronger when tested in adjacent fingers. Thus, the significant difference we found between the two groups might be accounted for by the fact that we tested lateral inhibition stimulating the thumb and index finger rather than two non-contiguous fingers as in the study by Tinazzi and colleagues. In addition, the difference in the sample size (19 vs 7 patients) might also explain

the different result. Overall, differences in SEP between patients and controls were observed in both temporal and spatial domains, suggesting a widespread deficit of sensory processing. However, the latter finding (impaired SIR) did not correlate with abnormal STDT, suggesting that increased STDT in dystonia is not merely owing to abnormal cortical activity, but is the result of specific abnormalities within circuits processing the temporal aspects of afferent inputs.

Finally, we found reduced e-HFO area in patients and a similar non-significant trend for l-HFO. HFO are low-amplitude, high-frequency wavelets superimposed on the N20 and P25 waves, with their early component suggested to represent activity from thalamocortical fibres projecting mainly to area 3b and 1 within S1, whereas the late component represents activity of S1 inhibitory interneurons³⁰⁰. In line with our results, a previous study in patients with CD found HFO to be reduced²⁹⁹. Hence, dystonic patients tend to have decreased inhibition at several levels of the somatosensory system when compared with HC.

While performing the neurophysiological investigations, we took great care to ensure that both patients and HC were seated comfortably and quietly to avoid the occurrence of involuntary movements, but we cannot entirely exclude that intermittent head movements in dystonic patients might have played a minor role in reducing inhibition within the sensory system because it is well known that movement gates sensory access to cortex^{317, 318}. Despite several differences found between the patients and control at both the cortical and subcortical levels, only the suppression of the N20/P25 at 5 millisecond ISI and the l-HFO individually correlated with STDT and were independently associated with STDT in the logistic regression model. These measures probably rely on local inhibition within S1^{182, 300, 305, 312, 313, 319}. Interestingly, both N20/P25 suppression and l-HFO are measures of temporal inhibition and, therefore, these inhibitory circuits within the S1 might act to sharpen the distinction between the first and the second afferent inputs in STDT¹⁶⁴.

The regression analysis indicated that a separate factor “dystonia group” was predictive of higher STDT. This suggests that there are one or more additional factors over and above our measures of cortical somatosensory inhibition that contributes to higher STDT in patients. This is somewhat supported by the fact that the regression model only explained 65% of the variance, indicating that other factors contribute to the behavioural performance. Previous imaging studies exploring abnormal STDT in dystonia have found somewhat contradictory results, reporting structural and functional abnormalities either at the subcortical (putamen)^{71, 72} and cortical (middle frontal, precentral, and postcentral giri) level^{72, 301}. We cannot conclude with any certainty whether the reduced inhibition in S1 developed secondarily to pathology in

the basal ganglia or occurred independently. This is consistent with the idea that dystonia should be construed as a network disorder, with higher STDT in dystonia being largely, but not completely, explained by reduced cortical inhibition^{71,72}. Abnormal activity within the basal ganglia^{320,321} might play an additional role in modulating STDT. Inhibitory mechanisms within S1 might theoretically represent a therapeutic target to reverse abnormal STDT in dystonia, as previously suggested^{74,208}. It remains to be seen whether targeting the cortical node of the sensorimotor network with the aim to increase inhibition efficacy will in turn ameliorate overt manifestations of dystonia.

4 High frequency somatosensory stimulation increases sensorimotor inhibition and leads to perceptual improvement in healthy subjects

4.1 Introduction

In a second set of experiments, we used a form of peripheral nerve stimulation, namely High-Frequency Repetitive Somatosensory Stimulation (HF-RSS), in an attempt to manipulate somatosensory function in HC, possibly by acting on intracortical inhibition mechanisms. Godde and coworkers²⁷⁵ were the first to demonstrate in HC that HF-RSS improves two-point discrimination in the stimulated area of the skin in humans. Since previous animal experiments³²² showed that HF-RSS enlarges cutaneous receptive fields in rat somatosensory cortex, it might have been expected that HF-RSS in humans would reduce spatial discrimination. However, the latter does not strictly relate to the size of individual neuron receptive field, but instead reflects the information present in the discharge of a large number of neurons^{275, 322, 323}. More neurons activated in response to stimulation of an area of skin with overlapping, but distinct receptive fields would code spatial representation with higher precision than single neurons. HF-RSS also improves STDT³⁰³; however, the reason for this effect is unclear since it is difficult to explain how larger spatial receptive fields can influence temporal discrimination between stimuli. In a previous work using TMS we argued that temporal threshold depends on the effectiveness of short duration inhibition in the somatosensory system, which is used to sharpen temporal processing following the arrival of the initial sensory input¹⁶⁴. The aim of the present experiment was to test whether HF-RSS might improve STDT by enhancing this inhibitory effect. If so, it would imply that HF-RSS has two consequences, both of which are spatially limited to the area of stimulation: increased size of spatial receptive fields and increased effectiveness of somatosensory inhibition. In fact, it could be that both effects are complementary. Thus, increased spatial discrimination between stimuli would benefit both from larger receptive fields as well as increased effectiveness of inhibitory connections between adjacent fields. Similarly, increased temporal discrimination might benefit from engagement of larger numbers of neurons in temporal processing, along with an augmented efficacy of inhibitory connections between them. We therefore correlated changes produced by HF-RSS on spatial and temporal discrimination with our measures of somatosensory inhibition

(recovery of P14 and N20/P25 waves with paired-pulse somatosensory evoked potentials and area of HFO) to test its relative contribution to temporal and spatial discrimination. We used STDT as our measure of temporal discrimination. For spatial discrimination we employed two different tests: the “bumps” test, which is a simple measure of tactile threshold, and the JVP test, which is a more complex measure of spatial discrimination that assesses the ability to detect the orientation of a tactile grating. Lastly, since HF-RSS has been further shown to improve motor performance³²⁴⁻³²⁶, we also explored possible effects of HF-RSS on processing in M1, using measures of short intracortical inhibition (SICI, putatively mediated by GABA-A receptors) and intracortical facilitation (ICF, putatively mediated by glutamatergic excitation).

4.2 Materials and methods

4.2.1 Subjects

Fifteen right handed³⁰² HC (11 male, 4 female, average age 54.5) participated in the study. They had no history of any diseases related to the central or peripheral nervous system; they did not have metal or electronic implants and were not on medications acting on the nervous system. Subjects signed a written informed consent before the experimental session. The local institutional review board approved the experimental procedure, which was conducted according with the Declaration of Helsinki and common safety guidelines. All experimental procedures were approved by the local ethical committee and conducted in accordance with the Declaration of Helsinki and according to international safety guidelines.

4.2.2 Somatosensory temporal discrimination threshold

STDT was tested by administering paired electrical stimuli, with an initial ISI of 0 ms (simultaneous pair) that was progressively increased in steps of 10 ms^{74, 208, 327}. This ascending method has been reported to yield results similar to common psychophysical assessment²¹¹. Stimulation was delivered separately to the third phalanx of the right and left thumb and index finger using surface electrodes separated by 0.5 cm (anode placed distally than the cathode). Current was applied by means of a constant current stimulator (Digitimer DS7A) in the form of square-wave pulses. The intensity for STDT testing was the lowest at which each subject could perceive a tactile stimulus in 10 out of 10 consecutive trials^{74, 208}. This was obtained by stimulation of the left index finger starting from 2 mA and increasing the current in steps of

0.5 mA; on the other fingers, the current intensity was adjusted to match the perceived intensity on the left index finger. Before the actual testing subjects had to familiarize with the task, achieving a stable performance. During the procedure, they had to report if they perceived a single stimulus or two discrete stimuli. The first of three consecutive ISI at which subjects reported two stimuli was considered the STDT. Each session consisted of four separate blocks; we entered in the analysis the average of four STDT values (i.e. one for each block). To keep subjects' attention level constant during the test some "catch" trials, consisting of single stimuli, were delivered at random during the procedure.

4.2.3 Tactile tasks

TSD was measured using a set of JVP domes²⁸¹. Each dome is a circular, convex grating surface of 20 mm diameter, on top of a cylindrical handle 30 mm long. The set is made of eight domes with equidistant groove and bar widths ranging from 3.0 to 0.35 mm. Testing was performed according to previous recommendations²⁸¹. Subjects were required to judge the orientation of the grating (i.e. horizontal or vertical to the fingertip). The thinnest grating which was reliably detected 75% of the times provided an estimate of the spatial resolution, as previously suggested²⁸¹. We avoided using two-point discrimination as a measure of TSD because its threshold often falls under the receptor spacing^{218, 222, 328}. Thus, several investigators have questioned the validity of two-point discrimination as a measure of spatial acuity^{222, 329-331}, while grating orientation can be considered a more rigorous alternative³³². TT was tested using the Bumps device (Kennedy et al., 2011). It is a smooth surface divided into 12 squares, each containing 5 coloured circles, only one of which one has a circular bump in the middle. Bumps are 550 μm in diameter but have different height. The device consists of two such plates (plates A and B), which are identical but for bumps heights: the latter are 2.5 - 8 μm and 8.5 - 14 μm , on plate A and B, respectively (e.g., bump heights on each plate increases in 0.5 μm increments). Participants were asked to locate the bump in each square (testing order: plate B always first). Two trials were performed for each plate and TT was defined as the lowest bump such that it and the following two higher bumps were successfully detected in either trial, as previously described²²⁷. Both tests were done on the right and the left index finger.

4.2.4 Somatosensory evoked potentials recording and analysis

To record the N20/P25 component of SEP the active electrode was placed at CP3 and the reference electrode at Fz, while P14 was recorded with the active electrode at Fz and the

reference electrode on the contralateral mastoid ^{280, 304}. Digital nerves of the right index finger were stimulated with a constant current stimulator (Digitimer DS7A) through ring electrodes, with the cathode placed at the base of the first phalanx and the anode placed two cm distally ^{165, 333}. Stimulation was delivered at 250% of the somatosensory threshold and consisted of square wave pulses given every 0.2 s (5 Hz). Signal was recorded from -20 to 100 ms with regard to the pulse, digitized with a 5 KHz sampling frequency and band-pass filtered (3 Hz - 2 KHz) ³⁰⁴. In a first block, N20 peak latency, N20/P25 peak-to-peak amplitude and P14 baseline-to-peak amplitude were calculated after averaging of 1000 sweeps. This block was further used to extract and measure high frequency oscillations (HFO) (see below). We recorded three more blocks to measure N20/P25 and P14 recovery cycle. In each, paired pulses at 5, 20 and 40 ms ISI were delivered in three separate sequences. Each sequence was made of 750 trials, and the sequences were randomized. In the frames obtained using two stimuli, responses following the second stimulus were obtained by subtracting the SEP waveform obtained by the first stimulus from the waveform following each double stimulus ^{306, 334}. R5, R20 and R40 were calculated as the ratio between the second and the first response. The position of the electrodes was kept constant throughout the whole experiment and care was taken to always keep impedance below 5 K Ω . In a further experimental session, we recorded SEP by stimulation of digital nerves of the right thumb before and after HF-RSS applied on the right index finger. Recording and stimulation parameters were similar to those used for SEP from the right index finger; 750 trials were recorded.

4.2.5 High frequency oscillations analysis

To measure HFO from N20/P25 SEP component the pulse artefact was deleted from -10 to +5 ms to avoid ringing due to filtering ³⁰⁷. The SEP original signal was band-pass filtered (400–800 Hz) and averaged. HFO were divided in e-HFO and l-HFO, separated by the N20 peak. Onset of e-HFO and offset of l-HFO were defined as their amplitudes exceeding the averaged background noise level by three standard deviations ³⁰⁸. e-HFO and l-HFO area was measured and analysed.

4.2.6 Transcranial magnetic stimulation and electromyographic recording

EMG activity was simultaneously recorded using Ag/AgCl electrodes placed over the right first dorsal interosseous (FDI), abductor pollicis brevis (APB) and abductor digiti minimi

(ADM) muscles in a belly-tendon fashion. EMG signal was digitized at 5 kHz with a CED 1401 A/D laboratory interface (Cambridge Electronic Design, Cambridge, UK) and bandpass filtered (5 Hz - 2 kHz) with a Digitimer D360 (Digitimer Ltd., Welwyn Garden City, Hertfordshire, UK). Data were stored on a laboratory computer for on-line visual display and further off-line analysis (Signal software, Cambridge Electronic Design, Cambridge, UK). EMG activity was monitored throughout the experiment to ensure complete muscle relaxation. TMS was performed using a Magstim 200² monophasic stimulator with a 70 mm figure-of-eight coil (Magstim Company Limited, Whitland, UK). First, the motor hotspot was found, defined as the site within M1 where the largest MEP in the APB could be obtained. Then, we found the resting motor threshold (RMT), active motor threshold (AMT), and the intensity able to elicit motor evoked potentials of approximately 1 mV amplitude from APB muscle (1 mV-int), which was later used for test pulses. RMT was defined as the lowest intensity able to evoke a MEP of at least 50 μ V in five out ten consecutive trials during rest³³⁵, while AMT was defined as the lowest intensity where a MEP of at least 200 μ V in five out ten consecutive trials could be obtained during a 10 - 15% voluntary activation of the target muscle³³⁶. SICI was obtained through a paired-pulse TMS, with an ISI of 3 ms between the first, conditioning stimulus and the second test stimulus. The test stimulus was set at 1 mV-int, while the conditioning stimulus was set at 70%, 80% and 90% AMT, as to obtain a recruitment curve²⁴⁷. Twenty paired stimuli for each different intensity of the conditioning stimuli and twenty single stimuli were delivered in a randomized order. SICI was calculated dividing the amplitude of conditioned/unconditioned MEP. ICF was obtained in a similar fashion, except that the ISI used was 10 ms and the intensity of the conditioning stimulus was 80% AMT²⁴⁷. Twenty paired stimuli were given during the same recording block used for SICI. ICF was obtained dividing the amplitude of conditioned/unconditioned MEP.

4.2.7 Experimental Procedure

Subjects underwent four measurements at baseline (T0), and specifically I – TSD and TT, II – STDT, III – SEP, IV – TMS. After the baseline evaluation, subjects underwent a single session of HF-RSS, and then repeated the four baseline measurements after the end of HF-RSS (T1). The sequence of measures I to IV was counterbalanced both at T0 and T1 and across subjects. Notice that at T1 the current intensity used for STDT testing was adjusted to match the intensity perceived at T0. Before application of HF-RSS it was ensured that subjects practiced the behavioural tests (STDT, TSD, TT) until a stable performance was reached.

4.2.8 Statistical analysis

Two three-way repeated measures ANOVA were used to evaluate the effect of HF-RSS on the current intensity used to test STDT and on STDT values using as factors of analysis “time” (T0, T1), “side” (right, left) and “finger” (thumb, index finger). Several dependent t-tests were used to evaluate the effect of HF-RSS on the latency and amplitude of N20/P25 and P14 recorded from the right thumb and right index finger. Two two-way repeated measures ANOVA with “time” (T0, T1) and “ISI” (R5, R20, R40) as factors of analysis were performed to investigate the effect of HF-RSS on N20/P25 and P14 recovery cycle. Two dependent t-tests were also performed to assess the effect of HF-RSS on N20 formed to compare changes induced by HF-RSS on the two waves (T1/T0 ratios). Two dependent t-tests were used to investigate possible effects of HF-RSS on e-HFO and l-HFO. Two different two-way repeated measures ANOVA with “time” (T0, T1) and “side” (right, left) were used to investigate possible effects of HF-RSS on bumps and domes tests. To explore possible correlations between baseline STDT measured on the right index finger, e-HFO area, l-HFO, SEPs recovery cycle, TSD and TT, Pearson’s correlation test was used. Correlation was also tested between electrophysiological variables and current intensity to elicit SEP from the right index finger to exclude intensity-related effects. The same test was used to investigate whether changes induced by HF-RSS on the same parameters from T0 and T1 were correlated. A three-way repeated measures ANOVA with “time” (T0, T1), “muscle” (FDI, APB, ADM) and “condition” (test pulse, SICI 70%, SICI 80%, SICI 90%, ICF) as factors of analysis was used to disclose possible effects of HF-RSS on SICI and ICF. Normality of distribution was assessed with the Shapiro-Wilks’ test, while Greenhouse-Geisser correction was used, if necessary, to correct for non-sphericity (i.e. Mauchly’s test < 0.05). P values < 0.05 were deemed significant. Bonferroni post-hoc test was used for post-hoc comparisons.

4.3 Results

Current intensity used to elicit SEP from the right index finger was 6.99 ± 1.65 mA, while the intensity for HF-RSS was 5.13 ± 2.02 mA (average \pm standard deviation).

4.3.1 Somatosensory temporal discrimination threshold

There was no significant difference in the threshold for perception of the electrical stimulus in the thumb and index finger in both sides (left and right) and at both time points (T0 and T1). As reported previously³⁰³, HF-RSS improved STDT in a spatially specific manner. This was confirmed by the 3-way ANOVA which revealed a significant “time × side × finger” interaction [F(1,14) = 8.823; p = 0.01] as well as significant interactions of “time × side” [F(1,14) = 35.681; p < 0.001] and “time × finger” [F(1,14) = 8.172; p = 0.013]. There was a significant main effect of “time” [F(1,14) = 14.624; p = 0.002], but not for “side” [F(1,14) = 1.104; p = 0.311] or “finger” [F(1,14) = 2.085; p = 0.171]. Post-hoc analyses showed that STDT significantly decreased in the right index finger from T0 to T1 (87.62 ± 36.01 vs. 68.60 ± 37.13; p < 0.001), while it remained unchanged in the other fingers (figure 4.1).

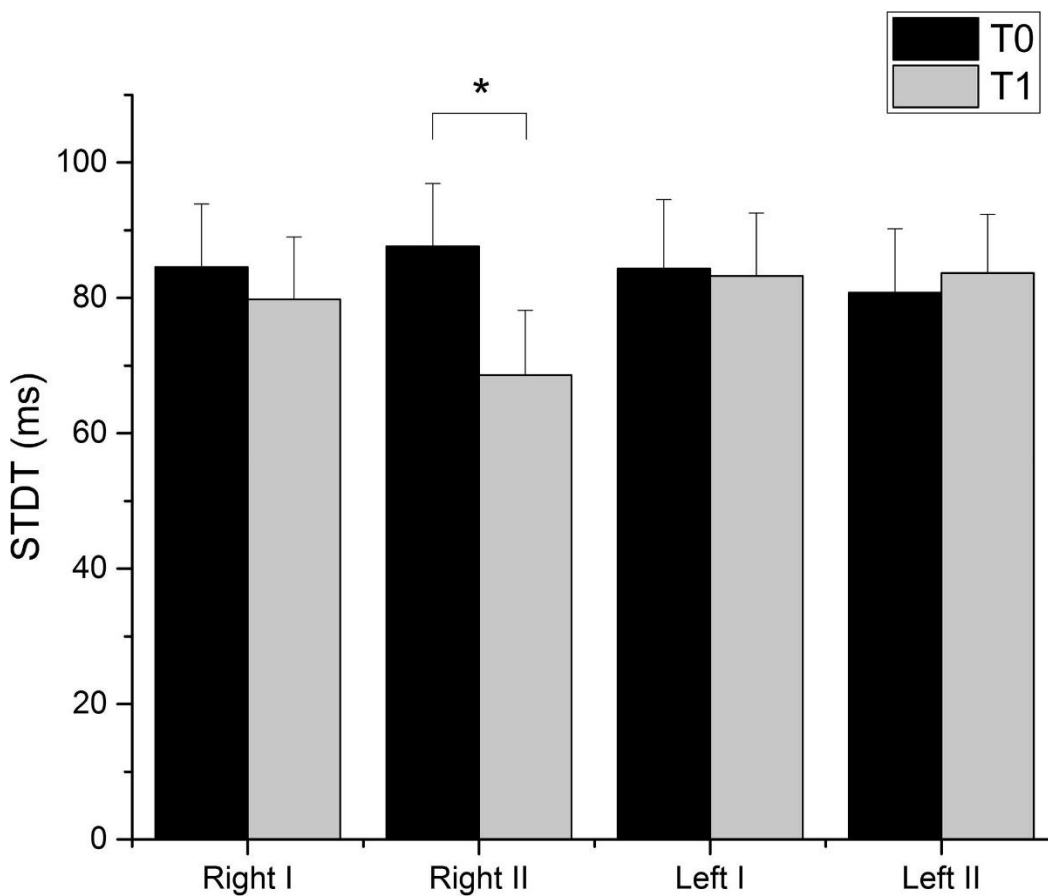


Figure 4.1: STDT values obtained from the thumb (I) and the index finger (II) of both hands before (T0) and immediately after (T1) HF-RSS applied on the right index finger. HF-RSS produced a significant decrease of STDT tested on the right index finger only (p < 0.001). Asterisks indicate statistical significance. Error bars indicate standard error.

4.3.2 N20/P25 and P14 latency and amplitude

HF-RSS had no effect on the latency of these early SEP components recorded by the right index finger (p values of all t -tests > 0.05), but significantly increased their amplitude. Thus, HF-RSS significantly increased the amplitude of N20/P25 [$t(14) = -11.386$; $p < 0.001$] and P14 [$t(14) = -10.862$; $p < 0.001$] obtained by stimulation of the right index finger. This increase in amplitude occurred both in the baseline N20 [$t(14) = -6.154$; $p < 0.001$, 0.30 ± 0.04 vs 0.33 ± 0.09] and baseline P25 [$t(14) = -7.490$; $p < 0.001$, 0.35 ± 0.05 vs 0.40 ± 0.11] measurement, and the changes induced in the two components were not significantly different (1.19 ± 0.14 vs 1.22 ± 0.11 for N20 and P25 respectively), [$t(14) = -0.868$; $p = 0.4$]. No changes were observed in N20/P25 and P14 amplitude recorded while stimulating the right thumb (all $p > 0.05$) (figure 4.2). HF-RSS had no effect on P14 and N20/P25 latency and amplitude recorded by stimulation of the right thumb (all p values > 0.05).

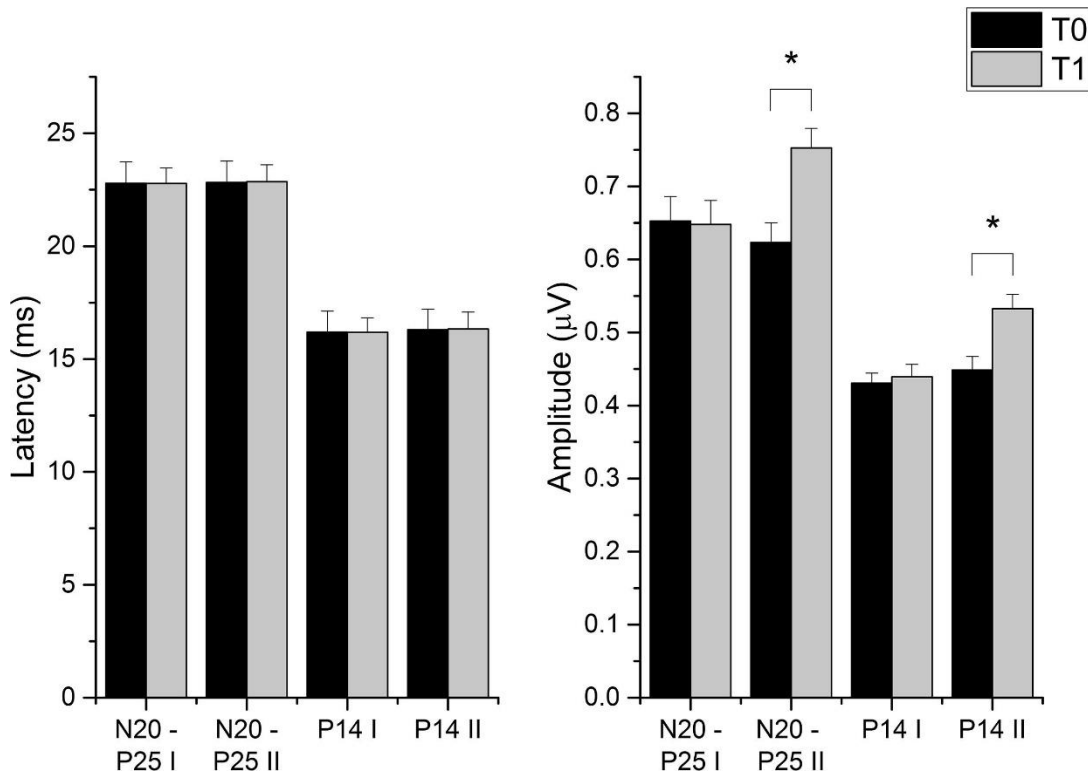


Figure 4.2: latency and amplitude of N20/P25 and P14 components of SEP obtained by stimulating the thumb (I) and the index finger (II) of the right hand before (T0) and immediately after (T1) HF-RSS applied on the right index finger. HF-RSS induced an increase in the amplitude of N20/P25 ($p < 0.001$) and P14 ($p < 0.001$) SEP components obtained from stimulation of the index finger but not the thumb. No changes in N20 or P14 latency were observed. Error bars indicate standard error. Asterisks indicate statistical significance. Error bars indicate standard error.

4.3.3 N20 and P14 recovery cycle

HF-RSS increased the amount of inhibition produced by the first stimulus of the pair on both the N20/P25 and P14 components. Thus, the recovery cycle was suppressed at all three intervals tested (figure 4.3). This was confirmed in the two way ANOVA on N20/P25 amplitude which showed a significant main effect of “time” [$F(1,14) = 70.02$; $p < 0.001$] and “ISI” [$F(1.479,17.234) = 38.816$; $p < 0.001$] and a significant interaction of “time \times ISI” [$F(1.949,27.282) = 4.014$; $p = 0.031$]. Post-hoc comparisons showed that inhibition increased from T0 and T1, and this was true for R5 (0.53 ± 0.19 vs. 0.37 ± 0.16 ; $p < 0.001$), R20 (0.72 ± 0.11 vs. 0.52 ± 0.12 ; $p < 0.001$) and R40 (0.92 ± 0.06 vs. 0.67 ± 0.14 ; $p < 0.001$) (figure 5). Similarly, the two-way ANOVA on P14 amplitude showed a significant main effect of “time” [$F(1,14) = 59.48$; $p < 0.001$] and “ISI” [$F(1.540,21.561) = 136.85$; $p < 0.001$] and a significant interaction of “time \times ISI” [$F(1.618,22.649) = 5.883$; $p = 0.012$]. Again, post-hoc comparisons showed an increase in inhibition from T0 and T1 for R5 (0.56 ± 0.15 vs. 0.40 ± 0.09 ; $p < 0.001$), R20 (0.78 ± 0.10 vs. 0.55 ± 0.08 ; $p < 0.001$) and R40 (0.92 ± 0.04 vs. 0.80 ± 0.06 ; $p < 0.001$) (figure 4.3).

4.3.4 Early and late high-frequency oscillations

The paired t-tests showed a significant increase of e-HFO [$t(15) = -5.860$; $p < 0.001$] and l-HFO [$t(15) = -5.279$; $p < 0.001$] after RSS (figure 4.4).

4.3.5 Tactile tasks

The two-way ANOVA on the bumps test showed a significant main effect of “time” [$F(1,14) = 16.227$; $p = 0.001$], a non-significant effect of “side” [$F(1,14) = 1.720$; $p = 0.211$] and a significant interaction of “time \times side” [$F(1,14) = 18.026$; $p = 0.001$]. Post hoc analyses showed that HF-RSS significantly reduced tactile threshold (TT) from T0 to T1 in the right hand (6.43 ± 0.59 vs. 4.80 ± 0.56 ; $p = 0.001$), while there was no effect on the left hand (6.35 ± 0.58 vs. 6.43 ± 0.60 ; $p > 0.05$). By contrast, performance on the JVP domes (tactile spatial discrimination, TSD) did not change after HF-RSS (all p values > 0.05) (figure 4.5).

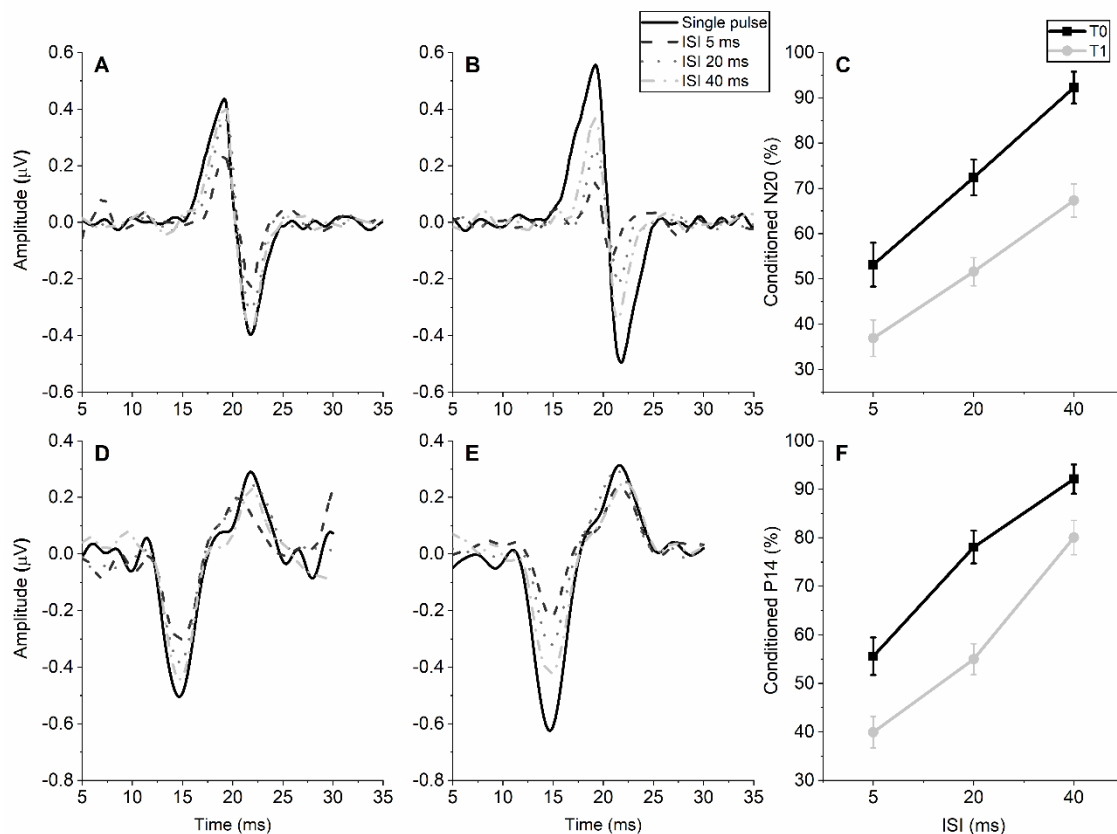


Figure 4.3: recovery cycle of N20/P25 (panels A, B, C) and P14 (panels D, E, F) components of SEP at ISIs of 5, 20 and 40 ms before (T0) and immediately after (T1) HF-RSS applied on the right index finger. HF-RSS increased the amplitude of unconditioned N20/P25 and P14 whereas it decreased the amplitude of PP-SEP (thus increasing the effectiveness of inhibition). For visualization purposes the raw signal was band-passed between 20 and 500 Hz. Artefact from electric stimulus (at 0.05 s) was removed. Error bars indicate standard error.

4.3.6 Correlation between the effect of HF-RSS on STDT and neurophysiological – behavioural measures

There was a strong correlation between changes induced by HFRSS in physiological measures of inhibition of the N20/P25 and l- HFO and in STDT (figure 4.6). The correlations were marginal for TT, and not significant for TSD. There was no correlation between current intensity to elicit SEP from the right index finger and any of the electrophysiological variables. At baseline (i.e. T0) there were significant correlations between STDT and R5 of the N20 ($r = 0.830$; $p < 0.001$); STDT and l-HFO area ($r = -0.887$; $p < 0.001$); and R5 (N20) and l-HFO area ($r = -0.690$; $p = 0.004$). In addition, the changes induced by HF-RSS in STDT were significantly correlated with the changes induced by HF-RSS on R5 (N20) ($r = 0.795$; $p < 0.001$) and on l-HFO area ($r = 0.746$; $p = 0.001$).

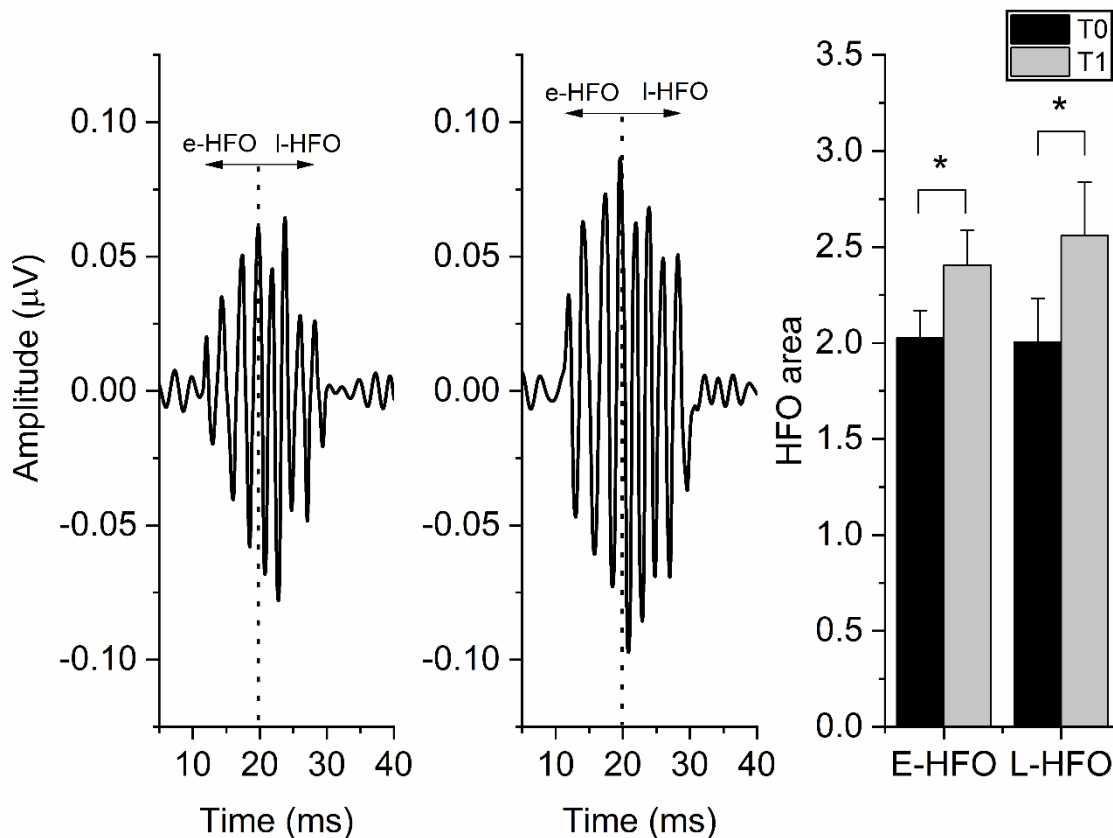


Figure 4.4: HFO area before (left panel, T0) and immediately after (middle panel, T1) HF-RSS applied on the right index finger. HF-RSS induced a significant increase of both early ($p < 0.001$) and late HFO ($p < 0.001$). HFO area in the right panel is expressed in $\mu V^2 \times 10^{-4}$. Artefact from electric stimulus (at 0.05 s) was removed. Asterisks indicate statistical significance. Error bars indicate standard error.

There was also a significant correlation between changes induced in R5 and in l-HFO ($r = 0.765$; $p = 0.001$). Despite a correlation between e-HFO and l-HFO was found ($r = 0.695$, $p = 0.04$), correlation between STDT and e-HFO was not significant ($r = -0.417$, $p = 0.122$). No correlations were found between STDT and SEP recovery at ISIs other than 5 ms, and no correlation was found between STDT and e-HFO. Notably, the changes induced by HF-RSS on R5 of the N20/P25 and P14 were not correlated. Neither was there any correlation between STDT and P14 recovery at any of the ISI explored. STDT was not correlated with TSD assessed with the JVP domes test at any time point (all p values > 0.05). Although not significant, there was a trend towards correlation between the STDT and TT at T0 ($r = 0.466$, $p = 0.08$) and T1 ($r = 0.424$, $p = 0.074$), and also the changes induced on the two variables by HF-RSS showed the same tendency ($r = 0.466$, $p = 0.08$).

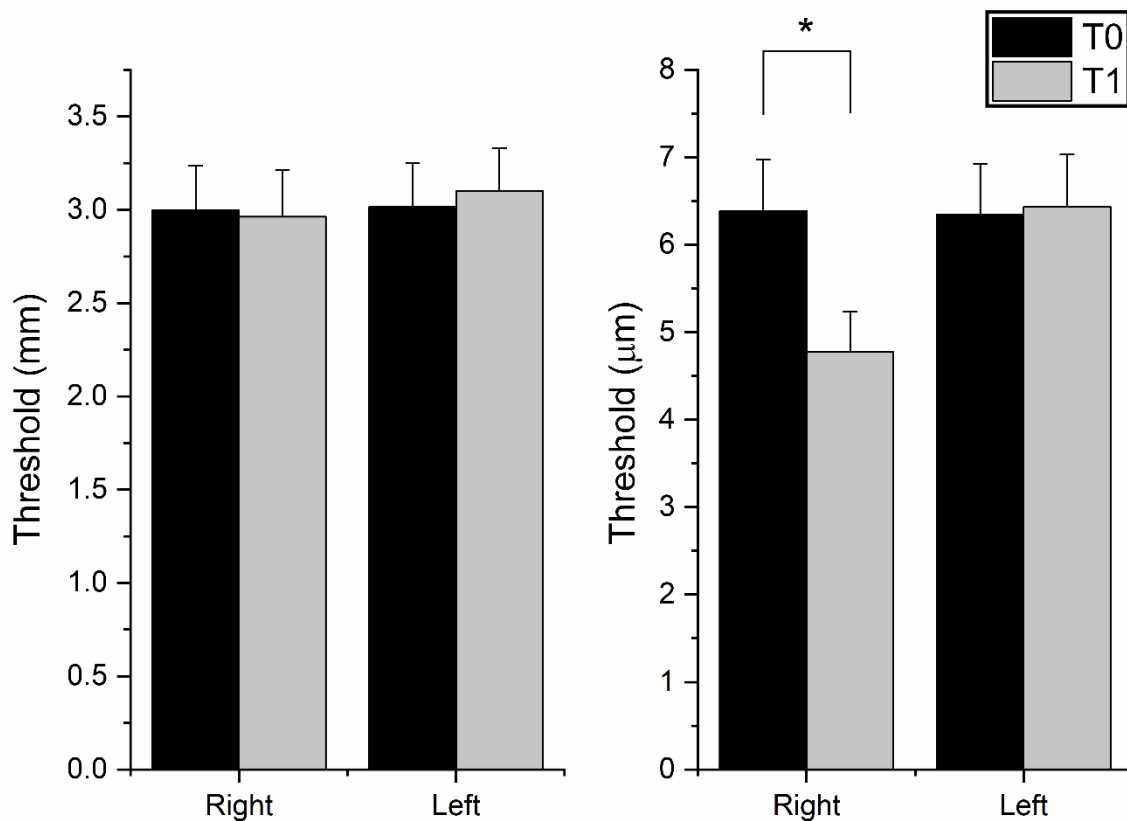


Figure 4.5: tactile spatial acuity assessed with the domes (left panel) and bumps (right panel) test before (T0) and immediately after (T1) HF-RSS applied on the right index finger. HF-RSS induced a significant decrease of threshold evaluated on the right index finger ($p = 0.001$), while no effect was observed on the contralateral index finger. By contrast, tactile threshold assessed by the domes test was not changed by HF-RSS on either side.

4.3.7 Effect of HF-RSS on inhibitory circuitry of the primary motor area

HF-RSS produced a focal increase of SICI in APB, but had no effect on other muscles nor on ICF (figure 4.7). The three-way ANOVA on SICI and ICF showed a non-significant main effect of “time” [$F(1,14) = 3.028$; $p = 0.104$], significant main effects of “muscle” [$F(1.907,26.702) = 33.952$; $p < 0.001$] and “condition” [$F(1.828,25.589) = 344.620$; $p < 0.001$] and significant interactions of “time \times muscle” [$F(1.761,24.658) = 3.771$; $p = 0.042$], “time \times condition” [$F(1.925,26.945) = 7.781$; $p = 0.002$], “muscle \times condition” [$F(2.938,41.135) = 136.131$; $p < 0.001$] and “time \times muscle \times condition” [$F(2.885,40.391) = 5.816$; $p = 0.002$]. Post hoc analyses showed that HF-RSS had no effect on unconditioned MEP, SICI and ICF recorded in FDI and ADM (all $p > 0.05$). On APB, by contrast, while HF-RSS had no effect on test MEP and ICF (all $p > 0.05$), the amount of SICI increased from T0 to T1 (i.e. there was

a decrease in the amplitude of the conditioned MEP), and this was true with a conditioning pulse set respectively at 70% (0.76 ± 0.10 mV vs. 0.63 ± 0.06 mV; $p < 0.001$), 80% (0.53 ± 0.10 mV vs. 0.43 ± 0.09 mV; $p < 0.001$), and 90% (0.38 ± 0.07 vs. 0.29 ± 0.09 ; $p < 0.001$) of AMT.

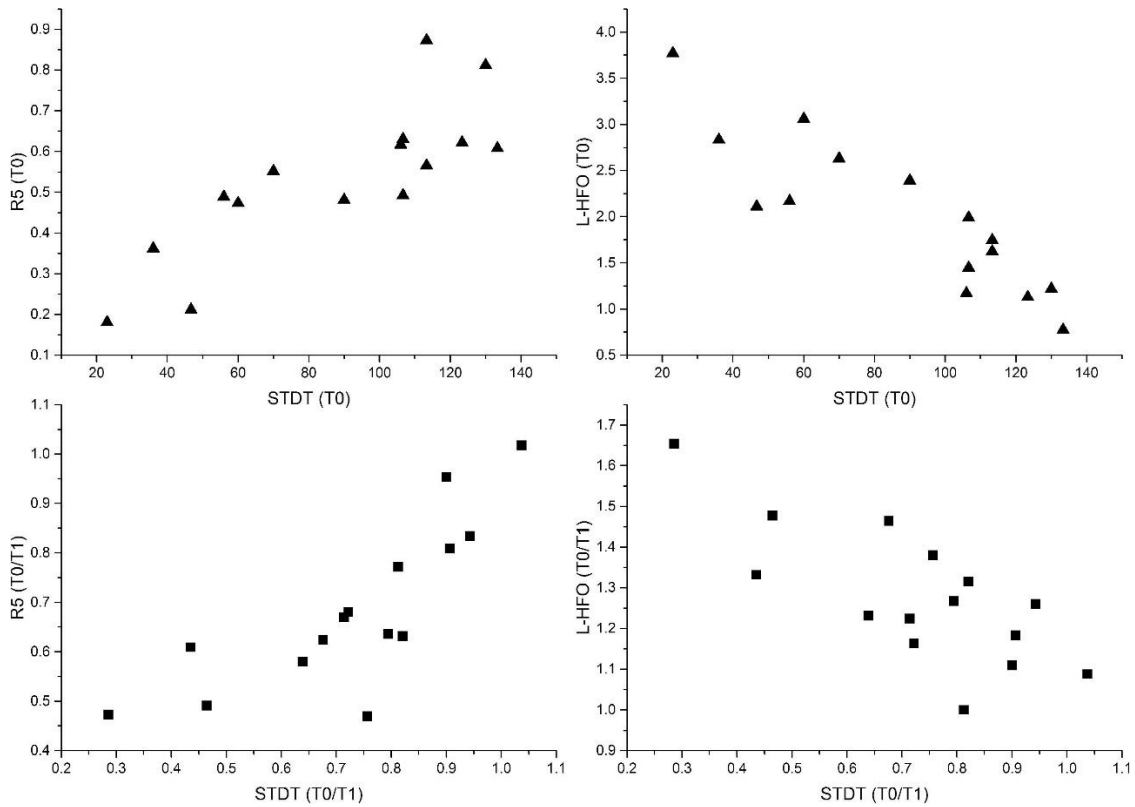


Figure 4.6: correlations between STDT, R5 and l-HFO. The upper panels show a significant correlation between baseline values of STDT and R5 (left) and between baseline values of STDT and l-HFO (right). There was also a significant correlation between the changes induced by HF-RSS on STDT and the changes induced, respectively, on R5 (left) and on l-HFO (right).

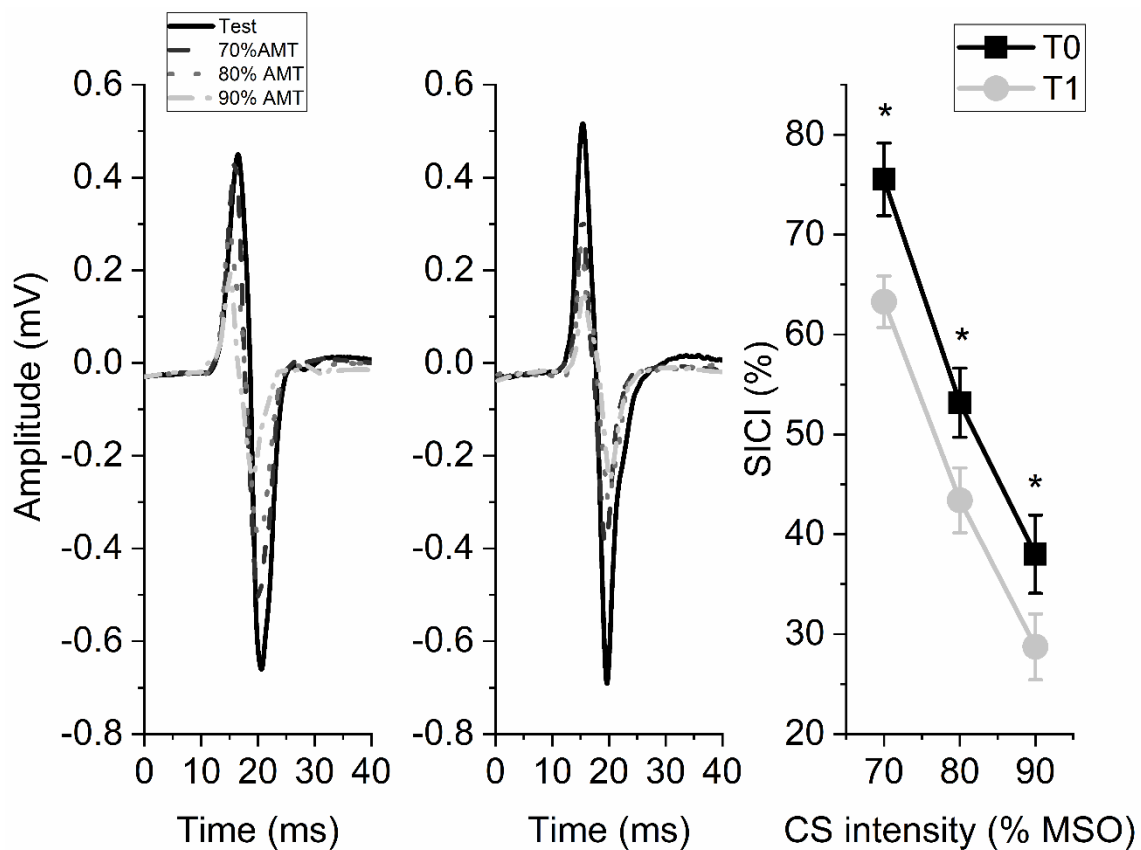


Figure 4.7: effect of HF-RSS on SICI on APB. Raw signal from a single subject before (left panel) and after (middle panel) on APB using different intensities of the conditioning TMS stimulus (CS) (70%, 80% and 90% of AMT). HF-RSS induced an increase in SICI irrespective of the strength of the conditioning TMS pulse (all p values < 0.001). Right panel shows SICI averaged among all subjects. Asterisks indicate statistical significance. Error bars indicate standard error.

4.4 Discussion

The present data show that the improvement in STDT produced by HF-RSS is associated with correlated increases in two measures of somatosensory inhibition (N20/P25 recovery curve and I-HFO area). HF-RSS also improved TT, as measured by the bumps test. Notably, the changes in STDT and TT were confined to the stimulated finger, which rules out any non-specific changes due to retest effect, impaired levels of alertness or attention. The fact that the improvement in TT was weakly correlated with changes in the somatosensory recovery curves may indicate that it partially depends on inhibitory interactions. However, there was no effect on TSD as assessed by the JVP domes, suggesting that HF-RSS may have less influence on more complex types of spatial processing. Surprisingly, HF-RSS also increased SICI in the

APB but not in other muscles, pointing to a focal transmission of HF-RSS effects to the motor system. Overall, we conclude that HF-RSS focally increased the excitability of inhibitory circuitry in the somatosensory system and that this sharpens temporal and some types of spatial processing. These effects are transmitted to M1.

4.4.1 Electrophysiological results

Somatosensory recovery curves reflect an inhibitory influence of the first stimulus on the response to the second stimulus. The present results suggest that HF-RSS increases the effectiveness of these interactions at both cortical and subcortical levels of the somatosensory afferent pathway. The N20 and P25 components of the SEP are generated in the posterior bank of the central sulcus and in the anterior crown of the postcentral gyrus respectively ³³⁷⁻³³⁹. N20/P25 suppression at ISI 5 ms is generally thought to be due to inhibitory interactions in sensory cortex ^{182, 340, 341}. Thus, increased R5 may indicate increased effectiveness of S1 inhibition. At longer ISIs inhibition of N20/P25 may involve subcortical structures within the somatosensory pathway, such as dorsal column nuclei or thalamus ^{157, 163}. Thus, increased inhibition at these intervals suggests that HF-RSS may also increase inhibitory interactions at subcortical levels. In the same way, P14 is a subcortical component of the SEP that is recorded as a far-field potential from the scalp and is probably generated at or near the first synaptic relay of the dorsal column-medial lemniscus system ³⁰⁴. Increased suppression of P14, which was independent from suppression of N20/P25, is also consistent with an increase in inhibition at subcortical stages of the somatosensory system. Our findings are apparently in contrast with those reported by Hoffken and co-workers ²⁷⁸, who found decreased suppression of PP-SEP after repetitive tactile stimulation. However, it is worth noting that in their study tactile stimuli were given at a random ISI based on a Poisson distribution (average frequency of 1 Hz) and the total stimulation duration was 3 h. This is very different from our HF-RSS. We also note that although our EEG montage was optimal for recording the N20/P25, this is not the case for the P14, which is best observed with a non-cephalic reference ³⁴². Nevertheless, although our montage underestimates the amplitude of the P14 it should have little effect on the intraindividual comparison of the recovery curves before and after HF-RSS.

HFOs are small wavelets with a frequency around 600 Hz superimposed on the N20 component of SEP. I-HFO are thought to depend on the activity of S1 inhibitory interneurons ^{180, 300} possibly producing feed-forward inhibition of cortical pyramidal neurons ³⁰⁰. Since HF-RSS produced an increase in I-HFO, it is likely that excitability of S1 inhibitory interneurons

was increased. Alternatively, it has also been proposed that S1 pyramidal chattering cells participate in the generation of l-HFO³⁴³, so an increase in excitability of these neural elements should also be considered. In contrast with l-HFO, e-HFO are supposed to originate from activity of thalamocortical fibres directed to areas 3b and 1 within S1³⁰⁰. As such, the increase in e-HFO area produced by HF-RSS might be interpreted as an increase in excitability of thalamocortical relay cells. Shimazu and coworkers³⁴⁴ have noted that l-HFO originate from a radial dipole, possibly due the fact that they are superimposed to P25, which is in area 1 and is a radial dipole as well. If this is correct, then our EEG montage may have been suboptimal for recording the orientation of the dipole. Although this may underestimate the amplitude of the l-HFO, it is unlikely to impact on the changes in amplitude observed here after RSS.

We have previously suggested that both short latency paired pulse interactions at R5 and l-HFO reflect activity in GABAergic neurons that are known to produce feedforward inhibition, at least at cortical level, of excitatory somatosensory inputs¹⁶⁴. These neurons sharpen the temporal profile of the incoming input by preventing overlap with later-arriving dispersed inputs in the same pathway. We speculate that repetitive activation of these neurons during HF-RSS increased the effectiveness of this feedforward inhibition, thus increasing the suppression of N20/P25 and P14 components of the SEP produced by the second stimulus of a pair. HF-RSS may also increase the excitability of post-synaptic neurons responsible for N20/P25 and P14 generation, consistent with the observed increase in amplitude of the cortical N20¹⁷⁷ and in the P14 from the nucleus cuneatus³⁰⁴. However, increased amplitude of the SEP did not correlate with changes in STDT suggesting that the change in temporal inhibition was the main factor influencing temporal discrimination. Interestingly, both behavioural and electrophysiological changes were spatially specific to input from the stimulated finger, with no effect on the SEP recorded by stimulation from the thumb, as previously found²⁷⁶.

4.4.2 Relation between temporal and spatial perception and electrophysiological inhibition

STDT showed the same spatial specificity as the N20/P25 and P14. It improved (i.e. decreased) only on the stimulated finger (i.e. the right index finger), while it showed no changes when tested on the right thumb or on the contralateral hand. As proposed in a previous study by Rocchi and coworkers¹⁶⁴, we suggest that increased excitability of feedforward somatosensory inhibition sharpens the temporal profile of afferent somatosensory stimuli; this, in turn, can contribute to the observed decrease in STDT^{164, 208}. The correlation between the changes produced by HF-RSS in STDT and electrophysiological inhibition further supports this

explanation. We examined two tests of spatial perception: the bumps test, which is a threshold detection task, and the JVP domes, which is an edge detection task. Given the relatively advanced age and wide distribution of our participants' sample, TSD and TT values are higher than reported in younger subjects^{227, 281}. However, in line with our results, it has been demonstrated that somatosensory perceptual abilities can also be modulated by repetitive tactile stimulation in subjects of advancing age^{303, 323}. The JVP domes test involves activity in slowly-adapting (SA) cutaneous afferents from Merkel cells, which have a high sensitivity to edge detection^{222, 224, 225}. In contrast, the bumps test, which entails the detection of small raised dots on a flat surface, is thought to depend on the activity of rapidly adapting (RA) skin receptors, represented by Meissner corpuscles^{228, 229}. Although RA receptors have a lower spatial acuity than the SA system, they are optimal for the detection of very small surface variations, such as small dots embedded in a flat surface²²⁰.

Why did HF-RSS modulate bumps perception but did not influence grating discrimination? It is known that cutaneous afferents project mainly to area 3b within S1. All neurons within each column in S1 respond to the same class of receptors, i.e. columns that receive afferents from cutaneous SA and RA receptors are distinct^{230, 231}. Accordingly, they are called, respectively, SA and RA cortical neurons²³⁰. A possible explanation is that HF RSS preferentially modulated the excitability of RA neurons in S1. This might be due to peripheral factors: while the receptive fields of RA and SA are more or less the same (11–12 square mm)³²⁸, the density of RA is considerably higher than SA on the volar surface of the fingers^{218, 220}. According to this view, a greater number of RA skin receptors might have been stimulated by HF-RSS. This could have two possible consequences. It could increase the excitability of cortical RA cells in S1 which, like skin RA receptors, increase their discharge in correspondence of application and removal of tactile stimuli^{224, 225}. This increase in cortical excitability might then contribute to the improved performance in the bumps test. It would also be consistent with the increase in amplitude of SEP to single stimuli. A second possibility is raised by the finding that there was a weak correlation between the change produced by HF-RSS in the bumps test and electrophysiological inhibition. RA cells involved in the bumps test fire with brief bursts of activity at the beginning and end of the stimulation as the finger pad is swept over the target area. It may be that repeated activation of peripheral RA input during HF-RSS can enhance feedforward inhibition in cortical RA columns. This may then sharpen detection of phasic sensory inputs as the finger pad is swept across the surface and improve perception.

4.4.3 HF-RSS effects on motor cortex inhibition

Since HF-RSS has been reported to affect motor performance³²⁴⁻³²⁶, we also investigated its effect on M1 excitability and inhibitory circuitry. The main finding was that HF-RSS increased SICI tested in APB, while leaving SICI in FDI and ADM and the unconditioned MEP unchanged. The lack of change of SICI in ADM is not entirely surprising according to the somatotopic organization of motor cortical input–output relationship described in previous investigations. Several authors have reported that in monkeys M1 receives sensory information from portions of limbs in close relation to the muscle to which it projects^{345, 346}. In humans, MEP amplitude is also modulated by stimulation of cutaneous fields close to the muscle involved^{347, 348}. Since HF-RSS was applied on skin closer to APB than ADM, it is plausible that modulation of SICI was clearer in APB. However, this does not explain why SICI in FDI was unaffected. The reason might be that TMS was centered over APB representation in M1; this means that activity in M1 evoked by TMS conditioning pulse was probably less effective in FDI representation and thus the effects of HF-RSS were less clear. We can only speculate on how HF-RSS effects were transmitted to M1. There are extensive and somatotopic connections between S1 and M1 directly targeting layer V pyramidal tract neurons³⁴⁹ or relaying in M1 cortical layers II/III^{350, 351}. It is also known that tetanic stimulation of S1 produces long-term potentiation in layers II/III of M1^{352, 353}. This could represent one pathway whereby HF-RSS might somatotopically increase excitability of the M1 GABAergic interneurons involved in SICI²⁴⁷. The lack of changes in MEP and ICF might be interpreted considering the higher sensitivity of SICI to low-intensity repetitive stimulation³⁵⁴.

4.4.4 Conclusion

In conclusion, we suggest that HF-RSS increases the effectiveness of inhibition at cortical and subcortical nodes of the somatosensory pathway. This leads to improved performance in behavioural tests of temporal discrimination and contributes to improved performance in some tests of spatial detection (i.e. STDT and the bumps test). Surprisingly, HF-RSS also affects short latency GABAergic inhibition in M1. Together these changes in S1 and M1 may underlie reported improvements in manual motor performance such as the pegboard test. HF-RSS might therefore be a suitable therapeutic tool in neurological disorders characterized by a loss of inhibition, such as dystonia³⁵⁵.

5 High Frequency Somatosensory Stimulation in Dystonia: Evidence for Defective Inhibitory Plasticity

5.1 Introduction

Dystonia is a syndrome characterized primarily by excessive muscle contractions giving rise to abnormal posture and involuntary twisting movements ¹. Formerly considered a motor disorder, dystonia is currently construed to represent a disorder of a network that also involves the somatosensory system. The latter argument stems from several behavioural ⁷⁰⁻⁷², electrophysiological ^{165, 311, 356}, and imaging ³⁵⁷⁻³⁵⁹ studies showing multiple deficits of sensory processing in dystonia. The hypothesis has been therefore raised that deranged processing of the somatosensory input in the central nervous system may lead to abnormal sensorimotor integration, thus contributing substantially to the generation of dystonic movements ^{58, 360}. At a behavioural level, the most consistent abnormality observed across different types of dystonia is increased STDT, that is thought to indicate a deficit of temporal sensory processing ⁶¹. STDT has been considered an endophenotype of dystonia ⁷⁵ because it does not correlate with disease severity ^{296, 297}, is abnormal in non-dystonic body regions ⁷³, and is altered in about half of the unaffected first-degree relatives of patients ⁷². In the previous experiments, we have shown that increased STDT in CD is well correlated with reduced PP-SEP suppression at short ISI and with reduced late component of SEP HFO ¹⁷, both of which reflect abnormal intracortical inhibitory mechanisms within S1. These results confirmed and expanded previous findings from Tamura and colleagues ²⁰², who showed impaired suppression of SEP with an ISI of 5 milliseconds in patients with FHD. Moreover, the argument that STDT involves synaptic activity within S1 is further corroborated by the finding that STDT can be modulated by repetitive TMS applied over S1 in healthy participants ²⁰⁸ and in patients with FHD ⁷⁴. However, it is hard to understand from these studies which specific mechanisms led to the observed changes in STDT. HF-RSS is a patterned electric stimulation applied to the skin through surface electrodes, which has been demonstrated to induce selective and reversible reorganization of receptive fields and cortical maps in somatosensory cortex of adult rats ³²². In humans, HF-RSS induces a reversible spatial discrimination improvement in the stimulated area that is scaled to the degree of spatially specific plastic changes localized in primary

somatosensory cortex^{275, 323}. We have recently demonstrated that HF-RSS is further capable of shortening STDT in healthy volunteers³⁰³; this finding was expanded in the present work, where we demonstrated that this improvement is driven by the enhancement of intracortical inhibitory mechanisms within S1³⁶¹. Thus, 45-minute HF-RSS enhances the suppression of N20/P25 at 5-millisecond ISI and increases l-HFO area and these, in turn, lead to a perceptual gain in terms of somatosensory timing abilities³⁶¹. We also showed that the augmented excitability of inhibitory circuitry in S1 was transmitted to M1, as demonstrated by increased SICI after HF-RSS³⁶¹. STDT, paired-pulse SEP, HFO, and SICI are all measures of inhibition and have been demonstrated to be abnormal in patients with dystonia, further consistent with the hypothesis of a widespread loss of inhibition in several areas of the central nervous system that might contribute to both motor and sensory deficits.³⁵⁵ The aim of the current study was therefore to test whether HF-RSS could enhance these defective inhibitory mechanisms, as well as improve STDT, in a group of patients with CD. We explored this by applying an extensive electrophysiological battery gathering several measures of excitability and inhibition in both motor and sensory systems.

5.2 Materials and methods

5.2.1 *Subjects and experimental protocol*

A total of 12 consecutive patients with a diagnosis of idiopathic isolated CD according to current criteria¹ were prospectively recruited from the outpatients clinic at the National Hospital for Neurology and Neurosurgery, Queen Square, London, United Kingdom. All patients were assessed at least three months after their last set of BoNT injections. As healthy controls HC, 12 volunteers with similar age (59.50 ± 13.73 vs 62.17 ± 9.80 , HC vs CD; $P = .589$), gender distribution (3 vs 6 women, HC vs CD; $\chi^2 = 1.6$, $P = .206$) and no family history for any neurological disorders were recruited. Patients' clinical details are provided in table 5.1. All participants underwent STDT testing, SEP recording, and TMS at baseline (T0) and after (T1) a single 45-minute session of HF-RSS. Overall, each session of electrophysiological testing lasted about 60 to 90 minutes. The experimental protocol was approved by the local institutional review board and conducted in accordance with the Declaration of Helsinki after each participant signed a written consent form.

5.2.2 *Somatosensory temporal discrimination threshold*

STDT was tested administering paired electrical stimuli, starting at an ISI of 0 ms (simultaneous pair) and progressively increasing the ISI in steps of 10 ms^{164, 208, 303}. Stimuli consisted of square-wave electrical pulses applied with a constant current stimulator (Digitimer DS7A) through surface skin electrodes, with the anode located 0.5 cm distally to the cathode. The right index finger, right thumb and left index finger were tested in separate sessions. As detailed below, HF-RSS was applied on the right index finger, which was therefore considered as the test finger to evaluate STDT changes after HF-RSS, whereas the right thumb and left index finger were used as control fingers^{303, 361}. The electrodes were applied on the distal phalanx of the examined finger. For the right index finger, stimulation intensity was obtained by delivering stimuli starting from 2 mA and increasing the current in steps of 0.5 mA; the intensity used for the STDT was the minimal intensity perceived by the subject in 10 of 10 consecutive stimuli^{164, 208}. For the other two fingers, the current intensity was adjusted to match the perceived intensity on the right index finger. Subjects familiarized with the task and achieved a stable performance before STDT testing^{164, 303}. During the procedure, they had to verbally report whether they perceived a single stimulus or two temporally separate stimuli. The first of three consecutive ISI at which participants consistently reported two stimuli was considered the STDT. To keep the subject's attention level constant during the test and to minimize the risk of perseverative responses, the STDT testing procedure included "catch" trials consisting of a single stimulus delivered randomly^{208, 211, 303}. Each finger was tested three times and the STDT was defined as the average the three obtained values and was entered in the data analysis.

5.2.3 Somatosensory evoked potentials recording and analysis

SEP were recorded from scalp Ag/AgCl surface electrodes arranged according to the international 10-20 system of EEG electrode placement²⁸⁰. To record the N20/P25 component the active electrode was placed at CP3 and the reference electrode at Fz, while the P14 component was recorded with the active electrode at Fz and the reference on the contralateral mastoid³⁰⁴. Digital nerves of the right index finger were stimulated with a constant current stimulator (Digitimer DS7A) through ring electrodes, with the cathode placed at the base of the first phalanx and the anode placed 2 cm distally^{165, 333}. Monophasic square wave pulses of 200 µsec duration were delivered at 250% of the somatosensory threshold and at a frequency of 5 Hz. Recordings were collected at a sampling rate of 5 KHz, beginning 20 ms before each stimulus and lasting for 100 ms. Data were band-passed filtered from 3 Hz to 2 kHz³⁰⁴. In a

first block, 1000 sweeps were averaged and N20 peak latency, N20/P25 peak-to-peak amplitude and P14 baseline-to-peak amplitude were measured. The recording from this block was also used to extract and measure HFO. Thus, the stimulus artefact was removed from -10 to +5 ms to avoid ringing due to filtering³⁰⁷. The SEP wide band signal was band pass filtered digitally (400-800 Hz) and averaged. HFO waveform was divided in two components, e-HFO and l-HFO, separated by the N20 peak. The onset of e-HFO and offset of l-HFO were defined as their amplitudes exceeding the averaged background noise level by three standard deviations³⁰⁸. e-HFO and l-HFO area was measured and entered into the analysis. Three more recording blocks of 750 frames each were performed to measure SEP recovery cycle. Thus, 750 trials were averaged and paired pulses at ISI of 5, 20 and 40 ms were delivered in each block^{306, 334}. In the paired-pulse condition, the responses following the second stimulus were obtained by subtracting the SEP waveform due to the first stimulus from the waveform following each double stimulus^{306, 334}. R5, R20 and R40 were defined as the ratio between the second and the first response at ISI of 5, 20 and 40 ms, respectively. Finally, 2 more blocks of 750 trials each were recorded, the first stimulating the right thumb only and the second simultaneously stimulating the right thumb and right index finger through two constant current stimulators. These two blocks were used to calculate the SIR of N20/P25 and P14; SIR was calculated as the ratio $TI/TII \times 100$, where TI is the SEP amplitude obtained by simultaneous stimulation of the thumb and index finger and TII is the arithmetic sum of the SEP obtained by the individual stimulation of the two fingers¹⁶⁵.

5.2.4 Transcranial magnetic stimulation and electromyographic recording

EMG activity was recorded through a pair of Ag/AgCl electrodes placed over the right FDI, APB and ADM muscles in a belly-tendon fashion. Raw signal, sampled at 5 kHz with a CED 1401 A/D laboratory interface (Cambridge Electronic Design, Cambridge, UK), was amplified and filtered (bandwidth 5 Hz - 2 kHz) with a Digitimer D360 (Digitimer Ltd., Welwyn Garden City, Hertfordshire, UK). Data were stored on a laboratory computer further off-line analysis (Signal software, Cambridge Electronic Design, Cambridge, UK). To ensure complete target muscle relaxation throughout the experiments, we continuously monitored EMG activity with audio and high-gain visual feedback. TMS was carried out using a Magstim 200 stimulator with a 70mm figure-of-eight coil (Magstim Company Limited, Whitland, UK), which produces monophasic waveform stimuli with a pulse width ~ 0.1 ms. First, the motor hotspot was found, defined as the site within M1 where TMS evoked the largest MEP in the APB muscle. Then,

we found the RMT, AMT, and the intensity able to elicit motor evoked potentials of approximately 1 mV amplitude from APB muscle (1mV-int), which was later used for test pulses. RMT was defined as the lowest intensity able to evoke a MEP of at least 50 μ V in five out of ten consecutive trials during rest³³⁵, while AMT was defined as the lowest intensity able to evoke a MEP of at least 200 μ V in five out of ten consecutive trials during a 10-15% voluntary contraction of the target muscle³³⁶. SICI was obtained through a paired-pulse TMS, with an ISI of 3 ms between the first, conditioning stimulus and the second test stimulus. The test stimulus was set at 1mV-int, while the conditioning stimulation intensity was set at 70%, 80% and 90% AMT, as to obtain a recruitment curve²⁴⁷. Twenty paired stimuli for each different intensity of the conditioning stimuli and twenty single stimuli were delivered in a randomized order. SICI was obtained dividing the amplitude of conditioned MEP by the amplitude of the unconditioned MEP. ICF was obtained in a similar fashion, except that the ISI used was 10 ms and CS intensity was 80% AMT²⁴⁷. Twenty paired stimuli were given during the same recording block used for SICI. ICF was obtained dividing the amplitude of conditioned MEP by the amplitude of the unconditioned MEP. To further characterize M1 circuitry, we also studied LICI in a separate block, by applying twenty test pulses (1mV-int) and twenty conditioned trials, where test stimuli were conditioned by TMS pulses delivered 100 ms before at 120% RMT intensity²⁵⁵. LICI was expressed as the ratio between amplitude of conditioned and unconditioned MEP.

5.2.5 High frequency repetitive somatosensory stimulation

HF-RSS consisted of 20 Hz trains of square wave electrical pulses of 200 μ s duration delivered for 1s, with 5 s intertrain intervals^{279, 303, 323}. The stimulation was applied for 45 min^{303, 361}. Stimuli were delivered with a constant current stimulator (Digitimer DS7A) through surface adhesive electrodes of approximately 1 cm² area, with the anode located on the distal phalanx of the right index finger and the cathode located on the proximal phalanx of the same finger. The intensity of the stimulation was set individually at the highest threshold that subjects could tolerate for the whole period of stimulation³⁶¹. This did not differ between groups (5.96 ± 2.78 vs 6.09 ± 3.04 mA, HC vs CD patients, $p > 0.05$) and corresponded to about 350% of the sensory threshold in both.

5.2.6 Statistical analysis

We first examined each variable for normality via the Shapiro–Wilk test, which was violated in the majority of cases ($p < 0.05$); therefore, nonparametric statistics were applied. Thus, the Friedman test, Wilcoxon signed-rank test, and Mann–Whitney U test were performed as appropriate. Data sets were first analysed in each group separately (HC and CD); in fact, baseline differences between the groups might have rendered interpretation difficult if both groups had been entered in the same analysis³⁷. Then, possible correlations between behavioural and electrophysiological data were evaluated in both groups with the Spearman correlation analysis with Bonferroni correction. Moreover, because we were mostly interested in possible correlations between changes induced by HF-RSS, and to further reduce the number of comparisons, each variable change was expressed as a ratio of measurements post/pre HF-RSS and entered in the Spearman model; p values < 0.05 was deemed significant. Unless otherwise stated, data are given as mean \pm standard deviation (SD).

5.3 Results

5.3.1 *Somatosensory temporal discrimination threshold*

As expected, at T0 STDT was higher in all tested fingers in CD patients when compared with those in HC (figure 5.1; for all p values < 0.01). In HC, the Friedman analysis of variance on the data from all fingers showed a significant effect of HF-RSS on STDT (Friedman $\chi^2 = 32.71$, $p = 0.006$) that was the result of a significant reduction of STDT (i.e. perceptual improvement) in the right index ($z = 3.10$; $p = 0.003$), but not in the other two fingers (for both, $p > 0.05$; figure 5.1). In CD patients, HF-RSS also produced an overall effect on STDT (Friedman $\chi^2 = 32.71$, $p = 0.003$), but in this case, it increased STDT in the right index finger ($z = -2.35$; $p = 0.001$) as well as the right thumb (figure 5.1; $z = -2.28$; $p = 0.005$), but had no effect on STDT in the left index ($z = 0.598$; $p = 0.178$).

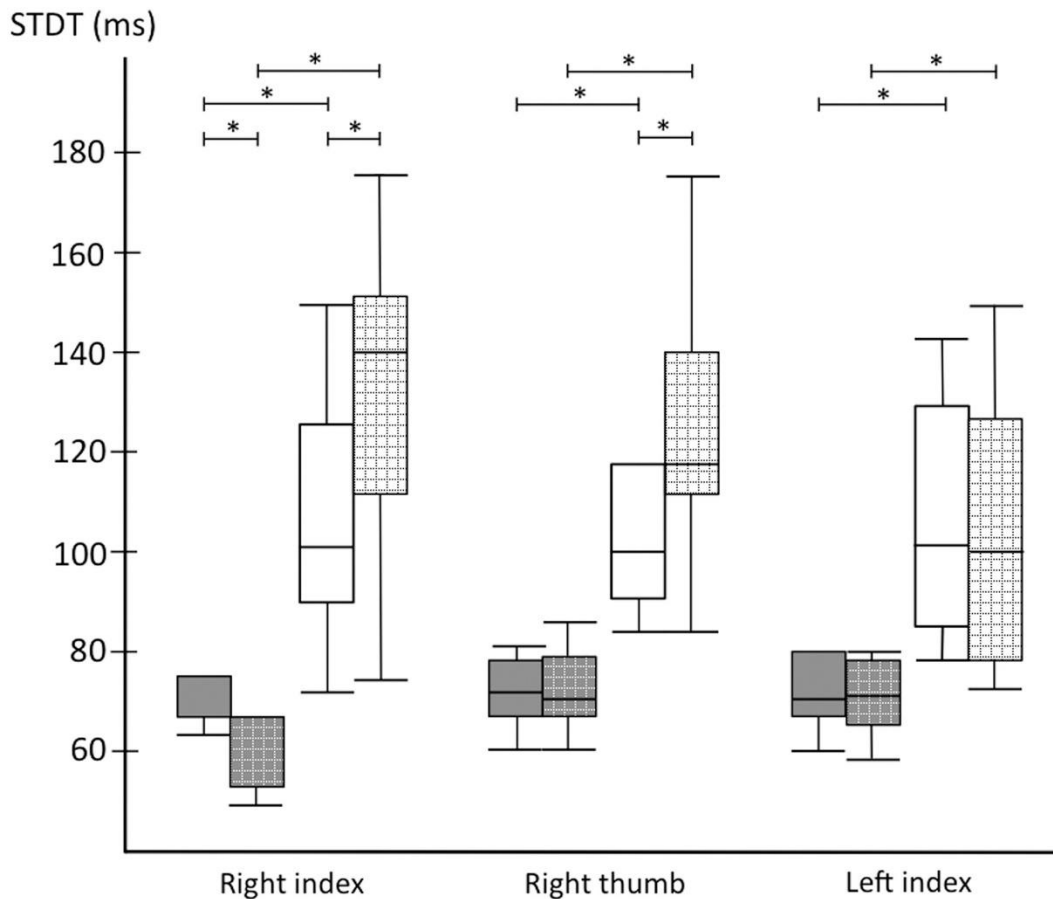


Figure 5.1: Box whisker plot showing the distribution of somatosensory temporal discrimination thresholds (STDT) in healthy participants (gray boxes) and patients (white boxes), before (plain boxes) and after (grid boxes) high-frequency repetitive somatosensory stimulation. Boxes indicate the extent of distributions, horizontal lines in the boxes indicate mean values, whiskers indicate standard deviations; stars indicate statistical significance ($P < .05$).

5.3.2 Somatosensory evoked potentials

The stimulation intensities used to record SEP from right index finger and right thumb were the same in patients and HC (both p values > 0.05 ; table 5.1). HF-RSS produced significant changes in the N20/P25 (Friedman $\chi^2 = 4.17$; $p = 0.036$) and P14 amplitudes (Friedman $\chi^2 = 10.66$; $p = 0.008$) after stimulation of the right index finger, but had no effect on SEP elicited from stimulation of the right thumb (for both N20/P25 and P14 component, Friedman $\chi^2 < 0.33$ and p values > 0.05). Post hoc Wilcoxon signed ranks tests for right index stimulation showed that HF-RSS significantly increased the amplitude of both N20/P25 ($0.61 \pm 0.11 \mu\text{V}$ vs $0.75 \pm 0.11 \mu\text{V}$, T0 vs T1, $z = -3.06$; $p = 0.002$) and P14 ($0.45 \pm 0.09 \mu\text{V}$ vs 0.52 ± 0.08

μV , T0 vs T1, $z = -3.06$; $p = 0.002$) in HC, whereas it had no significant effect in CD patients (for both N20/P25 and P14, $z < 0.58$ and $p > 0.05$). Thus, at T1 there were significant differences between groups in terms of N20/P25 amplitude (Mann–Whitney $z = 2.66$; $p = 0.006$) and P14 amplitude ($z = 3.52$; $p = 0.004$) after stimulation of the right index (table 5.2).

Age, years (mean \pm standard deviation)	62.17 \pm 9.80
Sex (M/F)	6/6
Disease duration, years (mean \pm standard deviation)	9.6 \pm 4.7
Disease severity, TWSTRS score	256.0 \pm 3.6

Table 5.1: *patients' clinical details.*

	Healthy subjects	CD patients	p
Index Finger			
Stimulation intensity, mA	7.4 (2.5)	7.3 (2.4)	> 0.05
N20-P25 latency T0, ms	22.8 (1.01)	22.67 (1.10)	> 0.05
P14 latency T0, ms	16.36 (0.70)	16.48 (0.62)	> 0.05
N20-P25 amplitude T0, μV	0.61 (.011)	0.57 (0.15)	> 0.05
P14 amplitude T0, μV	0.45 (0.09)	0.40 (0.07)	> 0.05
N20-P25 latency T1, ms	22.93 (0.97)	22.67 (1.04)	> 0.05
P14 latency T1, ms	16.40 (0.82)	16.42 (0.73)	> 0.05
N20-P25 amplitude T1, μV	0.75 (0.11)	0.57 (0.14)	< 0.01
P14 amplitude T1, μV	0.52 (0.08)	0.41 (0.06)	< 0.01
Thumb			
Stimulation intensity, mA	8.7 (3.1)	9.0 (3.0)	> 0.05
N20-P25 latency T0, ms	22.84 (1.02)	22.50 (1.09)	> 0.05
P14 latency T0, ms	16.25 (0.75)	16.34 (0.62)	> 0.05
N20-P25 amplitude T0, μV	0.64 (0.14)	0.57 (0.15)	> 0.05

P14 amplitude T0, μV	0.42 (0.05)	0.38 (0.07)	> 0.05
N20-P25 latency T1, ms	22.81 (1.00)	22.62 (1.04)	> 0.05
P14 latency T1, ms	16.26 (0.82)	16.26 (0.70)	> 0.05
N20-P25 amplitude T1, μV	0.64 (0.14)	0.57 (0.15)	> 0.05
P14 amplitude T1, μV	0.43 (0.07)	0.39 (0.08)	> 0.05
Double pulse stimulation			
N20 sum T0, μV	1.26 (.20)	1.15 (0.29)	> 0.05
N20 double pair T0, μV	0.95 (0.18)	1.17 (0.29)	< 0.01
SIR _{N20} T0	0.73 (0.06)	1.01 (0.05)	< 0.01
P14 sum T0, μV	0.87 (0.11)	0.78 (0.14)	> 0.05
P14 double pair T0, μV	0.64 (0.06)	0.79 (0.16)	< 0.01
SIR _{P14} T0	0.72 (0.08)	1.02 (0.08)	< 0.01
N20 sum T1, μV	1.38 (0.21)	1.14 (0.29)	< 0.01
N20 double pair T1, μV	0.78 (0.14)	1.36 (0.31)	< 0.01
SIR _{N20} T1	0.55 (0.05)	1.02 (0.05)	< 0.01
P14 sum T1, μV	0.96 (0.12)	0.79 (0.12)	< 0.01
P14 double pair T1, μV	0.49 (0.07)	0.97 (0.13)	< 0.01
SIR _{P14} T1	0.52 (0.07)	1.23 (0.08)	< 0.01

Table 5.2: SEP values. Data are expressed as mean (SD). Significant *p* values are expressed in bold.

5.3.3 Somatosensory evoked potentials recovery cycle

At baseline, there were significant between-group differences in R5 N20 (Mann–Whitney $z = -1.88$; $p = 0.034$) and R20 N20 (Mann–Whitney $z = -2.48$; $p = 0.019$), but not in R40 N20 (Mann–Whitney $z = -1.86$; $p = 0.063$) or at any ISI in the recovery cycle of the P14 (for all $z > -1.82$ and p values > 0.05). In HC, HF-RSS significantly enhanced inhibition (Friedman $\chi^2 = 51.33$; $p = 0.001$). Specifically, this occurred for R5 N20 (Wilcoxon signed ranks $z = 2.98$; $p = 0.002$), R20 N20 ($z = 3.06$; $p = 0.002$), R40 N20 ($z = 3.06$; $p = 0.002$), R5 P14 ($z = 2.85$; $p =$

0.003), R20 P14 ($z = 3.06$; $p = 0.002$), and R40 P14 ($z = 3.06$; $p = 0.002$; figure 5.2). In CD patients, HF-RSS also produced significant changes in the SEP recovery cycle (Friedman $\chi^2 = 50.97$; $p = 0.001$). In contrast to HC, this was the result of reduced inhibition at R5 N20 ($z = -2.83$; $p = 0.002$), R20 N20 ($z = -2.47$; $p = .003$), R5 P14 ($z = 3.06$; $p = 0.002$), and R20 P14 ($z = -2.58$; $p = 0.003$; figure 5.2). Consequently, there were significant differences between groups at T1 in terms of both N20 and P14 recovery cycles at all ISIs (for all Mann–Whitney, $z < -4.163$ and $p < 0.01$; figure 5.2).

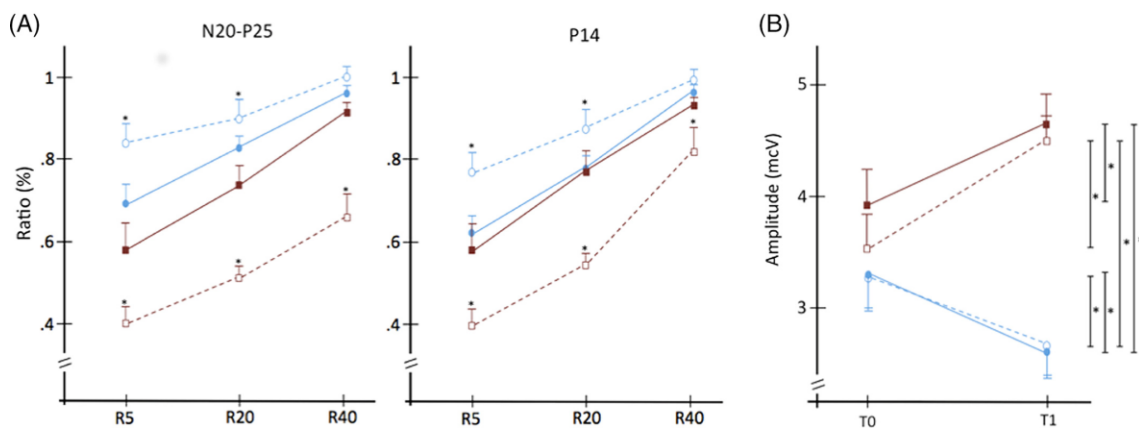


Figure 5.2: (A) SEP recovery cycles (N20 and P14 components, left and right panel, respectively) in patients (blue circles) and HC (red squares) before (plain squares/circles) and after (empty squares/circles) HF-RSS. Vertical bars represent standard errors. Only significant ($p < 0.05$) within-group comparisons are indicated with a star. For between-group comparisons see text. (B) HFO in patients (blue circles) and healthy controls (red squares). Plain squares/circles indicate e-HFO and empty squares/circles indicate l-HFO. Vertical bars represent standard errors. Stars indicate statistical significance ($p < 0.05$).

5.3.4 Somatosensory lateral inhibition

There were baseline differences between groups for both SIR N20 (Mann–Whitney $z = -4.16$; $p = 0.008$) and SIR P14 (Mann–Whitney $z = -4.16$; $p = 0.008$), with patients having a higher ratio than controls (table 5.2), indicative of less lateral inhibition. In HC, HF-RSS produced significant changes in both SIR N20 (Wilcoxon signed ranks $z = 3.06$; $p = 0.002$) and SIR P14 (Wilcoxon signed ranks $z = 3.06$; $p = 0.002$). In both cases, HF-RSS reduced the ratio (SIR N20, 0.73 ± 0.06 vs 0.55 ± 0.05 and SIR P14, 0.72 ± 0.08 vs 0.52 ± 0.07 , T0 vs T1), indicative of enhanced lateral inhibition. In CD patients, HF-RSS produced the opposite effect on both

SIR N20 (Wilcoxon signed ranks $z = 3.06$; $p = 0.002$) and SIR P14 (Wilcoxon signed ranks $z = 3.06$; $p = 0.002$). In both cases, the ratio was increased after HF-RSS (SIR N20, 1.01 ± 0.05 vs 1.20 ± 0.05 and SIR P14, 1.02 ± 0.08 vs 1.23 ± 0.08 , T0 vs T1), suggestive of reduced lateral inhibition (table 5.2). As expected, both SIR N20 (Mann–Whitney $z = -4.16$; $p = 0.008$) and SIR P14 (Mann–Whitney $z = -4.16$; $p = 0.008$) were significantly different between groups at T1 (table 5.2).

5.3.5 *High frequency oscillations*

No baseline differences were observed between groups in either e-HFO (Mann–Whitney $z = 1.44$; $p = 0.063$) or l-HFO ($z = 0.46$; $p = 0.078$). HF-RSS produced significant changes of HFO (Friedman $\chi^2 = 12.00$; $p = 0.007$) in HC, in whom both e-HFO (Wilcoxon signed ranks $z = -3.06$; $p = 0.002$) and l-HFO area ($z = -3.06$; $p = 0.002$) significantly increased (figure 5.2), suggestive of enhanced inhibition. HF-RSS also produced significant changes in CD patients (Friedman $\chi^2 = 5.3$; $p = 0.036$), but with an opposite pattern. In fact, both e-HFO (Wilcoxon signed ranks $z = 2.27$; $p = 0.047$) and l-HFO ($z = 2.82$; $p = 0.003$) were significantly reduced after HF-RSS (figure 5.2). Consequently, there were significant differences at T1 between groups for both e-HFO (Mann–Whitney $z = 4.02$; $p = 0.001$) and l-HFO (Mann–Whitney $z = 2.94$; $p = 0.006$) areas.

5.3.6 *Corticospinal excitability*

There were no differences between groups in the RMT (Mann–Whitney $z = -1.33$; $p = 0.05$), AMT ($z = 0.20$; $p = 0.738$), and 1mV-int ($z = 0.01$; $p = .887$). MEP amplitude after single pulses was found significantly different between groups for the FDI muscle (Mann–Whitney $z = -2.51$; $p = 0.013$) and ADM muscle ($z = -3.24$; $p = 0.003$), but not the abductor pollicis brevis APB muscle ($z = -0.26$; $p = 0.335$). In both former cases, patients had larger MEPs than HC. HF-RSS had no effect on MEP amplitude in any muscle in both HC (Friedman $\chi^2 = 4.03$; $p = 0.178$) and CD patients (Friedman $\chi^2 = 4.09$; $p = 0.176$). Thus, at T1 the same pattern was observed as at baseline, with patients having significantly larger MEPs in the FDI ($z = -2.74$; $p = 0.004$) and ADM ($z = -2.89$; $p = 0.003$), but not in the APB muscle ($z = -0.69$; $p = 0.665$) (table 5.3).

	Healthy subjects	CD patients	p
RMT %, mean (SD)	45.58 (9.66)	50.00 (8.2)	>0.05
AMT %, mean (SD)	39.88 (8.94)	41.08 (9.58)	>0.05
1mV-int %, mean (SD)	61.16 (12.34)	61.50 (11.45)	>0.05
MEP _{APB} amplitude T0, mean (SD)	0.98 (0.21)	1.01 (0.19)	>0.05
MEP _{FDI} amplitude T0, mean (SD)	0.95 (0.29)	1.27 (0.18)	<0.01
MEP _{ADM} amplitude T0, mean (SD)	0.44 (0.13)	0.70 (0.15)	<0.01
MEP _{APB} amplitude T1, mean (SD)	0.99 (0.23)	1.02 (0.14)	>0.05
MEP _{FDI} amplitude T1, mean (SD)	0.91 (0.26)	1.24 (0.16)	<0.01
MEP _{ADM} amplitude T1, mean (SD)	0.47 (0.15)	0.71 (0.18)	<0.01

Table 5.3: corticospinal excitability data are expressed as mean (SD). Significant p values are expressed in bold.

5.3.7 Cortical inhibition in the motor system

At baseline, there were significant differences between groups for all muscles, with patients having higher ratios at all CS intensities (all, p values < 0.01; figure 3). In HC, HF-RSS produced significant changes in the APB (Friedman $\chi^2 = 54.20$; p = 0.001), but not in the FDI or ADM muscles (for both, $\chi^2 < 4.12$; p > 0.05). Specifically, in the APB, SICI increased at CSI of 70% (Wilcoxon signed ranks z = 2.75; p = 0.003), 80% (z = 2.75; p = 0.003), and 90% (z = 2.35; p = 0.004; figure 5.3). In CD patients, HF-RSS significantly changed SICI in all muscles: APB (Friedman $\chi^2 = 49.43$; p = 0.001), FDI ($\chi^2 = 12.94$; p = 0.046), and ADM ($\chi^2 = 30.12$; p = 0.001). However, the effect was opposite to that seen in the HC. In the APB, SICI

was less effective at CS of 70% (Wilcoxon signed ranks $z = -2.86$; $p = 0.003$), 80% ($z = -2.71$; $p = 0.003$), and 90% ($z = -2.90$; $p = 0.003$; figure 5.3). In the FDI, it was significantly reduced at CSI of 90% ($z = -2.28$; $p = 0.004$), whereas in the ADM, there was a significant reduction in SICI at CS of 80% ($z = -2.51$; $p = 0.004$) and 90% ($z = -2.75$; $p < 0.01$). Between-group comparisons at T1 showed that HC and CD patients differed in terms of SICI at all CS and in all explored muscles (figure 5.3), with the exception of SICI 70% in the ADM muscle, where only a non-significant trend was observed (Mann–Whitney $z = -1.88$; $p = 0.063$). No differences were observed between groups in terms of LICI and ICF, either at T0 or at T1. HF-RSS did not induce any changes within groups (figure 5.4).

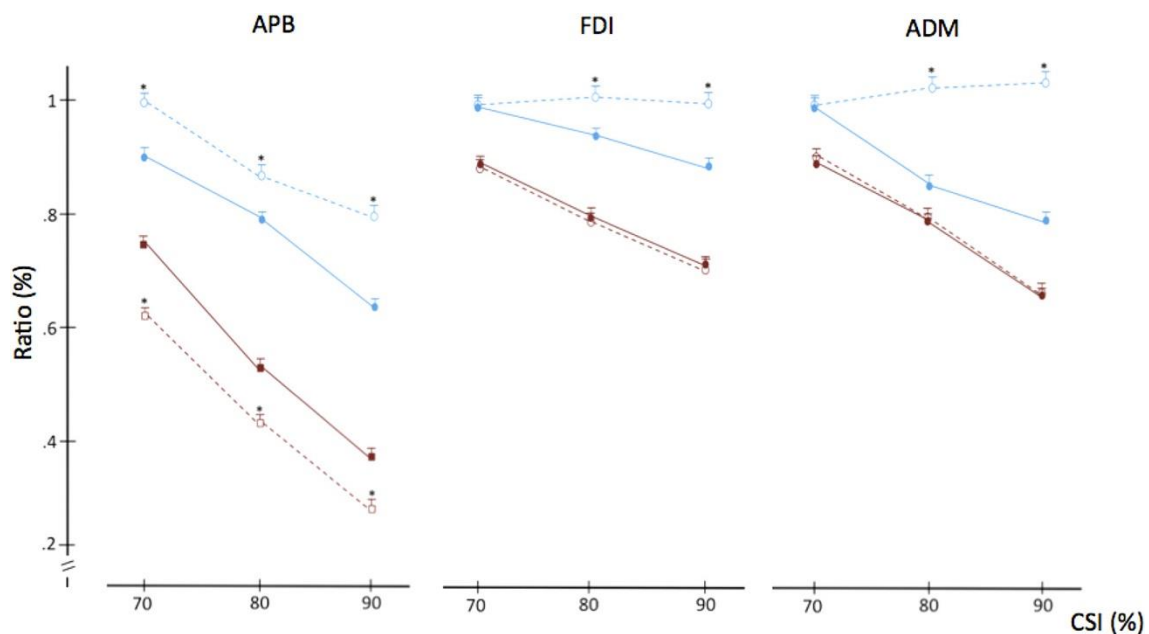


Figure 5.3: SICI in CD patients (blue circles) and HC (red squares) before (plain squares/circles) and after (empty squares/circles) HF-RSS. Vertical bars represent standard errors. Only significant ($p < 0.05$) within-group comparisons are indicated with a star. For between-group comparisons see text. FDI, First Dorsal Interosseous; APB, Abductor Pollicis Brevis; ADM, Abductor Digiti Minimi; CSI, conditioning stimulus intensities.

5.3.8 Correlations

In both groups, T1/T0 STDT ratio in the right index finger correlated with both T1/T0 R5 N20 ratio (Spearman ρ : 0.653 and 0.713, HC and CD, respectively; both $p < 0.01$; figure 5.5) and T1/T0 l-HFO ratio (Spearman ρ : -0.761 and -0.742 ; HC and CD, respectively; both $p < 0.01$; figure 5.5). There was also a significant correlation between T1/T0 l-HFO ratio and T1/T0 R5

N20 ratio (Spearman ρ : -0.767 and -0.692 , HC and CD, respectively; both $p < 0.01$). No other significant correlations were observed between behavioural and electrophysiological measures.

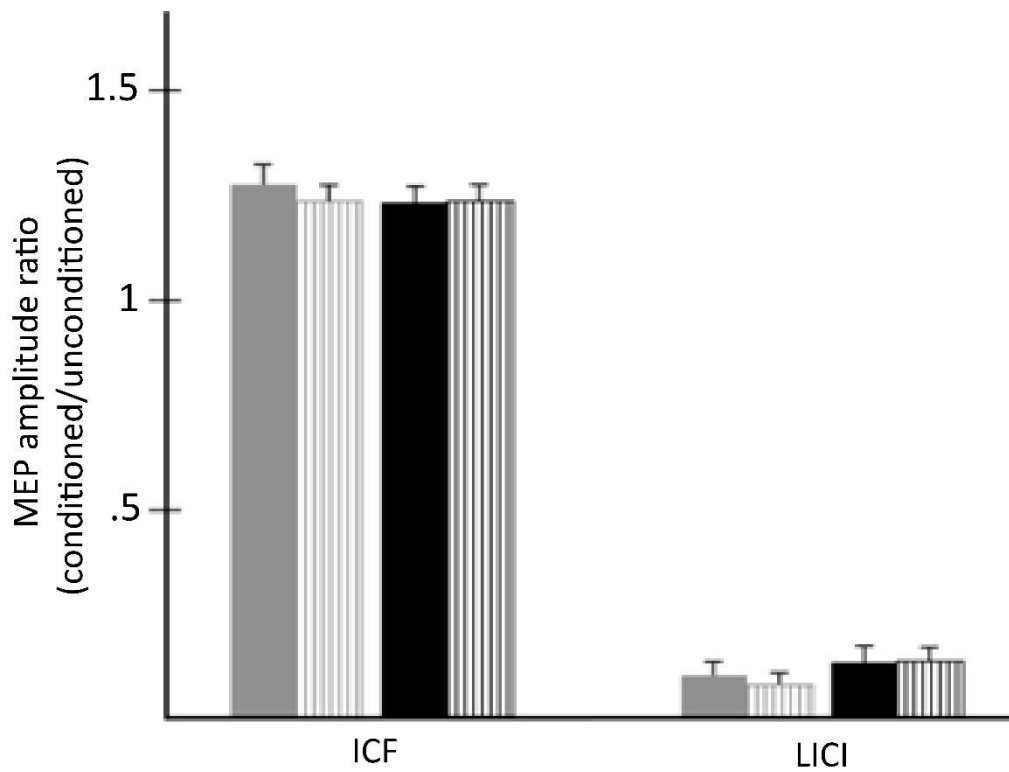


Figure 5.4: LICI and ICF in CD patients (grey columns) and HC (black columns), before (plain columns) and after (striped columns) HF-RSS. Vertical bars represent standard errors.

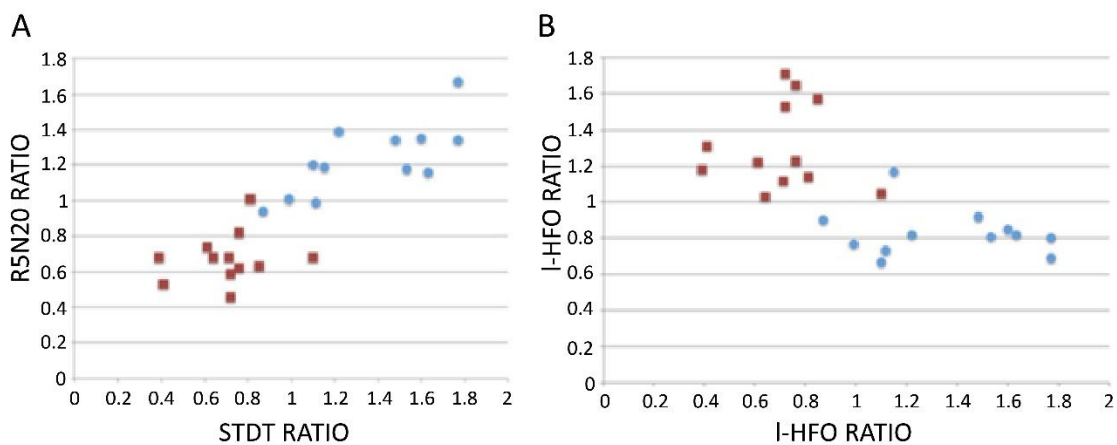


Figure 5.5: correlation between STDT ratio ($T1/T0$) and R5 N20 ratio ($T1/T0$; A) and l-HFO ratio ($T1/T0$; B) in CD patients (blue circles) and HC (red squares). HFO, high-frequency oscillation.

5.4 Discussion

Baseline comparisons between groups largely replicated previous findings showing that patients with dystonia have higher STDT⁷⁰⁻⁷³, reduced suppression of the recovery cycle of SEP²⁰², impaired lateral inhibition in both the somatosensory^{17, 165} and motor systems^{362, 363} and reduced SICI^{364, 365}. The evidence that single-pulse MEP in the FDI and ADM were higher in CD than in HC might further be an indirect measure of reduced lateral inhibition within M1. Altogether, these findings confirm previous suggestions of a widespread loss of inhibition in various areas of the central nervous system in dystonia³⁵⁵.

5.4.1 Paradoxical effect of HF-RSS in patients with idiopathic cervical dystonia

Novel to the current study is the difference in the aftereffects of HF-RSS on STDT and sensorimotor excitability between groups. We confirmed our previous observation in healthy volunteers that 45-minute HF-RSS raises the excitability of a number of facilitatory and inhibitory measures in somatosensory and motor cortex in a spatially selective fashion³⁶¹. HF-RSS increased the amplitude of cortical and subcortical SEP and enhanced excitability of several inhibitory mechanisms within the sensory system. Some of these measures (i.e. change in the suppression of the N20/P25 SEP component at short ISI and in the amplitude of l-HFO) correlated with the improvement in STDT. In addition, we verified that HF-RSS increased SICI in the motor system. The novel finding was the unexpected and paradoxical response to HF-RSS in patients with CD, which had the opposite behavioural and physiological effects to those in the healthy group. The patients' impaired STDT was made worse by HF-RSS, as were our physiological measures of inhibition; there was also no facilitation of SEP. Previously, we argued that the improvement in STDT after HF-RSS in HC was mainly the result of increased inhibitory activity within the somatosensory cortex³⁶¹. This was because changes in STDT correlated with changes in cortical sensory inhibition (i.e. PP-SEP suppression and amplitude of l-HFO), but not subcortical somatosensory inhibition (i.e. changes in the P14 recovery cycle and in the N20/P25 recovery cycle at longer ISI), nor with facilitatory effects on the amplitude of the SEP or on somatosensory lateral inhibition³⁶¹. Our hypothesis was that augmented feedforward somatosensory inhibition sharpens the temporal profile of excitatory somatosensory inputs, making it easier to detect two closely spaced stimuli^{211, 361}. This is

supported by our finding in this study that the deterioration of STDT in CD correlated with reductions in same measures of S1 inhibition.

5.4.2 Defective homeostatic plasticity in patients with idiopathic cervical dystonia

The main question is why HF-RSS had opposite effects on physiology and behaviour in CD. The aftereffects of HF-RSS have been described as a form of short-lasting synaptic plasticity²⁷⁹ that changes the excitability of a number of cortical and subcortical systems³⁶¹. Thus, the aftereffects of HF-RSS in dystonia might represent an abnormal plastic response of central neurons to peripheral inputs. However, most studies suggest that the main problem in dystonia is an increase in plasticity, rather than the reversal we observed. Thus, in the motor cortex, patients with dystonia are often reported to have an enhanced response to PAS, in which TMS is repeatedly paired with carefully timed somatosensory input^{25, 33, 36, 366, 367}. The same protocol has also been tested with TMS over S1 and in this case, it was reported that the amplitude of the P27 component of the SEP was enhanced in FHD more than in HC³⁶⁷. It was also found that baseline abnormal P27 suppression with paired pulses tended to normalize to the level of HC after PAS³⁶⁷. Another study³⁷ found that PAS paradoxically increased long-latency afferent inhibition (reflecting activity of somatosensory inputs to the motor cortex) in FHD, suggesting an abnormal homeostatic plasticity in the sensory cortex in FHD. However, in both latter studies^{37, 367}, the PAS protocol was applied to a dystonic body region, thus not clarifying whether the physiological abnormality observed within the sensory system represents a primary pathological condition or an adaptation process secondary to symptom manifestation. Here, HF-RSS has been applied to a non-dystonic body region, which makes us speculate that the observed abnormalities are primarily related to the pathophysiology of dystonia and are not merely consequential to abnormal posturing. Moreover, PAS entails associative stimulation of the somatosensory ascending pathways and M1³⁶⁸, thus making it difficult to specifically address the putative source of deranged plasticity. One observation in HC may be of major relevance. Höffken and colleagues²⁷⁸ had found that a much longer period of RSS (i.e. of three hours) reduced the suppression of PP-SEP compared with the increase we have observed in this study as well as in a previous article³⁶¹. Although the frequency and timing of the RSS stimuli were not the same as used in the present study, it is possible that the effects of RSS may differ for short versus long durations of stimulation. A similar effect has been described for

different plasticity protocols used on the motor cortex. Using transcranial direct current stimulation, the usual reduction of excitability that is observed after 13 minutes of anodal transcranial direct current stimulation reverses to facilitation if the stimulation duration is doubled ³⁶⁹. Similarly, conventional facilitatory intermittent theta-burst stimulation and inhibitory cTBS protocols reverse their effects when applied for twice as long ³⁷⁰. If a similar effect applies to HF-RSS, then it seems possible that what we observe in dystonia is a speeding up of the process: the response reverses after a shorter period of HF-RSS than in healthy individuals. Although a control condition with a shorter period of HF-RSS would have been necessary to confirm this hypothesis, it is to note that RSS durations as short as below 20 minutes might not induce any behavioural effects in HC ³⁷¹. The reversal of plasticity during long periods of stimulation is sometimes described as a form of homeostatic plasticity. For example, a previously high level of postsynaptic activity facilitates induction of long-term depression, whereas a previously low level of postsynaptic activity facilitates long-term potentiation ³⁷²⁻³⁷⁴. In terms of HF-RSS, this would mean that, although the initial effect might be to increase inhibition and reduce STDT, in prolonged protocols, this would interact with and reverse the effect of the later portions of HF-RSS, making the overall effect facilitatory and detrimental to STDT. In the case of CD patients, we might speculate that, because they have reduced baseline measures of somatosensory inhibition, this accelerates the inhibitory “priming” ³⁷⁵ of HF-RSS, which then reverses its effect even during a short protocol. Our results seem at odds with previous reports suggesting a lack of the normal homeostatic response to plasticity inducing protocols in CD ^{25, 33, 36, 366}. However, the results are difficult to compare because in those studies the homeostatic interaction was between discrete applications of two plasticity protocols, whereas the present observations refer to homeostatic interactions within a single long-lasting protocol. Finally, it is interesting to note that the abnormal effects of HF-RSS were also seen in the motor areas. As reported previously, HF-RSS increased the effectiveness of SICI in a topographically selective way in HC ³⁶¹, whereas in patients with CD, HF-RSS reduced the effectiveness of SICI in the target muscle as well as two “distant” muscles, ADM and FDI. This transfer of sensory effects to the motor system would further support the notion that spatially and temporally distorted sensory information could lead to abnormal motor programs in dystonia ^{58, 165}. Yet, these abnormalities were demonstrated in a non-dystonic body region. This implies that, although some of these defective inhibitory mechanisms are able to explain impaired temporal sensory processing, as demonstrated by increased STDT, they are per se not sufficient to produce dystonic symptoms.

5.4.3 Limitations

Although our findings specifically point to a defective homeostatic plasticity of inhibitory circuits within S1 correlating with the behavioural changes, we cannot entirely rule out a possible contribution of subcortical origin. Differences in subcortical processing of sensory input in dystonia compared with HC might theoretically contribute to the overall differences we observed. In fact, despite no baseline differences being observed between groups as to the P14 SEP and its recovery curve, HF-RSS induced opposite effects in the P14 recovery cycle between groups, as it was observed for the N20/P25 components. Moreover, because we tested our patients at least three months after their last set of BoNT injections, we cannot entirely exclude that the aftereffects of HF-RSS might have been partially influenced by proprioceptive overflow related to neck dystonia. This confounding factor can be specifically addressed in future studies by applying HF-RSS soon after BoNT injections. Finally, we acknowledge the relatively small sample size that might prevent us to draw firm conclusions. However, the results were strikingly different between groups and we propose that the abnormal response to HF-RSS can be interpreted as an impaired homeostatic plasticity, most likely driven by a dysfunction in inhibitory circuits in S1. Moreover, the fact that these results have been obtained by stimulation of a non-dystonic body part would suggest that the described alterations likely represent a primary dysfunction and are not related to abnormal posturing. Further studies are needed to investigate the relationship between these alterations and overt development of dystonia.

6 Defective inhibition and plasticity in the somatosensory system are not required to develop dystonia

6.1 Introduction

Dystonia is a heterogeneous disorder with variable distribution (from focal to generalised), phenomenology (isolated or combined to additional signs) and aetiology (inherited, acquired or idiopathic) ¹. Treatment strategies and their outcomes also differ between dystonia subtypes ⁴⁵⁻⁴⁷. Such features are consistent with the concept that different dystonias may have different neuroanatomical substrates ⁴³ and pathophysiology ⁴⁴. Evidence for the latter comes from studies in the motor system. Although some physiological features are common to many types of dystonia, such as reduced intracortical inhibition in motor cortex, others, such as motor plasticity cortex, are not ^{16, 19-25, 376-378}. Plasticity is abnormal in forms of idiopathic dystonia ^{23, 32}, but does not seem to be required for the clinical expression of dystonia secondary to basal ganglia lesions ²³, even though dystonia normally develops months after the brain insult, suggesting an underlying plastic reorganization.

Although clinical symptoms of dystonia relate to disorders of movement, there are clear abnormalities in the somatosensory system, at least in idiopathic dystonia. One of the most consistent findings is an increased STDT ^{79, 379, 380}. As described in the previous chapters of this thesis, physiologically, this is associated with reduced excitability of the inhibitory circuits in S1 ^{361, 381} that are required to heighten temporal acuity. In healthy volunteers, STDT and S1 inhibition are improved by a period of HF-RSS, whereas it has the opposite, deleterious, effect in idiopathic dystonia ³⁸¹. This has been attributed to abnormal somatosensory plasticity akin to that observed in the motor system.

In the present chapter we tested whether these abnormalities of STDT, S1 inhibition and S1 plasticity that are seen in patients with idiopathic dystonia also occur in patients with dystonia acquired to basal ganglia damage. In addition, to evaluate interaction between sensory and motor systems, the inhibitory circuitry within M1 was also investigated before and after HF-RSS. Our hypothesis was that the findings in secondary dystonia would differ from those previously reported in idiopathic dystonia, providing further evidence that dystonia can arise from different, probably independent, mechanisms.

6.2 Materials and methods

Ten patients affected by acquired dystonia secondary to structural brain lesions (here named secondary dystonia – SD), were consecutively recruited from the National Hospital for Neurology and Neurosurgery, Queen Square, London, United Kingdom. Inclusion criteria comprised: 1) unilateral distribution of dystonia, with upper limb mostly affected, 2) no significant pyramidal signs or somatosensory abnormalities of the limbs affected by dystonia, 3) structural brain lesion involving the basal ganglia, contralateral to the clinically affected side, confirmed by brain MRI. All patients were assessed at least 3 months after their last set of BoNT injections or off medications that act on the central nervous system. Disease severity was assessed with the UDRS. A control group of twelve, age-matched, HC was also studied. All experimental procedures were performed as previously reported in the previous chapter of this thesis^{17, 303, 361, 381}. In summary, all participants underwent electrophysiological testing at baseline (T0) and after (T1) a single 45-minute session of HF-RSS, which consist of 20 Hz trains of square wave electrical pulses of 200 μ s duration delivered for 1 second, with 5-second intertrain intervals, applied on the tip of the index finger (test finger – TF) of the dystonic hand and of the right hand in HC (test hand). Electrophysiological testing consisted of: 1) STDT applied on the TF and three control fingers (thumb of the test hand, thumb and index finger of the contralateral hand, named respectively F1, F2 and F3); 2) SEP obtained by stimulating TF and F1 and including measurement of SEP e-HFO, l-HFO and SIR of N20/P25 (Q20) and P14 (Q14); 3) PP-SEP recovery cycle obtained by stimulating TF; 4) SICI recorded from the APB and ADM muscles, the first being the target muscle for TMS. T0 and T1 measurements were counterbalanced across participants. Results were compared with those obtained from twelve age-matched HC. The experimental protocol was approved by the local institutional review board and conducted in accordance with the Declaration of Helsinki after each participant signed a written consent form.

6.2.1 *Statistical analysis*

Statistical analyses were conducted similarly to the other projects in the current thesis. Briefly, age, HF-RSS threshold and stimulation intensity, SEP intensity for thumb and index finger, RMT and 1 mV intensity were compared between the two groups by means of an unpaired t-test. Gender was compared with the Fisher's exact test. Several mixed ANOVAs were

performed to assess the effect of HF-RSS in the two groups. Therefore, several mixed ANOVAs with “group” (SD, HC) and “time” (T0, T1) as factors of analysis were used on the following variables: SEP N20 and P14 latencies and amplitudes, Q20, Q14, area of e-HFO and l-HFO. The structure of the ANOVAs changes for other variables. To investigate STDT intensities and values, two three-way mixed ANOVAs with the added factor “finger” (TF, F1, F2, F3) were performed. Similarly, for N20 and P14 recovery cycle, the factor “ISI” (R5, R20, R40) was added. Lastly, to investigate the effect of HF-RSS on SICI, a four-way mixed ANOVA with “group” (SD, HC) “time” (T0, T1), “muscle” (APB, ADM) and “condition” (test pulse, SICI 70%, SICI 80%, SICI 90%) as factors of analysis was performed on SICI ratios. Normality of distribution was assessed with the Shapiro-Wilks’ test, while Greenhouse-Geisser correction was used, if necessary, to correct for non-sphericity (i.e. Mauchly’s test < 0.05). Levene’s test was performed to investigate homogeneity of variances. P values < 0.05 were deemed significant. Bonferroni post-hoc test was used for post-hoc comparisons.

6.3 Results

There were no differences in age, gender, TMS thresholds and stimulation intensities between groups (table 6.1).

	Healthy controls	Secondary dystonia	Statistics values	p values
Disease duration	-	8.7 ± 3.4	-	-
UDRS	-	30.4 ± 4.2	-	-
Age (years)	51.3 ± 9.2	52.3 ± 9.5	t(20) = -0.242	0.81
Gender	3F, 9M	5F, 5M	$\chi^2(1) = 1.63$	0.20
SEP intensity I	8.9 ± 2.5	8.4 ± 2.2	t(20) = 0.50	0.62
SEP intensity II	7.4 ± 1.6	7.6 ± 2.3	t(20) = -0.29	0.77
HF-RSS threshold	1.6 ± 0.4	1.8 ± 0.6	t(20) = -0.52	0.606
HF-RSS stim	5.5 ± 2.0	5.6 ± 2.0	t(20) = -0.13	0.898
RMT	50.08 ± 9.38	52.6 ± 9.5	t(20) = -0.62	0.54

AMT	42.08 ± 8.94	43.3 ± 9.26	t(20) = - 0.31	0.76
1mV-int	61.17 ± 12.34	64.6 ± 11.57	t(20) = -0.67	0.51

Table 6.1: values related to demographic and clinical variables, thresholds and stimulation intensities. Where appropriate, variables have been compared by means on unpaired t-tests or the Fisher's exact test (for age). Values are expressed as mean ± standard deviation. Thresholds and stimulation intensities (stim) for electrical stimulation are quantified in mA, whereas RMT, AMT and 1mV-int are expressed in maximal stimulator output units. I and II refers to thumb and index finger, respectively.

Unlike the typically elevated STDT in idiopathic dystonia, there was no significant difference in STDT values between controls and patients, in all fingers tested. HF-RSS had no effect, in both groups, on the stimulation intensity used for STDT, N20 and P14 latencies, and test MEP recorded from APB and ADM (raw values for these variables are listed in table 6.2), as confirmed by the ANOVAs. Main effects and interactions of all ANOVAs are listed in table 6.3.

	Healthy controls		Secondary dystonia	
	T0	T1	T0	T1
STDT Intensity F1	13.4 ± 4.99	14.80 ± 5.15	10.02 ± 3.57	10.20 ± 3.88
STDT Intensity TF	11.20 ± 3.89	11.93 ± 4.65	9.49 ± 3.77	9.79 ± 3.69
STDT Intensity F2	12.41 ± 5.92	13.11 ± 5.97	10.18 ± 4.68	10.40 ± 4.61
STDT Intensity F3	10.67 ± 3.98	11.09 ± 3.90	9.50 ± 3.22	9.74 ± 3.44
N20 latency thumb	22.90 ± 0.93	22.86 ± 0.93	22.17 ± 1.39	22.31 ± 1.57
N20 latency index	22.93 ± 0.82	22.86 ± 0.94	22.42 ± 1.44	22.44 ± 1.42
P14 latency thumb	16.28 ± 0.68	16.29 ± 0.75	16.45 ± 0.75	16.33 ± 0.94
P14 latency index	16.37 ± 0.57	16.46 ± 0.72	16.68 ± 0.74	16,66 ± 0.93
Test MEP APB	1.00 ± 0.23	1.09 ± 0.26	0.84 ± 0.15	0.88 ± 0.23
Test MEP ADM	0.43 ± 0.12	0.45 ± 0.17	0.51 ± 0.11	0.54 ± 0.15

Table 6.2: raw values of variables unchanged by HF-RSS. Values are expressed as mean \pm standard deviation. Stimulation intensities for STDT are measured in mA, latencies in ms and test MEP size in mV. RI, RII, LI and LII refer to the right thumb, right index finger, left thumb and left index finger, respectively.

Significant results are represented in figures 6.1 and 6.2. Except from SICI, all baseline values of the electrophysiological variables tested were not significantly different in the two groups (all p values > 0.05).

Overall, there were no significant differences in the effects of HF-RSS in HC and SD patients. In both groups, HF-RSS increased the amplitude of the subcortical P14 and cortical N20/P25 components of the SEP and decreased (i.e. improved) STDT in the TF but not F1 (all p values < 0.001) (figure 1). Figure 1D shows effects on SICI assessed with three different intensities of conditioning stimulus. Baseline SICI was less effective in SD than HC, but was enhanced in the APB muscle to the same degree in both groups after HF-RSS (all p values < 0.05). There was no change in SICI in the distant ADM muscle.

Figure 2 shows that the effectiveness of somatosensory intracortical inhibition was enhanced after HF-RSS in both groups, as indicated by the increase in e-HFO and l-HFO area (p values < 0.01), and the increased amount of inhibition in the N20/P25 and P14 PP-SEP recovery cycle, in both groups and at all ISI (all p values < 0.001). SIR was also improved in HC and SD patients, as indicated by the decrease in Q14 and Q20 (both p values < 0.01).

	Main effects and interactions	F statistics	p values
STDT stim	Group	$F_{1,20} = 1.723$	$p = 0.204$
	Time	$F_{1,20} = 1.576$	$p = 0.220$
	Finger	$F_{3,60} = 1.649$	$p = 0.188$
	Group \times time	$F_{1,20} = 2.471$	$p = 0.130$
	Group \times finger	$F_{1,20} = 0.756$	$p = 0.523$
	Time \times finger	$F_{3,60} = 1.178$	$p = 0.326$
	Group \times time \times finger	$F_{3,60} = 1.776$	$p = 0.161$

STDT values	Group	$F_{1,20} = 0.12$	$p = 0.914$
	Time	$F_{1,20} = 10.126$	$p = 0.005$
	Finger	$F_{3,60} = 3.020$	$p = 0.037$
	Group \times time	$F_{1,20} = 3.635$	$p = 0.071$
	Group \times finger	$F_{3,20} = 0.505$	$p = 0.680$
	Time \times finger	$F_{3,60} = 32.036$	$p < 0.001$
	Group \times time \times finger	$F_{3,60} = 1.791$	$p = 0.158$
N20 latency I	Group	$F_{1,20} = 1.569$	$p = 0.225$
	Time	$F_{1,20} = 0.650$	$p = 0.430$
	Group \times time	$F_{1,20} = 2.466$	$p = 0.132$
N20 latency II	Group	$F_{1,20} = 0.890$	$p = 0.357$
	Time	$F_{1,20} = 0.231$	$p = 0.636$
	Group \times time	$F_{1,20} = 0.772$	$p = 0.390$
P14 latency I	Group	$F_{1,20} = 0.089$	$p = 0.768$
	Time	$F_{1,20} = 0.969$	$p = 0.337$
	Group \times time	$F_{1,20} = 1.601$	$p = 0.220$
P14 latency II	Group	$F_{1,20} = 0.651$	$p = 0.429$
	Time	$F_{1,20} = 0.284$	$p = 0.600$
	Group \times time	$F_{1,20} = 0.702$	$p = 0.412$
N20/P25 amp I	Group	$F_{1,20} = 0.419$	$p = 0.525$
	Time	$F_{1,20} = 0.675$	$p = 0.421$
	Group \times time	$F_{1,20} = 0.978$	$p = 0.334$
N20/P25 amp II	Group	$F_{1,20} = 1.456$	$p = 0.242$
	Time	$F_{1,20} = 143.140$	$p < 0.001$
	Group \times time	$F_{1,20} = 1.456$	$p = 0.242$
P14 amplitude I	Group	$F_{1,20} = 2.177$	$p = 0.162$
	Time	$F_{1,20} = 2.473$	$p = 0.130$

	Group × time	$F_{1,20} = 0.84$	$p = 0.775$
P14 amplitude II	Group	$F_{1,20} = 2.162$	$p = 0.157$
	Time	$F_{1,20} = 40.01$	$p < 0.001$
	Group × time	$F_{1,20} = 0.031$	$p = 0.862$
N20/P25 rec	Group	$F_{1,20} = 0.042$	$p = 0.841$
	Time	$F_{1,20} = 146.859$	$p < 0.001$
	ISI	$F_{2,40} = 81.751$	$p < 0.001$
	Group × time	$F_{1,20} = 0.118$	$p = 0.735$
	Group × ISI	$F_{2,40} = 0.247$	$p = 0.783$
	Time × ISI	$F_{2,40} = 10.621$	$p < 0.001$
	Group × time × ISI	$F_{2,40} = 2.990$	$p = 0.062$
P14 rec	Group	$F_{1,20} = 1.689$	$p = 0.207$
	Time	$F_{1,20} = 69.277$	$p < 0.001$
	ISI	$F_{2,40} = 125.71$	$p < 0.001$
	Group × time	$F_{1,20} = 2.788$	$p = 0.111$
	Group × ISI	$F_{2,40} = 0.196$	$p = 0.823$
	Time × ISI	$F_{2,40} = 2.612$	$p = 0.086$
	Group × time × ISI	$F_{2,40} = 2.042$	$p = 0.143$
Q20	Group	$F_{1,20} = 1.580$	$p = 0.223$
	Time	$F_{1,20} = 132.426$	$p < 0.001$
	Group × time	$F_{1,20} = 0.005$	$p = 0.946$
Q14	Group	$F_{1,20} = 3.676$	$p = 0.070$
	Time	$F_{1,20} = 48.226$	$p < 0.001$
	Group × time	$F_{1,20} = 2.072$	$p = 0.165$
e-HFO	Group	$F_{1,20} = 2.035$	$p = 0.169$
	Time	$F_{1,20} = 89.248$	$p < 0.001$
	Group × time	$F_{1,20} = 0.255$	$p = 0.619$

I-HFO	Group	$F_{1,20} = 0.038$	$p = 0.847$
	Time	$F_{1,20} = 122.388$	$p < 0.001$
	Group \times time	$F_{1,20} = 0.139$	$p = 0.713$
Test MEP APB	Group	$F_{1,20} = 2.636$	$p = 0.120$
	Time	$F_{1,20} = 0.360$	$p = 0.555$
	Group \times time	$F_{1,20} = 0.423$	$p = 0.523$
Test MEP ADM	Group	$F_{1,20} = 2.419$	$p = 0.136$
	Time	$F_{1,20} = 1.754$	$p = 0.200$
	Group \times time	$F_{1,20} = 0.117$	$p = 0.736$
SICI	Group	$F_{1,20} = 15.545$	$p = 0.001$
	Time	$F_{1,20} = 15.011$	$p = 0.001$
	Muscle	$F_{1,20} = 142.310$	$p < 0.001$
	Intensity	$F_{2,40} = 53.823$	$p < 0.001$
	Group \times time	$F_{1,20} = 1.058$	$p = 0.316$
	Group \times muscle	$F_{1,20} = 18.407$	$p < 0.001$
	Group \times intensity	$F_{2,40} = 7.080$	$p = 0.002$
	Time \times muscle	$F_{1,20} = 8.369$	$p = 0.009$
	Time \times intensity	$F_{2,40} = 0.922$	$p = 0.406$
	Muscle \times intensity	$F_{2,40} = 3.707$	$p = 0.033$
	Group \times time \times muscle	$F_{1,20} = 0.206$	$p = 0.655$
	Group \times time \times intensity	$F_{2,40} = 2.257$	$p = 0.118$
	Time \times muscle \times intensity	$F_{2,40} = 4.257$	$p = 0.021$
	Group \times time \times muscle \times intensity	$F_{2,40} = 0.998$	$p = 0.378$

Table 6.3: statistics relative to main effects and interactions of the ANOVAs. Values are expressed as mean \pm standard deviation. Bold characters indicate statistically significant p values. Stimulation intensities for STDT are measured in mA, latencies in ms and test MEP size in mV. I and II refer to the stimulated thumb and index finger, respectively. Measuring units for variables are as follows: STDT stimulation intensity (stim): mA; STDT values: ms;

latencies: ms; P14 and N20/P25 amplitudes (amp): μV ; e-HFO and l-HFO: $\mu\text{V}2 \times 10^{-4}$; test MEP: mV; N20/P25 recovery (rec), Q14, Q20 and SICI are adimensional.

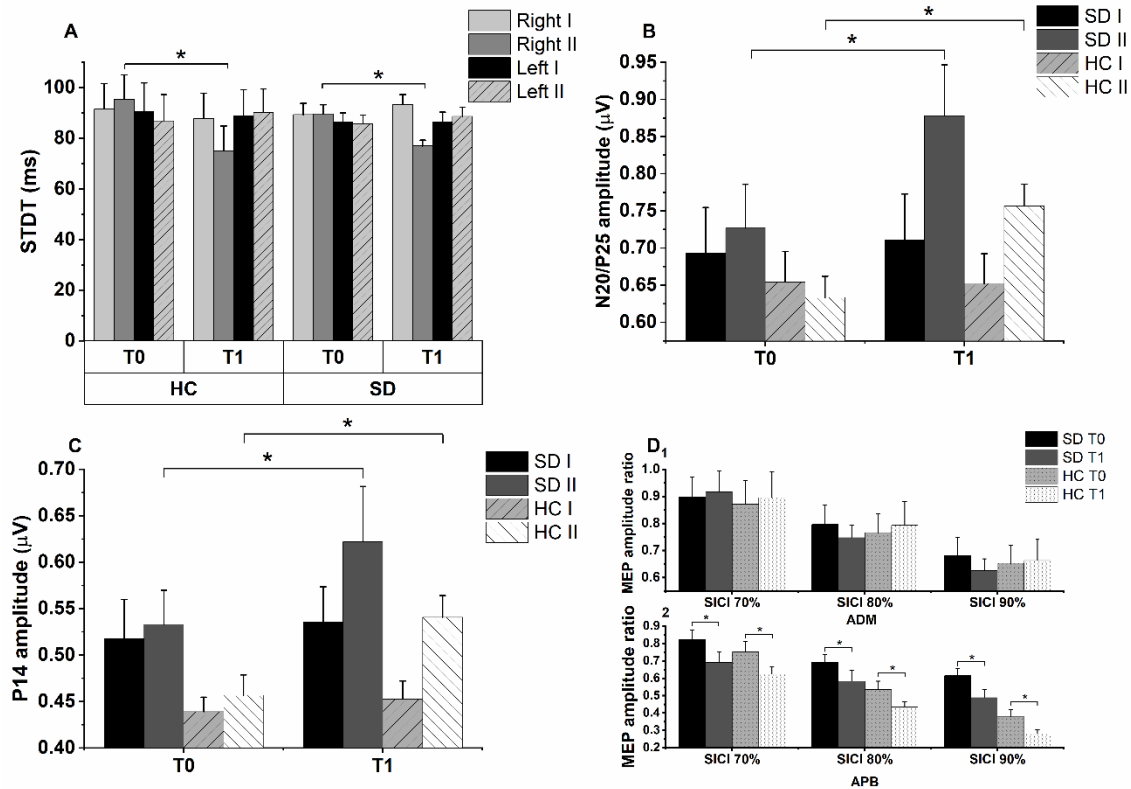


Figure 6.1: panel A: STDT values obtained from the thumb (F1) and the index finger (TF) of the test hand, and thumb (F2) and index finger (F3) of the contralateral hand, before (T0) and immediately after (T1) HF-RSS applied on the TF, in healthy control (HC) and patients with secondary dystonia (SD). HF-RSS produced a significant decrease of STDT TF only ($p < 0.001$). Panel B and C: Amplitude of N20/P25 (B) and P14 (C) components of SEP obtained by stimulating the thumb (F1) and the index finger (TF) of the test hand in HC and SD, before (T0) and after (T1) HF-RSS applied on the TF. HF-RSS induced a significant increase of N20/P25 amplitude ($p < 0.001$ in both cases) as well as an increase in P14 (both p values < 0.001). Panel D: Effect of HF-RSS on SICI on APB and ADM at different intensities of the conditioning TMS stimulus (CS) (70%, 80% and 90% of AMT), in HC and SD, at T0 and T1. HF-RSS induced an increase in SICI irrespective of the strength of the conditioning TMS pulse in the APB, but not in the ADM (all p values < 0.05). Asterisks indicate statistical significance. Error bars indicate standard error.

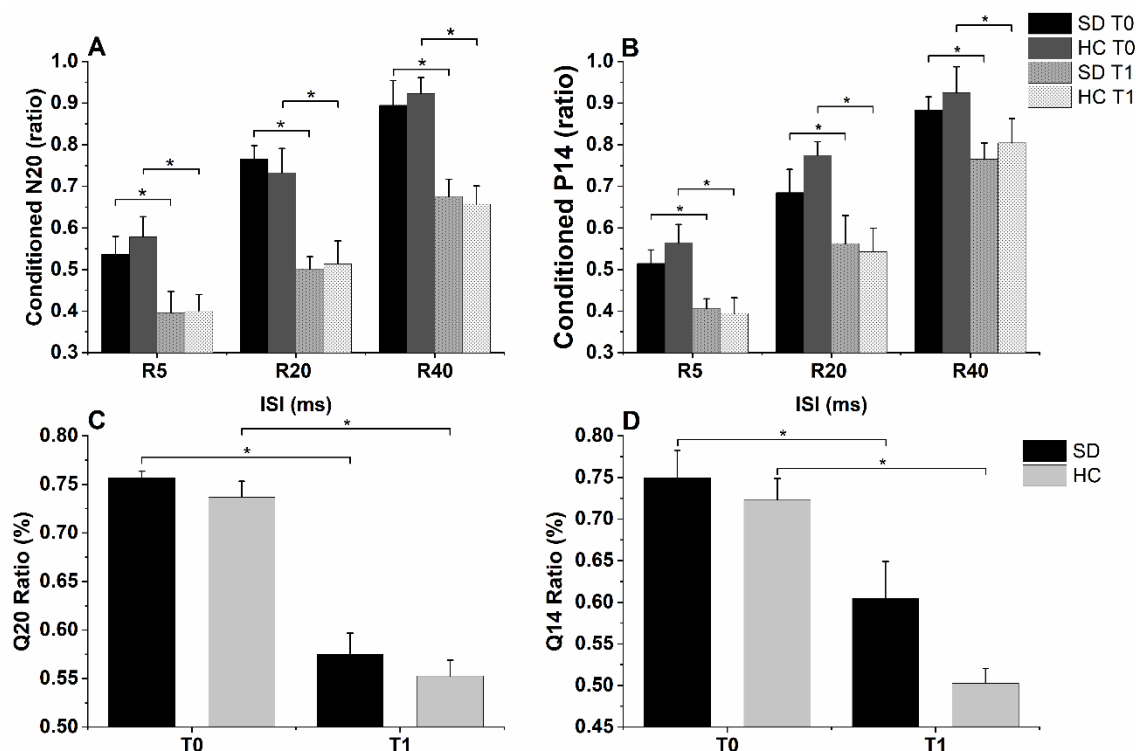


Figure 6.2: Recovery cycle of N20/P25 (panel A) and P14 (panel B) components of SEP at ISIs of 5, 20 and 40 ms before (T0) and immediately after (T1) HF-RSS applied on the TF HF-RSS significantly increased the amount of inhibition produced by the first stimulus of the pair on both the N20-P25 (all p values < 0.001) and P14 (all p values < 0.01) components, in both groups and at all ISI. Spatial inhibition ratio of N20/P25, represented by Q20 (panel C), and P14, represented by Q14 (panel D), before (T0) and after (T1) HF-RSS, in HC and SD. HF-RSS increased somatosensory surround inhibition in both groups by decreasing the Q20 (both p values < 0.001) and the Q14 (both p values < 0.01). Asterisks indicate statistical significance. Error bars indicate standard error.

6.4 Discussion

The main finding of the present study is that patients with SD due to lesions in the basal ganglia do not differ from HC in all the electrophysiological variables tested, before and after HF-RSS, except for SICI, which was reduced at baseline in SD compared to HC. This means that STDT and somatosensory inhibition, investigated by PP-SEP, SIR and HFO, as well as cortical

plasticity induced by HF-RSS, are normal in SD, whereas motor inhibitory mechanisms are defective, as previously described ²³.

This is the first study to report that STDT is normal in SD. STDT reflects the ability to discriminate two consecutive cutaneous electrical stimuli; it relies on inhibitory mechanisms within S1 ^{17, 202, 211, 382} and on functional integrity of the basal ganglia ³⁸³. Increased STDT is the most consistent behavioural abnormality observed in idiopathic dystonia ^{17, 61, 70-72, 200, 381, 384}. Indeed, it has been proposed to be an endophenotypic trait of dystonia ^{75, 383}, since it does not correlate with disease severity, it is abnormal in body parts not affected by dystonia and in unaffected first-degree relatives of patients with sporadic and genetic dystonia, and it does not change with treatment ^{59, 61, 68, 72}. In view of this evidence, the finding of normal STDT in SD is unexpected. It indicates that although all our patients displayed basal ganglia lesions, this is not sufficient to affect temporal discrimination, for which a dopaminergic deficit is required ^{200, 383}. In addition, the increased STDT is consistent with our physiological data. Increased STDT in idiopathic dystonia is associated with reduced excitability of inhibitory circuits in S1 ^{17, 72, 380, 381}, whereas in the present study, S1 inhibitory excitability was normal in SD patients. Finally, our result is in line with the concept of STDT being an idiopathic dystonic endophenotype, not related to the motor phenotype.

The measures of somatosensory inhibition applied in this study have never been investigated in SD, other than in SD due to lesions in the somatosensory pathways ^{385, 386}. None of our patients presented with lesions involving the somatosensory system, which was intact from a functional point of view. However, the results differed from those in idiopathic dystonia, in which there is reduced suppression of the SEP recovery cycle ^{202, 381}, impaired SIR ^{17, 165, 381} and reduced HFO ^{17, 381}. This implies that, while the loss of somatosensory inhibition has a role in the pathophysiology of idiopathic dystonia, it is of less relevance in patients affected by SD due to basal ganglia lesions.

In contrast with the preserved inhibition in the somatosensory system, we found that, as reported by others, motor cortex SICI is reduced in SD ^{23, 387}. Reduced SICI is considered a hallmark feature of dystonia, although this notion has been recently questioned and its pathophysiological significance is still not clear ¹². SICI can be reduced also in other basal ganglia diseases ^{15, 388, 389}, but also in functional dystonia ^{24, 25} and unaffected DYT1 gene mutations carriers ¹⁶. It is therefore suspected that other abnormalities, together with the lack of inhibition, are required for dystonia to manifest ^{12, 390}.

Disordered control of plasticity has been a frequent finding in M1, and, more recently, also in S1 of patients with idiopathic dystonia ^{23, 32, 33, 35, 366, 381}. However, our present results in S1 indicate, that as previously reported in M1 ²³, plasticity may be normal in SD. Thus, HF-RSS induced the same amount of plasticity as controls: it led to a short-term increase in the excitability of inhibitory circuitry within S1 and M1 which was similar to that in healthy subjects ³⁶¹. This result in striking contrast to the opposite effect of HF-RSS on S1 inhibition in idiopathic dystonia ³⁸¹, and there are a number of possible explanations for it. First, in our previous study ³⁸¹, HF-RSS was applied over a body part not affected by dystonia. However, this would unlikely account for the normal STDT and homeostatic plasticity found in SD, as similar abnormalities are seen when testing body parts uninvolved in dystonia ^{380,391}. Secondly, our SD patients were affected by hemi- or segmental dystonia and not focal dystonia, and it is possible that the pathophysiological mechanisms are different ⁴⁴. Finally, and more importantly, in cervical dystonia, HF-RSS acted on top of a defective somatosensory system (due to lack of inhibition), and this could contribute to the paradoxical response. Whatever the explanation, the data shows that abnormally enhanced cortical plasticity is not required for the clinical expression of all types of dystonia and that it is not necessarily linked to basal ganglia damage.

Although classically considered a basal ganglia disorder, dystonia has more recently been framed as network dysfunction, involving the thalamus, cerebellum and sensorimotor cortices ^{42,79}. Albeit the present data suggest normal sensorimotor plasticity and altered M1 inhibition in SD, they do not exclude that other nodes of the network might play a role. In particular, whether the cerebellum contributes to the development of SD has not been investigated and might be the object for future research.

7 Reversal of abnormal somatosensory temporal discrimination in cervical dystonia following low-frequency repetitive sensory stimulation

7.1 Introduction

In the previous investigations, we have demonstrated that HF-RSS is able to induce, in HC, a reversible shortening of STDT on the stimulated area by potentiating intracortical inhibitory mechanisms within S1³⁶¹. We have also shown that HF-RSS induces an opposite response in patients with CD, with a worsening in STDT paralleled by a decreased effectiveness of intracortical inhibition mechanisms within S1 and M1³⁸¹. This has been interpreted as evidence of abnormal homeostatic inhibitory plasticity in dystonia. In healthy individuals, application of a standard inhibitory protocol for twice its usual duration (e.g. 20 min v 10 min of cathodal transcranial direct current stimulation), can reverse the after-effect from inhibition to excitation^{369, 370}. It is thought that the expected inhibition in the first part of the protocol biases the response during the second part to excitation (i.e. a homeostatic reversal of effect). We previously suggested that this tendency was increased in dystonia, reversing the expected excitatory effect of long-lasting HF-RSS into inhibition.

Low frequency RSS (LF-RSS) has been shown to cause a decline in tactile spatial discrimination performance in HC, arguably mediated by long-term depression (LTD)-like processes. However, as for HF-RSS^{278, 381}, it is possible that CD patients exhibit a reversal of plastic effects induced by LF-RSS so that the overall response is excitatory. Following this line of reasoning, by applying a LF-RSS protocol able to induce a worsening of sensory performance in HC, we might expect an opposite response in CD patients. Therefore, we hypothesized that, by applying 45 minutes of LF-RSS, patients with CD would show enhancement of inhibitory intracortical mechanisms and, in turn, manifest a perceptual gain. We tested this hypothesis by gathering several measures of inhibition in both motor and sensory systems and by testing, at the behavioural level, the STDT before and after LF-RSS.

7.2 Materials and methods

Thirteen consecutive patients with a diagnosis of idiopathic isolated CD without tremor according to current criteria¹ were recruited from the outpatient clinic at the National Hospital for Neurology and Neurosurgery, Queen Square, London, UK. All patients were assessed at least 3 months after their last set of BoNT injections. Disease severity was assessed with the TWSTRS. Thirteen volunteers with similar age (57.23 ± 12.36 vs 58.15 ± 9.21 , HC vs CD; $t(1) = 0.180$, $p = 0.860$), gender distribution (5 vs 6 female, HC vs CD; $\chi^2(1) = 0.77$, $p = 0.782$) and no family history for any neurological disorders served as HC. All experimental procedures were performed as described in previous chapters^{17, 361, 381}. Briefly, all subjects underwent a neurophysiological battery to gather measures of somatosensory (PP-SEP, HFO, SIR) and motor inhibition (SICI) at baseline (T0) and after (T1) a single 45-min session of LF-RSS, which consists of square wave electrical pulses of 200 μ s duration, delivered at a frequency of 1 Hz through surface electrodes applied on the tip of the right index finger²⁷⁹. STDT testing was performed with the ascending method²⁹⁶ on the right index finger (i.e., the stimulate area) as well as in three “control” fingers (i.e., adjacent = right thumb; and non-adjacent = left thumb and index). T0 and T1 measurements were counterbalanced across subjects. The experimental protocol was approved by the local institutional review board and conducted in accordance with the Declaration of Helsinki after signing a written consent form.

7.2.1 *Statistical analysis*

Statistical analyses were conducted similarly to the other projects in the current thesis. HF-RSS threshold and stimulation intensity, electrical intensities to obtain SEPs by stimulation of the thumb and index finger, RMT and TMS intensity to get a 1 mV MEP were compared between the two groups by means of unpaired t-tests. Age was compared with the Fisher’s exact test. Several mixed ANOVAs were performed to assess the effect of LF-RSS in the two groups. Therefore, several mixed ANOVAs with “group” (SD, HC) and “time” (T0, T1) as factors of analysis were used on the following variables: SEP N20 and P14 latencies and amplitudes (considered separately for the thumb and index finger), Q20, Q14, area of e-HFO and l-HFO. The structure of the ANOVAs changes for other variables. To investigate STDT intensities and values, two three-way mixed ANOVAs with the added factor “finger” (right thumb, right index finger, left thumb, left index finger) were performed. Similarly, for N20/P25 and P14 recovery cycle, the factor “ISI” (R5, R20, R40) was added. Lastly, to investigate the effect of HF-RSS

on SICI, a four-way mixed ANOVA with “group” (SD, HC) “time” (T0, T1), “muscle” (APB, ADM) and “condition” (test pulse, SICI 70%, SICI 80%, SICI 90%, ICF) as factors of analysis was performed on SICI ratios. Normality of distribution was assessed with the Shapiro-Wilks’ test, while Greenhouse-Geisser correction was used, if necessary, to correct for non-sphericity (i.e. Mauchly’s test < 0.05). Levene’s test was performed to investigate homogeneity of variances. P values < 0.05 were deemed significant. Bonferroni post-hoc test was used for post-hoc comparisons.

7.3 Results

Age, gender, thresholds and stimulation intensities did not show significant differences between groups (table 7.1).

	Healthy controls	Cervical dystonia	Statistics values	p values
Disease duration	-	24.9 ± 5.1	-	-
TWSTRS	-	9.1 ± 4.9	-	-
Age (years)	57.23 ± 12.36	58.15 ± 9.21	t(24) = 0.180	0.860
Gender	5F, 8M	6F, 7M	$\chi^2(1) = 0.77$	0.782
SEP intensity I	9.6 ± 2.5	9.2 ± 2.8	t(24) = -0.369	0.715
SEP intensity II	9.2 ± 2.4	8.7 ± 2.5	t(24) = -0.563	0.578
HF-RSS threshold	3.7 ± 1.0	3.5 ± 1.0	t(24) = -0.563	0.578
HF-RSS stim	12.9 ± 3.3	11.9 ± 3.4	t(24) = -0.759	0.455
RMT	56.62 ± 8.07	54.02 ± 7.66	t(24) = -0.848	0.405
AMT	48.23 ± 7.36	46.22 ± 6.77	t(24) = -0.721	0.478
1mV-int	69.85 ± 10.37	67.15 ± 8.29	t(24) = -0.731	0.472

Table 7.1: values related to demographic and clinical variables, thresholds and stimulation intensities. Where appropriate, variables were compared by means of unpaired t-tests or the Fisher’s exact test (for age). Values are expressed as mean ± standard deviation. Thresholds

and stimulation intensities (*stim*) for electrical stimulation are quantified in mA, whereas RMT, AMT and 1mV-int are expressed in maximal stimulator output units. I and II refers to thumb and index finger, respectively.

HF-RSS had no effect, in both groups, on the stimulation intensity used for STDT, N20 and P14 latencies, and test MEP amplitude recorded from APB and ADM (raw values for these variables are in table 7.2), as confirmed by the ANOVAs. Main effects and interactions of all ANOVAs are listed in table 7.3.

	Healthy controls		Cervical dystonia	
	T0	T1	T0	T1
STDT Intensity RI	9.42 ± 1.87	9.66 ± 2.07	9.75 ± 1.70	9.55 ± 1.44
STDT Intensity RII	9.15 ± 1.77	9.57 ± 1.84	9.22 ± 1.82	8.96 ± 1.76
STDT Intensity LI	9.77 ± 2.00	9.84 ± 1.96	9.86 ± 1.55	10.22 ± 1.43
STDT Intensity LII	9.26 ± 2.10	9.31 ± 2.12	9.36 ± 1.74	9.74 ± 1.73
N20 latency thumb	23.01 ± 1.39	22.89 ± 1.28	22.72 ± 1.35	22.98 ± 1.17
N20 latency index	23.37 ± 1.39	23.02 ± 1.19	22.94 ± 1.10	23.15 ± 1.29
P14 latency thumb	16.32 ± 0.93	16.35 ± 0.82	16.50 ± 1.06	16.52 ± 0.83
P14 latency index	16.55 ± 0.93	16.54 ± 0.89	16.72 ± 1.05	16.68 ± 1.27
Test MEP APB	0.87 ± 0.18	0.91 ± 0.20	0.91 ± 0.18	0.94 ± 0.17
Test MEP ADM	0.58 ± 0.12	0.62 ± 0.14	0.63 ± 0.13	0.65 ± 0.17

Table 7.2: raw values of variables unchanged by LF-RSS. Values are expressed as mean ± standard deviation. Stimulation intensities for STDT are measured in mA, latencies in ms and test MEP size in mV. RI, RII, LI and LII refer to the right thumb, right index finger, left thumb and left index finger, respectively.

Significant effects induced by LF-RSS are represented in figures 7.1, 7.2, 7.3. LF-RSS increased STDT in RII in HC ($p < 0.01$), whereas it decreased STDT in the right thumb and

index finger in CD patients (both p values < 0.05). The effects of HF-RSS on global excitability of the somatosensory system were similar in the two groups, with a decreased amplitude of both N20/P25 and P14 recorded following stimulation of the index finger (p values < 0.01); however, this effect spread in CD patients, affecting both N20/P25 and P14 SEP components obtained by stimulation of the thumb (both p values < 0.01). Overall, the effects of LF-RSS on S1 inhibition were opposite in CD, compared to HC. In HC, the conditioning protocol induced a decrease in the effectiveness of cortical and subcortical somatosensory inhibition, reflected by a decreased suppression of N20/P25 and P14 amplitude obtained with PP-SEP (p values < 0.01), increased Q20 and Q14 (p values < 0.01) and decreased e-HFO and l-HO area (both p values < 0.01). By contrast, in CD patients, LF-RSS induced an increase in paired-pulse suppression of N20/P25 and P14 (p values < 0.01), an increase in Q20 and Q14 (p values < 0.01) and in e-HFO and l-HO area (both p values < 0.01). Similar, opposite effects were observed with regards to M1 inhibition. LF-RSS increase SICI in the APB and the ADM in CD, for all three CS intensities tested (all p values < 0.01); in HC, SICI on the APB decreased for 80% and 90% CS intensities (p = 0.001 and p < 0.001, respectively), while it was left unaffected on the ADM.

	Main effects and interactions	F statistics	P values
STDT stim	Group	$F_{1,24} = 0.016$	$p = 0.902$
	Time	$F_{1,24} = 0.312$	$p = 0.681$
	Finger	$F_{3,72} = 1.474$	$p = 0.346$
	Group × time	$F_{1,24} = 1.958$	$p = 0.174$
	Group × finger	$F_{3,72} = 1.561$	$p = 0.206$
	Time × finger	$F_{3,72} = 1.918$	$p = 0.134$
	Group × time × finger	$F_{3,72} = 0.92$	$p = 0.434$
STDT values	Group	$F_{1,24} = 7.836$	p = 0.010
	Time	$F_{1,24} = 15.802$	p = 0.001
	Finger	$F_{3,72} = 5.725$	p = 0.001
	Group × time	$F_{1,24} = 45.281$	p < 0.001
	Group × finger	$F_{3,72} = 11.228$	p < 0.001

	Time × finger	$F_{3,72} = 14.014$	p < 0.001
	Group × time × finger	$F_{3,72} = 33.480$	p < 0.001
N20 latency I	Group	$F_{1,24} = 0.042$	p = 0.839
	Time	$F_{1,24} = 0.457$	p = 0.505
	Group × time	$F_{1,24} = 3.041$	p = 0.094
N20 latency II	Group	$F_{1,24} = 0.096$	p = 0.760
	Time	$F_{1,24} = 1.448$	p = 0.241
	Group × time	$F_{1,24} = 0.623$	p = 0.561
P14 latency I	Group	$F_{1,24} = 0.235$	p = 0.632
	Time	$F_{1,24} = 0.073$	p = 0.789
	Group × time	$F_{1,24} = 0.008$	p = 0.929
P14 latency II	Group	$F_{1,24} = 0.162$	p = 0.691
	Time	$F_{1,24} = 0.072$	p = 0.791
	Group × time	$F_{1,24} = 0.032$	p = 0.860
N20/P25 amp I	Group	$F_{1,24} = 0.330$	p = 0.571
	Time	$F_{1,24} = 22.744$	p < 0.001
	Group × time	$F_{1,24} = 21.444$	p < 0.001
N20/P25 amp II	Group	$F_{1,24} = 0.001$	p = 0.976
	Time	$F_{1,24} = 69.950$	p < 0.001
	Group × time	$F_{1,24} = 0.689$	p = 0.415
P14 amplitude I	Group	$F_{1,24} = 0.004$	p = 0.948
	Time	$F_{1,24} = 2.644$	p = 0.117
	Group × time	$F_{1,24} = 7.889$	p = 0.010
P14 amplitude II	Group	$F_{1,24} = 0.036$	p = 0.850
	Time	$F_{1,24} = 41.616$	p < 0.001
	Group × time	$F_{1,24} = 2.091$	p = 0.161
N20/P25 rec	Group	$F_{1,24} = 0.231$	p = 0.635

	Time	$F_{1,24} = 44.826$	p < 0.001
	ISI	$F_{2,48} = 91.859$	p < 0.001
	Group × time	$F_{1,24} = 49.296$	p < 0.001
	Group × ISI	$F_{2,48} = 1.551$	p = 0.222
	Time × ISI	$F_{2,48} = 2.530$	p = 0.090
	Group × time × ISI	$F_{2,48} = 0.985$	p = 0.381
P14 rec	Group	$F_{1,24} = 1.060$	p = 0.314
	Time	$F_{1,24} = 17.747$	p < 0.001
	ISI	$F_{2,48} = 18.174$	p < 0.001
	Group × time	$F_{1,24} = 16.512$	p < 0.001
	Group × ISI	$F_{2,48} = 0.833$	p = 0.441
	Time × ISI	$F_{2,48} = 0.917$	p = 0.407
	Group × time × ISI	$F_{2,48} = 0.994$	p = 0.378
Q20	Group	$F_{1,24} = 12.556$	p = 0.002
	Time	$F_{1,24} = 6.168$	p = 0.020
	Group × time	$F_{1,24} = 105.143$	p < 0.001
Q14	Group	$F_{1,24} = 1.202$	p = 0.284
	Time	$F_{1,24} = 10.435$	p = 0.004
	Group × time	$F_{1,24} = 121.814$	p < 0.001
e-HFO	Group	$F_{1,24} = 6.684$	p = 0.016
	Time	$F_{1,24} = 1.261$	p = 0.273
	Group × time	$F_{1,24} = 24.785$	p < 0.001
l-HFO	Group	$F_{1,24} = 3.304$	p = 0.082
	Time	$F_{1,24} = 2.009$	p = 0.169
	Group × time	$F_{1,24} = 31.789$	p < 0.001
Test MEP APB	Group	$F_{1,24} = 0.355$	p = 0.557
	Time	$F_{1,24} = 1.498$	p = 0.233

	Group × time	$F_{1,24} = 0.068$	$p = 0.796$
Tet MEP ADM	Group	$F_{1,24} = 0.578$	$p = 0.454$
	Time	$F_{1,24} = 2.150$	$p = 0.156$
	Group × time	$F_{1,24} = 0.439$	$p = 0.514$
SICI	Group	$F_{1,24} = 3.532$	$p = 0.072$
	Time	$F_{1,24} = 5.242$	$p = 0.031$
	Muscle	$F_{1,24} = 0.557$	$p = 0.463$
	Intensity	$F_{2,48} = 35.951$	$p < 0.001$
	Group × time	$F_{1,24} = 39.034$	$p < 0.001$
	Group × muscle	$F_{1,24} = 0.043$	$p = 0.838$
	Group × intensity	$F_{2,48} = 2.517$	$p = 0.091$
	Time × muscle	$F_{1,24} = 0.779$	$p = 0.386$
	Time × intensity	$F_{2,48} = 0.769$	$p = 0.469$
	Muscle × intensity	$F_{2,48} = 0.797$	$p = 0.457$
	Group × time × muscle	$F_{1,24} = 0.894$	$p = 0.354$
	Group × time × intensity	$F_{2,48} = 13.717$	$p < 0.001$
	Time × muscle × intensity	$F_{2,48} = 2.029$	$p = 0.143$
	Group × time × muscle × intensity	$F_{2,48} = 0.279$	$p = 0.758$

Table 7.3: *statistics relative to main effects and interactions of the ANOVAs. Values are expressed as mean \pm standard deviation. Bold characters indicate statistically significant p values. Stimulation intensities for STDT are measured in mA, latencies in ms and test MEP size in mV. I and II refer to the stimulated thumb and index finger, respectively. Measuring units for variables are as follows: STDT stimulation intensity (stim): mA; STDT values: ms; latencies: ms; P14 and N20/P25 amplitudes (amp): μV ; e-HFO and l-HFO: $\mu\text{V}^2 \times 10^{-4}$; test MEP: mV; N20/P25 recovery (rec), Q14, Q20 and SICI are adimensional.*

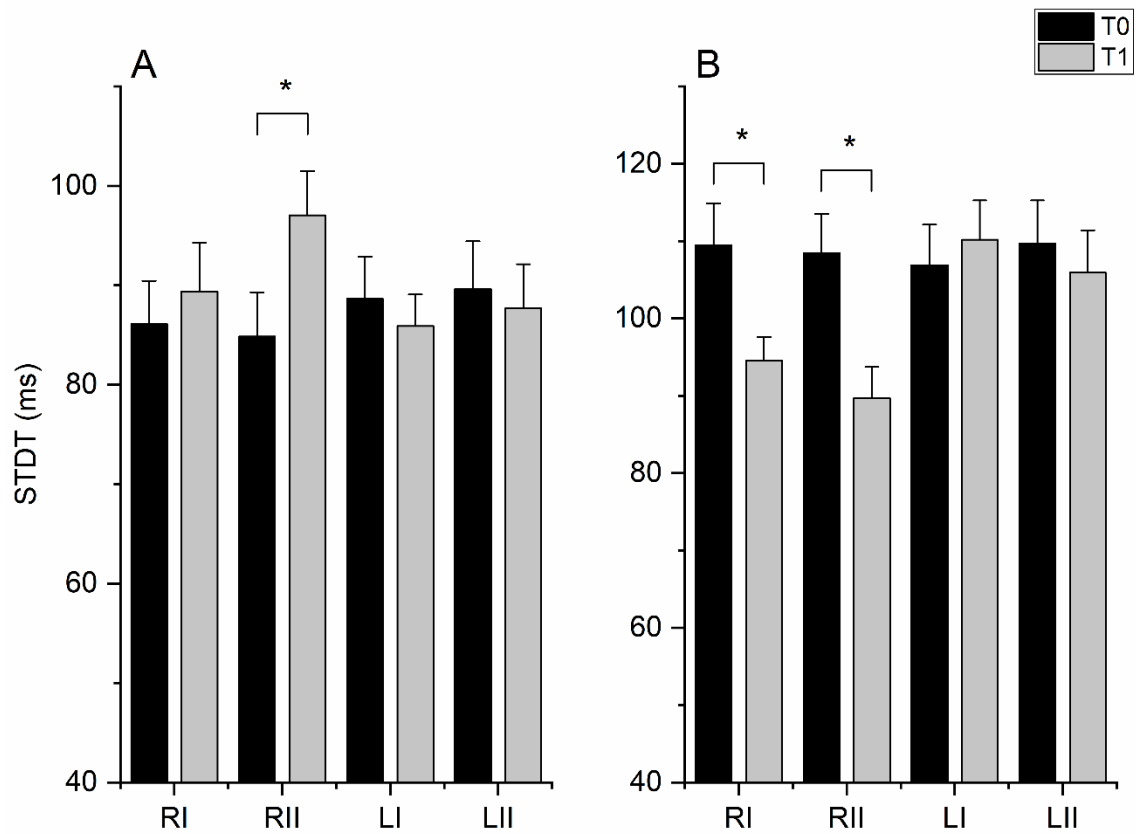


Figure 7.1: effects of LF-RSS on STDT. LF-RSS increased STDT in the right thumb in HC (panel A), whereas it decreased STDT in the right thumb and index finger in CD patients (panel B). Error bars indicate the standard error of the mean. Asterisks indicate statistically significant comparisons ($p < 0.05$).

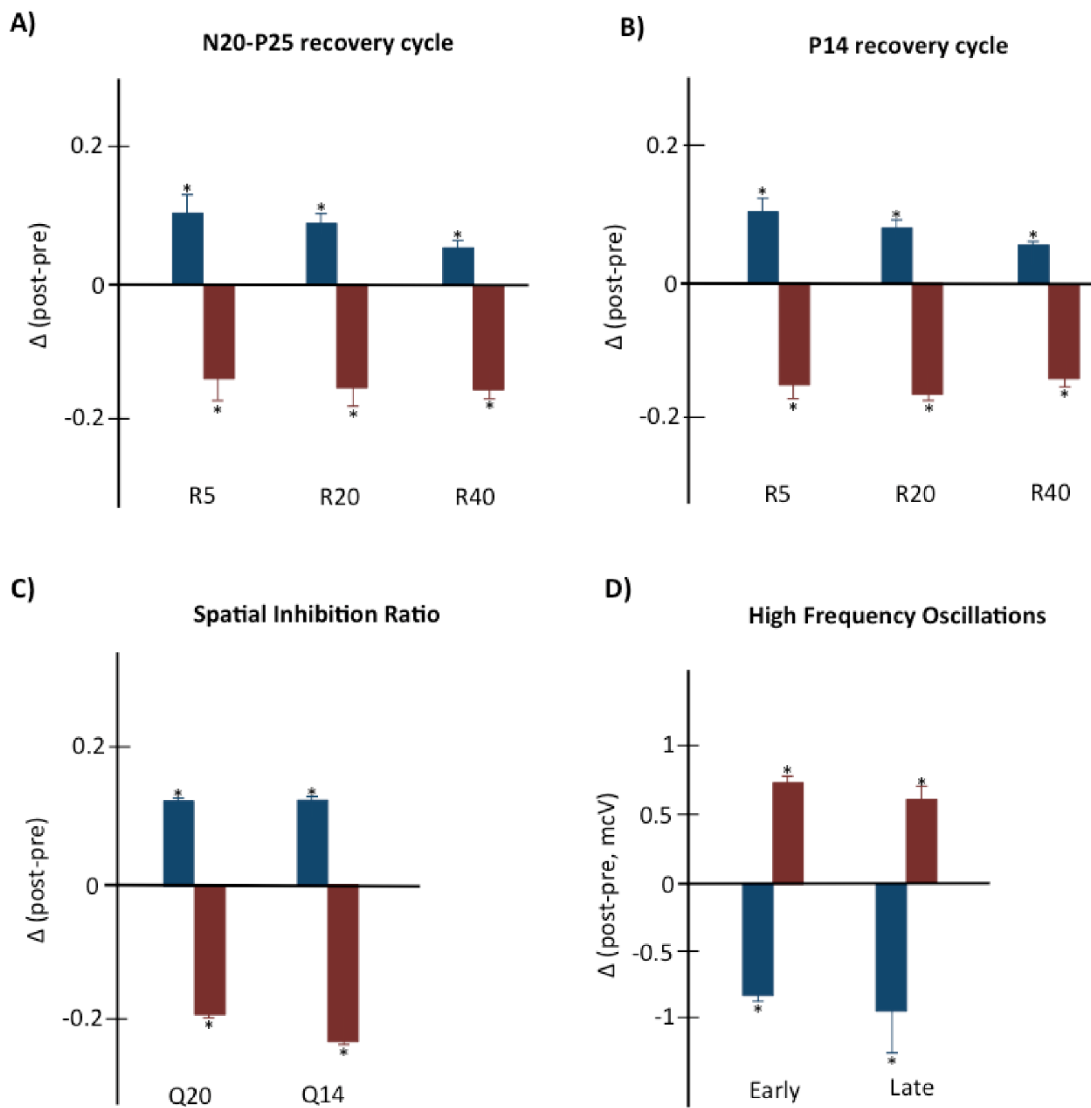


Figure 7.2: effects of LF-RSS on N20/P25 recovery cycle (panel A), P14 recovery cycle (panel B), SIR (panel C), HFO (panel D). Blue bars represent values from HC, red bars from CD patients. Error bars represent indicate the standard error of the mean. Asterisks indicate statistically significant comparisons ($p < 0.05$).

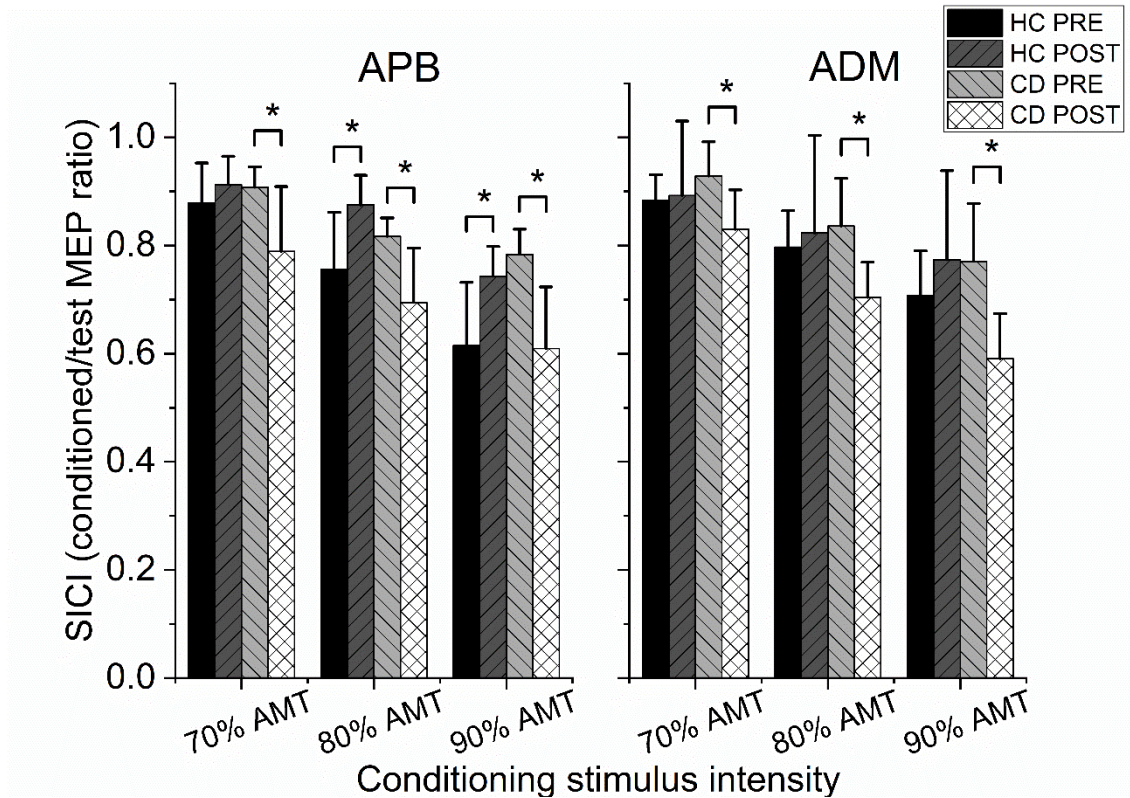


Figure 7.3: effects of LF-RSS on SICI. LF-RSS increased SICI in the APB and the ADM in CD, for all three CS intensities tested; in HC, SICI on the APB decreased for 80% and 90% CS intensities, while it was left unaffected on the ADM. Error bars indicate the standard error of the mean. Asterisks indicate statistically significant comparisons ($p < 0.05$).

In both groups, STDT change on the right index finger correlated with changes of both N20/P25 R5 ($r = .894$ and $.826$, HC and CD patients, respectively) and I-HFO area ($r = -.763$ and $-.793$, HC and CD patients, respectively) (figure 7.4).

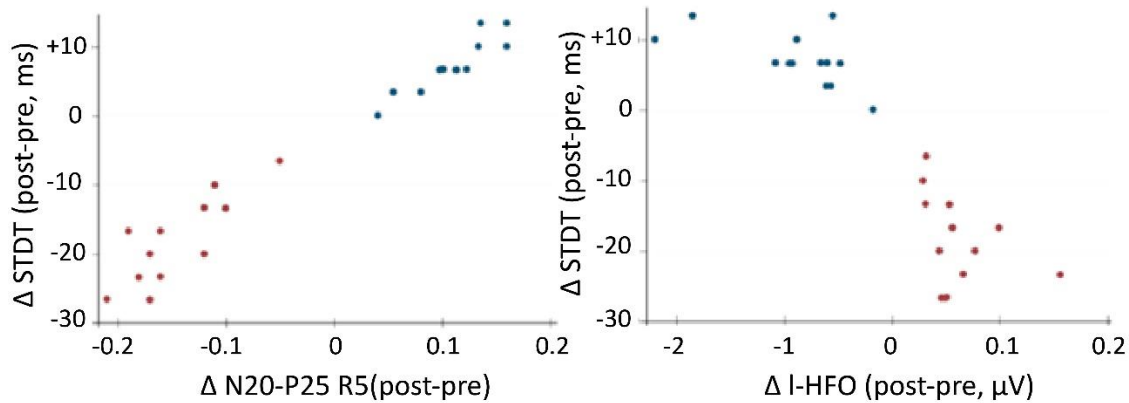


Figure 7.4: correlation between changes induced by HF-RSS on STDT and N20/P25 recovery cycle at 5 ms ISI (left panel) and between STDT and l-HFO (right panel). In both cases STDT refers to the stimulated right index finger. Blue dots represent values from HC, whereas red dots from CD patients.

7.4 Discussion

Baseline comparisons between groups largely confirmed previous findings, showing that patients with CD have higher STDT^{17, 71, 72}, reduced suppression of the recovery cycle of SEP^{17, 202}, impaired lateral inhibition in the sensory system^{17, 165} as well as reduced SICI^{364, 365}. Altogether, these findings support previous suggestions of a widespread loss of inhibition in the CNS in dystonia³⁵⁵. Novel to the current study, however, is the difference in the aftereffects of LF-RSS on STDT and sensorimotor inhibition between the two tested groups. As expected from previous observations in healthy subjects, showing that LF-RSS decreases perceptual performance²⁷⁹, our control group showed a spatially-selective increase in STDT (i.e., on the stimulated area) that correlated with reduced intracortical inhibition within S1. Conversely, in patients with CD, LF-RSS enhanced sensory cortical inhibition and shortened STDT not only in the stimulated area (i.e., right index), but also in adjacent areas (i.e., right thumb), arguably as a result of strengthened lateral inhibition. Interestingly, similar but smaller, aftereffects were observed in the motor systems. Thus, while LF-RSS induced modest detrimental changes in terms of SICI in HC, stronger changes in the opposite direction (i.e., inhibitory enhancement) were observed in patients in both the “target” and “non-target” adjacent muscles (i.e., abductor pollicis brevis and abductor digiti minimi, respectively). The reversal of plasticity after long periods of stimulation has been attributed to the ability of neurons to regulate their own excitability relative to network activity and is described as homeostatic plasticity³⁷¹. It might

be speculated that, in the case of LF-RSS, an initial decrease in inhibition would interact with and reverse the effect of the later part of stimulation, reversing the final effect into an increase in cortical inhibition. Alternatively, baseline low levels of postsynaptic inhibitory activity in patients may facilitate LTP-like changes^{372, 374} and drive a perceptual gain. Our findings seem at odds with previous research suggesting a lack of the normal homeostatic response to plasticity-inducing protocols in CD^{33, 366}. However, our results are difficult to compare since in those studies, the homeostatic interaction was checked between discrete applications of two plasticity protocols, while we used a single, long lasting protocol. In addition, there is the possibility of homeostatic interactions of baseline physiological status of patients with the plasticity protocol. Finally, at variance with previous studies^{33, 366}, stimulation was applied to a non-dystonic body region, suggesting that the observed abnormalities are primarily related to the pathophysiology of dystonia and are not a consequence of abnormal posturing. Interestingly, the aftereffects seen in our S1 excitability measures were also observed in SICI; this transfer of plastic effects to the motor system supports the concept that spatially and temporally distorted sensory information could drive abnormal motor programs in dystonia^{58, 165}. It should be noted, however, that these abnormalities were demonstrated in a non-dystonic body region, which suggests that these defective inhibitory mechanisms might be able to explain impaired sensory processing as demonstrated by increased STDT, but are not sufficient to produce dystonic symptoms. Nonetheless, our findings might provide the rationale to apply LF-RSS to dystonic body regions, particularly in the view of the fact that our intervention enhanced inhibition in subcortical structures as well as the cortex. Indeed, one of the unique advantages of RSS compared to other stimulation paradigms is the fact that inputs travel through somatosensory pathways relaying both at cortical and subcortical levels^{275, 322, 323}, in areas that are putatively involved in the pathophysiology of dystonia. We acknowledge the relatively small sample size prevents us from drawing firm conclusions. However, the results were strikingly different between groups. We therefore suggest that the abnormal response to RSS can be interpreted as impaired homeostatic inhibitory plasticity in dystonia. This abnormality might be specifically leveraged with LF-RSS to enhance sensorimotor inhibition, normalise STDT and, possibly, ameliorate motor symptoms.

8 Amelioration of focal hand dystonia via low-frequency repetitive somatosensory stimulation

8.1 Introduction

In this last project, we sought to characterize the effects of RSS applied directly on muscles involved in dystonia. In the previous sections, we demonstrated the following: a) inhibitory circuitry in S1 can be characterized *in vivo* by measuring PP-SEP, SIR and HFO extracted from standard SEP, and they show typical abnormalities in dystonic patients¹⁷; b) the effectiveness of inhibitory interactions in S1 and M1 can be manipulated, in healthy subjects, by applying RSS on digital nerves³⁶¹; c) CD patients have a paradoxical response to both HF-RSS and LF-RSS: the first leads to a decrease in effectiveness of sensorimotor inhibitory mechanisms³⁸¹, whereas the second induces opposite changes; this findings are opposite to those obtained in HC²⁷⁹.

It is to note that, in the experiments outlined in the previous sections of this work, we probed the effects of RSS on sensorimotor circuitry by applying the conditioning protocol on a body part not affected by dystonia. Indeed, RSS was applied on digital nerves, whereas patients were affected by CD. It is not known whether delivering RSS on a dystonic body part would lead to the same results. At least one line of evidence would point to this direction, i.e. the known increase in STDT described in dystonia. This abnormality is usually not directly linked to dystonic symptoms^{62,63}, can be found in unaffected relatives of patients with dystonia⁷⁵ and is not specific to affected body parts or correlated with disease severity^{61,71}. Since it was suggested that STDT represents a behavioural correlate of S1 inhibitory mechanisms²¹¹, it is possible that deranged inhibition and possibly abnormal homeostatic inhibitory plasticity are present globally in the somatosensory system of dystonic patients, regardless of the distribution of dystonia.

A further important reason to test the effects of RSS applied on dystonic body parts comes from previous findings in stroke patients. Smith and coworkers³²⁵ found that RSS delivered on the fingers of patients affected by chronic stroke, presenting with motor and somatosensory impairment, could improve not only sensory performance, but also motor hand function. This could not be tested in our previous investigations since RSS was applied in a non-dystonic body area. However, an important finding was noted: the changes in S1

inhibition, observed after RSS, were paralleled by similar changes in M1 inhibition assessed with SICI. We speculated that this effect could be mediated by the somatotopic connections between S1 and M1^{349, 351} and be analogous to the LTP induced in M1 by tetanic stimulation of S1 in animal models^{352, 353}. It is therefore possible that an increased effectiveness of inhibitory M1 circuitry subserving hand function could lead to improvement in focal hand dystonia.

We therefore tested the hypothesis whether RSS is able to enhance defective inhibitory mechanisms in patients with FHD. Patients were divided into three groups, according to the stimulation pattern received. In the first two groups, we used either HF-RSS or LF-RSS, based on the results of our previous investigations. We expected that, due to altered homeostatic plasticity, HF-RSS delivered synchronously over dystonic muscles would decrease the effectiveness of inhibition at the boundary of their representation in the somatosensory and motor areas, increasing their simultaneous contraction and thus worsening dystonia. By contrast, we would expect LF-RSS to lead to the opposite response, i.e. a refinement in inhibition and a consequent improvement of dystonia. The stimulation used in the third group is different and is based on the principle of STDP. A well-established approach to test plasticity in humans in a non-invasive way is PAS, that combines repetitive electrical stimulation of a nerve with subsequent TMS of the contralateral M1. The direction of PAS-induced cortical excitability changes depends on the exact sequence of events induced in M1 by each of the stimulation modalities³⁹², similar to the SDTP of synaptic efficacy observed in brain preparations of animals²⁷³. Using PAS, it has been demonstrated that both LTP-like and LTD-like plasticity are enhanced in patients with writer's cramp, which is a form of FHD^{34, 393}. Based on this principle, in the third group of FHD patients we delivered LF-RSS asynchronously over affected muscles. In this case, we hypothesized that the asynchronicity would act at the cortical level by LTD-like mechanism following the principle of STDP, possibly inducing inhibition of the abnormal muscle synergies characterizing dystonia.

8.2 Materials and methods

8.2.1 Patients and clinical evaluation

Forty-five patients with a diagnosis of FHD (22 male, 23 female, mean age 55.13 ± 13.04) were enrolled in the study (their characteristics are summarized in table 8.1). They were recruited from those attending the outpatients clinic of the Clinical Neurophysiology

Department of the Institute of Neurology, University College London. Patients were assessed at least 3 months after their last BoNT injection, and they were not treated with other drugs for their dystonia. Handedness was assessed by the Edinburgh handedness Inventory ³⁰² and dystonia was clinically assessed by means of the UDRS and ADDS. All experimental procedures were approved by the local institutional review board and conducted in accordance with the Declaration of Helsinki according to international safety guidelines.

8.2.2 Hand motor function tasks

Hand dexterity was assessed with the BBT and the NHPT. In the BBT, patients had to move, one by one, the maximum number of blocks from one compartment of a box to another of equal size, within sixty seconds. The number of blocks moved was used as a variable for following analyses. In the NHPT, subjects were asked to put, as fast as possible, nine wooden pegs from a container into holes in a board, and then back. The behavioural variable of interest, which was measured and used for further analyses, was the time in seconds to complete the task.

8.2.3 Electromyographic recording and transcranial magnetic stimulation

EMG activity was recorded using Ag/AgCl electrodes placed over the two most affected by dystonia and were primarily chosen based on BoNT treatment (table 8.1). In case patients received injection in only one, or no muscles, recording sites were chosen based on clinical observation of dystonia (i.e. muscles where involuntary contraction was more clearly seen at examination). No patients had BoNT injections in more than two forearm sites. EMG signals were digitized at 5 kHz with a CED 1401 A/D laboratory interface (Cambridge Electronic Design, Cambridge, UK) and bandpass filtered (5 Hz - 2 kHz) with a Digitimer D360 (Digitimer Ltd., Welwyn Garden City, Hertfordshire, UK). Data were stored on a laboratory computer for on-line visual display and further off-line analysis (Signal software, Cambridge Electronic Design, Cambridge, UK). EMG activity was monitored throughout the experiment. TMS was performed using a Magstim 200 monophasic stimulator with a 70 mm figure-of-eight coil (Magstim Company Limited, Whitland, UK).

Group 1 – HF-RSS

Age	Gen	Hand	Disease duration	UDRS	ADDS	M1	M2
-----	-----	------	------------------	------	------	----	----

1	50	F	R	1	2.50	85.95	FCR	FDS
2	74	F	R	18	6.50	72.86	PT	FCU
3	74	M	R	11	14.00	42.86	FCU	BR
4	68	M	R	20	4.50	55.71	FCR	ECR
5	50	F	L	15	3.50	77.14	EDC	FCR
6	63	M	R	7	8.50	68.57	ADM	FCU
7	58	F	L	6	9.00	81.43	FCR	FDI
8	55	F	R	15	6.00	90.48	FCR	ECR
9	58	F	R	12	12.00	47.14	FCR	FPL
10	51	M	R	7	8.00	58.81	PT	FCU
11	42	M	R	8	4.00	85.71	FDS	FPL
12	49	F	L	4	8.50	42.86	FCU	BR
13	55	M	R	5	9.00	47.14	FCR	ECR
14	51	F	L	6	6.00	85.95	ADM	FCU
15	48	M	R	14	14.00	47.14	FDS	FPL
AV	56.4			9.9	7.73	65.98		
SD	9.6			5.5	3.57	17.92		

Group 2 – LF-RSS

	Age	Gen	Hand	Disease duration	UDRS	ADDS	M1	M2
1	58	F	L	6.00	8.50	81.43	FCR	FDI
2	52	M	R	10.00	26.50	68.57	FCU	ECR
3	53	F	R	6.00	8.00	95.24	FPL	APL
4	41	M	R	15.00	4.50	72.38	FCR	FPL
5	45	F	R	15.00	2.50	72.38	FDS	FPL
6	44	F	R	10.00	4.00	90.48	FDS	FPL
7	66	M	R	20.00	7.00	38.57	FDS	FCR
8	58	F	R	7.00	14.00	55.71	FCR	ECR

9	58	M	R	9.00	9.00	55.71	FCU	ECR
10	53	F	R	10.00	5.50	38.57	FCR	ECR
11	49	M	R	5.00	5.00	85.95	PT	FCU
12	67	F	R	7.00	8.50	47.14	FDS	ECR
13	64	F	R	9.00	9.50	60.00	ADM	FCU
14	66	M	R	12.00	11.50	72.38	FCR	PT
15	74	M	L	13.00	12.00	42.86	FDS	FPL
AV	56.5			10.27	9.07	65.16		
SD	9.6			4.13	5.78	18.62		

Group 3 – LFas-RSS

	Age	Gen	Hand	Disease duration	UDRS	ADDS	M1	M2
1	71	M	R	6.00	5.00	34.29	FCR	FCU
2	45	F	R	10.00	3.00	55.71	FCR	FDS
3	63	M	R	7.00	8.50	68.57	ADM	FCU
4	45	M	R	2.50	7.00	30.00	EPL	EDC
5	66	M	R	20.00	7.00	38.57	FDS	FCR
6	48	M	L	1.00	13.00	17.14	FDS	ECR
7	71	F	R	13.00	2.00	85.71	FCU	PT
8	45	F	R	8.00	6.00	85.95	FCU	ADM
9	63	M	R	6.00	14.00	64.29	FCR	ECR
10	45	F	R	9.00	6.50	90.48	FCR	ECR
11	66	M	R	13.00	14.50	54.29	FCR	EDC
12	52	F	L	16.00	2.50	85.71	FDS	ECR
13	76	F	R	11.00	8.50	76.90	FDS	FPL
14	72	F	R	7.00	10.00	72.38	PT	FCU
15	65	M	R	11.00	13.50	68.57	FDS	EDC
AV	59.5			9.37	8.07	61.9		

SD 11.5 4.94 4.2 22.96

Table 8.1: *patient variables. Abbreviations for muscles: ADM: abductor digiti minimi; APL: abductor pollicis longus; BR: brachioradialis; ECR: extensor carpi radialis; EDC: extensor digitorum communis; EPL: extensor pollicis longus; FCR: flexor carpi radialis; FCU: flexor carpi ulnaris; FDI: first dorsal interosseous; FDS: flexor digitorum superficialis; FPL: flexor pollicis longus; PT: pronator teres. Other abbreviations: AV: average; Hand: hand affected by dystonia; Gen: gender; AV: average; SD: standard deviation.*

First, the motor hotspot was found. Differently from the other experiments, here we were interested mostly in EMG activity from forearm muscles; therefore, the hotspot was defined as the M1 location where the largest MEP with respect to forearm muscles could be obtained. Then, we found the RMT related to the less excitable of the two forearm muscles, and we measured the intensity able to elicit motor evoked potentials of at least 0.5 mV (0.5 mV-int) in both of them. RMT was defined as the lowest intensity able to evoke a MEP of at least 50 μ V in five out ten consecutive trials during rest³³⁵. SICI was obtained through a paired-pulse TMS, with an ISI of 3 ms between the CS and the test stimulus. The test stimulus was set at 0.5 mV-int, while the CS was set at 50%, 60% 70%, 80%, 90% and 100% RMT, to obtain a recruitment curve²⁴⁷. Fifteen paired stimuli for each different intensity of the CS and fifteen single pulses were delivered in a randomized order. SICI was calculated dividing the amplitude of conditioned/unconditioned MEP.

8.2.4 Somatosensory evoked potentials recording and analysis

To record the N20/P25 component of SEP, the active electrode was placed at CP3 or CP4 (contralateral to the dystonic arm) and the reference electrode at Fz, while P14 was recorded with the active electrode at Fz and the reference electrode on the contralateral mastoid^{280, 304} (Klem et al., 1999; Cruccu et al., 2008). For stimulation, we used the same electrodes used to record EMG signals from the forearm sites of interest, but this time they were connected to two current stimulator (Digitimer DS7A). Monophasic square wave pulses of 200 μ s duration were delivered at a frequency of 3 Hz. Since the stimulation was not applied on a nerve trunk, as for standard SEP, the brain potential recorded would be due to afferent activity due to muscle contraction, with a little contribution from stimulation of the overlying skin. This would result

in a considerably smaller signal; to try to overcome this limitation, the stimulation intensity was the highest that subject could tolerate without generating pain. The somatosensory threshold was also recorded at each site, defined as the minimum current intensity able to elicit a consistent percept. Signals were recorded from -20 to +100 ms with regard to the pulse, digitized with a 5 KHz sampling frequency and band-pass filtered (3 Hz - 2 KHz) ³⁰⁴. Three blocks, of 500 trials each, were recorded by stimulation at each forearm site separately, one with single pulse stimulation, and the other two with paired-pulse stimulation with ISI of 5 and 30 ms. In the frames obtained using two stimuli, responses following the second stimulus were obtained by subtracting the SEP waveform obtained by the first stimulus from the waveform following each double stimulus ^{306, 334}. R5 and R30 were calculated as the ratio between the second and the first response. In a further block, again of 500 trials, stimulation was given at the two forearm sites at the same time. As in the previous chapters, the SIR of N20/P25 (Q20) and P14 (Q14) were calculated as the ratio $M1M2/(M1+M2) \times 100$, where M1M2 is the SEP amplitude obtained by simultaneous stimulation of the two forearm sites and M1+M2 is the arithmetic sum of the SEP obtained by the individual stimulation at the two sites ¹⁶⁵. All blocks were recorded in a randomized order. The position of the electrodes was kept constant throughout the whole experiment and care was taken to always keep impedances below 5 K Ω .

8.2.5 Repetitive somatosensory stimulation

RSS was delivered on the forearm sites located as described before for SEP. Each of the three groups of patients underwent a different RSS protocol, but the overall duration of each was the same (45 minutes). As for SEP, the somatosensory threshold was measured for each protocol, and conditioning was applied at the maximum tolerable, non-painful intensity. HF-RSS consisted of 20 Hz trains of stimuli (0.2 ms square wave electrical pulses) of 1 s duration, with 5 s inter-train interval, applied to both forearm sites at the same time. LF-RSS was delivered in a similar way, exception made for the different pattern of stimulation, which consisted of 1 pulse applied every second. Lastly, in its asynchronous variant (LFas-RSS), electric pulses were applied intermittently on each muscle site, with a 0.5 s interval.

8.2.6 Experimental procedure

Subjects were seated in a comfortable chair for the whole duration of the experiment. First, they underwent clinical assessment with the UDRS and ADDS. Several baseline (T0) measurements were then performed, as detailed above, including 1) hand function tests (BBT, NHPT); 2) EMG measurement in two blocks of postural activity (arms outstretched and holding a pen, one minute each); 3) TMS (including SICI); 4) SEP recording (single pulse, R5, R30, SIR). These measures were randomized and repeated after RSS (T1). To note that, since most of these variables relied on thresholds, the latter were measured again after RSS and the various stimulation intensities were adjusted accordingly where needed.

8.2.7 Statistical analysis

In this section and the Results one, groups will be identified with the stimulation protocol received (i.e. HF-RSS, LF-RSS, LFas-RSS). Age, disease duration, scores of UDRS and ADDS, thresholds and stimulation intensities for RSS were compared by means of one-way between group ANOVAs. Several two-way mixed ANOVAs with “group” (HF-RSS, LF-RSS, LFas-RSS) and “time” (T0, T1) as factors of analysis were performed on thresholds and stimulation values, including RMT, 0.5 mV-int, somatosensory threshold and stimulation intensities for SEP; this was done to compare baseline values in the three groups and to assess the effect of RSS on these variables. ANOVAs with the same factors were performed to investigate the effect of RSS on the following variables: a) number of blocks moved in 60 seconds in the BBT; b) time to complete the NHPT; c) root mean square (RMS) of the EMG activity recorded at sites M1 and M2 during postural activity (arms outstretched, holding a pen).

The effect of RSS on SICI was investigated with two separate three-way mixed ANOVAs with factors “group” (HF-RSS, LF-RSS, LFas-RSS), “time” (T0, T1) and “intensity” (50%, 60%, 70%, 80%, 90%, 100% RMT, indicating the intensity of the conditioning pulse), one for each forearm site (M1, M2). To exclude that possible changes in SICI were biased by changes in test MEP amplitude, two separate two-way mixed ANOVAs with “group” (HF-RSS, LF-RSS, LFas-RSS) and “time” (T0, T1) as factors of analysis were performed on the latter variable, separately for M1 and M2 sites.

The effect of RSS on latencies (P14, N20) and amplitudes (P14, N20/P25) of SEP evoked by single pulse stimulation at M1 and M2 sites, as well as the effects of RSS on Q14 and Q20, was investigated by several mixed ANOVAs with “group” (HF-RSS, LF-RSS, LFas-

RSS) and “time” (T0, T1) as factors of analysis. The recovery cycle of P14 and N20/P25 amplitude was assessed with a similar ANOVA, but with the addition of “ISI” (5 ms, 30 ms) as a within-subject factor of analysis. Lastly, the effects of RSS on SIR was investigated with two separate mixed ANOVAs with “group” (HF-RSS, LF-RSS, LFas-RSS) and “time” (T0, T1) as factors of analysis, one for P14 and the other for N20/P25 amplitude. Possible correlations between the effects induced by RSS on different variables were investigated with Pearson’s correlation coefficient. For this analysis, we considered the maximum SICI obtained at the group level, averaged between M1 and M2. Additionally, correlation analyses were run after pooling data from all groups together. Normality of distribution was assessed with the Shapiro-Wilks’ test, while Greenhouse-Geisser correction was used, if necessary, to correct for non-sphericity (i.e. Mauchly’s test < 0.05). P values < 0.05 were deemed significant. Homogeneity of variance across groups was tested with the Levene’s test. Bonferroni post-hoc test was used for post-hoc comparisons following ANOVAs and for correlations.

8.3 Results

No side effects were recorded during the experimental sessions. The three groups of patients examined did not significantly differ in terms of age, disease duration, ADDS, UDRS, thresholds and stimulation values; additionally, the latter two variables were not changed by RSS, as demonstrated by the ANOVAs (values of the mentioned variables, as well as statistics of the ANOVAs, are summarized in table 8.2).

	Group 1		Group 2		Group 3		Group	Time	Group × Time
	(HF-RSS)		(LF-RSS)		(LFas-RSS)				
	T0	T1	T0	T1	T0	T1			
Age	56.4		56.5		59.5		F=0.45		
	±		±		±		p=0.64		
	9.6		9.5		11.5				
DD	9.9		10.3		59.5		F=0.13		
			±		±		p=0.88		

	±		4.1		4.9				
	5.6								
UDRS	7.7		9.1		8.1		F=0.34		
	±		±		±		p=0.71		
	3.6		5.8		4.2				
ADDS	65.9		65.2		61.9		F=0.18		
	±		±		±		p=0.84		
	17.9		18.6		22.9				
RMT	51.20	51.67	53.0	53.67	51.60	52.27	F=0.15	F=0.41	F=0.95
	±	±	±	±	±	±	p=0.87	p=0.65	p=0.91
	11.82	11.87	6.55	6.44	10.93	10.96			
0.5 mV-int	64.07	64.20	65.60	64.93	64.60	63.80	F=0.04	F=1.18	F=1.92
	±	±	±	±	±	±	p=0.96	p=0.42	p=0.16
	14.39	13.70	7.93	8.06	13.52	12.91			
SEP ST	3.1	3.2	2.8	2.9	3.2	3.4	F=1.28	F=1.10	F=2.18
M1	±	±	±	±	±	±	p=0.29	p=0.48	p=0.09
	0.9	0.9	0.8	0.8	0.8	0.7			
SEP ST	3.1	3.2	2.9	3.0	3.2	3.3	F=0.38	F=1.56	F=1.15
M2	±	±	±	±	±	±	p=0.68	p=0.15	p=0.33
	1.1	1.1	1.0	1.0	0.8	0.8			
SEP STIM	10.1	10.4	10.2	10.5	11.1	11.3	F=0.21	F=1.23	F=0.66
M1	±	±	±	±	±	±	p=0.21	p=0.32	p=0.53
	2.6	2.5	5.0	4.8	4.6	4.5			
SEP STIM	9.2	9.6	10.3	10.8	10.6	10.9	F=0.57	F=1.41	F=0.44
M2	±	±	±	±	±	±	p=0.57	p=0.22	p=0.65
	2.3	2.4	4.7	4.9	3.5	3.5			
RSS ST	2.6		2.8		3.2		F=1.51		
M1	±		±		±		p=0.23		
	1.3		0.8		0.8				

RSS ST	2.5	3.2	3.3	F=2.01
M2	±	±	±	p=0.15
	1.3	1.2	0.8	
RSS STIM	8.7	11.4	13.1	F=1.53
M1	±	±	±	p=0.22
	3.0	5.6	6.8	
RSS STIM	8.9	11.3	13.6	F=2.01
M2	±	±	±	p=0.15
	3.1	5.1	4.3	

Table 8.2: effects of RSS on thresholds and stimulation intensities. DD: disease duration; ST: somatosensory threshold; STIM: stimulation condition (refers to both SEP and RSS). M1 and M2 indicate the two forearm sites where stimulation was delivered (see text for details). Values are expressed as mean ± standard deviation. Note that degrees of freedom and error were 1,42 for main effects of “group” and “time”, and 2,42 for “group×time” interaction.

Statistics of the ANOVAs are summarized in table 8.3, and a description of the results, including post-hoc comparisons, is given in relevant subsections.

	Main effects and interactions	F statistics	P values
BBT	Group	F _{1,42} = 0.803	p = 0.455
	Time	F _{1,42} = 16.490	p < 0.001
	Group × time	F _{2,42} = 39.787	p < 0.001
NHPT	Group	F _{1,42} = 1.442	p = 0.248
	Time	F _{1,42} = 9.131	p = 0.004
	Group × time	F _{2,42} = 45.853	p < 0.001
RMS M1 outstretched	Group	F _{1,42} = 0.700	p = 0.502
	Time	F _{1,42} = 6.849	p = 0.012

	Group × time	$F_{2,42} = 22.773$	p < 0.001
RMS M1 pen	Group	$F_{1,42} = 0.349$	p = 0.708
	Time	$F_{1,42} = 9.271$	p = 0.004
	Group × time	$F_{2,42} = 24.223$	p < 0.001
RMS M2 outstretched	Group	$F_{1,42} = 1.560$	p = 0.222
	Time	$F_{1,42} = 8.475$	p = 0.006
	Group × time	$F_{2,42} = 15.700$	p < 0.001
RMS M2 pen	Group	$F_{1,42} = 0.593$	p = 0.557
	Time	$F_{1,42} = 9.218$	p = 0.004
	Group × time	$F_{2,42} = 20.541$	p < 0.001
Test MEP M1	Group	$F_{1,42} = 0.806$	p = 0.453
	Time	$F_{1,42} = 0.612$	p = 0.439
	Group × time	$F_{2,42} = 0.392$	p = 0.678
Test MEP M2	Group	$F_{1,42} = 0.949$	p = 0.395
	Time	$F_{1,42} = 1.645$	p = 0.217
	Group × time	$F_{2,42} = 0.094$	p = 0.910
SICI M1	Group	$F_{1,42} = 1.850$	p = 0.170
	Time	$F_{1,42} = 90.217$	p < 0.001
	Intensity	$F_{5,210} = 382.88$	p < 0.001
	Group × time	$F_{2,42} = 140.995$	p < 0.001
	Group × int	$F_{10,210} = 3.563$	p < 0.001
	Time × int	$F_{5,210} = 0.988$	p = 0.426
	Group × time × int	$F_{10,210} = 13.225$	p < 0.001
SICI M2	Group	$F_{1,42} = 2.257$	p = 0.117
	Time	$F_{1,42} = 33.375$	p < 0.001
	Intensity	$F_{5,210} = 305.61$	p < 0.001
	Group × time	$F_{2,42} = 63.899$	p < 0.001

	Group × int	$F_{10,210} = 2.872$	p < 0.001
	Time × int	$F_{5,210} = 2.657$	p = 0.024
	Group × time × int	$F_{10,210} = 5.168$	p < 0.001
SEP N20 latency M1	Group	$F_{1,42} = 0.963$	p = 0.390
	Time	$F_{1,42} = 2.912$	p = 0.425
	Group × time	$F_{2,42} = 0.872$	p = 0.425
SEP N20 latency M2	Group	$F_{1,42} = 0.711$	p = 0.497
	Time	$F_{1,42} = 0.031$	p = 0.861
	Group × time	$F_{2,42} = 0.187$	p = 0.830
SEP P14 latency M1	Group	$F_{1,42} = 1.759$	p = 0.185
	Time	$F_{1,42} = 0.106$	p = 0.746
	Group × time	$F_{2,42} = 0.265$	p = 0.768
SEP P14 latency M2	Group	$F_{1,42} = 0.348$	p = 0.828
	Time	$F_{1,42} = 1.517$	p = 0.225
	Group × time	$F_{2,42} = 0.190$	p = 0.828
SEP N20/P25 amp M1	Group	$F_{1,42} = 1.657$	p = 0.214
	Time	$F_{1,42} = 36.647$	p < 0.001
	Group × time	$F_{2,42} = 146.281$	p < 0.001
SEP N20/P25 amp M2	Group	$F_{1,42} = 2.541$	p = 0.125
	Time	$F_{1,42} = 8.201$	p = 0.007
	Group × time	$F_{2,42} = 60.386$	p < 0.001
SEP P14 amplitude M1	Group	$F_{1,42} = 1.984$	p = 0.127
	Time	$F_{1,42} = 25.436$	p < 0.001
	Group × time	$F_{2,42} = 65.569$	p < 0.001
SEP P14 amplitude M2	Group	$F_{1,42} = 2.781$	p = 0.103
	Time	$F_{1,42} = 50.082$	p < 0.001
	Group × time	$F_{2,42} = 151.986$	p < 0.001

SEP Q20	Group	$F_{1,42} = 1.293$	$p = 0.264$
	Time	$F_{1,42} = 8.709$	$p = 0.005$
	Group \times time	$F_{2,42} = 43.183$	$p < 0.001$
SEP Q14	Group	$F_{1,42} = 2.447$	$p = 0.139$
	Time	$F_{1,42} = 7.032$	$p = 0.011$
	Group \times time	$F_{2,42} = 21.401$	$p < 0.001$
SEP N20/P25 recovery M1	Group	$F_{1,42} = 17.874$	$p < 0.001$
	Time	$F_{1,42} = 137.991$	$p < 0.001$
	ISI	$F_{1,42} = 196.593$	$p < 0.001$
	Group \times time	$F_{2,42} = 322.446$	$p < 0.001$
	Group \times ISI	$F_{2,42} = 0.894$	$p = 0.417$
	Time \times ISI	$F_{1,42} = 32.061$	$p < 0.001$
	Group \times time \times ISI	$F_{2,42} = 1.146$	$p = 0.328$
SEP N20/P25 recovery M2	Group	$F_{1,42} = 21.037$	$p < 0.001$
	Time	$F_{1,42} = 256.769$	$p < 0.001$
	ISI	$F_{1,42} = 213.856$	$p < 0.001$
	Group \times time	$F_{2,42} = 578.0.7$	$p < 0.001$
	Group \times ISI	$F_{2,42} = 1.141$	$p = 0.329$
	Time \times ISI	$F_{1,42} = 24.448$	$p < 0.001$
	Group \times time \times ISI	$F_{2,42} = 3.103$	$p = 0.055$
SEP P14 recovery M1	Group	$F_{1,42} = 33.025$	$p < 0.001$
	Time	$F_{1,42} = 175.700$	$p < 0.001$
	ISI	$F_{1,42} = 239.572$	$p < 0.001$
	Group \times time	$F_{2,42} = 512.329$	$p < 0.001$
	Group \times ISI	$F_{2,42} = 2.149$	$p < 0.001$
	Time \times ISI	$F_{1,42} = 22.409$	$p < 0.001$
	Group \times time \times ISI	$F_{2,42} = 0.413$	$p = 0.664$

SEP P14 recovery M2			
	Group	$F_{1,42} = 9.914$	p < 0.001
	Time	$F_{1,42} = 167.258$	p < 0.001
	ISI	$F_{1,42} = 211.008$	p < 0.001
	Group × time	$F_{2,42} = 488.688$	p < 0.001
	Group × ISI	$F_{2,42} = 3.065$	p = 0.057
	Time × ISI	$F_{1,42} = 22.235$	p < 0.001
	Group × time × ISI	$F_{2,42} = 0.499$	p = 0.611

Table 8.3: *statistics relative to main effects and interactions of the ANOVAs. Values are expressed as mean ± standard deviation. In the statistics for SICI, “int” refers to the intensity of the conditioning stimulus. Bold characters indicate statistically significant p values.*

8.3.1 Hand motor function tests and EMG activity during posture

Baseline scores of the BBT and the NHPT were not significantly different across groups. Overall, HF-RSS caused a worsening of motor performance, whereas both LF-RSS and LFas-RSS induced a slight improvement in hand motor function, more marked in the second case. In particular, after HF-RSS, the number of boxes moved in the BBT was smaller at T1 than T0 (p < 0.01), and this was paralleled by an increase in the time taken by subjects to complete the NHPT (p < 0.01). By contrast, after LF-RSS, patients were able to move more boxes in the BBT (p < 0.01) and to perform the NHPT in a smaller time (p < 0.01). The same effect, but slightly more marked, was observed after LFas-RSS (p values < 0.01 for both the BBT and the NHPT) (figure 8.1).

The RMS of the EMG activity, while subjects kept their arms outstretched, increased both in M1 (p < 0.01) and M2 (p = 0.07) after HF-RSS, whereas it decreased after LF-RSS (p = 0.02 for M1 and p = for M2) and after LFas-RSS (p < 0.01 for both M1 and M2). Similar changes in EMG RMS occurred when subjects held a pen, with RMS increasing after HF-RSS (p < 0.01 for M1 and p = 0.02 for M2) and decreasing after LF-RSS (p = 0.01 for both M1 and M2) and LFas-RSS (p < 0.01 for both M1 and M2) (figure 8.1).

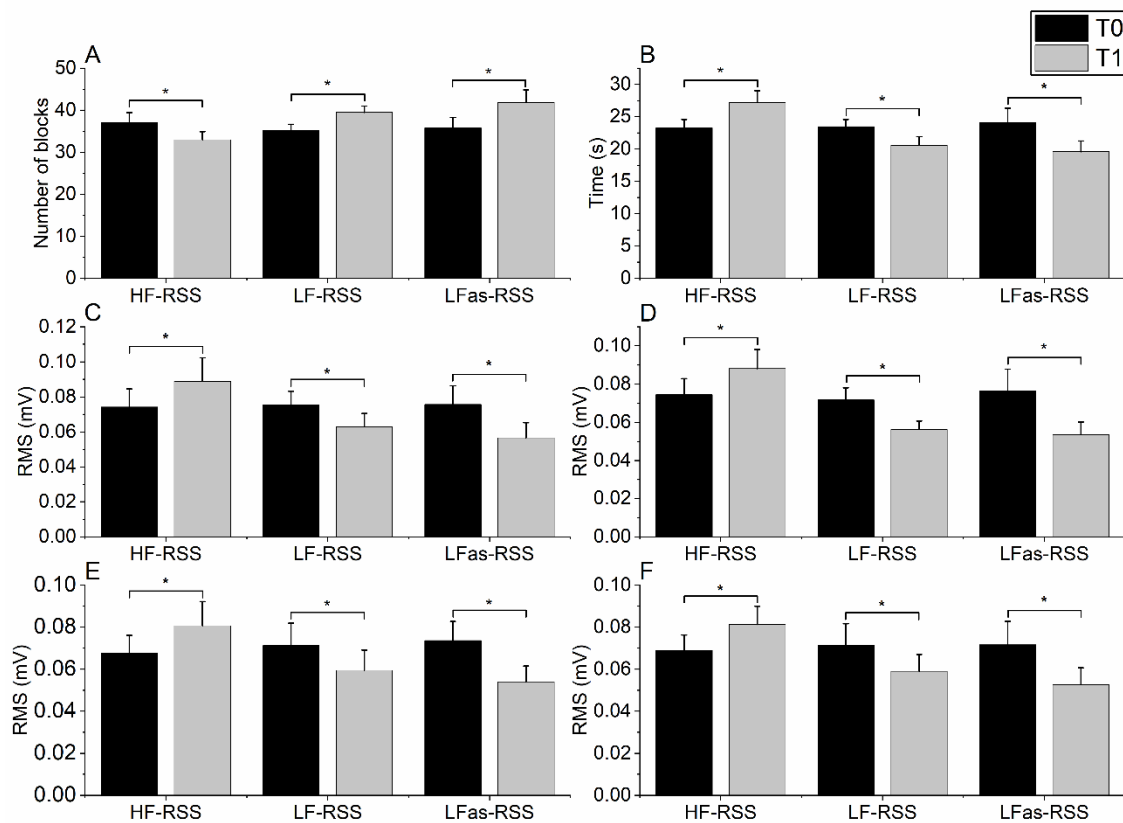


Figure 8.1: effects of RSS on BBT (panel A), NHPT (panel B), RMS of EMG recorded from M1 when arms were outstretched (panel C), RMS of EMG recorded from M2 when arms were outstretched (panel D), RMS of EMG recorded from M1 while holding a pen (panel E), RMS of EMG recorded from M2 while holding a pen (panel F). Error bars indicate the standard error of the mean. Brackets with asterisks indicate statistically significant comparisons.

8.3.2 Motor evoked potentials and short intracortical inhibition

Results are summarized in figure 8.2. Maximum SICI was found, in all groups and time points, for CS intensity of 80% RMT, consistent with previous reports²⁴⁷. There was no effect of RSS on test MEP. HF-RSS induced a decrease in SICI at T1 in both M1 and M2; this decrease was statistically significant for 80% ($p = 0.013$) and 90% ($p = 0.018$) CS intensities for M1, and for 60% ($p = 0.022$), 80% ($p = 0.023$) and 90% ($p = 0.025$) CS intensities for M2. LF-RSS induced opposite effects, i.e. an overall improvement in SICI. This was statistically significant for 80% ($p = 0.009$), 90% ($p = 0.007$) and 100% ($p = 0.039$) CS intensities for M1, and for 70% ($p = 0.029$), 80% ($p = 0.013$), 90% ($p = 0.015$) and 100% ($p = 0.036$) CS intensities for M1. LFas-RSS caused an improvement in SICI as well, slightly more marked than LF-RSS. SICI increase

was statistically significant, when considering M1, for 60% ($p = 0.026$), 70% ($p = 0.021$), 80% ($p = 0.017$), 90% ($p = 0.012$) and 100% ($p = 0.015$) CS intensities. A similar pattern was observed for M2, where an increase in SICI after LFas-RSS occurred for 60% ($p = 0.024$), 70% ($p = 0.019$), 80% ($p = 0.018$), 90% ($p = 0.016$) and 100% ($p = 0.009$) CS intensities.

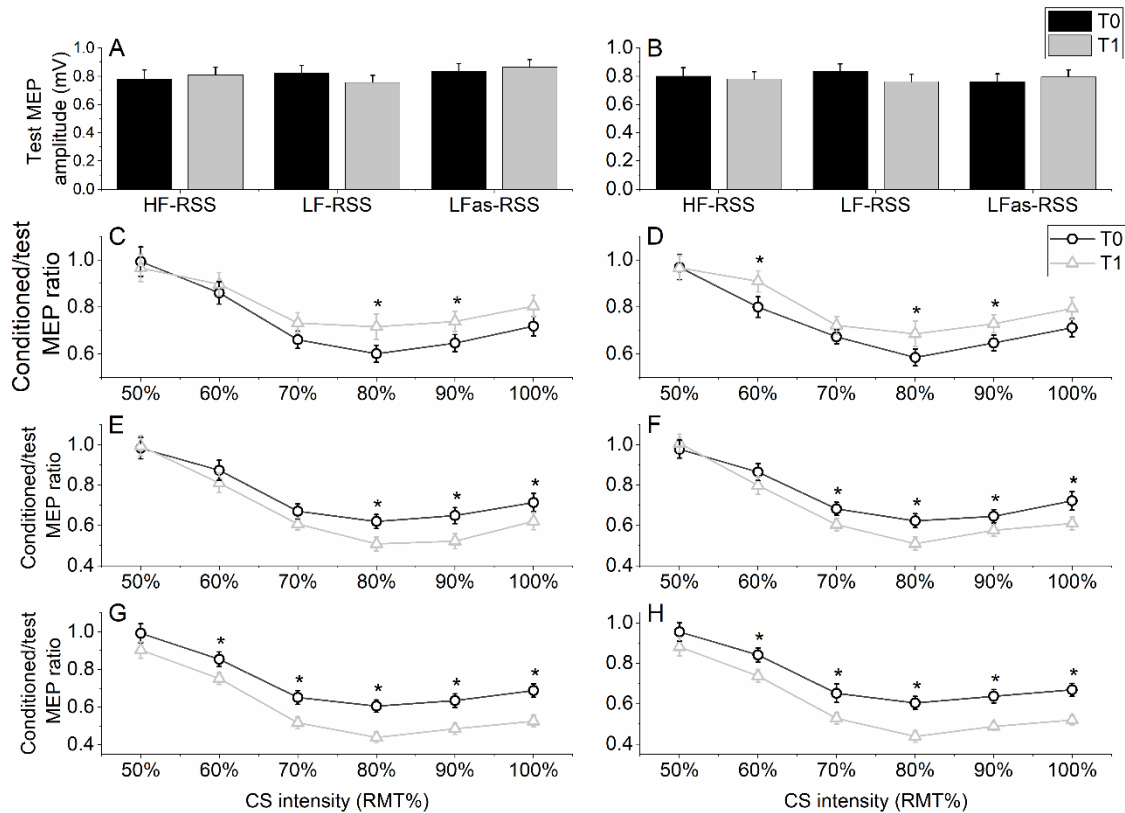


Figure 8.2: panels A and B show the effects of RSS on test MEP recorded from M1 and M2, respectively. Panels C-F show the effect of RSS on SICI; in particular, HF-RSS-M1 (panel C), HF-RSS-M2 (panel D), LF-RSS-M1 (panel E), LF-RSS-M2 (panel F), LFas-RSS-M1 (panel G), LF-RSS-M2 (panel H). Error bars indicate the standard error of the mean. Asterisks indicate statistically significant comparisons.

8.3.3 Somatosensory evoked potentials

Electrical stimulation at muscle sites evoked signals which closely resembled SEP obtained by peripheral nerve stimulation, although of smaller amplitude (figure 8.3).

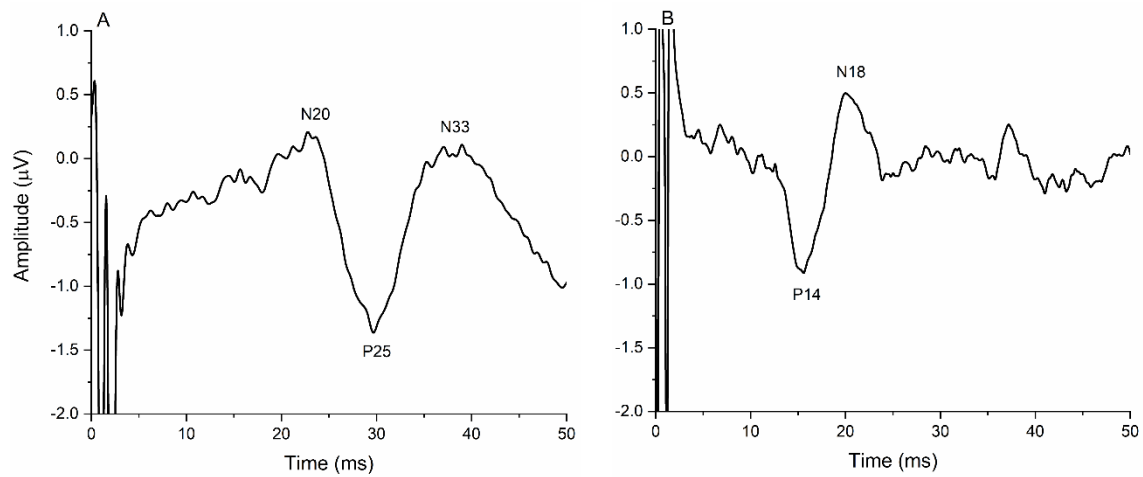


Figure 8.3: SEP obtained by single pulse stimulation over one muscle site in a representative subject. Signals resemble SEP obtained by stimulation of a peripheral nerve, although they are of smaller amplitude. Panel A: parietal components (N20, P25, N33) measures with CP3/4-FCz montage. Panel B: central components (P14, N18) recorded with Fz-contralateral mastoid montage.

RSS had no effect on latencies of N20 and P14 SEP components (figure 8.4).

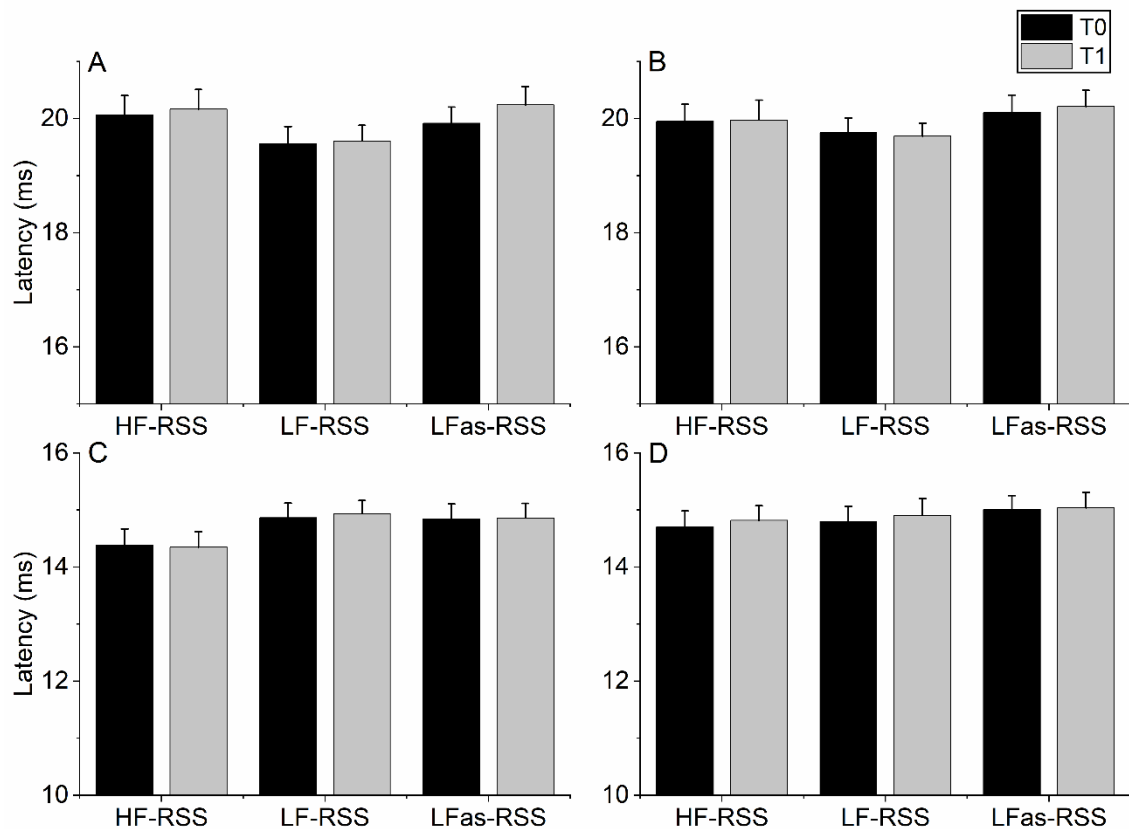


Figure 8.4: effects of RSS on latencies of SEP. Panel A: N20 M1 latency; panel B: N20 M2 latency; panel C: P14 M1 latency; panel D: P14 M2 latency. Error bars indicate the standard error of the mean.

Overall, excitability in the somatosensory system was increased by HF-RSS and decreased by LF-RSS and LFas-RSS; this was reflected by differential modulation of SEP components evoked from stimulation at both M1 and M2 sites. Specifically, HF-RSS increased the amplitude of the P14 (M1: $p = 0.004$; M2: $p = 0.008$) and the N20/P25 complex of SEP (M1: $p = 0.004$; M2: $p = 0.013$), whereas LF-RSS and LFas-RSS had an opposite effect, i.e. they decreased the amplitude of P14 (LF-RSS M1: $p = 0.021$; LF-RSS M2: $p = 0.023$; LFas-RSS M1: $p = 0.015$; LFas-RSS M2: $p = 0.008$) and N20/P25 (LF-RSS M1: $p = 0.018$; LF-RSS M2: $p = 0.028$; LFas-RSS M1: $p = 0.004$; LFas-RSS M2: $p = 0.011$) (figure 8.5).

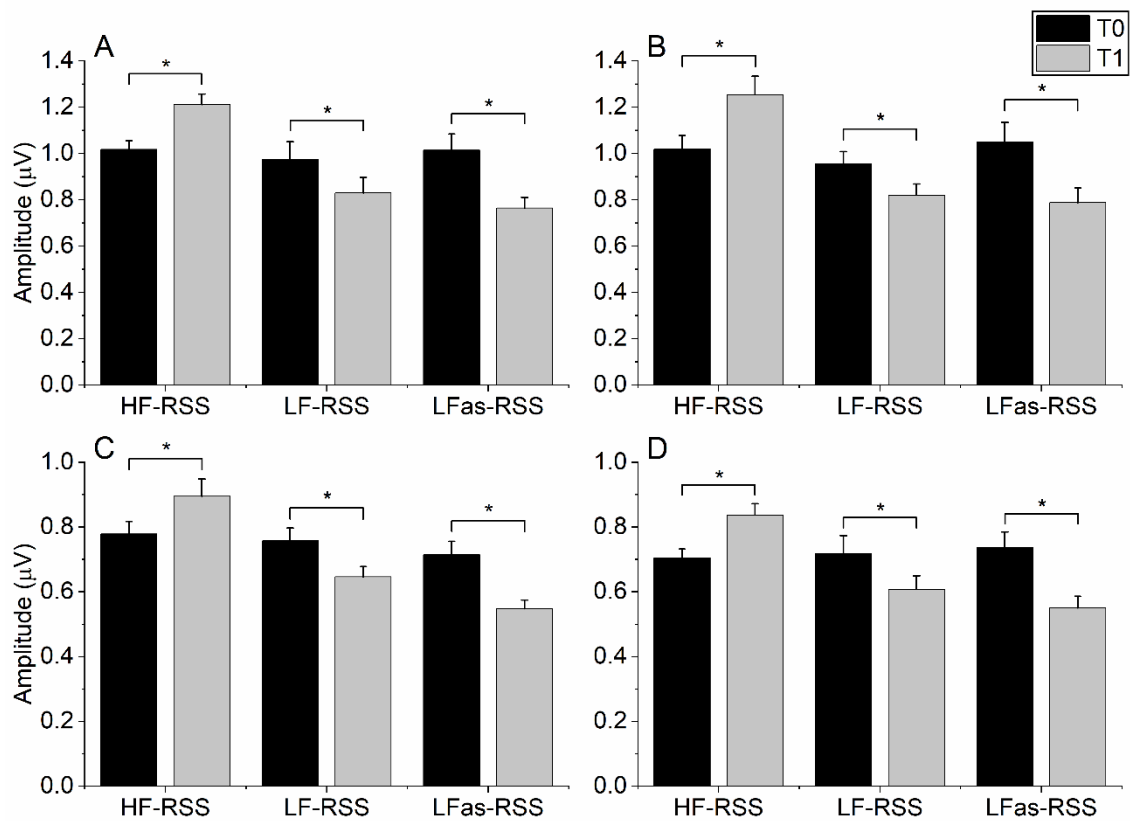


Figure 8.5: effects of RSS on SEP amplitude. Panel A: N20/P25 M1 amplitude; panel B: N20/P25 M2 amplitude; panel C: P14 M1 amplitude; panel D: P14 M2 amplitude. Error bars indicate the standard error of the mean. Brackets with asterisks indicate statistically significant comparisons.

The effects of RSS on PP-SEP were variable according to the stimulation pattern used (figure 8.6). HF-RSS increased PP-SEP suppression in both the ISI tested, reflected by a decrease in R5 and R30. The effect was statistically significant for both N20/P25 and P14 SEP components, obtained by stimulation of M1 and M2 (M1, N20/P25, R5: $p = 0.024$; M1, P14, R5: $p = 0.028$; M1, N20/P25, R30, $p = 0.017$; M1, P14, R30, $p = 0.015$; M2, N20/P25, R5: $p = 0.008$; M2, P14, R5: $p = 0.033$; M2, N20/P25, R30, $p = 0.038$; M2, P14, R30, $p = 0.019$). The effect was opposite (i.e. increase in PP-SEP suppression) after LF-RSS (M1, N20/P25, R5: $p = 0.011$; M1, P14, R5: $p = 0.012$; M1, N20/P25, R30, $p = 0.018$; M1, P14, R30, $p = 0.022$; M2, N20/P25, R5: $p = 0.004$; M2, P14, R5: $p = 0.022$; M2, N20/P25, R30, $p = 0.025$; M2, P14, R30, $p = 0.008$) and LFas-RSS (LFas-RSS M1, N20/P25, R5: $p = 0.003$; M1, P14, R5: $p = 0.008$; M1, N20/P25, R30, $p = 0.006$; M1, P14, R30, $p = 0.009$; M2, N20/P25, R5: $p = 0.014$; M2, P14, R5: $p = 0.018$; M2, N20/P25, R30, $p = 0.005$; M2, P14, R30, $p = 0.003$), and it was slightly more marked in the latter case.

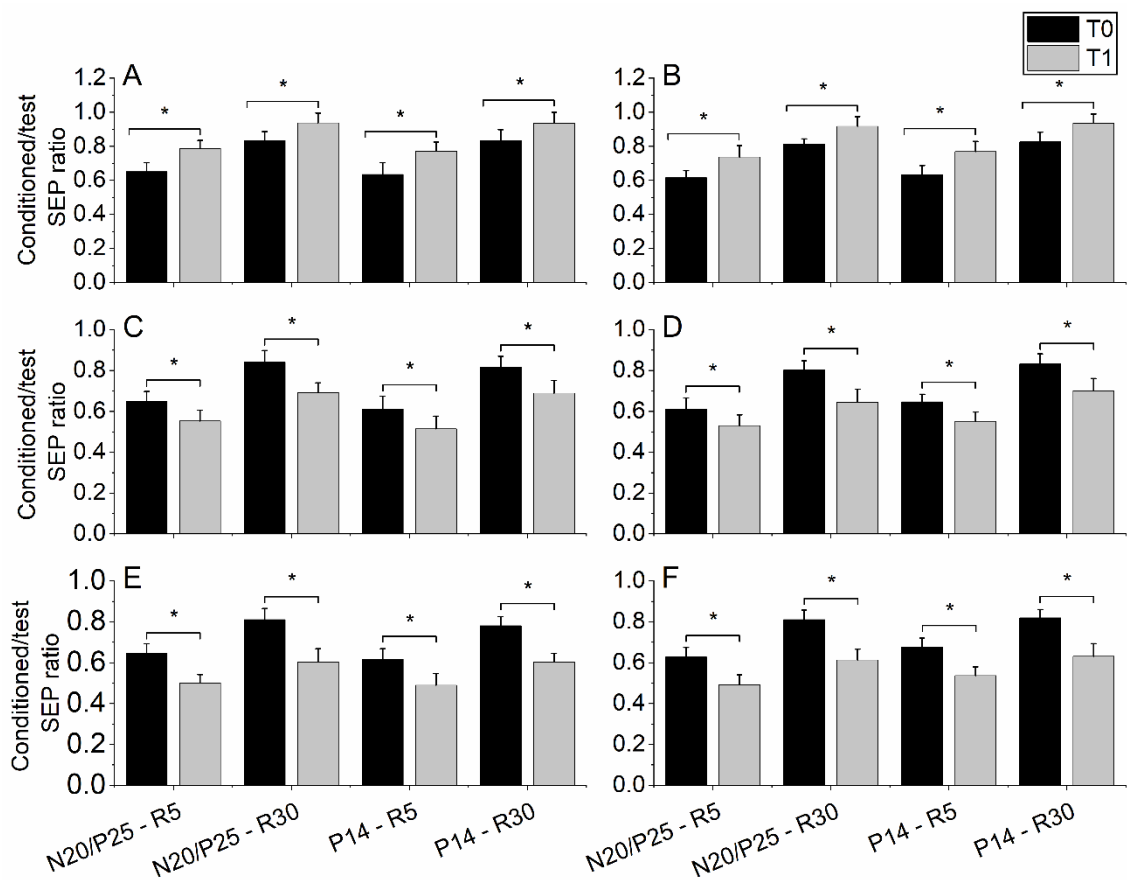


Figure 8.6: effects of RSS on PP-SEP suppression. Panel A: HF-RSS on N20/P25 and P14, M1. Panel B: HF-RSS on N20/P25 and P14, M2; Panel C: LF-RSS on N20/P25 and P14, M1; Panel D: LF-RSS on N20/P25 and P14, M2; Panel E: LFas-RSS on N20/P25 and P14, M1; Panel F: LFas-RSS on N20/P25 and P14, M2. Error bars indicate the standard error of the mean. Brackets with asterisks indicate statistically significant comparisons.

There were no baseline differences across groups in Q20 and Q14. HF-RSS caused a significant increase in Q20 ($p = 0.002$), whereas it decreased after LF-RSS ($p = 0.005$) and LFas-RSS ($p = 0.003$). The same pattern was observed for Q14 ($p = 0.002$, $p = 0.003$ and $p = 0.005$ for HF-RSS, LF-RSS and LFas-RSS, respectively) (figure 8.7).

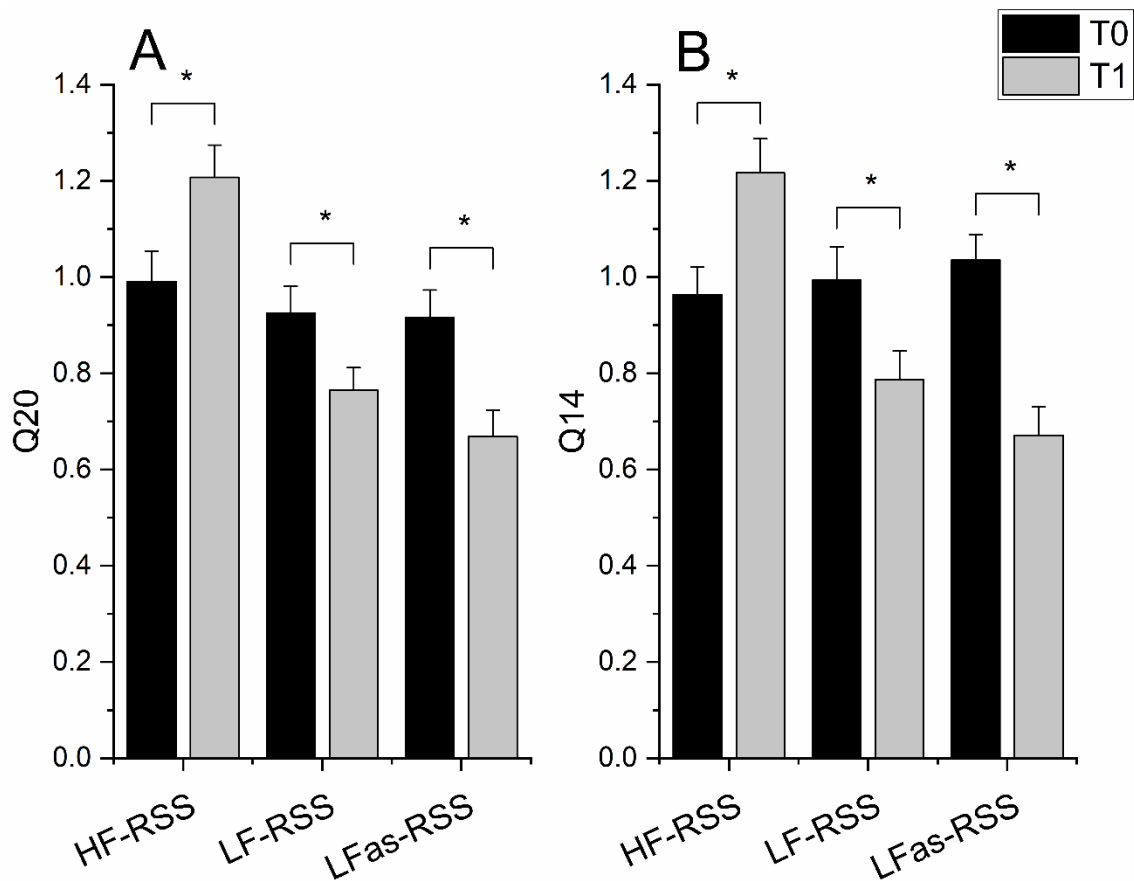


Figure 8.7: effects of RSS on Q20 (panel A) and Q14 (panel B). Error bars indicate the standard error of the mean. Brackets with asterisks indicate statistically significant comparisons.

8.3.4 Correlations

RSS induced correlated changes in several variables linked to somatosensory and motor functions (figure 8.8). Specifically, significant correlations were found between the following variables: SICI and EMG RMS outstretched tested on M1 ($r = 0.734$, $p = 0.018$); SICI and EMG RMS pen tested on M1 ($r = 0.694$, $p = 0.020$); SICI and EMG RMS outstretched tested on M2 ($r = 0.620$, $p = 0.021$); SICI and EMG RMS pen tested on M2 ($r = 0.571$, $p = 0.027$); Q20 and average EMG RMS outstretched ($r = 0.689$, $p = 0.013$); Q20 and average EMG RMS pen ($r = 0.691$, $p = 0.015$); Q20 and average SICI ($r = 0.634$, $p = 0.028$).

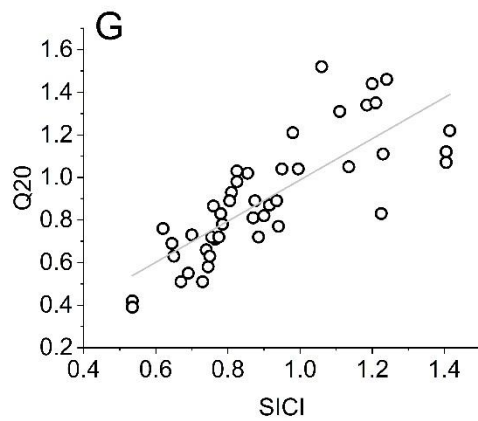
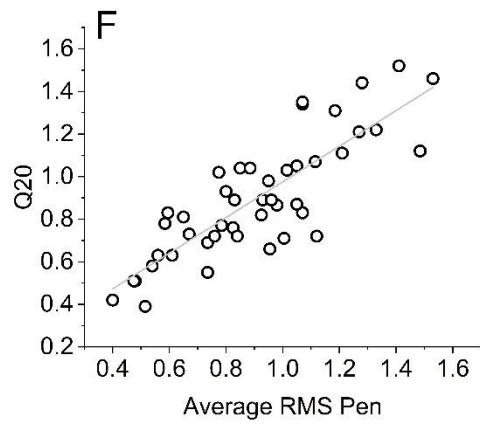
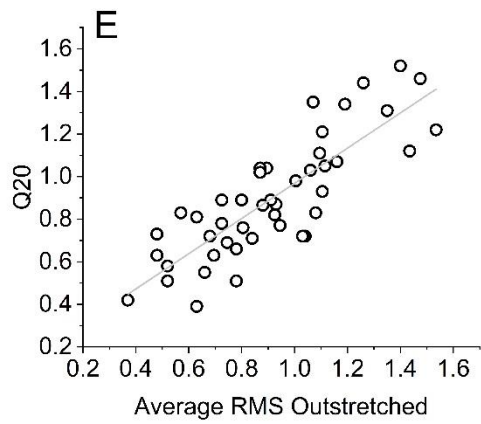
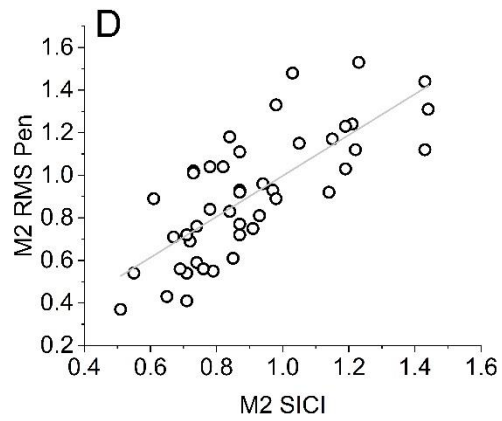
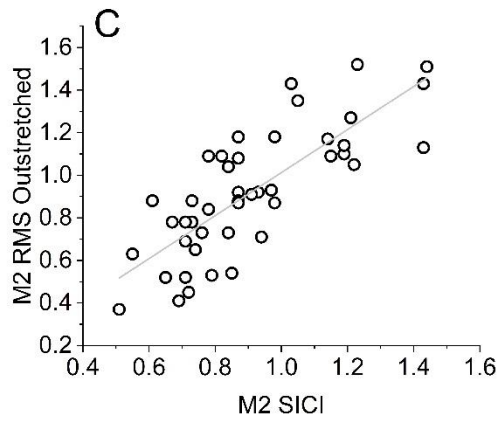
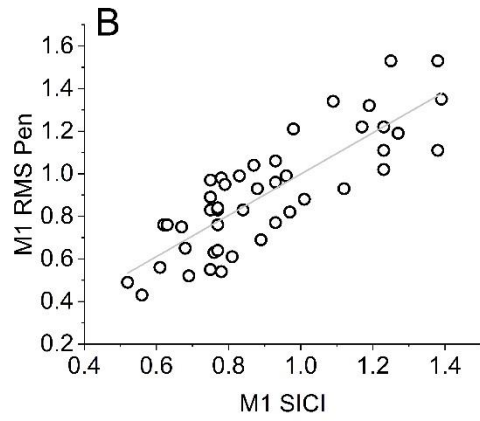
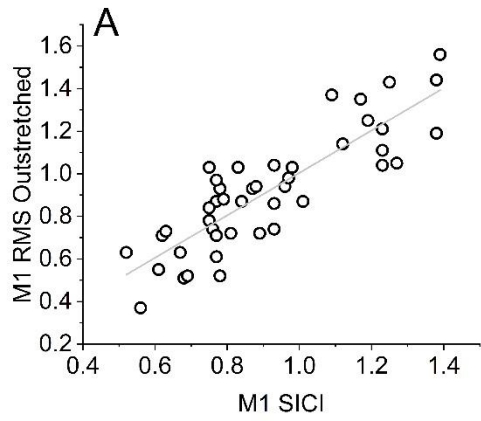


Figure 8.8: correlations. Panel A: M1 SICI, RMS outstretched; panel B: M1 SICI, RMS pen; panel C: M2 SICI, RMS outstretched; panel D: M2 SICI, RMS pen; panel E: Q20, average RMS outstretched; panel F: Q20, average RMS pen; panel G: Q20, average SICI.

8.4 Discussion

In this project, we confirmed the effects previously observed, i.e. that HF-RSS induces a paradoxical response in sensorimotor inhibition when delivered to dystonic patients, whereas LF-RSS has the opposite effects. Additionally, we expanded these results in several ways. The described changes in cortical inhibition hold true when stimulation is delivered on muscles affected by dystonia, and not only on digital nerves. Importantly, the effects of RSS on somatosensory and motor intracortical circuitry are reflected in changes in hand function. Lastly, we found that low-frequency stimulation is more effective when delivered asynchronously on dystonic muscles. Overall, this section demonstrates that peripheral stimulation is effective in modulating cortical and subcortical excitability in dystonia when applied on affected muscles and provide initial results about the effectiveness of this conditioning as a means for ameliorating motor symptoms in this disease.

8.4.1 Effects of RSS on somatosensory function

There was no effect of RSS on SEP latencies, suggesting that our conditioning protocol left transmission along the somatosensory pathway unchanged. By contrast, RSS had differential effects on other measures derived from the SEP. Similar to what was observed with stimulation of digital nerves, HF-RSS induced a global increase in excitability of S1, reflected in enlarged SEP evoked by single pulses, whereas the opposite occurred with LF-RSS and LFas-RSS. According to current theories about SEP generators, this effect might be due to changes in excitability of post-synaptic neurons responsible for SEP generation in S1 (N20/P25) and in the nucleus cuneatus (P14)^{177,304}. RSS also had differential effects on somatosensory inhibition tested with PP-SEP. This form of suppression decreased after HF-RSS and increased after LF-RSS and LFas-RSS. Two pieces of evidence suggest that these effects were widespread in the somatosensory system. First, the amount of suppression was changed when both ISI of 5 ms and 30 ms were used. It is thought that, at short ISI (5 ms), local inhibitory mechanisms are tested^{182, 340, 341}, whereas at longer ISI (30 ms, in the present experiment) inhibition can occur

via more complex loops involving distant structures^{157, 163}. Second, changes in PP-SEP suppression occurred both for N20/P25 and P14 components, whose generators are thought to reside in S1 and in the nucleus cuneatus, respectively³⁰⁴. Based on the findings explained in the previous sections^{17, 361, 381}, as well as past literature^{164, 208}, it is plausible that the effects of RSS on PP-SEP suppression (at least for 5 ms ISI) reflect changes in the effectiveness of inhibition mediated by fast-spiking inhibitory interneurons, which limit discharges by cortical principal cells via feedforward inhibition. However, this might not be the only mechanism through which RSS exerts its effects on the CNS. After RSS, we observed changes in somatosensory lateral inhibition, reflected by the degree of suppression due to simultaneous stimulation of dystonic muscles. Specifically, this decreased after HF-RSS, and increased after LF-RSS and LFas-RSS. It is known that some interneurons have axons that extend beyond the local area where their soma is located, terminating in different cortical columns¹³¹, and that they can provide feedback inhibition to neighbouring populations of principal cells located at a certain distance that may not have provided excitation to that particular interneuron population. We speculate that this phenomenon, better known as surround inhibition, might explain the observed changes in Q20 and Q14. In the present setting, principal cells receiving afferent from one stimulated muscle would activate interneurons responsible for the suppression of activity generated within the cortical representation in S1 of the other muscle.

8.4.2 Effects of RSS on motor function

Similar to the previous sections, we found that the effects of RSS were not confined to the somatosensory system, but spread to the motor cortex as well. Whereas there was no effect on MEP evoked by single TMS pulses, their suppression by conditioning stimuli was affected by the intervention. Specifically, SICI decreased after HF-RSS, whereas it increased following LF-RSS and LFas-RSS. We propose that the processes underlying the relay of the effects to M1 GABAergic interneurons mediating SICI²⁴⁷ are similar to those hypothesized for the stimulation of digital nerves, but this time involving proprioceptive information. Briefly, it is likely that changes in excitability are transmitted by somatotopic connections between S1 and M1 directly targeting layer V pyramidal tract neurons³⁴⁹ or relaying in M1 cortical layers II/III³⁵¹, in a way similar to the induction of long-term potentiation in layers II/III of M1 following tetanic stimulation of S1^{352, 353}.

Differently from previous sections, here we also tested whether RSS had more direct functional effects on motor function, the rationale being that conditioning was applied directly on muscles. Consistent with our hypothesis, we observed that RSS modulated spontaneous muscle activity, estimated by the RMS of surface EMG recorded during two different postural tasks (i.e. arms outstretched and holding a pen) which elicited dystonia. During both tasks, EMG RMS was increased by HF-RSS and decreased by LF-RSS and LFas-RSS, indicating that dystonic muscles were more or less active, respectively. Additionally, this modulation of muscle activity was reflected in changes in performance in the BBT and NHPT. HF-RSS, which induced an increase in EMG activity, led to a worsening in performance in the BBT and NHPT. By contrast, the decrease in EMG activity which followed LF-RSS and LFas-RSS was paralleled by better scores in the BBT and NHPT. It is plausible that the excess of involuntary muscle activity induced by HF-RSS hampered motor skills necessary for the two tasks, whereas the opposite occurred when low-frequency stimulation was applied.

8.4.3 Correlations and putative mechanisms underlying the effect of RSS

A significant correlation was found between the effects of RSS on SICI and the magnitude of EMG RMS on each muscle. SICI is thought to depend on the activity of GABAergic interneurons within M1²⁴⁷. Although the link between SICI and motor function is still not completely clarified, it is known that GABAergic interneurons contribute to shaping M1 activity. In particular, evidence suggest that inhibition in M1 play an important role in determining selective output from pyramidal cells during voluntary movement⁹⁴, which is partially lost in dystonia³⁵⁵. It is possible that the same class of interneurons is tested by SICI. Therefore, in the present experiment, RSS would modulate the effectiveness of inhibition in M1, leading to correlated changes in SICI and involuntary muscle activity during postural tasks. Interestingly, based on our correlation analysis, the effects observed on motor variables are correlated to the degree of change in lateral inhibition in S1. A possible speculation is that the effects of RSS are particularly relevant for inhibitory interneurons at the boundary of the two muscles stimulated by RSS, which are responsible for surround inhibition. Since we hypothesized that the effects of RSS occurring in S1 are transmitted to M1 via somatotopic connections, it is possible that changes in excitability in M1 take place prominently at the level of circuits responsible for lateral inhibition in the same muscles; this would lead to related changes in the simultaneous activation of the two muscles in dystonia.

As for the other investigations described in this thesis, we can only speculate about the interaction between the effects of RSS and the pathophysiology of dystonia. We note, however, that the effects observed with RSS applied directly on muscles seem to follow the same pattern of those obtained with stimulation of digital nerves, so we propose a similar explanation, involving deranged inhibitory homeostatic plasticity. Briefly, for HF-RSS, an initial effect might be to increase inhibition; however, with prolonged stimulation, this would interact with and reverse the effect of the later portions of HF-RSS, making the overall effect facilitatory and detrimental for dystonia. The opposite would occur with LF-RSS: an initial decrease in inhibition would interact with and reverse the effect of the later part of stimulation, resulting in a final net effect of increased cortical inhibition. Compared to the previous ones, however, this last experiment introduced a third form of stimulation, different from HF-RSS and LF-RSS, i.e. LFas-RSS. This was done based on the altered STDP in dystonia, previously investigated with PAS^{34, 393}. Our initial hypothesis, based on the finding of increased LTD-like plasticity in writer's cramp investigated by PAS, was that an asynchronous delivery of peripheral, low-frequency stimulation, would promote LTD-like effects in FHD. The present data seem to confirm our expectation; it is plausible that the greater effectiveness of LFas-RSS, compared to LF-RSS, is due to inhibition via STDP, superimposed to that of frequency-dependent effect of LF-RSS. STDP might have worked by inhibiting the simultaneous activation of dystonic muscles at the cortical level.

Some final comments are necessary about the complex effects of RSS on different electrophysiological variables. Interestingly, the direction of plastic effects induced by RSS on measures of inhibition in S1 (SEP recovery, SIR) were opposite to those on SEP amplitude obtained by single pulses. It has been proposed that The N20/P25 and P14 components are generated by post-synaptic neurons in S1 and nucleus cuneatus, respectively^{177, 304}, whereas inhibition tested with PP-SEP and SIR rely on inhibitory intracortical circuitry^{17, 211}. Therefore, it is possible that the described dissociation in the effects of RSS is due to the different neural elements tested in the present experiment. This result also suggest that the hypothesized abnormal homeostatic plasticity in the somatosensory system possibly involves inhibitory intracortical circuitry, more than excitatory synapses between afferent fibres and principal cells.

A variability in the effects of RSS has also been observed in M1. RSS induced a pattern of changes in SICI similar to inhibition measures in S1, whereas the amplitude of test MEP was not affected by the conditioning. Given that the primary site of conditioning was S1,

this result suggests that inhibitory interneurons in M1 are more easily modulated than the principal cells and connected excitatory interneurons responsible for MEP generation. Previous literature suggested that, compared to excitatory neurons, inhibitory interneurons have faster time constants and stronger excitatory inputs, allowing for larger and faster membrane potential changes; consequently, they can reach threshold more often and exhibit more spiking activity for non-preferred stimuli and hence broader tuning³⁹⁴. Excitatory inputs to inhibitory interneurons tend also to be stronger^{116, 156} and to exhibit more convergence^{125, 395} than those to pyramidal cells. Although the present data do not address this issue directly, it is possible that one or more of the mentioned factors led to the differential effects of RSS on MEP and SICI.

Lastly, it is interesting that only the effects of RSS on SICI and Q20, but not PP-SEP, were correlated with changes in motor hand function. A possible explanation might lie in the heterogeneity of interneuronal circuits tested in the present investigations, and in their different relationship with clinical expression of dystonia. Based on the present findings, as well as those in previous chapters of this thesis, we can speculate that the pathophysiological mechanisms underlying dystonia involve at least two subset of interneurons in the somatosensory cortex. A first one possibly acts on principal cells via a feedforward mechanism and can be probed with PP-SEP suppression and I-HFO. This ensemble is probably linked to somatosensory discrimination deficits (e.g. STDT), but does not seem to produce dystonia. By contrast, a different subset of inhibitory interneurons responsible for surround inhibition in S1, possibly via a feedback mechanism¹³³, appears more involved in the expression of motor symptoms in dystonia.

8.5 Conclusions and limitations

In conclusion, we have observed that abnormal homeostatic plasticity in the sensorimotor system is present in patients with FHD and involves inhibitory circuits rather specifically. Importantly, this abnormal response can be used for therapeutical purposes by means of low-frequency electrical stimulation applied directly over dystonic muscles. One caveat is that, by applying electrical stimulation over muscles, we have inevitably stimulated cutaneous nerve fibres as well. Therefore, it is difficult to ascertain whether the observed effects are due to stimulation of muscle afferents alone, or they are the result of afferent activity from a mixed population of muscle and skin afferents. Regardless of the exact nature of the afferent activity

mediating the effect, low-frequency stimulation was able to improve hand function in patients with FHD and therefore represent a viable option as an aid to therapy for FHD. Clearly more attempts are needed to further optimize stimulation parameters (e.g. duration and intensity) and to investigate response on larger patient samples.

9 GENERAL DISCUSSION

This final chapter will bring together the evidence laid out in this thesis in order to present a clear account of the findings. It is also useful, at this point, to give an account of the overlap between healthy subjects and patients tested in the various projects of the thesis, to estimate the total number of participants and the consistency of basic results.

	STUDY 1 (CD,HC)	STUDY 2 (HC)	STUDY 3 (CD,HC)	STUDY 4 (HC,SD)	STUDY 5 (CD,HC)	STUDY 6 (FHD)
STUDY 1 (CD,HC)						
STUDY 2 (HC)	10 (53%)					
STUDY 3 (CD,HC)	12 (63%)	8 (53%)				
STUDY 4 (HC,SD)	8 (42%)	6 (40%)	8 (66%)			
STUDY 5 (CD,HC)	0	5 (33%)	4 (33%)	8 (62%)		
STUDY 6 (FHD)	*	*	*	*	*	

Table 9.1: overlap between healthy controls tested across different projects. * no overlap possible for one or more reasons (i.e. one of the two studies being compared only has healthy controls or only patients). CD: cervical dystonia; FHD: focal hand dystonia; HC: healthy subjects; SD: secondary dystonia.

	STUDY 1 (CD,HC)	STUDY 2 (HC)	STUDY 3 (CD,HC)	STUDY 4 (HC,SD)	STUDY 5 (CD,HC)	STUDY 6 (FHD)
STUDY 1 (CD,HC)						
STUDY 2 (HC)	*					
STUDY 3 (CD,HC)	8 (42%)	*				
STUDY 4 (HC,SD)	*	*	*			
STUDY 5 (CD,HC)	2 (11%)	*	2 (15%)	*		
STUDY 6 (FHD)	*	*	*	*	*	

Table 9.2: overlap between patients tested across different projects. * no overlap possible for one or more reasons (i.e. one of the two studies being compared only has healthy controls or only patients, or patients' diagnoses are different). CD: cervical dystonia; FHD: focal hand dystonia; HC: healthy subjects; SD: secondary dystonia.

9.1 Evidence for defective inhibition in the somatosensory system in dystonia

In the first chapter, we investigated the correlation between behavioural (STDT) and electrophysiological (PP-SEP, HFO) markers of S1 inhibition in patients with CD. It was previously known that STDT is impaired in many forms of dystonia³⁸⁰; however, the question of where this abnormality is generated was still open. Indeed, increased STDT is not specific for dystonia, but is found in other basal ganglia diseases, such as Parkinson's diseases and Multiple System Atrophy³²⁷. However, as detailed in the first chapter, we found a correlation between STDT and electrophysiological measures of S1 inhibition (recovery of SEP at 5 ms ISI, I-HFO area) in patients with CD, similarly to healthy subjects²¹¹, indicating a disorder of a short latency inhibitory pathway in the somatosensory cortex in these patients.

Several questions were left open by this first investigation, the most important being the clinical significance of the described defective somatosensory inhibition. STDT has been showed not to be correlated with clinical symptoms of dystonia and to be altered in unaffected relatives of dystonic patients^{61, 62, 71, 75, 76, 383}. Since we found a correlation between STDT and electrophysiological measures of S1 inhibition, it might be argued that the latter does not play a prominent role in the clinical expression of dystonia. However, at least two lines of reasoning

prompted further investigations. The first is that the correlation between STDT and electrophysiological markers of S1 inhibition was not perfect. Indeed, STDT is a behavioural variable, which might receive contribution from several mechanisms in addition to somatosensory inhibition; therefore, it is possible that the variance unexplained by the behavioural-electrophysiological correlation might also account for the lack of relation between STDT and dystonia expression, whereas somatosensory inhibition per se might be more closely linked to motor manifestations of dystonia. Additionally, the origin of S1 inhibition abnormality is not completely understood, and it is possibly the result of a more widespread dysfunction. Indeed, dystonia has recently been construed as a network disorders, the somatosensory system being one of the dysfunctional nodes ⁷⁹. Based on these arguments, we speculated that a non-invasive brain stimulation method aimed at improving somatosensory inhibition, either directly or indirectly by restoring a more physiological activity in a more widespread brain network, could be useful to ameliorate dystonia as well.

9.2 Evidence for defective inhibitory plasticity in idiopathic dystonia

In the second chapter, we tested the effects of a patterned form of repetitive somatosensory electrical stimulation (HF-RSS), applied on digital nerves, on a sample of healthy participants. This form of conditioning is known to improve spatial discrimination in humans ²⁷⁹ and to improve motor performance in healthy elderly subjects and patients who developed motor impairment after stroke ³²⁴⁻³²⁶; we speculated that these improvements might involve refinement in inhibition in the sensorimotor system. Overall, we found that HF-RSS could improve measures of somatosensory (STDT, PP-SEP, HFO) and motor (SICI) inhibition. We concluded that HF-RSS focally increased the excitability of inhibitory circuitry in the somatosensory system and that this effect was at least partly transmitted to M1; this latter finding led to the perspective of a possible improvement in motor function due to better inhibition, although this was not tested from a functional point of view. The next step, in chapter three, was to test whether the effects of HF-RSS observed in healthy subjects would occur in dystonic patients as well. To this aim, the same protocol, in terms of conditioning and variables tested, was applied to patients with CD. Unexpectedly, the opposite effect was found: instead of improving the outcomes, HF-RSS led to a substantial decrease in measures of somatosensory (STDT, PP-SEP, HFO) and motor (SICI) inhibition. We suggested that patients with dystonia have abnormal homeostatic plasticity in the inhibitory circuitry within the

somatosensory cortex and that this is responsible for their paradoxical response to HF-RSS. We also proposed that this alteration in inhibitory somatosensory plasticity represents a primary alteration, since it is obtained by stimulation of digital nerves in patients with CD; thus, it could hardly be ascribed to abnormal posturing. At this point, one interesting question was whether this abnormal plasticity represents a primary alteration of dystonia, or it is secondary to dysfunction in areas not strictly part of the somatosensory system. To clarify this, as explained in chapter six, we applied the same HF-RSS protocol to patients affected by dystonia acquired following lesions involving the basal ganglia. Interestingly, the effects of HF-RSS on this group of patients were similar to those obtained in healthy controls, suggesting that abnormal somatosensory plasticity is specific to idiopathic dystonia and is not required to develop dystonia.

9.3 Low-frequency repetitive somatosensory stimulation as a means to ameliorate dystonia

In chapter seven, we again directed our attention to the potential use of peripheral stimulation as a therapy for dystonia. Since we hypothesized that the paradoxical effect of HF-RSS in CD patients was caused by abnormal homeostatic plasticity, we reasoned that one solution to obtain opposite effects might be to use a shorter period of conditioning. However, it has also been suggested that RSS durations as short as below 20 minutes might not induce any behavioural effects in HC ³⁷¹. Instead, we chose to use LF-RSS, a form of stimulation known to have opposite behavioural effects in healthy subjects, i.e. a decline in tactile spatial discrimination. We hypothesized that CD patients would exhibit a reversal of plastic effects that LF-RSS is known to induce in healthy subjects, so that the effect on intracortical circuitry would be excitatory. Our prediction turned out to be correct, since LF-RSS enhanced sensory cortical inhibition, shortened STDT increased SICI in patients with cervical dystonia; opposite results were found in healthy controls. Therefore, in the last chapter, we aimed to target this abnormal plasticity with LF-RSS to ameliorate motor symptoms in dystonia. This time, conditioning was applied directly over dystonic muscles, with three different stimulating protocols in three separate groups of patients with FHD: HF-RSS, LF-RSS, and LFas-RSS, a variant of the former, with which we tried to summate the effect of STDP to that of LF-RSS. Differently from the experiment explained in other chapters, in this one we also had the possibility of testing the effects of RSS on hand function, since conditioning was applied on the body part affected by dystonia. Overall, the effects on the somatosensory system confirmed the pattern

observed in CD when digital nerves were stimulated. HF-RSS induced again a paradoxical response, consisting in decreased inhibition in paired-pulse and lateral inhibition measured with SEP obtained by stimulation of affected muscles, and decreased inhibition in the motor cortex measured with SICI. The opposite effects were observed with LF-RSS and LFas-RSS, the latter being slightly more prominent. Importantly, the results on electrophysiological variables were paralleled by changes in hand function: patients' performance in hand functions tests worsened after HF-RSS, whereas it improved after LF-RSS and LFas-RSS. Although we did not provide direct findings about cellular elements involved, we speculated that the observed effect was mediated by excitability changes in a specific subset of interneurons involved in the expression of motor symptoms of dystonia.

9.4 Contribution of the present findings to the understanding of the pathophysiology of dystonia

This section summarizes the most important findings of the thesis (figure 9.1). The first key contribution of the present work to the understanding of the pathophysiology of dystonia is the definition of the relationship between the STDT and electrophysiological markers of S1 inhibition in patients with CD. A further finding is the widespread alteration of synaptic plasticity in the somatosensory system. While abnormal plasticity was known in dystonia^{12,79}, it had been mostly characterized in M1, by means of PAS^{23,33-35}. The present investigations extend this findings by providing direct evidence of deranged synaptic plasticity in S1 and in the nucleus cuneatus, by means of SEP, in patients with CD. New to the present set of studies is also the definition of putative cellular elements involved. Whereas previous literature focussed on MEP, which represents a global readout of M1 excitability³⁹⁶, our results indicated that the mentioned abnormal plasticity specifically involves synapses between inhibitory interneurons and principal cells, both in the somatosensory system and in M1. Lastly, the present findings help to define the nature of abnormal plasticity in dystonia, pointing to a specific alteration in homeostatic plasticity, consisting in a decrease in the threshold for reversing the direction of plastic changes.

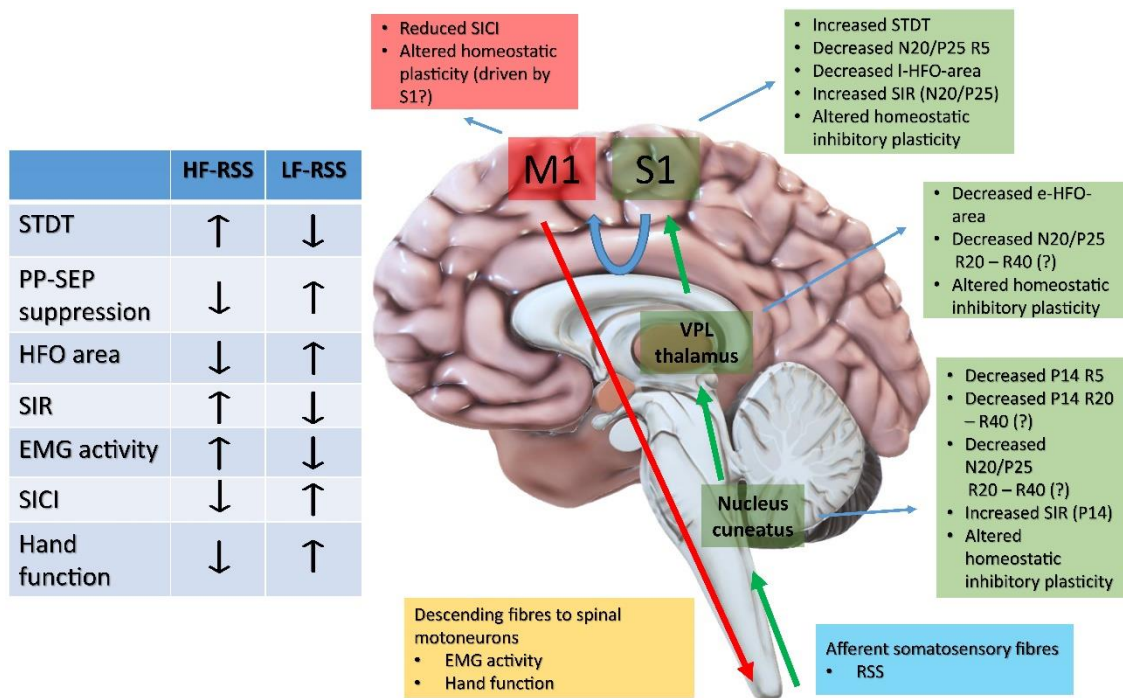


Figure 9.1: graphical summary of the key findings of the PhD projects. Green and red boxes (related to the somatosensory and motor systems, respectively) illustrate the alterations showed in dystonic patients with regards to the main electrophysiological variables tested and their putative anatomical generators (S1, M1, thalamus, nucleus cuneatus). The light blue box indicate the site of action of RSS (afferent somatosensory fibres), while the orange box indicate the outcome measures used to assess the effects of RSS on dystonia in FHD (EMG activity, hand function tests). Arrows represent main somatosensory and motor pathways (green and red, respectively). The blue arrow indicate U fibres connecting S1 and M1. The table summarizes the main effects of HF-RSS and LF-RSS in the electrophysiological variables tested in dystonic patients.

The relationship between decreased somatosensory inhibition and clinical aspects of dystonia is difficult to clarify. Some of the somatosensory alterations found in dystonia, such as the STDT, do not seem to be related to motor symptoms^{60, 61, 68, 70-73}. Since previous literature and part of the present investigations point to a close relationship between STDT and inhibitory function of S1^{211, 361}, one might suppose that inhibition in the somatosensory system would not be related to motor symptoms of dystonia as well. However, it should be noted that STDT relies on a more complex network of brain structures than S1 alone, including the basal ganglia^{71, 203}. Also, other lines of evidence might suggest that alterations in the basal ganglia and somatosensory function in dystonia might be relatively independent. As described in the

first chapter of this thesis, electrophysiological markers of S1 inhibition and dystonia were independently associated with abnormal STDT, leading to speculate that other factors beyond alterations in S1 computation might contribute to increased STDT, such as basal ganglia dysfunction. This would be in line with the results of chapter 6, which suggest that structural damage in the basal ganglia does not necessarily lead to somatosensory dysfunction. Lastly, while there seems to be a clear relationship between S1 inhibition and STDT, dystonic patients also showed altered inhibition at subcortical stages of the somatosensory pathway, the latter being not clearly involved in the STDT. Taken together, these data point to the fact that STDT and somatosensory inhibition might represent only partially overlapping variables.

One way to frame altered somatosensory inhibition and motor symptoms in the same picture is to consider the former in the context of deranged plasticity, which has indeed been suggested to reflect dystonia more closely ³². It is possible that derangement in the regulation of somatosensory inhibitory plasticity represents a dysfunctional background on which other factors act and induce typical dystonic symptoms. One of these factors could be overtraining, which is thought to induce changes in the connectivity in sensory and motor cortices, leading to inappropriate association between sensory input and motor outputs, which in turn would cause errors in selecting muscles used in voluntary movement ³⁹³. If we hypothesize that, in the context of motor training, afferent somatosensory input plays a prominent role in sensorimotor plastic changes, it is possible that, in our experimental setting, overtraining was at least partly mimicked by HF-RSS. On the other side, when applied directly over muscles, LF-RSS led to a decrease in involuntary activity: this represents another novel finding and points towards the possibility by peripheral stimulation to partly restore a more physiological inhibitory function in sensorimotor circuits of patients affected by dystonia.

It is important to note that the aforementioned concepts seem to be true for idiopathic dystonia, but not for dystonia caused by damage to the basal ganglia. In this regard, our findings expand those of a previous report, where M1 plasticity investigated by PAS was found to be normal in secondary dystonia ²³. The absence of deranged somatosensory plasticity in acquired dystonia is also in keeping with the fact that sensory trick is much more prevalent in idiopathic, rather than acquired dystonia ³⁹⁷⁻³⁹⁹.

9.5 Limitations and future perspectives

There are several general limitations to the present set of studies. First, the researchers who measured the data were not blinded with regards to the groups being investigated (patients or

healthy controls). Only electrophysiological outcomes relative to the primary somatosensory and motor cortices (SEP, MEP) were employed, whereas the effect of RSS might cause changes in other structures; this should prompt future investigations to assess the outcome of RSS application on different structures (e.g. the cerebellum and the spinal cord), by using a combination of electrophysiological, behavioural and imaging techniques.

Several pathophysiological questions remain open. First, we were only able to speculate about the fact that the effects observed with both HF-RSS and LF-RSS on dystonic patients were due to deranged homeostatic plasticity. A control condition with a shorter period of RSS would have been necessary to confirm this hypothesis, and it might be possible to test it in future studies. Second, albeit we were able to demonstrate clear pathophysiological differences between idiopathic and acquired dystonia, we were not able to give a clear account of how involuntary movements are generated in the latter condition, given that cortical plasticity is normal.

Lastly, there were limitations specific to the investigation described in the last chapter of the thesis. The observed effects were probably due to mixed stimulation of muscle and skin afferents; this limits the understanding of the mechanisms underlying the action of RSS. It is not clear yet whether the effectiveness of stimulation can be improved by changing parameters and whether there would be an additive effect with multiple sessions. The beneficial effects of LF-RSS were not put into the context of other therapies for dystonia; therefore, more investigations are needed to understand how LF-RSS could be used together with other therapeutic options (e.g. in terms of indication, timing and possible synergy of effects). Finally, as this was mainly a pathophysiological study, a relatively low number of patients was tested; future research should include a larger cohort of subjects investigated in a double-blind trial.

9.6 Conclusion

Overall, this thesis has expanded current knowledge about altered inhibition in dystonia, first characterizing its electrophysiological and behavioural features, and then showing their relationship with deranged homeostatic plasticity. We demonstrated that these alterations are specific to idiopathic dystonia, and that they can be used as a therapeutic target with repetitive peripheral electrical stimulation. We anticipate that the findings in this thesis will impact a range of clinical and non-clinical neuroscientists interested in dystonia and hopefully that they will lead to the development of larger scale studies to explore the therapeutic potential of RSS in dystonia.

10 REFERENCES

1. Albanese A, Bhatia K, Bressman SB, et al. Phenomenology and classification of dystonia: a consensus update. *Mov Disord* 2013;28(7):863-873.
2. Balint B, Mencacci NE, Valente EM, et al. Dystonia. *Nature reviews Disease primers* 2018;4(1):25.
3. DeLong MR. Primate models of movement disorders of basal ganglia origin. *Trends Neurosci* 1990;13(7):281-285.
4. Mitchell IJ, Luquin R, Boyce S, et al. Neural mechanisms of dystonia: evidence from a 2-deoxyglucose uptake study in a primate model of dopamine agonist-induced dystonia. *Mov Disord* 1990;5(1):49-54.
5. Vitek JL. Pathophysiology of dystonia: a neuronal model. *Mov Disord* 2002;17 Suppl 3:S49-62.
6. Vitek JL, DeLong MR, Starr PA, Hariz MI, Metman LV. Intraoperative neurophysiology in DBS for dystonia. *Mov Disord* 2011;26 Suppl 1:S31-36.
7. Vitek JL, Chockkan V, Zhang JY, et al. Neuronal activity in the basal ganglia in patients with generalized dystonia and hemiballismus. *Ann Neurol* 1999;46(1):22-35.
8. Barow E, Neumann WJ, Brucke C, et al. Deep brain stimulation suppresses pallidal low frequency activity in patients with phasic dystonic movements. *Brain* 2014;137:3012-3024.
9. Silberstein P, Kuhn AA, Kupsch A, et al. Patterning of globus pallidus local field potentials differs between Parkinson's disease and dystonia. *Brain* 2003;126:2597-2608.
10. Hutchison WD, Lang AE, Dostrovsky JO, Lozano AM. Pallidal neuronal activity: implications for models of dystonia. *Ann Neurol* 2003;53(4):480-488.
11. Wichmann T, Dostrovsky JO. Pathological basal ganglia activity in movement disorders. *Neuroscience* 2011;198:232-244.
12. Latorre A, Rocchi L, Berardelli A, Bhatia KP, Rothwell JC. The interindividual variability of transcranial magnetic stimulation effects: Implications for diagnostic use in movement disorders. *Mov Disord* 2019;34(7):936-949.
13. Rothwell JC, Obeso JA, Day BL, Marsden CD. Pathophysiology of dystonias. *Adv Neurol* 1983;39:851-863.
14. Marsden CD, Rothwell JC. The physiology of idiopathic dystonia. *Can J Neurol Sci* 1987;14(3 Suppl):521-527.
15. Ridding MC, Inzelberg R, Rothwell JC. Changes in excitability of motor cortical circuitry in patients with Parkinson's disease. *Ann Neurol* 1995;37(2):181-188.
16. Edwards MJ, Huang YZ, Wood NW, Rothwell JC, Bhatia KP. Different patterns of electrophysiological deficits in manifesting and non-manifesting carriers of the DYT1 gene mutation. *Brain* 2003;126:2074-2080.
17. Antelmi E, Erro R, Rocchi L, et al. Neurophysiological correlates of abnormal somatosensory temporal discrimination in dystonia. *Mov Disord* 2017;32(1):141-148.
18. Chen R, Cros D, Curra A, et al. The clinical diagnostic utility of transcranial magnetic stimulation: report of an IFCN committee. *Clin Neurophysiol* 2008;119(3):504-532.

19. Gilio F, Curra A, Inghilleri M, et al. Abnormalities of motor cortex excitability preceding movement in patients with dystonia. *Brain* 2003;126:1745-1754.
20. Gilio F, Curra A, Lorenzano C, Modugno N, Manfredi M, Berardelli A. Effects of botulinum toxin type A on intracortical inhibition in patients with dystonia. *Ann Neurol* 2000;48(1):20-26.
21. Hanajima R, Okabe S, Terao Y, et al. Difference in intracortical inhibition of the motor cortex between cortical myoclonus and focal hand dystonia. *Clin Neurophysiol* 2008;119(6):1400-1407.
22. Huang YZ, Trender-Gerhard I, Edwards MJ, Mir P, Rothwell JC, Bhatia KP. Motor system inhibition in dopa-responsive dystonia and its modulation by treatment. *Neurology* 2006;66(7):1088-1090.
23. Kojovic M, Parees I, Kassavetis P, et al. Secondary and primary dystonia: pathophysiological differences. *Brain* 2013;136:2038-2049.
24. Espay AJ, Morgante F, Purzner J, Gunraj CA, Lang AE, Chen R. Cortical and spinal abnormalities in psychogenic dystonia. *Ann Neurol* 2006;59(5):825-834.
25. Quartarone A, Rizzo V, Terranova C, et al. Abnormal sensorimotor plasticity in organic but not in psychogenic dystonia. *Brain* 2009;132:2871-2877.
26. Rona S, Berardelli A, Vacca L, Inghilleri M, Manfredi M. Alterations of motor cortical inhibition in patients with dystonia. *Mov Disord* 1998;13(1):118-124.
27. Brighina F, Romano M, Giglia G, et al. Effects of cerebellar TMS on motor cortex of patients with focal dystonia: a preliminary report. *Exp Brain Res* 2009;192(4):651-656.
28. Kagi G, Ruge D, Brugger F, et al. Endophenotyping in idiopathic adult onset cervical dystonia. *Clin Neurophysiol* 2017;128(7):1142-1147.
29. Ganos C, Ferre ER, Marotta A, et al. Cortical inhibitory function in cervical dystonia. *Clin Neurophysiol* 2017.
30. Hermsen AM, Haag A, Duddek C, et al. Test-retest reliability of single and paired pulse transcranial magnetic stimulation parameters in healthy subjects. *J Neurol Sci* 2016;362:209-216.
31. Brown KE, Lohse KR, Mayer IMS, et al. The reliability of commonly used electrophysiology measures. *Brain stimulation* 2017;10(6):1102-1111.
32. Edwards MJ, Huang YZ, Mir P, Rothwell JC, Bhatia KP. Abnormalities in motor cortical plasticity differentiate manifesting and nonmanifesting DYT1 carriers. *Mov Disord* 2006;21(12):2181-2186.
33. Quartarone A, Bagnato S, Rizzo V, et al. Abnormal associative plasticity of the human motor cortex in writer's cramp. *Brain* 2003;126:2586-2596.
34. Weise D, Schramm A, Stefan K, et al. The two sides of associative plasticity in writer's cramp. *Brain* 2006;129:2709-2721.
35. Belvisi D, Suppa A, Marsili L, et al. Abnormal experimentally- and behaviorally-induced LTP-like plasticity in focal hand dystonia. *Exp Neurol* 2013;240:64-74.
36. Kang JS, Terranova C, Hilker R, Quartarone A, Ziemann U. Deficient homeostatic regulation of practice-dependent plasticity in writer's cramp. *Cereb Cortex* 2011;21(5):1203-1212.
37. Meunier S, Russmann H, Shamim E, Lamy JC, Hallett M. Plasticity of cortical inhibition in dystonia is impaired after motor learning and paired-associative stimulation. *Eur J Neurosci* 2012;35(6):975-986.
38. Sadnicka A, Hamada M, Bhatia KP, Rothwell JC, Edwards MJ. A reflection on plasticity research in writing dystonia. *Mov Disord* 2014;29(8):980-987.

39. Teo JT, van de Warrenburg BP, Schneider SA, Rothwell JC, Bhatia KP. Neurophysiological evidence for cerebellar dysfunction in primary focal dystonia. *J Neurol Neurosurg Psychiatry* 2009;80(1):80-83.
40. Sadnicka A, Teo JT, Kojovic M, et al. All in the blink of an eye: new insight into cerebellar and brainstem function in DYT1 and DYT6 dystonia. *Eur J Neurol* 2015;22(5):762-767.
41. Antelmi E, Di Stasio F, Rocchi L, et al. Impaired eye blink classical conditioning distinguishes dystonic patients with and without tremor. *Parkinsonism Relat Disord* 2016;31:23-27.
42. Jinnah HA, Neychev V, Hess EJ. *The Anatomical Basis for Dystonia: The Motor Network Model. Tremor and other hyperkinetic movements* (New York, NY) 2017;7:506.
43. Neychev VK, Gross RE, Lehericy S, Hess EJ, Jinnah HA. The functional neuroanatomy of dystonia. *Neurobiol Dis* 2011;42(2):185-201.
44. Quartarone A, Ruge D. How Many Types of Dystonia? Pathophysiological Considerations. *Front Neurol* 2018;9:12.
45. Jinnah HA, Alterman R, Klein C, et al. Deep brain stimulation for dystonia: a novel perspective on the value of genetic testing. *Journal of neural transmission* (Vienna, Austria : 1996) 2017;124(4):417-430.
46. Dressler D, Altenmueller E, Bhidayasiri R, et al. Strategies for treatment of dystonia. *Journal of neural transmission* (Vienna, Austria : 1996) 2016;123(3):251-258.
47. van den Heuvel C, Tijssen MAJ, van de Warrenburg BPC, Delnooz CCS. The Symptomatic Treatment of Acquired Dystonia: A Systematic Review. *Movement disorders clinical practice* 2016;3(6):548-558.
48. Pirazzini M, Rossetto O, Eleopra R, Montecucco C. Botulinum Neurotoxins: Biology, Pharmacology, and Toxicology. *Pharmacol Rev* 2017;69(2):200-235.
49. Albanese A, Barnes MP, Bhatia KP, et al. A systematic review on the diagnosis and treatment of primary (idiopathic) dystonia and dystonia plus syndromes: report of an EFNS/MDS-ES Task Force. *Eur J Neurol* 2006;13(5):433-444.
50. Balash Y, Giladi N. Efficacy of pharmacological treatment of dystonia: evidence-based review including meta-analysis of the effect of botulinum toxin and other cure options. *Eur J Neurol* 2004;11(6):361-370.
51. Lumsden DE, Kaminska M, Tomlin S, Lin JP. Medication use in childhood dystonia. *Eur J Paediatr Neurol* 2016;20(4):625-629.
52. Pirio Richardson S, Wegele AR, Skipper B, Deligtisch A, Jinnah HA, Dystonia Coalition I. Dystonia treatment: Patterns of medication use in an international cohort. *Neurology* 2017;88(6):543-550.
53. Bruggemann N, Kuhn A, Schneider SA, et al. Short- and long-term outcome of chronic pallidal neurostimulation in monogenic isolated dystonia. *Neurology* 2015;84(9):895-903.
54. Schrader C, Capelle HH, Kiefe TM, et al. GPi-DBS may induce a hypokinetic gait disorder with freezing of gait in patients with dystonia. *Neurology* 2011;77(5):483-488.
55. Mills KA, Scherzer R, Starr PA, Ostrem JL. Weight change after globus pallidus internus or subthalamic nucleus deep brain stimulation in Parkinson's disease and dystonia. *Stereotact Funct Neurosurg* 2012;90(6):386-393.
56. Baizabal Carvallo JF, Mostile G, Almaguer M, Davidson A, Simpson R, Jankovic J. Deep brain stimulation hardware complications in patients with movement

- disorders: risk factors and clinical correlations. *Stereotact Funct Neurosurg* 2012;90(5):300-306.
57. Horisawa S, Ochiai T, Goto S, et al. Safety and long-term efficacy of ventro-oral thalamotomy for focal hand dystonia: A retrospective study of 171 patients. *Neurology* 2019;92(4):e371-e377.
 58. Tinazzi M, Rosso T, Fiaschi A. Role of the somatosensory system in primary dystonia. *Mov Disord* 2003;18(6):605-622.
 59. Bradley D, Whelan R, Kimmich O, et al. Temporal discrimination thresholds in adult-onset primary torsion dystonia: an analysis by task type and by dystonia phenotype. *J Neurol* 2012;259(1):77-82.
 60. Fiorio M, Tinazzi M, Scontrini A, et al. Tactile temporal discrimination in patients with blepharospasm. *J Neurol Neurosurg Psychiatry* 2008;79(7):796-798.
 61. Scontrini A, Conte A, Defazio G, et al. Somatosensory temporal discrimination in patients with primary focal dystonia. *J Neurol Neurosurg Psychiatry* 2009;80(12):1315-1319.
 62. Conte A, Defazio G, Ferrazzano G, et al. Is increased blinking a form of blepharospasm? *Neurology* 2013;80(24):2236-2241.
 63. Conte A, Ferrazzano G, Defazio G, Fabbrini G, Hallett M, Berardelli A. Increased blinking may be a precursor of blepharospasm: a longitudinal study. *Movement disorders clinical practice* 2017;4(5):733-736.
 64. Johnson KO. The roles and functions of cutaneous mechanoreceptors. *Curr Opin Neurobiol* 2001;11(4):455-461.
 65. Ganos C, Ferrè ER, Marotta A, et al. Cortical inhibitory function in cervical dystonia. *Clin Neurophysiol* 2018;129(2):466-472.
 66. Sadnicka A, Daum C, Cordivari C, et al. Mind the gap: temporal discrimination and dystonia. *Eur J Neurol* 2017;24(6):796-806.
 67. Kimmich O, Bradley D, Whelan R, et al. Sporadic adult onset primary torsion dystonia is a genetic disorder by the temporal discrimination test. *Brain* 2011;134:2656-2663.
 68. Sadnicka A, Kimmich O, Pisarek C, et al. Pallidal stimulation for cervical dystonia does not correct abnormal temporal discrimination. *Mov Disord* 2013;28(13):1874-1877.
 69. Kägi G, Ruge D, Brugger F, et al. Endophenotyping in idiopathic adult onset cervical dystonia. *Clin Neurophysiol* 2017;128(7):1142-1147.
 70. Fiorio M, Gambarin M, Valente EM, et al. Defective temporal processing of sensory stimuli in DYT1 mutation carriers: a new endophenotype of dystonia? *Brain* 2007;130:134-142.
 71. Bradley D, Whelan R, Walsh R, et al. Temporal discrimination threshold: VBM evidence for an endophenotype in adult onset primary torsion dystonia. *Brain* 2009;132:2327-2335.
 72. Kimmich O, Molloy A, Whelan R, et al. Temporal discrimination, a cervical dystonia endophenotype: penetrance and functional correlates. *Mov Disord* 2014;29(6):804-811.
 73. Scontrini A, Conte A, Fabbrini G, et al. Somatosensory temporal discrimination tested in patients receiving botulinum toxin injection for cervical dystonia. *Mov Disord* 2011;26(4):742-746.
 74. Conte A, Rocchi L, Ferrazzano G, et al. Primary somatosensory cortical plasticity and tactile temporal discrimination in focal hand dystonia. *Clin Neurophysiol* 2014;125(3):537-543.

75. Hutchinson M, Kimmich O, Molloy A, et al. The endophenotype and the phenotype: temporal discrimination and adult-onset dystonia. *Mov Disord* 2013;28(13):1766-1774.
76. Conte A, Ferrazzano G, Belvisi D, et al. Does the Somatosensory Temporal Discrimination Threshold Change over Time in Focal Dystonia? *Neural Plast* 2017;2017:9848070.
77. Aglioti SM, Fiorio M, Forster B, Tinazzi M. Temporal discrimination of cross-modal and unimodal stimuli in generalized dystonia. *Neurology* 2003;60(5):782-785.
78. Fiorio M, Tinazzi M, Bertolasi L, Aglioti SM. Temporal processing of visuotactile and tactile stimuli in writer's cramp. *Ann Neurol* 2003;53(5):630-635.
79. Conte A, Rocchi L, Latorre A, Belvisi D, Rothwell JC, Berardelli A. Ten-Year Reflections on the Neurophysiological Abnormalities of Focal Dystonias in Humans. *Mov Disord* 2019;34(11):1616-1628.
80. Merchant H, de Lafuente V, Pena-Ortega F, Larriva-Sahd J. Functional impact of interneuronal inhibition in the cerebral cortex of behaving animals. *Prog Neurobiol* 2012;99(2):163-178.
81. Silberberg G, Grillner S, LeBeau FE, Maex R, Markram H. Synaptic pathways in neural microcircuits. *Trends Neurosci* 2005;28(10):541-551.
82. Mountcastle VB. Modality and topographic properties of single neurons of cat's somatic sensory cortex. *J Neurophysiol* 1957;20(4):408-434.
83. Hubel DH, Wiesel TN. Receptive fields of single neurones in the cat's striate cortex. *J Physiol* 1959;148:574-591.
84. Horton JC, Adams DL. The cortical column: a structure without a function. *Philos Trans R Soc Lond B Biol Sci* 2005;360(1456):837-862.
85. Douglas RJ, Martin KA. Mapping the matrix: the ways of neocortex. *Neuron* 2007;56(2):226-238.
86. Mountcastle VB. The columnar organization of the neocortex. *Brain* 1997;120:701-722.
87. Buxhoeveden DP, Casanova MF. The minicolumn hypothesis in neuroscience. *Brain* 2002;125:935-951.
88. Mountcastle VB, Talbot WH, Sakata H, Hyvarinen J. Cortical neuronal mechanisms in flutter-vibration studied in unanesthetized monkeys. Neuronal periodicity and frequency discrimination. *J Neurophysiol* 1969;32(3):452-484.
89. Krimer LS, Zaitsev AV, Czanner G, et al. Cluster analysis-based physiological classification and morphological properties of inhibitory neurons in layers 2-3 of monkey dorsolateral prefrontal cortex. *J Neurophysiol* 2005;94(5):3009-3022.
90. Zaitsev AV, Povysheva NV, Gonzalez-Burgos G, et al. Interneuron diversity in layers 2-3 of monkey prefrontal cortex. *Cereb Cortex* 2009;19(7):1597-1615.
91. Atencio CA, Schreiner CE. Spectrotemporal processing differences between auditory cortical fast-spiking and regular-spiking neurons. *J Neurosci* 2008;28(15):3897-3910.
92. Tamura H, Kaneko H, Kawasaki K, Fujita I. Presumed inhibitory neurons in the macaque inferior temporal cortex: visual response properties and functional interactions with adjacent neurons. *J Neurophysiol* 2004;91(6):2782-2796.
93. Cohen JY, Pouget P, Heitz RP, Woodman GF, Schall JD. Biophysical support for functionally distinct cell types in the frontal eye field. *J Neurophysiol* 2009;101(2):912-916.
94. Merchant H, Naselaris T, Georgopoulos AP. Dynamic sculpting of directional tuning in the primate motor cortex during three-dimensional reaching. *J Neurosci* 2008;28(37):9164-9172.

95. Isomura Y, Harukuni R, Takekawa T, Aizawa H, Fukai T. Microcircuitry coordination of cortical motor information in self-initiation of voluntary movements. *Nat Neurosci* 2009;12(12):1586-1593.
96. Murray PD, Keller A. Somatosensory response properties of excitatory and inhibitory neurons in rat motor cortex. *J Neurophysiol* 2011;106(3):1355-1362.
97. Kaufman MT, Churchland MM, Santhanam G, et al. Roles of monkey premotor neuron classes in movement preparation and execution. *J Neurophysiol* 2010;104(2):799-810.
98. Yokoi I, Komatsu H. Putative pyramidal neurons and interneurons in the monkey parietal cortex make different contributions to the performance of a visual grouping task. *J Neurophysiol* 2010;104(3):1603-1611.
99. Mitchell JF, Sundberg KA, Reynolds JH. Differential attention-dependent response modulation across cell classes in macaque visual area V4. *Neuron* 2007;55(1):131-141.
100. Chen Y, Martinez-Conde S, Macknik SL, Bereshpolova Y, Swadlow HA, Alonso JM. Task difficulty modulates the activity of specific neuronal populations in primary visual cortex. *Nat Neurosci* 2008;11(8):974-982.
101. Cardin JA. Dissecting local circuits in vivo: integrated optogenetic and electrophysiology approaches for exploring inhibitory regulation of cortical activity. *J Physiol Paris* 2012;106(3-4):104-111.
102. Cardin JA, Carlen M, Meletis K, et al. Driving fast-spiking cells induces gamma rhythm and controls sensory responses. *Nature* 2009;459(7247):663-667.
103. Constantinidis C, Williams GV, Goldman-Rakic PS. A role for inhibition in shaping the temporal flow of information in prefrontal cortex. *Nat Neurosci* 2002;5(2):175-180.
104. Kloc M, Maffei A. Target-specific properties of thalamocortical synapses onto layer 4 of mouse primary visual cortex. *J Neurosci* 2014;34(46):15455-15465.
105. Takesian AE, Kotak VC, Sharma N, Sanes DH. Hearing loss differentially affects thalamic drive to two cortical interneuron subtypes. *J Neurophysiol* 2013;110(4):999-1008.
106. Wang HX, Gao WJ. Development of calcium-permeable AMPA receptors and their correlation with NMDA receptors in fast-spiking interneurons of rat prefrontal cortex. *J Physiol* 2010;588:2823-2838.
107. Simons DJ, Carvell GE, Kyriazi HT. Alterations in functional thalamocortical connectivity following neonatal whisker trimming with adult regrowth. *J Neurophysiol* 2015;114(3):1912-1922.
108. Buzsaki G, Geisler C, Henze DA, Wang XJ. Interneuron Diversity series: Circuit complexity and axon wiring economy of cortical interneurons. *Trends Neurosci* 2004;27(4):186-193.
109. Bormann J. The 'ABC' of GABA receptors. *Trends Pharmacol Sci* 2000;21(1):16-19.
110. Kullmann DM, Ruiz A, Rusakov DM, Scott R, Semyanov A, Walker MC. Presynaptic, extrasynaptic and axonal GABA receptors in the CNS: where and why? *Prog Biophys Mol Biol* 2005;87(1):33-46.
111. Glickfeld LL, Roberts JD, Somogyi P, Scanziani M. Interneurons hyperpolarize pyramidal cells along their entire somatodendritic axis. *Nat Neurosci* 2009;12(1):21-23.
112. Tseng GF, Haberly LB. Characterization of synaptically mediated fast and slow inhibitory processes in piriform cortex in an in vitro slice preparation. *J Neurophysiol* 1988;59(5):1352-1376.

113. Isaacson JS, Scanziani M. How inhibition shapes cortical activity. *Neuron* 2011;72(2):231-243.
114. Kubota Y, Karube F, Nomura M, Kawaguchi Y. The Diversity of Cortical Inhibitory Synapses. *Frontiers in neural circuits* 2016;10:27.
115. Cruikshank SJ, Ahmed OJ, Stevens TR, et al. Thalamic control of layer 1 circuits in prefrontal cortex. *J Neurosci* 2012;32(49):17813-17823.
116. Gabernet L, Jadhav SP, Feldman DE, Carandini M, Scanziani M. Somatosensory integration controlled by dynamic thalamocortical feed-forward inhibition. *Neuron* 2005;48(2):315-327.
117. Inoue T, Imoto K. Feedforward inhibitory connections from multiple thalamic cells to multiple regular-spiking cells in layer 4 of the somatosensory cortex. *J Neurophysiol* 2006;96(4):1746-1754.
118. Hull C, Isaacson JS, Scanziani M. Postsynaptic mechanisms govern the differential excitation of cortical neurons by thalamic inputs. *J Neurosci* 2009;29(28):9127-9136.
119. Bagnall MW, Hull C, Bushong EA, Ellisman MH, Scanziani M. Multiple clusters of release sites formed by individual thalamic afferents onto cortical interneurons ensure reliable transmission. *Neuron* 2011;71(1):180-194.
120. Alonso JM, Swadlow HA. Thalamocortical specificity and the synthesis of sensory cortical receptive fields. *J Neurophysiol* 2005;94(1):26-32.
121. Pinto DJ, Brumberg JC, Simons DJ. Circuit dynamics and coding strategies in rodent somatosensory cortex. *J Neurophysiol* 2000;83(3):1158-1166.
122. Wehr M, Zador AM. Balanced inhibition underlies tuning and sharpens spike timing in auditory cortex. *Nature* 2003;426(6965):442-446.
123. Wilentz WB, Contreras D. Dynamics of excitation and inhibition underlying stimulus selectivity in rat somatosensory cortex. *Nat Neurosci* 2005;8(10):1364-1370.
124. Bruno RM, Sakmann B. Cortex is driven by weak but synchronously active thalamocortical synapses. *Science* 2006;312(5780):1622-1627.
125. Bruno RM, Simons DJ. Feedforward mechanisms of excitatory and inhibitory cortical receptive fields. *J Neurosci* 2002;22(24):10966-10975.
126. Cardin JA, Kumbhani RD, Contreras D, Palmer LA. Cellular mechanisms of temporal sensitivity in visual cortex neurons. *J Neurosci* 2010;30(10):3652-3662.
127. Pinto DJ, Hartings JA, Brumberg JC, Simons DJ. Cortical damping: analysis of thalamocortical response transformations in rodent barrel cortex. *Cereb Cortex* 2003;13(1):33-44.
128. Higley MJ, Contreras D. Balanced excitation and inhibition determine spike timing during frequency adaptation. *J Neurosci* 2006;26(2):448-457.
129. Fino E, Yuste R. Dense inhibitory connectivity in neocortex. *Neuron* 2011;69(6):1188-1203.
130. Packer AM, Yuste R. Dense, unspecific connectivity of neocortical parvalbumin-positive interneurons: a canonical microcircuit for inhibition? *J Neurosci* 2011;31(37):13260-13271.
131. Helmstaedter M, Staiger JF, Sakmann B, Feldmeyer D. Efficient recruitment of layer 2/3 interneurons by layer 4 input in single columns of rat somatosensory cortex. *J Neurosci* 2008;28(33):8273-8284.
132. Katzel D, Zemelman BV, Buetfering C, Wolfel M, Miesenböck G. The columnar and laminar organization of inhibitory connections to neocortical excitatory cells. *Nat Neurosci* 2011;14(1):100-107.
133. Adesnik H, Bruns W, Taniguchi H, Huang ZJ, Scanziani M. A neural circuit for spatial summation in visual cortex. *Nature* 2012;490(7419):226-231.

134. Muzyka IM, Estephan B. Somatosensory evoked potentials. *Handb Clin Neurol* 2019;160:523-540.
135. Dumitru D, Jewett DL. Far-field potentials. *Muscle Nerve* 1993;16(3):237-254.
136. Aminoff MJ, Eisen AA. AAEM minimonograph 19: somatosensory evoked potentials. *Muscle Nerve* 1998;21(3):277-290.
137. Lee EK, Seyal M. Generators of short latency human somatosensory-evoked potentials recorded over the spine and scalp. *J Clin Neurophysiol* 1998;15(3):227-234.
138. Yiannikas C, Shahani BT, Young RR. The investigation of traumatic lesions of the brachial plexus by electromyography and short latency somatosensory potentials evoked by stimulation of multiple peripheral nerves. *J Neurol Neurosurg Psychiatry* 1983;46(11):1014-1022.
139. Desmedt JE, Cheron G. Non-cephalic reference recording of early somatosensory potentials to finger stimulation in adult or aging normal man: differentiation of widespread N18 and contralateral N20 from the prerolandic P22 and N30 components. *Electroencephalogr Clin Neurophysiol* 1981;52(6):553-570.
140. Lueders H, Dinner DS, Lesser RP, Klem G. Origin of far-field subcortical evoked potentials to posterior tibial and median nerve stimulation. A comparative study. *Arch Neurol* 1983;40(2):93-97.
141. Emerson RG, Seyal M, Pedley TA. Somatosensory evoked potentials following median nerve stimulation. I. The cervical components. *Brain* 1984;107:169-182.
142. Desmedt JE, Cheron G. Central somatosensory conduction in man: neural generators and interpeak latencies of the far-field components recorded from neck and right or left scalp and earlobes. *Electroencephalogr Clin Neurophysiol* 1980;50(5-6):382-403.
143. Mauguière F, Courjon J. The origins of short-latency somatosensory evoked potentials in humans. *Ann Neurol* 1981;9(6):607-611.
144. Emerson RG, Pedley TA. Generator sources of median somatosensory evoked potentials. *J Clin Neurophysiol* 1984;1(2):203-218.
145. Tomberg C, Desmedt JE, Ozaki I, Noël P. Nasopharyngeal recordings of somatosensory evoked potentials document the medullary origin of the N18 far-field. *Electroencephalogr Clin Neurophysiol* 1991;80(6):496-503.
146. Urasaki E, Uematsu S, Lesser RP. Short latency somatosensory evoked potentials recorded around the human upper brain-stem. *Electroencephalogr Clin Neurophysiol* 1993;88(2):92-104.
147. Noël P, Ozaki I, Desmedt JE. Origin of N18 and P14 far-fields of median nerve somatosensory evoked potentials studied in patients with a brain-stem lesion. *Electroencephalogr Clin Neurophysiol* 1996;98(2):167-170.
148. Sonoo M. Anatomic origin and clinical application of the widespread N18 potential in median nerve somatosensory evoked potentials. *J Clin Neurophysiol* 2000;17(3):258-268.
149. Mauguière F, Desmedt JE, Courjon J. Neural generators of N18 and P14 far-field somatosensory evoked potentials studied in patients with lesion of thalamus or thalamo-cortical radiations. *Electroencephalogr Clin Neurophysiol* 1983;56(4):283-292.
150. Klostermann F, Funk T, Vesper J, Siedenberg R, Curio G. Double-pulse stimulation dissociates intrathalamic and cortical high-frequency (>400Hz) SEP components in man. *Neuroreport* 2000;11(6):1295-1299.
151. Ragert P, Becker M, Tegenthoff M, Pleger B, Dinse HR. Sustained increase of somatosensory cortex excitability by 5 Hz repetitive transcranial magnetic

- stimulation studied by paired median nerve stimulation in humans. *Neurosci Lett* 2004;356(2):91-94.
152. Sparing R, Dambeck N, Stock K, Meister IG, Huetter D, Boroojerdi B. Investigation of the primary visual cortex using short-interval paired-pulse transcranial magnetic stimulation (TMS). *Neurosci Lett* 2005;382(3):312-316.
 153. McLaughlin DF, Kelly EF. Evoked potentials as indices of adaptation in the somatosensory system in humans: a review and prospectus. *Brain Res Brain Res Rev* 1993;18(2):151-206.
 154. Chung S, Li X, Nelson SB. Short-term depression at thalamocortical synapses contributes to rapid adaptation of cortical sensory responses in vivo. *Neuron* 2002;34(3):437-446.
 155. Petersen CC. Short-term dynamics of synaptic transmission within the excitatory neuronal network of rat layer 4 barrel cortex. *J Neurophysiol* 2002;87(6):2904-2914.
 156. Cruikshank SJ, Lewis TJ, Connors BW. Synaptic basis for intense thalamocortical activation of feedforward inhibitory cells in neocortex. *Nat Neurosci* 2007;10(4):462-468.
 157. Hoffken O, Lenz M, Tegenthoff M, Schwenkreis P. Multichannel SEP-recording after paired median nerve stimulation suggests origin of paired-pulse inhibition rostral of the brainstem. *Neurosci Lett* 2010;468(3):308-311.
 158. Dinse HR, Ragert P, Pleger B, Schwenkreis P, Tegenthoff M. Pharmacological modulation of perceptual learning and associated cortical reorganization. *Science* 2003;301(5629):91-94.
 159. Hess G, Aizenman CD, Donoghue JP. Conditions for the induction of long-term potentiation in layer II/III horizontal connections of the rat motor cortex. *J Neurophysiol* 1996;75(5):1765-1778.
 160. Castro-Alamancos MA, Connors BW. Short-term synaptic enhancement and long-term potentiation in neocortex. *Proc Natl Acad Sci U S A* 1996;93(3):1335-1339.
 161. Deisz RA, Prince DA. Frequency-dependent depression of inhibition in guinea-pig neocortex in vitro by GABAB receptor feed-back on GABA release. *J Physiol* 1989;412:513-541.
 162. Mennerick S, Zorumski CF. Paired-pulse modulation of fast excitatory synaptic currents in microcultures of rat hippocampal neurons. *J Physiol* 1995;488:85-101.
 163. Luders H, Lesser R, Gurd A, Klem G. Recovery functions of spinal cord and subcortical somatosensory evoked potentials to posterior tibial nerve stimulation: intrasurgical recordings. *Brain Res* 1984;309(1):27-34.
 164. Rocchi L, Casula E, Tocco P, Berardelli A. Somatosensory Temporal Discrimination Threshold Involves Inhibitory Mechanisms in the Primary Somatosensory Area. 2016;36(2):325-335.
 165. Tinazzi M, Priori A, Bertolasi L, Frasson E, Mauguiere F, Fiaschi A. Abnormal central integration of a dual somatosensory input in dystonia. Evidence for sensory overflow. *Brain* 2000;123:42-50.
 166. Hsieh CL, Shima F, Tobimatsu S, Sun SJ, Kato M. The interaction of the somatosensory evoked potentials to simultaneous finger stimuli in the human central nervous system. A study using direct recordings. *Electroencephalogr Clin Neurophysiol* 1995;96(2):135-142.
 167. Burke D, Gandevia SC, McKeon B, Skuse NF. Interactions between cutaneous and muscle afferent projections to cerebral cortex in man. *Electroencephalogr Clin Neurophysiol* 1982;53(4):349-360.

168. Gandevia SC, Burke D, McKeon BB. Convergence in the somatosensory pathway between cutaneous afferents from the index and middle fingers in man. *Exp Brain Res* 1983;50(2-3):415-425.
169. Okajima Y, Chino N, Saitoh E, Kimura A. Interactions of somatosensory evoked potentials: simultaneous stimulation of two nerves. *Electroencephalogr Clin Neurophysiol* 1991;80(1):26-31.
170. Huttunen J, Ahlfors S, Hari R. Interaction of afferent impulses in the human primary sensorimotor cortex. *Electroencephalogr Clin Neurophysiol* 1992;82(3):176-181.
171. Cracco RQ, Cracco JB. Somatosensory evoked potential in man: far field potentials. *Electroencephalogr Clin Neurophysiol* 1976;41(5):460-466.
172. Abbruzzese M, Favale E, Leandri M, Ratto S. New subcortical components of the cerebral somatosensory evoked potential in man. *Acta Neurol Scand* 1978;58(6):325-332.
173. Eisen A, Roberts K, Low M, Hoirch M, Lawrence P. Questions regarding the sequential neural generator theory of the somatosensory evoked potential raised by digital filtering. *Electroencephalogr Clin Neurophysiol* 1984;59(5):388-395.
174. Maccabee PJ, Hassan NF, Cracco RQ, Schiff JA. Short latency somatosensory and spinal evoked potentials: power spectra and comparison between high pass analog and digital filter. *Electroencephalogr Clin Neurophysiol* 1986;65(3):177-187.
175. Yamada T, Kameyama S, Fuchigami Y, Nakazumi Y, Dickins QS, Kimura J. Changes of short latency somatosensory evoked potential in sleep. *Electroencephalogr Clin Neurophysiol* 1988;70(2):126-136.
176. Curio G, Mackert BM, Burghoff M, Koetitz R, Abraham-Fuchs K, Harer W. Localization of evoked neuromagnetic 600 Hz activity in the cerebral somatosensory system. *Electroencephalogr Clin Neurophysiol* 1994;91(6):483-487.
177. Hashimoto I, Mashiko T, Imada T. Somatic evoked high-frequency magnetic oscillations reflect activity of inhibitory interneurons in the human somatosensory cortex. *Electroencephalogr Clin Neurophysiol* 1996;100(3):189-203.
178. Ozaki I, Suzuki C, Yaegashi Y, Baba M, Matsunaga M, Hashimoto I. High frequency oscillations in early cortical somatosensory evoked potentials. *Electroencephalogr Clin Neurophysiol* 1998;108(6):536-542.
179. Klostermann F, Nolte G, Curio G. Multiple generators of 600 Hz wavelets in human SEP unmasked by varying stimulus rates. *Neuroreport* 1999;10(8):1625-1629.
180. Curio G. Linking 600-Hz "spikelike" EEG/MEG wavelets ("sigma-bursts") to cellular substrates: concepts and caveats. *J Clin Neurophysiol* 2000;17(4):377-396.
181. Gobbele R, Waberski TD, Simon H, et al. Different origins of low- and high-frequency components (600 Hz) of human somatosensory evoked potentials. *Clin Neurophysiol* 2004;115(4):927-937.
182. Emori T, Yamada T, Seki Y, et al. Recovery functions of fast frequency potentials in the initial negative wave of median SEP. *Electroencephalogr Clin Neurophysiol* 1991;78(2):116-123.
183. Urasaki E, Genmoto T, Akamatsu N, Wada S, Yokota A. The effects of stimulus rates on high frequency oscillations of median nerve somatosensory-evoked potentials--direct recording study from the human cerebral cortex. *Clin Neurophysiol* 2002;113(11):1794-1797.
184. Mochizuki H, Machii K, Terao Y, et al. Recovery function of and effects of hyperventilation on somatosensory evoked high-frequency oscillation in Parkinson's disease and myoclonus epilepsy. *Neurosci Res* 2003;46(4):485-492.

185. Ikeda H, Leyba L, Bartolo A, Wang Y, Okada YC. Synchronized spikes of thalamocortical axonal terminals and cortical neurons are detectable outside the pig brain with MEG. *J Neurophysiol* 2002;87(1):626-630.
186. Kimura T, Ozaki I, Hashimoto I. Impulse propagation along thalamocortical fibers can be detected magnetically outside the human brain. *J Neurosci* 2008;28(47):12535-12538.
187. Nakano S, Hashimoto I. The later part of high-frequency oscillations in human somatosensory evoked potentials is enhanced in aged subjects. *Neurosci Lett* 1999;276(2):83-86.
188. Haueisen J, Heuer T, Nowak H, et al. The influence of lorazepam on somatosensory-evoked fast frequency (600 Hz) activity in MEG. *Brain Res* 2000;874(1):10-14.
189. Jones MS, Barth DS. Effects of bicuculline methiodide on fast (>200 Hz) electrical oscillations in rat somatosensory cortex. *J Neurophysiol* 2002;88(2):1016-1025.
190. Ozaki I, Yaegashi Y, Kimura T, Baba M, Matsunaga M, Hashimoto I. Dipole orientation differs between high frequency oscillations and N20m current sources in human somatosensory evoked magnetic fields to median nerve stimulation. *Neurosci Lett* 2001;310(1):41-44.
191. Ozaki I, Hashimoto I. Neural mechanisms of the ultrafast activities. *Clin EEG Neurosci* 2005;36(4):271-277.
192. Jones MS, MacDonald KD, Choi B, Dudek FE, Barth DS. Intracellular correlates of fast (>200 Hz) electrical oscillations in rat somatosensory cortex. *J Neurophysiol* 2000;84(3):1505-1518.
193. Galarreta M, Hestrin S. A network of fast-spiking cells in the neocortex connected by electrical synapses. *Nature* 1999;402(6757):72-75.
194. Gibson JR, Beierlein M, Connors BW. Two networks of electrically coupled inhibitory neurons in neocortex. *Nature* 1999;402(6757):75-79.
195. Hestrin S, Galarreta M. Electrical synapses define networks of neocortical GABAergic neurons. *Trends Neurosci* 2005;28(6):304-309.
196. Swadlow HA, Beloozerova IN, Sirota MG. Sharp, local synchrony among putative feed-forward inhibitory interneurons of rabbit somatosensory cortex. *J Neurophysiol* 1998;79(2):567-582.
197. Porter JT, Johnson CK, Agmon A. Diverse types of interneurons generate thalamus-evoked feedforward inhibition in the mouse barrel cortex. *J Neurosci* 2001;21(8):2699-2710.
198. Fukuda T, Kosaka T. Ultrastructural study of gap junctions between dendrites of parvalbumin-containing GABAergic neurons in various neocortical areas of the adult rat. *Neuroscience* 2003;120(1):5-20.
199. Lacruz F, Artieda J, Pastor MA, Obeso JA. The anatomical basis of somaesthetic temporal discrimination in humans. *J Neurol Neurosurg Psychiatry* 1991;54(12):1077-1081.
200. Conte A, Ferrazzano G, Belvisi D, et al. Somatosensory temporal discrimination in Parkinson's disease, dystonia and essential tremor: Pathophysiological and clinical implications. *Clin Neurophysiol* 2018;129(9):1849-1853.
201. Artieda J, Pastor MA, Lacruz F, Obeso JA. Temporal discrimination is abnormal in Parkinson's disease. *Brain* 1992;115:199-210.
202. Tamura Y, Matsushashi M, Lin P, et al. Impaired intracortical inhibition in the primary somatosensory cortex in focal hand dystonia. *Mov Disord* 2008;23(4):558-565.
203. Pastor MA, Day BL, Macaluso E, Friston KJ, Frackowiak RS. The functional neuroanatomy of temporal discrimination. *J Neurosci* 2004;24(10):2585-2591.

204. Lewis PA, Miall RC. A right hemispheric prefrontal system for cognitive time measurement. *Behavioural processes* 2006;71(2-3):226-234.
205. Koch G, Oliveri M, Caltagirone C. Neural networks engaged in milliseconds and seconds time processing: evidence from transcranial magnetic stimulation and patients with cortical or subcortical dysfunction. *Philos Trans R Soc Lond B Biol Sci* 2009;364(1525):1907-1918.
206. Ivry RB, Spencer RM, Zelaznik HN, Diedrichsen J. The cerebellum and event timing. *Ann N Y Acad Sci* 2002;978:302-317.
207. Kotani S, Kawahara S, Kirino Y. Purkinje cell activity during learning a new timing in classical eyeblink conditioning. *Brain Res* 2003;994(2):193-202.
208. Conte A, Rocchi L, Nardella A, et al. Theta-burst stimulation-induced plasticity over primary somatosensory cortex changes somatosensory temporal discrimination in healthy humans. *PLoS One* 2012;7(3):e32979.
209. Bolognini N, Papagno C, Moroni D, Maravita A. Tactile temporal processing in the auditory cortex. *J Cogn Neurosci* 2010;22(6):1201-1211.
210. Hannula H, Neuvonen T, Savolainen P, et al. Navigated transcranial magnetic stimulation of the primary somatosensory cortex impairs perceptual processing of tactile temporal discrimination. *Neurosci Lett* 2008;437(2):144-147.
211. Rocchi L, Casula E, Tocco P, Berardelli A, Rothwell J. Somatosensory Temporal Discrimination Threshold Involves Inhibitory Mechanisms in the Primary Somatosensory Area. *J Neurosci* 2016;36(2):325-335.
212. Salinas E, Hernandez A, Zainos A, Romo R. Periodicity and firing rate as candidate neural codes for the frequency of vibrotactile stimuli. *J Neurosci* 2000;20(14):5503-5515.
213. Romo R, Hernández A, Zainos A, Lemus L, Brody CD. Neuronal correlates of decision-making in secondary somatosensory cortex. *Nat Neurosci* 2002;5(11):1217-1225.
214. Romo R, Salinas E. Flutter discrimination: neural codes, perception, memory and decision making. *Nat Rev Neurosci* 2003;4(3):203-218.
215. García-Larrea L, Lukaszewicz AC, Mauguière F. Somatosensory responses during selective spatial attention: The N120-to-N140 transition. *Psychophysiology* 1995;32(6):526-537.
216. Valeriani M, Ranghi F, Giaquinto S. The effects of aging on selective attention to touch: a reduced inhibitory control in elderly subjects? *Int J Psychophysiol* 2003;49(1):75-87.
217. Halata Z, Munger BL. The sensory innervation of primate facial skin. II. Vermilion border and mucosa of lip. *Brain Res* 1983;286(1):81-107.
218. Johansson RS, Vallbo AB. Tactile sensibility in the human hand: relative and absolute densities of four types of mechanoreceptive units in glabrous skin. *J Physiol* 1979;286:283-300.
219. Darian-Smith I, Kenins P. Innervation density of mechanoreceptive fibres supplying glabrous skin of the monkey's index finger. *J Physiol* 1980;309:147-155.
220. Johnson KO, Hsiao SS. Neural mechanisms of tactual form and texture perception. *Annu Rev Neurosci* 1992;15:227-250.
221. Van Boven RW, Johnson KO. A psychophysical study of the mechanisms of sensory recovery following nerve injury in humans. *Brain* 1994;117:149-167.
222. Johnson KO, Phillips JR. Tactile spatial resolution. I. Two-point discrimination, gap detection, grating resolution, and letter recognition. *J Neurophysiol* 1981;46(6):1177-1192.

223. Loomis JM. An investigation of tactile hyperacuity. *Sens Processes* 1979;3(4):289-302.
224. Phillips JR, Johnson KO. Tactile spatial resolution. II. Neural representation of Bars, edges, and gratings in monkey primary afferents. *J Neurophysiol* 1981;46(6):1192-1203.
225. Phillips JR, Johnson KO. Tactile spatial resolution. III. A continuum mechanics model of skin predicting mechanoreceptor responses to bars, edges, and gratings. *J Neurophysiol* 1981;46(6):1204-1225.
226. Rosenfeld AK, AC. *Digital picture processing*. 2nd ed: Academic Press, 1982.
227. Kennedy WR, Selim MM, Brink TS, et al. A new device to quantify tactile sensation in neuropathy. *Neurology* 2011;76(19):1642-1649.
228. Johansson RS, LaMotte RH. Tactile detection thresholds for a single asperity on an otherwise smooth surface. *Somatosens Res* 1983;1(1):21-31.
229. LaMotte RH, Whitehouse J. Tactile detection of a dot on a smooth surface: peripheral neural events. *J Neurophysiol* 1986;56(4):1109-1128.
230. Sur M, Wall JT, Kaas JH. Modular segregation of functional cell classes within the postcentral somatosensory cortex of monkeys. *Science* 1981;212(4498):1059-1061.
231. Sur M, Wall JT, Kaas JH. Modular distribution of neurons with slowly adapting and rapidly adapting responses in area 3b of somatosensory cortex in monkeys. *J Neurophysiol* 1984;51(4):724-744.
232. Okun M, Lampl I. Instantaneous correlation of excitation and inhibition during ongoing and sensory-evoked activities. *Nat Neurosci* 2008;11(5):535-537.
233. Georgopoulos AP, Stefanis CN. Local shaping of function in the motor cortex: motor contrast, directional tuning. *Brain research reviews* 2007;55(2):383-389.
234. Georgopoulos AP, Kalaska JF, Caminiti R, Massey JT. On the relations between the direction of two-dimensional arm movements and cell discharge in primate motor cortex. *J Neurosci* 1982;2(11):1527-1537.
235. Amirikian B, Georgopoulos AP. Modular organization of directionally tuned cells in the motor cortex: is there a short-range order? *Proc Natl Acad Sci U S A* 2003;100(21):12474-12479.
236. Georgopoulos AP, Merchant H, Naselaris T, Amirikian B. Mapping of the preferred direction in the motor cortex. *Proc Natl Acad Sci U S A* 2007;104(26):11068-11072.
237. Naselaris T, Merchant H, Amirikian B, Georgopoulos AP. Large-scale organization of preferred directions in the motor cortex. II. Analysis of local distributions. *J Neurophysiol* 2006;96(6):3237-3247.
238. Matsumura M, Sawaguchi T, Kubota K. GABAergic inhibition of neuronal activity in the primate motor and premotor cortex during voluntary movement. *J Neurophysiol* 1992;68(3):692-702.
239. Stefanis C, Jasper H. Recurrent collateral inhibition in pyramidal tract neurons. *J Neurophysiol* 1964;27:855-877.
240. Stefanis C, Jasper H. Intracellular microelectrode studies of antidromic responses in cortical pyramidal tract neurons. *J Neurophysiol* 1964;27:828-854.
241. Di Lazzaro V, Rothwell J, Capogna M. Noninvasive Stimulation of the Human Brain: Activation of Multiple Cortical Circuits. *Neuroscientist* 2018;24(3):246-260.
242. Di Lazzaro V, Oliviero A, Profice P, et al. Comparison of descending volleys evoked by transcranial magnetic and electric stimulation in conscious humans. *Electroencephalogr Clin Neurophysiol* 1998;109(5):397-401.
243. Di Lazzaro V, Oliviero A, Profice P, et al. Effects of voluntary contraction on descending volleys evoked by transcranial electrical stimulation over the motor cortex hand area in conscious humans. *Exp Brain Res* 1999;124(4):525-528.

244. Kaneko K, Kawai S, Fuchigami Y, Morita H, Ofuji A. The effect of current direction induced by transcranial magnetic stimulation on the corticospinal excitability in human brain. *Electroencephalogr Clin Neurophysiol* 1996;101(6):478-482.
245. Di Lazzaro V, Restuccia D, Oliviero A, et al. Effects of voluntary contraction on descending volleys evoked by transcranial stimulation in conscious humans. *J Physiol* 1998;508:625-633.
246. Baker SN, Curio G, Lemon RN. EEG oscillations at 600 Hz are macroscopic markers for cortical spike bursts. *J Physiol* 2003;550:529-534.
247. Kujirai T, Caramia MD, Rothwell JC, et al. Corticocortical inhibition in human motor cortex. *J Physiol* 1993;471:501-519.
248. Miyaguchi S, Kojima S, Sasaki R, Tamaki H, Onishi H. Modulation of short-latency afferent inhibition and short-interval intracortical inhibition by test stimulus intensity and motor-evoked potential amplitude. *Neuroreport* 2017;28(18):1202-1207.
249. Di Lazzaro V, Restuccia D, Oliviero A, et al. Magnetic transcranial stimulation at intensities below active motor threshold activates intracortical inhibitory circuits. *Exp Brain Res* 1998;119(2):265-268.
250. Ziemann U, Lonnecker S, Steinhoff BJ, Paulus W. The effect of lorazepam on the motor cortical excitability in man. *Exp Brain Res* 1996;109(1):127-135.
251. Di Lazzaro V, Oliviero A, Meglio M, et al. Direct demonstration of the effect of lorazepam on the excitability of the human motor cortex. *Clin Neurophysiol* 2000;111(5):794-799.
252. Ziemann U, Rothwell JC, Ridding MC. Interaction between intracortical inhibition and facilitation in human motor cortex. *J Physiol* 1996;496:873-881.
253. Ilic TV, Meintzschel F, Cleff U, Ruge D, Kessler KR, Ziemann U. Short-interval paired-pulse inhibition and facilitation of human motor cortex: the dimension of stimulus intensity. *J Physiol* 2002;545:153-167.
254. Hasenstaub A, Shu Y, Haider B, Kraushaar U, Duque A, McCormick DA. Inhibitory postsynaptic potentials carry synchronized frequency information in active cortical networks. *Neuron* 2005;47(3):423-435.
255. Valls-Sole J, Pascual-Leone A, Wassermann EM, Hallett M. Human motor evoked responses to paired transcranial magnetic stimuli. *Electroencephalogr Clin Neurophysiol* 1992;85(6):355-364.
256. Chen R. Interactions between inhibitory and excitatory circuits in the human motor cortex. *Exp Brain Res* 2004;154(1):1-10.
257. Brasil-Neto JP, Cammarota A, Valls-Sole J, Pascual-Leone A, Hallett M, Cohen LG. Role of intracortical mechanisms in the late part of the silent period to transcranial stimulation of the human motor cortex. *Acta Neurol Scand* 1995;92(5):383-386.
258. Nakamura H, Kitagawa H, Kawaguchi Y, Tsuji H. Intracortical facilitation and inhibition after transcranial magnetic stimulation in conscious humans. *J Physiol* 1997;498:817-823.
259. Chen R, Lozano AM, Ashby P. Mechanism of the silent period following transcranial magnetic stimulation. Evidence from epidural recordings. *Exp Brain Res* 1999;128(4):539-542.
260. Di Lazzaro V, Oliviero A, Mazzone P, et al. Direct demonstration of long latency cortico-cortical inhibition in normal subjects and in a patient with vascular parkinsonism. *Clin Neurophysiol* 2002;113(11):1673-1679.
261. Douglas RJ, Martin KA. A functional microcircuit for cat visual cortex. *J Physiol* 1991;440:735-769.

262. McDonnell MN, Orekhov Y, Ziemann U. The role of GABA(B) receptors in intracortical inhibition in the human motor cortex. *Exp Brain Res* 2006;173(1):86-93.
263. Di Lazzaro V, Pilato F, Oliviero A, et al. Origin of facilitation of motor-evoked potentials after paired magnetic stimulation: direct recording of epidural activity in conscious humans. *J Neurophysiol* 2006;96(4):1765-1771.
264. Ni Z, Gunraj C, Wagle-Shukla A, et al. Direct demonstration of inhibitory interactions between long interval intracortical inhibition and short interval intracortical inhibition. *J Physiol* 2011;589:2955-2962.
265. Wiegel P, Niemann N, Rothwell JC, Leukel C. Evidence for a subcortical contribution to intracortical facilitation. *Eur J Neurosci* 2018;47(11):1311-1319.
266. Bliss TV, Lomo T. Long-lasting potentiation of synaptic transmission in the dentate area of the anaesthetized rabbit following stimulation of the perforant path. *J Physiol* 1973;232(2):331-356.
267. Abraham WC, Williams JM. Properties and mechanisms of LTP maintenance. *Neuroscientist* 2003;9(6):463-474.
268. Stanton PK, Sejnowski TJ. Associative long-term depression in the hippocampus induced by hebbian covariance. *Nature* 1989;339(6221):215-218.
269. Bliss TV, Collingridge GL. A synaptic model of memory: long-term potentiation in the hippocampus. *Nature* 1993;361(6407):31-39.
270. Nicoll RA, Malenka RC. Contrasting properties of two forms of long-term potentiation in the hippocampus. *Nature* 1995;377(6545):115-118.
271. Bi G, Poo M. Synaptic modification by correlated activity: Hebb's postulate revisited. *Annu Rev Neurosci* 2001;24:139-166.
272. Yao H, Dan Y. Stimulus timing-dependent plasticity in cortical processing of orientation. *Neuron* 2001;32(2):315-323.
273. Dan Y, Poo MM. Spike timing-dependent plasticity of neural circuits. *Neuron* 2004;44(1):23-30.
274. Markram H, Gerstner W, Sjöström PJ. A history of spike-timing-dependent plasticity. *Front Synaptic Neurosci* 2011;3:4.
275. Godde B, Stauffenberg B, Spengler F, Dinse HR. Tactile coactivation-induced changes in spatial discrimination performance. *J Neurosci* 2000;20(4):1597-1604.
276. Pleger B, Dinse HR, Ragert P, Schwenkreis P, Malin JP, Tegenthoff M. Shifts in cortical representations predict human discrimination improvement. *Proc Natl Acad Sci U S A* 2001;98(21):12255-12260.
277. Pleger B, Foerster AF, Ragert P, et al. Functional imaging of perceptual learning in human primary and secondary somatosensory cortex. *Neuron* 2003;40(3):643-653.
278. Hoffken O, Veit M, Knossalla F, et al. Sustained increase of somatosensory cortex excitability by tactile coactivation studied by paired median nerve stimulation in humans correlates with perceptual gain. *J Physiol* 2007;584:463-471.
279. Ragert P, Kalisch T, Bliem B, Franzkowiak S, Dinse HR. Differential effects of tactile high- and low-frequency stimulation on tactile discrimination in human subjects. *BMC Neurosci* 2008;9:9.
280. Klem GH, Luders HO, Jasper HH, Elger C. The ten-twenty electrode system of the International Federation. *The International Federation of Clinical Neurophysiology. Electroencephalogr Clin Neurophysiol Suppl* 1999;52:3-6.
281. Van Boven RW, Johnson KO. The limit of tactile spatial resolution in humans: grating orientation discrimination at the lip, tongue, and finger. *Neurology* 1994;44(12):2361-2366.

282. Mathiowetz V, Volland G, Kashman N, Weber K. Adult norms for the Box and Block Test of manual dexterity. *Am J Occup Ther* 1985;39(6):386-391.
283. Chen HM, Chen CC, Hsueh IP, Huang SL, Hsieh CL. Test-retest reproducibility and smallest real difference of 5 hand function tests in patients with stroke. *Neurorehabil Neural Repair* 2009;23(5):435-440.
284. Siebers A, Oberg U, Skargren E. The effect of modified constraint-induced movement therapy on spasticity and motor function of the affected arm in patients with chronic stroke. *Physiother Can* 2010;62(4):388-396.
285. Earhart GM, Cavanaugh JT, Ellis T, Ford MP, Foreman KB, Dibble L. The 9-hole PEG test of upper extremity function: average values, test-retest reliability, and factors contributing to performance in people with Parkinson disease. *J Neurol Phys Ther* 2011;35(4):157-163.
286. Mathiowetz V, Kashman N, Volland G, Weber K, Dowe M, Rogers S. Grip and pinch strength: normative data for adults. *Arch Phys Med Rehabil* 1985;66(2):69-74.
287. Sommerfeld DK, Eek EU, Svensson AK, Holmqvist LW, von Arbin MH. Spasticity after stroke: its occurrence and association with motor impairments and activity limitations. *Stroke* 2004;35(1):134-139.
288. Heller A, Wade DT, Wood VA, Sunderland A, Hewer RL, Ward E. Arm function after stroke: measurement and recovery over the first three months. *J Neurol Neurosurg Psychiatry* 1987;50(6):714-719.
289. Oxford Grice K, Vogel KA, Le V, Mitchell A, Muniz S, Vollmer MA. Adult norms for a commercially available Nine Hole Peg Test for finger dexterity. *Am J Occup Ther* 2003;57(5):570-573.
290. Comella CL, Stebbins GT, Goetz CG, Chmura TA, Bressman SB, Lang AE. Teaching tape for the motor section of the Toronto Western Spasmodic Torticollis Scale. *Mov Disord* 1997;12(4):570-575.
291. Jost WH, Hefter H, Stenner A, Reichel G. Rating scales for cervical dystonia: a critical evaluation of tools for outcome assessment of botulinum toxin therapy. *Journal of neural transmission (Vienna, Austria : 1996)* 2013;120(3):487-496.
292. Comella CL, Leurgans S, Wu J, Stebbins GT, Chmura T. Rating scales for dystonia: a multicenter assessment. *Mov Disord* 2003;18(3):303-312.
293. Zeuner KE, Peller M, Knutzen A, et al. How to assess motor impairment in writer's cramp. *Mov Disord* 2007;22(8):1102-1109.
294. Humes LE, Busey TA, Craig JC, Kewley-Port D. The effects of age on sensory thresholds and temporal gap detection in hearing, vision, and touch. *Attention, perception & psychophysics* 2009;71(4):860-871.
295. Molloy FM, Carr TD, Zeuner KE, Dambrosia JM, Hallett M. Abnormalities of spatial discrimination in focal and generalized dystonia. *Brain* 2003;126:2175-2182.
296. Tinazzi M, Frasson E, Bertolasi L, Fiaschi A, Aglioti S. Temporal discrimination of somesthetic stimuli is impaired in dystonic patients. *Neuroreport* 1999;10(7):1547-1550.
297. Sanger TD, Tarsy D, Pascual-Leone A. Abnormalities of spatial and temporal sensory discrimination in writer's cramp. *Mov Disord* 2001;16(1):94-99.
298. Bara-Jimenez W, Shelton P, Hallett M. Spatial discrimination is abnormal in focal hand dystonia. *Neurology* 2000;55(12):1869-1873.
299. Inoue K, Hashimoto I, Shirai T, et al. Disinhibition of the somatosensory cortex in cervical dystonia-decreased amplitudes of high-frequency oscillations. *Clin Neurophysiol* 2004;115(7):1624-1630.

300. Ozaki I, Hashimoto I. Exploring the physiology and function of high-frequency oscillations (HFOs) from the somatosensory cortex. *Clin Neurophysiol* 2011;122(10):1908-1923.
301. Termsarasab P, Ramdhani RA, Battistella G, et al. Neural correlates of abnormal sensory discrimination in laryngeal dystonia. *NeuroImage Clinical* 2016;10:18-26.
302. Oldfield RC. The assessment and analysis of handedness: the Edinburgh inventory. *Neuropsychologia* 1971;9(1):97-113.
303. Erro R, Rocchi L, Antelmi E, et al. High frequency repetitive sensory stimulation improves temporal discrimination in healthy subjects. *Clin Neurophysiol* 2016;127(1):817-820.
304. Cruccu G, Aminoff MJ, Curio G, et al. Recommendations for the clinical use of somatosensory-evoked potentials. *Clin Neurophysiol* 2008;119(8):1705-1719.
305. Meyer-Hardting E, Wiederholt WC, Budnick B. Recovery function of short-latency components of the human somatosensory evoked potential. *Arch Neurol* 1983;40(5):290-293.
306. Vollono C, Ferraro D, Miliucci R, Vigevano F, Valeriani M. The abnormal recovery cycle of somatosensory evoked potential components in children with migraine can be reversed by topiramate. *Cephalalgia* 2010;30(1):17-26.
307. Katayama T, Suppa A, Rothwell JC. Somatosensory evoked potentials and high frequency oscillations are differently modulated by theta burst stimulation over primary somatosensory cortex in humans. *Clin Neurophysiol* 2010;121(12):2097-2103.
308. Murakami T, Sakuma K, Nomura T, Nakashima K, Hashimoto I. High-frequency oscillations change in parallel with short-interval intracortical inhibition after theta burst magnetic stimulation. *Clin Neurophysiol* 2008;119(2):301-308.
309. Hoshiyama M, Kakigi R, Tamura Y. Temporal discrimination threshold on various parts of the body. *Muscle Nerve* 2004;29(2):243-247.
310. Giersch A, Lalanne L, Corves C, et al. Extended visual simultaneity thresholds in patients with schizophrenia. *Schizophr Bull* 2009;35(4):816-825.
311. Frasson E, Priori A, Bertolasi L, Mauguiere F, Fiaschi A, Tinazzi M. Somatosensory disinhibition in dystonia. *Mov Disord* 2001;16(4):674-682.
312. Sonoo M, Genba-Shimizu K, Mannen T, Shimizu T. Detailed analysis of the latencies of median nerve somatosensory evoked potential components, 2: Analysis of subcomponents of the P13/14 and N20 potentials. *Electroencephalogr Clin Neurophysiol* 1997;104(4):296-311.
313. Araki A, Yamada T, Ito T, et al. Dissociation between upper and lower neck N13 potentials following paired median nerve stimuli. *Electroencephalogr Clin Neurophysiol* 1997;104(1):68-73.
314. Lueders H, Lesser RP, Hahn J, Dinner DS, Klem G. Cortical somatosensory evoked potentials in response to hand stimulation. *J Neurosurg* 1983;58(6):885-894.
315. Helmstaedter M, Sakmann B, Feldmeyer D. Neuronal correlates of local, lateral, and translaminar inhibition with reference to cortical columns. *Cereb Cortex* 2009;19(4):926-937.
316. Kolasinski J, Makin TR, Jbabdi S, Clare S, Stagg CJ, Johansen-Berg H. Investigating the Stability of Fine-Grain Digit Somatotopy in Individual Human Participants. *J Neurosci* 2016;36(4):1113-1127.
317. Rushton DN, Rothwell JC, Craggs MD. Gating of somatosensory evoked potentials during different kinds of movement in man. *Brain* 1981;104(3):465-491.
318. Murase N, Kaji R, Shimazu H, et al. Abnormal premovement gating of somatosensory input in writer's cramp. *Brain* 2000;123:1813-1829.

319. Jones EG, Burton H. Areal differences in the laminar distribution of thalamic afferents in cortical fields of the insular, parietal and temporal regions of primates. *J Comp Neurol* 1976;168(2):197-247.
320. Peller M, Zeuner KE, Munchau A, et al. The basal ganglia are hyperactive during the discrimination of tactile stimuli in writer's cramp. *Brain* 2006;129:2697-2708.
321. Schneider SA, Pleger B, Draganski B, et al. Modulatory effects of 5Hz rTMS over the primary somatosensory cortex in focal dystonia--an fMRI-TMS study. *Mov Disord* 2010;25(1):76-83.
322. Godde B, Spengler F, Dinse HR. Associative pairing of tactile stimulation induces somatosensory cortical reorganization in rats and humans. *Neuroreport* 1996;8(1):281-285.
323. Dinse HR, Kleibel N, Kalisch T, Ragert P, Wilimzig C, Tegenthoff M. Tactile coactivation resets age-related decline of human tactile discrimination. *Ann Neurol* 2006;60(1):88-94.
324. Kalisch T, Tegenthoff M, Dinse HR. Improvement of sensorimotor functions in old age by passive sensory stimulation. *Clin Interv Aging* 2008;3(4):673-690.
325. Smith PS, Dinse HR, Kalisch T, Johnson M, Walker-Batson D. Effects of repetitive electrical stimulation to treat sensory loss in persons poststroke. *Arch Phys Med Rehabil* 2009;90(12):2108-2111.
326. Kalisch T, Tegenthoff M, Dinse HR. Repetitive electric stimulation elicits enduring improvement of sensorimotor performance in seniors. *Neural Plast* 2010;2010:690531.
327. Rocchi L, Conte A, Nardella A, et al. Somatosensory temporal discrimination threshold may help to differentiate patients with multiple system atrophy from patients with Parkinson's disease. *Eur J Neurol* 2013;20(4):714-719.
328. Johansson RS, Vallbo AB. Spatial properties of the population of mechanoreceptive units in the glabrous skin of the human hand. *Brain Res* 1980;184(2):353-366.
329. Stevens JC, Patterson MQ. Dimensions of spatial acuity in the touch sense: changes over the life span. *Somatosens Mot Res* 1995;12(1):29-47.
330. Lundborg G, Rosen B. The two-point discrimination test--time for a re-appraisal? *J Hand Surg Br* 2004;29(5):418-422.
331. Tong J, Mao O, Goldreich D. Two-point orientation discrimination versus the traditional two-point test for tactile spatial acuity assessment. *Front Hum Neurosci* 2013;7:579.
332. Craig JC, Johnson KO. The Two-Point Threshold: Not a Measure of Tactile Spatial Resolution. *Curr Dir Psychol Sci* 2000 9:29-32.
333. Kwast-Rabben O, Libelius R, Heikkila H. Somatosensory evoked potentials following stimulation of digital nerves. *Muscle Nerve* 2002;26(4):533-538.
334. Valeriani M, Rinalduzzi S, Vigeveno F. Multilevel somatosensory system disinhibition in children with migraine. *Pain* 2005;118(1-2):137-144.
335. Rossini PM, Barker AT, Berardelli A, et al. Non-invasive electrical and magnetic stimulation of the brain, spinal cord and roots: basic principles and procedures for routine clinical application. Report of an IFCN committee. *Electroencephalogr Clin Neurophysiol* 1994;91(2):79-92.
336. Huang YZ, Edwards MJ, Rounis E, Bhatia KP, Rothwell JC. Theta burst stimulation of the human motor cortex. *Neuron* 2005;45(2):201-206.
337. Allison T, McCarthy G, Wood CC, Darcey TM, Spencer DD, Williamson PD. Human cortical potentials evoked by stimulation of the median nerve. I. Cytoarchitectonic areas generating short-latency activity. *J Neurophysiol* 1989;62(3):694-710.

338. McCarthy G, Wood CC, Allison T. Cortical somatosensory evoked potentials. I. Recordings in the monkey *Macaca fascicularis*. *J Neurophysiol* 1991;66(1):53-63.
339. Allison T, Wood CC, McCarthy G, Spencer DD. Cortical somatosensory evoked potentials. II. Effects of excision of somatosensory or motor cortex in humans and monkeys. *J Neurophysiol* 1991;66(1):64-82.
340. Ugawa Y, Genba-Shimizu K, Kanazawa I. Somatosensory evoked potential recovery (SEP-R) in various neurological disorders. *Electroencephalogr Clin Neurophysiol* 1996;100(1):62-67.
341. Mochizuki H, Hanajima R, Kowa H, et al. Somatosensory evoked potential recovery in myotonic dystrophy. *Clin Neurophysiol* 2001;112(5):793-799.
342. Tomberg C, Desmedt JE, Ozaki I. Right or left ear reference changes the voltage of frontal and parietal somatosensory evoked potentials. *Electroencephalogr Clin Neurophysiol* 1991;80(6):504-512.
343. Restuccia D, Della Marca G, Valeriani M, et al. Influence of cholinergic circuitries in generation of high-frequency somatosensory evoked potentials. *Clin Neurophysiol* 2003;114(8):1538-1548.
344. Shimazu H, Kaji R, Tsujimoto T, et al. High-frequency SEP components generated in the somatosensory cortex of the monkey. *Neuroreport* 2000;11(12):2821-2826.
345. Rosen I, Asanuma H. Peripheral afferent inputs to the forelimb area of the monkey motor cortex: input-output relations. *Exp Brain Res* 1972;14(3):257-273.
346. Asanuma H. Functional role of sensory inputs to the motor cortex. *Prog Neurobiol* 1981;16(3-4):241-262.
347. Classen J, Steinfelder B, Liepert J, et al. Cutaneomotor integration in humans is somatotopically organized at various levels of the nervous system and is task dependent. *Exp Brain Res* 2000;130(1):48-59.
348. Tamburin S, Manganotti P, Zanette G, Fiaschi A. Cutaneomotor integration in human hand motor areas: somatotopic effect and interaction of afferents. *Exp Brain Res* 2001;141(2):232-241.
349. Porter LL. Somatosensory input onto pyramidal tract neurons in rodent motor cortex. *Neuroreport* 1996;7(14):2309-2315.
350. Kaneko T, Caria MA, Asanuma H. Information processing within the motor cortex. I. Responses of morphologically identified motor cortical cells to stimulation of the somatosensory cortex. *J Comp Neurol* 1994;345(2):161-171.
351. Kaneko T, Caria MA, Asanuma H. Information processing within the motor cortex. II. Intracortical connections between neurons receiving somatosensory cortical input and motor output neurons of the cortex. *J Comp Neurol* 1994;345(2):172-184.
352. Sakamoto T, Porter LL, Asanuma H. Long-lasting potentiation of synaptic potentials in the motor cortex produced by stimulation of the sensory cortex in the cat: a basis of motor learning. *Brain Res* 1987;413(2):360-364.
353. Keller A, Iriki A, Asanuma H. Identification of neurons producing long-term potentiation in the cat motor cortex: intracellular recordings and labeling. *J Comp Neurol* 1990;300(1):47-60.
354. McAllister SM, Rothwell JC, Ridding MC. Selective modulation of intracortical inhibition by low-intensity Theta Burst Stimulation. *Clin Neurophysiol* 2009;120(4):820-826.
355. Hallett M. Neurophysiology of dystonia: The role of inhibition. *Neurobiol Dis* 2011;42(2):177-184.
356. Abbruzzese G, Marchese R, Buccolieri A, Gasparetto B, Trompetto C. Abnormalities of sensorimotor integration in focal dystonia: a transcranial magnetic stimulation study. *Brain* 2001;124:537-545.

357. Elbert T, Candia V, Altenmuller E, et al. Alteration of digital representations in somatosensory cortex in focal hand dystonia. *Neuroreport* 1998;9(16):3571-3575.
358. Meunier S, Garnero L, Ducorps A, et al. Human brain mapping in dystonia reveals both endophenotypic traits and adaptive reorganization. *Ann Neurol* 2001;50(4):521-527.
359. Candia V, Wienbruch C, Elbert T, Rockstroh B, Ray W. Effective behavioral treatment of focal hand dystonia in musicians alters somatosensory cortical organization. *Proc Natl Acad Sci U S A* 2003;100(13):7942-7946.
360. Stamelou M, Edwards MJ, Hallett M, Bhatia KP. The non-motor syndrome of primary dystonia: clinical and pathophysiological implications. *Brain* 2012;135:1668-1681.
361. Rocchi L, Erro R, Antelmi E, et al. High frequency somatosensory stimulation increases sensori-motor inhibition and leads to perceptual improvement in healthy subjects. *Clin Neurophysiol* 2017;128(6):1015-1025.
362. Sohn YH, Hallett M. Disturbed surround inhibition in focal hand dystonia. *Ann Neurol* 2004;56(4):595-599.
363. Beck S, Richardson SP, Shamim EA, Dang N, Schubert M, Hallett M. Short intracortical and surround inhibition are selectively reduced during movement initiation in focal hand dystonia. *J Neurosci* 2008;28(41):10363-10369.
364. McDonnell MN, Thompson PD, Ridding MC. The effect of cutaneous input on intracortical inhibition in focal task-specific dystonia. *Mov Disord* 2007;22(9):1286-1292.
365. Huang YZ, Rothwell JC, Lu CS, Wang J, Chen RS. Restoration of motor inhibition through an abnormal premotor-motor connection in dystonia. *Mov Disord* 2010;25(6):696-703.
366. Quartarone A, Rizzo V, Bagnato S, et al. Homeostatic-like plasticity of the primary motor hand area is impaired in focal hand dystonia. *Brain* 2005;128:1943-1950.
367. Tamura Y, Ueki Y, Lin P, et al. Disordered plasticity in the primary somatosensory cortex in focal hand dystonia. *Brain* 2009;132:749-755.
368. Classen J, Wolters A, Stefan K, et al. Paired associative stimulation. *Suppl Clin Neurophysiol* 2004;57:563-569.
369. Monte-Silva K, Kuo MF, Hessenthaler S, et al. Induction of late LTP-like plasticity in the human motor cortex by repeated non-invasive brain stimulation. *Brain stimulation* 2013;6(3):424-432.
370. Gamboa OL, Antal A, Moliadze V, Paulus W. Simply longer is not better: reversal of theta burst after-effect with prolonged stimulation. *Exp Brain Res* 2010;204(2):181-187.
371. Bliem B, Muller-Dahlhaus JF, Dinse HR, Ziemann U. Homeostatic metaplasticity in the human somatosensory cortex. *J Cogn Neurosci* 2008;20(8):1517-1528.
372. Bear MF. Mechanism for a sliding synaptic modification threshold. *Neuron* 1995;15(1):1-4.
373. Bienenstock EL, Cooper LN, Munro PW. Theory for the development of neuron selectivity: orientation specificity and binocular interaction in visual cortex. *J Neurosci* 1982;2(1):32-48.
374. Gentner R, Wankerl K, Reinsberger C, Zeller D, Classen J. Depression of human corticospinal excitability induced by magnetic theta-burst stimulation: evidence of rapid polarity-reversing metaplasticity. *Cereb Cortex* 2008;18(9):2046-2053.
375. Abraham WC. Metaplasticity: tuning synapses and networks for plasticity. *Nat Rev Neurosci* 2008;9(5):387.

376. Ridding MC, Sheean G, Rothwell JC, Inzelberg R, Kujirai T. Changes in the balance between motor cortical excitation and inhibition in focal, task specific dystonia. *J Neurol Neurosurg Psychiatry* 1995;59(5):493-498.
377. Sommer M, Ruge D, Tergau F, Beuche W, Altenmuller E, Paulus W. Intracortical excitability in the hand motor representation in hand dystonia and blepharospasm. *Mov Disord* 2002;17(5):1017-1025.
378. Huang YZ, Edwards MJ, Bhatia KP, Rothwell JC. One-Hz repetitive transcranial magnetic stimulation of the premotor cortex alters reciprocal inhibition in DYT1 dystonia. *Mov Disord* 2004;19(1):54-59.
379. Tinazzi M, Fiorio M, Stanzani C, et al. Temporal discrimination of two passive movements in writer's cramp. *Mov Disord* 2006;21(8):1131-1135.
380. Conte A, Defazio G, Hallett M, Fabbrini G, Berardelli A. The role of sensory information in the pathophysiology of focal dystonias. *Nat Rev Neurol* 2019;15(4):224-233.
381. Erro R, Rocchi L, Antelmi E, et al. High frequency somatosensory stimulation in dystonia: Evidence for defective inhibitory plasticity. *Mov Disord* 2018.
382. Leodori G, Formica A, Zhu X, et al. The third-stimulus temporal discrimination threshold: focusing on the temporal processing of sensory input within primary somatosensory cortex. *J Neurophysiol* 2017;118(4):2311-2317.
383. Conte A, McGovern EM, Narasimham S, et al. Temporal Discrimination: Mechanisms and Relevance to Adult-Onset Dystonia. *Front Neurol* 2017;8:625.
384. Govert F, Becktepe J, Balint B, et al. Temporal discrimination is altered in patients with isolated asymmetric and jerky upper limb tremor. *Mov Disord* 2020;35(2):306-315.
385. Liepert J, Gorsler A, van Eimeren T, Munchau A, Weiller C. Motor excitability in a patient with a somatosensory cortex lesion. *Clin Neurophysiol* 2003;114(6):1003-1008.
386. Tamburin S, Zanette G. Abnormalities of sensory processing and sensorimotor interactions in secondary dystonia: a neurophysiological study in two patients. *Mov Disord* 2005;20(3):354-360.
387. Trompetto C, Avanzino L, Marinelli L, et al. Corticospinal excitability in patients with secondary dystonia due to focal lesions of the basal ganglia and thalamus. *Clin Neurophysiol* 2012;123(4):808-814.
388. Ziemann U, Paulus W, Rothenberger A. Decreased motor inhibition in Tourette's disorder: evidence from transcranial magnetic stimulation. *Am J Psychiatry* 1997;154(9):1277-1284.
389. Orth M, Rothwell JC. Motor cortex excitability and comorbidity in Gilles de la Tourette syndrome. *J Neurol Neurosurg Psychiatry* 2009;80(1):29-34.
390. Meunier S, Hallett M. Endophenotyping: a window to the pathophysiology of dystonia. *Neurology* 2005;65(6):792-793.
391. Quartarone A, Morgante F, Sant'angelo A, et al. Abnormal plasticity of sensorimotor circuits extends beyond the affected body part in focal dystonia. *J Neurol Neurosurg Psychiatry* 2008;79(9):985-990.
392. Wolters A, Sandbrink F, Schlottmann A, et al. A temporally asymmetric Hebbian rule governing plasticity in the human motor cortex. *J Neurophysiol* 2003;89(5):2339-2345.
393. Quartarone A, Hallett M. Emerging concepts in the physiological basis of dystonia. *Mov Disord* 2013;28(7):958-967.
394. Cardin JA, Palmer LA, Contreras D. Stimulus feature selectivity in excitatory and inhibitory neurons in primary visual cortex. *J Neurosci* 2007;27(39):10333-10344.

395. Swadlow HA, Gusev AG. Receptive-field construction in cortical inhibitory interneurons. *Nat Neurosci* 2002;5(5):403-404.
396. Ibáñez J, Hannah R, Rocchi L, Rothwell JC. Premovement Suppression of Corticospinal Excitability may be a Necessary Part of Movement Preparation. *Cereb Cortex* 2020;30(5):2910-2923.
397. Martino D, Liuzzi D, Macerollo A, Aniello MS, Livrea P, Defazio G. The phenomenology of the geste antagoniste in primary blepharospasm and cervical dystonia. *Mov Disord* 2010;25(4):407-412.
398. Dagostino S, Ercoli T, Gigante AF, Pellicciari R, Fadda L, Defazio G. Sensory trick in upper limb dystonia. *Parkinsonism Relat Disord* 2019;63:221-223.
399. Svetel M, Ivanović N, Marinković J, Jović J, Dragasević N, Kostić VS. Characteristics of dystonic movements in primary and symptomatic dystonias. *J Neurol Neurosurg Psychiatry* 2004;75(2):329-330.